



**This electronic thesis or dissertation has been
downloaded from Explore Bristol Research,
<http://research-information.bristol.ac.uk>**

Author:

Frysz, Monika

Title:

Describing the development of hip shape in adolescence, and environmental and genetic influences on this process, in ALSPAC offspring

General rights

Access to the thesis is subject to the Creative Commons Attribution - NonCommercial-No Derivatives 4.0 International Public License. A copy of this may be found at <https://creativecommons.org/licenses/by-nc-nd/4.0/legalcode> This license sets out your rights and the restrictions that apply to your access to the thesis so it is important you read this before proceeding.

Take down policy

Some pages of this thesis may have been removed for copyright restrictions prior to having it been deposited in Explore Bristol Research. However, if you have discovered material within the thesis that you consider to be unlawful e.g. breaches of copyright (either yours or that of a third party) or any other law, including but not limited to those relating to patent, trademark, confidentiality, data protection, obscenity, defamation, libel, then please contact collections-metadata@bristol.ac.uk and include the following information in your message:

- Your contact details
- Bibliographic details for the item, including a URL
- An outline nature of the complaint

Your claim will be investigated and, where appropriate, the item in question will be removed from public view as soon as possible.

**Describing the development of hip shape in
adolescence, and environmental and genetic
influences on this process, in ALSPAC offspring**

Monika Renata Frysz

A dissertation submitted to the University of Bristol in
accordance with the requirements for award of the degree
of PhD in the Faculty of Health Sciences

Population Health Sciences

September 2018

Word count 56,812

Abstract

Hip shape is an important determinant of hip osteoarthritis (OA) and osteoporotic hip fracture; however, little is known about its development in childhood and adolescence. In this thesis, I aimed to address this question by exploring factors influencing hip shape in adolescence.

Hip DXA scans were collected in offspring from the Avon Longitudinal Study of Parents and Children, at mean ages of 13.8 and 17.8 years. These images were analysed in Shape software to quantify hip morphology using a 53-point Statistical Shape Model (SSM). Principal component analysis was used to generate independent modes of variation (hip shape modes (HSMs) and scores from an adult reference SSM (based on 19,379 images) were applied to adolescent data to aid comparability between the time points. The top ten HSMs were selected as outcomes and associations with sex, tempo (marker of pubertal timing) and BMD were examined, and genome-wide association study (GWAS) explored genetic influences on hip shape at both time points.

Several HSMs showed sex differences. At age 14, there was strong evidence of relationships between tempo and hip shape, particularly in males, whereas at age 18 these associations were weaker in both sexes. Consistent associations between BMD and hip shape were observed in males and females, and at both time points. GWAS identified five independent variants associated with hip shape ($p < 5 \times 10^{-8}$).

These findings suggest that sexual dimorphism in hip shape can be discerned in early adolescence, and that puberty is a critical period for hip shape development. Observed relationships between BMD and hip shape could be partially explained by shared genetic factors underlying these traits. Finally, genetic variants implicated in endochondral bone formation, which were previously found to be associated with adult hip shape, appear to influence hip shape in adolescents, consistent with a contribution of longitudinal growth to hip shape.

Acknowledgements

Firstly, I would like to thank the Wellcome Trust for funding this research.

My sincerest thanks go to Professor Jon Tobias for your guidance, patience and enthusiasm for research which kept me motivated throughout this PhD. Thank you so much for believing in me and the opportunity I was given to embark on this journey.

Heartfelt thanks also go to Dr Lavinia Paternoster, for always listening and for your invaluable advice regarding my research and beyond, for your constructive feedback and challenging questions. Thank you to both of you, I could not have imagined having better supervisors and mentors for this PhD. I would also like to thank Dr Jenny Gregory for her assistance with Shape and help with resolving any issues.

I would also like to thank the members of the Musculoskeletal Research Unit: Dr Emma Clark for encouraging me to undertake this PhD, Adrian Sayers, Kevin Deere and Dr Erik Lenguerrand for your help with statistics and for kindly sharing your Stata code with me, Dr Denis Baird for being an R geek and for helping with genetic analyses, Dr Ben Faber for stimulating discussions, Sofia Mouchti for lunchtime walks and April Hartley, my running buddy, for providing much needed distraction throughout this journey; for our training runs, parkruns and memorable races. I am also very grateful to other members of Bristol Medical School, particularly Beverly Evanson and Sharen O'Keefe for all of your admin support and to the staff and students in the Southmead and Clifton offices, whom I have had the pleasure of working with, for making it enjoyable and stimulating place to work over the course of my studentship.

I am extremely grateful to ALSPAC participants, without whom this research would not be possible, also to the midwives for their help in recruiting them, and the whole ALSPAC team, which includes interviewers, computer and laboratory technicians, clerical workers, research scientists, volunteers, managers, receptionists, and nurses.

Last, but by no means least, I am profoundly grateful to my family: my parents and sisters for your unconditional support even when thousand miles away. Thank you!

Author's declaration

I declare that the work in this dissertation was carried out in accordance with the requirements of the University's *Regulations and Code of Practice for Research Degree Programmes* and that it has not been submitted for any other academic award. Except where indicated by specific reference in the text, the work is the candidate's own work. Work done in collaboration with, or with the assistance of, others, is indicated as such. Any views expressed in the dissertation are those of the author.

SIGNED: DATE:.....

Research outputs arising from this thesis

Submitted publications

1. **Frysz, M.**, Howe, L.D., Tobias, J.H., Paternoster, L., *Using SITAR (SuperImposition by Translation and Rotation) to estimate age at peak height velocity in Avon Longitudinal Study of Parents and Children*. Wellcome Open Research, 2018. **3** [available online, under review]

Planned publications

1. Data note describing generation of Statistical Shape Modelling data in ALSPAC offspring.
2. Gender differences in proximal femur shape: findings from a population-based study in adolescents.
3. The effect of pubertal timing on proximal femur shape.
4. Bone mineral density is related to proximal femur shape.
5. Investigating the influence of adult hip shape genetic variants across the life course: findings from a population-based study in adolescents.

Oral presentations

1. The effect of age and puberty on proximal femur shape. Osteoarthritis Research International (OARSI), Las Vegas, NV, USA: 27- 30 April 2017
2. Investigating the influence of adult hip shape genetic variants across the life course: findings from a population-based study in adolescents. American Society for Bone and Mineral Research (ASBMR), Montreal, Canada: 28 September – 1 October 2018 [**plenary oral**]

Poster presentations

1. Gender differences in proximal femur shape: findings from a population-based study in adolescents. ASBMR, Atlanta, GA, USA: 16- 19 September 2016 [**plenary poster**]

2. Investigation of relationships between hip bone mineral density and hip shape in adolescent and adult females. OARSI, Las Vegas, NV, USA: 27- 30 April 2017
3. Bone mineral density is related to proximal femur shape: findings from a cross-sectional study in middle aged women. ASBMR, Denver, Colorado, USA: 8 -11 September 2017 **[plenary poster]**
4. Age at peak height velocity is related to proximal femur shape in adolescents. OARSI, Liverpool, UK: 26-29 April 2018

Data generated as a result of this thesis

Data generated as a result of this thesis has been returned to ALSPAC and is now available to access by other researchers via the Research Proposal System (which can be accessed via the following link <https://proposals.epi.bristol.ac.uk/>).

1. Pubertal growth data (age at peak height velocity, size, tempo, velocity and peak velocity) as described in the above-mentioned publication.
2. Hip shape as quantified using Statistical Shape Modelling at age 14 and 18 in ALSPAC offspring.

Statement of contribution

Jenny Gregory and collaborators at the University of Aberdeen developed Shape software which was used to generate the outcome data (hip shape) used throughout this thesis. Jenny uploaded all images in Shape (which I then aligned) and provided help and advice with all queries regarding Shape. She assisted with building and generating the reference template for adult hip shape which was subsequently applied to ALSPAC adolescent and mothers' data used in this thesis. I used this template to generate hip shape mode scores for adolescent and mothers' data and carried out all statistical analyses. Jenny Gregory also provided valuable comments on Chapter 2 of this thesis.

Olly Butters, ALSPAC data manager, located hip DXA scans collected as part of ALSPAC research clinics and assisted with secure transfer of these images to collaborators in Aberdeen. Prior to transfer, all images were processed by Denis Baird. All adolescent hip DXA images were aligned in Shape by myself, whereas ALSPAC mothers' images, which generated data used as outcomes in Chapter 6, were aligned by Denis Baird and Ben Faber.

Kevin Deere, Adrian Sayers, Erik Lenguerrand and Hannah Sallis provided statistical advice and helped with Stata queries. Laura Howe provided guidance on generating puberty measures based on height data in ALSPAC offspring used in Chapter 4. Ruth Mitchell provided me with code to extract SNP data from ALSPAC and generate genetic risk score used to run analyses in Chapter 5. In my MR analysis in Chapter 6, I used summary statistics from GWAS of hip shape in ALSPAC mothers previously performed by Denis Baird. Scripts written by Lavinia Paternoster were adapted and used to perform GWAS described in Chapter 7.

Contents

Abstract	iii
Acknowledgements.....	v
Author’s declaration	vii
Research outputs arising from this thesis.....	ix
Statement of contribution	xiii
Contents	xv
List of tables	xxiii
List of figures	xxvii
List of abbreviations	xxxii
Chapter 1. Introduction and aims of this PhD	1
1.1. Structure and function of bone.....	2
1.2. Bone development.....	3
1.3. Bone maintenance	6
1.4. Joints	7
1.4.1. Types of joints	7
1.4.2. Joint tissues	8
1.5. Development and anatomy of the hip joint.....	11
1.5.1. Development of the hip joint.....	11
1.5.2. Anatomy of the hip joint	12
1.6. Osteoarthritis	13
1.6.1. Definition of OA.....	13
1.6.2. Classification of OA	15
1.6.3. Burden of OA.....	16
1.6.4. OA diagnosis.....	16

1.6.5. OA pathogenesis.....	17
1.6.6. OA epidemiology	19
1.6.6.1. Prevalence and incidence.....	19
1.6.6.2. OA risk factors	20
1.6.7. Hip morphology and OA.....	23
1.6.7.1. Acetabular dysplasia.....	24
1.6.7.2. Femoroacetabular impingement	25
1.6.8. Genetics of OA.....	26
1.6.8.1. Heritability.....	26
1.6.8.2. Candidate gene studies, linkage studies, GWAS studies.....	27
1.6.8.3. OA-associated endophenotypes and genetics of hip shape	28
1.6.9. OA management	29
1.7. Osteoporosis.....	31
1.7.1. Definition and burden of OP	31
1.7.2. OP diagnosis	32
1.7.3. OP pathogenesis.....	32
1.7.4. OP epidemiology	33
1.7.4.1. Risk factors	33
1.7.5. Genetics of OP	34
1.7.6. OP management.....	35
1.8. Relationship between osteoporosis and osteoarthritis.....	36
1.9. Statistical Shape Model (SSM).....	37
1.10. Hypotheses and aims to be addressed in thesis	38
1.10.1. Knowledge gaps to be addressed in this thesis	39
1.10.2. Summary and aims of this PhD	40

Chapter 2. Methods	43
2.1. Cohort description	44
2.1.1. ALSPAC cohort.....	44
2.1.2. Ethical approval.....	44
2.2. Data	45
2.2.1. Outcome – hip shape	45
2.2.1.1. ALSPAC offspring.....	45
2.2.1.2. ALSPAC mothers’	46
2.2.2. Exposure and covariate data.....	48
2.2.2.1. ALSPAC offspring.....	48
2.2.2.2. ALSPAC mothers.....	50
2.2.3. Genotyping and imputation	51
2.3. Defining and quantifying proximal femur shape	52
2.3.1. Statistical Shape Modelling.....	52
2.3.2. Definition of shape.....	53
2.3.3. Analytical steps involved in Statistical Shape Modelling	53
2.4. Building the Statistical Shape Model in ALSPAC children	57
2.4.1. Model checking (effect of hip abduction and adduction on hip shape mode scores)	57
2.4.2. Repeatability and reproducibility of point placement.....	63
2.4.3. SSMs in ALSPAC offspring	67
2.5. Applying external reference SSM to adolescent HSMs	72
2.5.1. Building and applying scores from adult reference Statistical Shape Model .	72
2.5.2. Comparing adolescent HSM scores with HSM scores based on adult reference SSM.....	73
2.5.3. Checking independence of standardized HSMs.....	82

2.6. Statistical methods	85
2.6.1. Data checking and descriptive statistics	85
2.6.2. Regression analysis.....	85
2.6.3. Testing for interaction.....	89
2.6.4. P value threshold.....	89
2.6.5. Mendelian randomization (MR) analysis	89
2.6.6. Composite hip shape figures.....	91
Chapter 3. Age and sex differences in hip shape.....	93
3.1. Introduction and chapter aims.....	93
3.2. Methods	94
3.2.1. Subjects	94
3.2.2. Measures.....	94
3.2.2.1. Outcome.....	94
3.2.2.2. Exposure and covariate data.....	94
3.2.3. Statistical analysis.....	94
3.3. Results	95
3.3.1. Participant characteristics.....	95
3.3.2. Differences in hip shape between age 14 and 18.....	97
3.3.3. Univariate associations between confounders and hip shape	100
3.3.4. Sex differences in hip shape.....	100
3.4. Discussion	107
Chapter 4. Influence of pubertal growth on hip shape.....	110
4.1. Introduction and chapter aims.....	110
4.2. Methods	111
4.2.1. Subjects	111
4.2.2. Measures.....	112

4.2.2.1. Outcome.....	112
4.2.2.2. Exposures	112
4.2.2.3. Confounding variables	115
4.2.3. Statistical analysis	115
4.3. Results	116
4.3.1. Assessment of puberty.....	116
4.3.2. Study participant characteristics.....	116
4.3.3. Relationship between tempo and hip shape	122
4.3.3.1. Age 14.....	122
4.3.3.2. Age 18.....	137
4.4. Discussion.....	143
Chapter 5. Investigating the relationship between BMD and hip shape in ALSPAC offspring.....	149
5.1. Introduction and chapter aims	149
5.2. Methods	151
5.2.1. Subjects	151
5.2.2. Measures.....	151
5.2.2.1. Outcome.....	151
5.2.2.2. Exposure and covariate data.....	152
5.2.2.3. Genotyping.....	152
5.2.3. Statistical analysis	152
5.2.3.1. Observational associations	152
5.2.3.2. Mendelian randomization.....	153
5.3. Results	153
5.3.1. Participant characteristics.....	153
5.3.2. Observational associations	156

5.3.2.1. Age 14.....	156
5.3.2.2. Age 18.....	161
5.3.3. Can sex differences in hip shape be explained by differences in BMD.....	165
5.3.4. Mendelian randomization	168
5.3.4.1. Association between BMD GRS and hip BMD.....	168
5.3.4.2. Association between BMD GRS and confounders	168
5.3.4.3. Mendelian randomization results	168
5.4. Discussion	172
Chapter 6. Investigating the relationship between BMD and hip shape in middle-aged women.....	178
6.1. Introduction chapter aims.....	178
6.2. Methods	179
6.2.1. Study population	179
6.2.1.1. Outcome.....	179
6.2.1.2. Exposure and covariate data.....	179
6.2.1.3. Genotyping.....	179
6.2.2. Statistical analysis.....	180
6.2.2.1. Cross-sectional analysis.....	180
6.2.2.2. Mendelian randomization	180
6.3. Results	181
6.3.1. Sample characteristics.....	181
6.3.2. Cross-sectional associations.....	185
6.3.2.1. Confounder- exposure and confounder- outcome associations	185
6.3.2.2. Total hip BMD and FN BMD associations.....	185
6.3.2.3. Adolescent vs. adult results	188
6.3.3. Two-sample Mendelian randomization	189

6.4. Discussion.....	192
Chapter 7. Genetic variants associated with hip shape in adolescents	197
7.1. Introduction and chapter aims	197
7.2. Methods	198
7.2.1. Study population	198
7.2.2. Data	198
7.2.2.1. Genome- wide genetic data.....	198
7.2.2.2. Outcome and covariate data	198
7.2.3. Analysis.....	199
7.2.3.1. GWAS analysis.....	199
7.2.3.2. Replication	199
7.2.3.3. The effect of adult hip shape variants on adolescent hip shape	200
7.2.3.4. Look-up of known OA variants in adolescent hip shape	200
7.2.3.5. Genetic correlation between hip shape and other phenotypes	202
7.3. Results	203
7.3.1. Participant characteristics.....	203
7.3.2. GWAS at age 14, 18 and replication in adult cohort.....	203
7.3.3. The effect of adult hip shape variants on adolescent hip shape	213
7.3.4. Look-up of known OA variants in adolescent hip shape.....	215
7.3.5. Genetic correlation between hip shape and other phenotypes.....	221
7.4. Discussion.....	234
Chapter 8. Discussion.....	240
8.1. Aims of this PhD	240
8.2. Key findings of this research	241
8.2.1. Variation in hip shape in relation to sex and pubertal timing	241
8.2.2. Relationship between BMD and hip shape.....	242

8.2.3. Genetic influences on adolescent hip shape.....	243
8.3. Contribution of this research	245
8.4. Strengths and limitations	247
8.5. Future research	252
8.6. Conclusions.....	255
Chapter 9. References	256
Chapter 10. Appendices.....	276
10.1. Appendix 1.....	276
10.2. Appendix 2.....	282
10.3. Appendix 3.....	286
10.4. Appendix 4.....	295
10.5. Appendix 5.....	303
10.5.2. Power in MR analysis.....	311
10.6. Appendix 6.....	314

List of tables

Table 2.1; ALSPAC offspring hip shape data at age 14.....	47
Table 2.2; ALSPAC offspring hip shape data at age 18.....	47
Table 2.3; ALSPAC mothers’ hip shape data	48
Table 2.4; Number of puberty questionnaires sent to ALSPAC participants and number of questionnaires returned	50
Table 2.5; Description of the key landmark points shown in red in Figure 2.2	56
Table 2.6; Number of hips with positioning errors.....	61
Table 2.7; Percentage of hip shape variation at age 18 (TF 4) explained by the top 10 HSMs in SSMs based on all images vs. SSM which excluded hips with positioning errors	61
Table 2.8; Cross-correlations between the top ten HSMs based on SSM built on all images vs. SSM built after excluding images with positioning errors	62
Table 2.9; Cohorts contributing to the adult reference Statistical Shape Model.....	72
Table 2.10; Mean HSM scores for the top ten HSMs based on ALSPAC adolescent and mothers’ images, after applying adult reference model (compared with mean=0 and SD=1 when data from each time point included as its own reference)	76
Table 2.11; Percentage of variance explained by the first ten HSMs by different SSMs .	76
Table 2.12; Correlations between first ten HSMs at age 14 vs. the adult reference model	77
Table 2.13; Correlations between top ten HSMs at age 18 vs. the adult reference model	78
Table 2.14; Summary of the key morphological features described by the top ten HSMs based on combined adult reference model.....	81
Table 2.15; Correlation matrix for the top ten standardized HSM scores at age 14 to assess the number of independent variables using matrix Spectral Decomposition (matSpD)	83
Table 2.16; Correlation matrix for the top ten standardized HSM scores at age 18 to assess the number of independent variables using matrix Spectral Decomposition (matSpD)	84

Table 2.17; A comparison of characteristics between adolescents who did and did not participate in the TF 2 assessment clinic.....	87
Table 2.18; A comparison of characteristics between adolescents who did and did not participate in the TF 4 assessment clinic.....	87
Table 3.1; Characteristics of participants who attended TF 2 and TF 4 assessment clinics	96
Table 3.2; Differences in mean HSM scores, between age 14 and 18, for the top ten HSMs based on adolescent images, after applying the combined adult reference model (N= 3,188).....	98
Table 3.3; Differences in mean HSM scores between age 14 and age 18 after applying the combined adult reference model, stratified by sex.....	99
Table 3.4; Differences in hip shape mode scores between males and females (age 14)	103
Table 3.5; Differences in hip shape mode scores between males and females (age 18)	104
Table 4.1; Descriptive statistics of ALSPAC study participants	118
Table 4.2; Mean aPHV and years since aPHV by quintiles of tempo stratified by gender, in children who attended TF 2 clinic (mean age at attendance 13.8 years).....	119
Table 4.3; Mean aPHV and years since aPHV by quintiles of tempo stratified by gender, in children who attended TF 4 clinic (mean age at attendance 17.7 years).....	119
Table 4.4; Age distribution by pubertal status for 3,003 individuals with complete outcome, Tanner stage and covariate data at age 14.....	120
Table 4.5; Number of individuals in each Tanner stage category (assessed at a mean age of 13.2 years) per quintile of tempo	121
Table 4.6; Associations between tempo and the top ten HSMs in ALSPAC adolescents at age 14 (N=3,827)	125
Table 4.7; Associations between tempo and the top ten HSMs in ALSPAC males at age 14 (N=1,797).....	126
Table 4.8; Associations between tempo and the top ten HSMs in ALSPAC females at age 14 (N=2,030).....	127

Table 4.9; Test for linear trend between Tanner stages and the top ten HSMs in ALSPAC adolescents at age 14 (N=3,003).....	134
Table 4.10; Test for linear trend between Tanner stages and the top ten HSMs in ALSPAC males at age 14 (N=1,364)	135
Table 4.11; Test for linear trend between Tanner stages and the top ten HSMs in ALSPAC females at age 14 (N=1,639)	136
Table 4.12; Associations between tempo (continuous measure) and the top ten HSMs in ALSPAC adolescents at age 18 (N=3,507)	139
Table 4.13; Associations between tempo (continuous measure) and the top ten hip shape modes in ALSPAC males (N=1,597)	140
Table 4.14; Association between tempo and the top ten HSMs in ALSPAC females at age 18 (N=1,910).....	141
Table 5.1; Characteristics of participants who attended TF 2 and TF 4 assessment clinics	155
Table 5.2; Differences in hip shape mode scores between males and females (age 14).....	166
Table 5.3; Differences in hip shape mode scores between males and females (age 18).....	167
Table 5.4; Associations between genetic risk score and total hip and FN BMD at age 14 and 18.....	170
Table 5.5; Associations between genetic risk score and confounders at age 14 and 18	170
Table 6.1; Baseline characteristics in women who attended the research clinic, and had data available for exposure, outcome and main confounder variables, and women initially recruited but did not attend the first follow up clinic assessment of mothers .	183
Table 6.2; Characteristics of participating ALSPAC cohort study adult women (N=4,289)	184
Table 6.3; Summary statistics for the top ten HSMs in ALSPAC mothers (N= 4,289) based on the adult reference SSM template.....	184

Table 7.1; List of SNPs associated with hip OA available from previously published literature.....	201
Table 7.2; Genome-wide significant hits for hip shape at age 14 in ALSPAC adolescents and a look-up of these loci in adolescent and adult GWAS	205
Table 7.3; Genome-wide significant hits for hip shape at age 18 in ALSPAC adolescents and a look-up of these loci in adolescent and adult GWAS	205
Table 7.4; Look-up of rs8079830 associated with HSM1 at age 14 in MR Base PheWAS showing traits associated with this SNP reaching suggestive genome-wide significance level ($P < 5 \times 10^{-5}$)	211
Table 7.5; Look-up of rs8111495, associated with HSM5 at age 18, in MR Base PheWAS showing traits associated with this SNP reaching suggestive ($P < 5 \times 10^{-5}$) and genome-wide significance level ($P < 5 \times 10^{-8}$)	211
Table 7.6; Look-up of rs1111767 associated with HSM6 at age 18 in MR Base PheWAS showing traits associated with this SNP reaching suggestive genome-wide significance level ($P < 5 \times 10^{-5}$)	212
Table 7.7; Hip shape meta-analysis results (adjusted for age and gender) and look-up in ALSPAC adolescent GWAS (adjusted for age and gender)	214

List of figures

Figure 1.1 Compact and spongy bone.....	2
Figure 1.2 Steps involved in endochondral ossification.	6
Figure 1.3 Schematic diagram and histological section of articular cartilage zones.	10
Figure 1.4 Anatomy of hip joint.	13
Figure 1.5 Schematic diagram showing pincer and cam femoroacetabular impingement.	26
Figure 1.6 Overview of PhD content indicating relationships to be explored during this PhD.....	42
Figure 2.1 Outline of proximal femur shape and point positions.....	54
Figure 2.2 Key landmark points.....	55
Figure 2.3 Example of hip abduction on DXA images. Left hand side represents lower degree of abduction. Right hand side represents higher degree of abduction.....	58
Figure 2.4 Example of hip adduction on DXA image. Left hand side represents lower degree of adduction. Right hand side represents higher degree of adduction.....	59
Figure 2.5 Example of correctly positioned hip	59
Figure 2.6 Intra-observer repeatability assessed by mean point-to-point repeatability showing mean and median differences in pixels for each point and right-hand figure showing points with the highest intra-observer repeatability error values.....	65
Figure 2.7 Inter-observer repeatability assessed by mean point-to-point repeatability showing mean and median differences in pixels for each point and right-hand figure showing points with the highest intra-observer repeatability error values (>2 pixels) ...	66
Figure 2.8 Variation in hip shape described by modes 1 - 5 at age 14 (SSM based on age 14 images)	68
Figure 2.9 Variation in hip shape described by modes 6 -10 at age 14 (SSM based on age 14 images).....	69
Figure 2.10 Variation in hip shape described by modes 1 - 5 at age 18 (SSM based on age 18 images).....	70

Figure 2.11 Variation in hip shape described by modes 6 - 10 at age 18 (SSM based on age 18 images).....	71
Figure 2.12 Variation in hip shape at ages 14 and 18 described by modes 1 - 5, based on adult reference SSM	79
Figure 2.13 Variation in hip shape at ages 14 and 18 described by modes 6 -10, based on adult reference SSM	80
Figure 2.14 Flow chart of participants included in the ALSPAC study and number of participants included in each analysis chapter	88
Figure 2.15 Directed acyclic graph illustrating Mendelian randomization and its underlying assumptions.	90
Figure 2.16 Example hip shape features referred to throughout this thesis.....	92
Figure 3.1 Sex differences in hip shape at age 14 based on the difference in mean HSM scores. Sex beta coefficients (for all modes with $p < 0.005$) magnified 4-fold were modelled in Shape to represent the average overall hip shape between males and females.	105
Figure 3.2 Sex differences in hip shape at age 18 based on the difference in mean HSM scores. Sex beta coefficients (for all modes with $p < 0.005$) magnified 4-fold were modelled in Shape to represent the average overall hip shape between males and females.	106
Figure 4.1 Illustration of the SITAR model for height in puberty.....	113
Figure 4.2 The overall difference in hip shape at age 14 between early vs. late matures (changes in hip shape associated with unit change in tempo) based on adjusted beta coefficients.	128
Figure 4.3 Unadjusted mean (and 95% CIs) HSM1 and HSM2 scores per quintile of tempo in males and females.....	129
Figure 4.4 Unadjusted mean (and 95% CIs) HSM3 and HSM4 scores per quintile of tempo in males and females.	130
Figure 4.5 Unadjusted mean (and 95% CIs) HSM5 and HSM6 scores per quintile of tempo in males and females.....	131

Figure 4.6 Unadjusted mean (and 95% CIs) HSM7 and HSM8 scores per quintile of tempo in males and females.	132
Figure 4.7 Unadjusted mean (and 95% CIs) HSM9 and HSM10 scores per quintile of tempo in males and females.	133
Figure 4.8 The overall difference in hip shape at age 18 between early vs. late matures (changes in hip shape associated with unit change in tempo) based on adjusted beta coefficients.	142
Figure 5.1 Schematic diagram representing relationship to be explored in this chapter (dashed blue line) and known pathways relevant to this analysis (solid black lines).. ..	151
Figure 5.2 Linear regression coefficients with 95% CIs for the association between total hip BMD and the top ten HSMs in ALSPAC adolescents at age 14 (N=4,428).	158
Figure 5.3 Linear regression coefficients with 95% CIs for the association between total hip BMD and the top ten HSMs in ALSPAC adolescents at age 14, stratified by gender.	159
Figure 5.4 Composite hip shape changes associated with higher hip BMD at age 14 based on fully adjusted coefficients (model 2) multiplied by a factor of 10.	160
Figure 5.5 Linear regression coefficients with 95% CIs for the association between total hip BMD and the top ten HSMs in ALSPAC adolescents at age 18 (N= 4,369).	162
Figure 5.6 Linear regression coefficients with 95% CIs for the association between total hip BMD and the top ten HSMs in ALSPAC adolescents at age 18, stratified by gender..	163
Figure 5.7 Composite hip shape changes associated with higher hip BMD at age 18 based on fully adjusted coefficients (model 2) multiplied by a factor of 10. Dotted line (mean hip shape), solid line (overall change in hip shape per 10 x SD increase in BMD).	164
Figure 5.8 Fully adjusted observational (dashed grey line) and MR (solid navy line) estimates and 95% CIs for the association between BMD and hip shape in ALSPAC adolescents at age 14.	171
Figure 5.9 Fully adjusted observational (dashed grey line) and MR (solid navy line) estimates and 95% CIs for the association between BMD and hip shape in ALSPAC adolescents at age 18.	171

Figure 6.1 Linear regression coefficients (black and dashed grey lines) with 95% CIs for the association between total hip BMD and the top ten HSMs.	186
Figure 6.2 Hip shape changes observed per SD increase in total hip BMD based on fully adjusted coefficients (model 2) (to aid visualisation each coefficient was multiplied by a factor of 10).....	187
Figure 6.3 Linear regression coefficients with 95% CIs for the association between total hip BMD and the top ten HSMs in adolescent females at age 14 (yellow line) and 18 (blue line) years and adult women (red line).	188
Figure 6.4 Linear regression (dashed grey lines) and Mendelian randomization (using inverse variance weighted method) estimates (solid navy line) between BMD and the top ten HSMs.....	190
Figure 6.5 One-sample (TSLs) and two-sample (IVW) MR estimates for the association between BMD and hip shape in ALSPAC adolescents at age 14 (yellow line) and 18 (blue line) and ALSPAC mothers (red line).	191
Figure 7.1 Regional association plot for rs8079830 locus associated with HSM1 at age 14.....	206
Figure 7.2 Regional association plot for rs10857102 (in high LD >0.8 with rs1827922) locus associated with HSM3 at age 14.....	207
Figure 7.3 Regional association plot for rs7969867 (in high LD >0.8 with rs10748285) locus associated with HSM1 at age 18.	208
Figure 7.4 Regional association plot for rs8111495 locus associated with HSM5 at age 18.....	209
Figure 7.5 Regional association plot for rs7025847 (in high LD >0.8 with rs1111767) locus associated with HSM6 at age 18.	210
Figure 7.6 A look-up of published hip OA variants in ALSPAC HSM1 and HSM2 GWASes at age 14 (in black) and age 18 (in blue).....	216
Figure 7.7 A look-up of published hip OA variants in ALSPAC HSM3 and HSM4 GWASes at age 14 (in black) and age 18 (in blue).....	217

Figure 7.8 A look-up of published hip OA variants in ALSPAC HSM5 and HSM6 GWASes at age 14 (in black) and age 18 (in blue).	218
Figure 7.9 A look-up of published hip OA variants in ALSPAC HSM7 and HSM8 GWASes at age 14 (in black) and age 18 (in blue).	219
Figure 7.10 A look-up of published hip OA variants in ALSPAC HSM9 and HSM10 GWASes at age 14 (in black) and age 18 (in blue).	220
Figure 7.11 Volcano plot for genetic correlation results between HSM1 at age 14 and a range of traits.....	223
Figure 7.12 Volcano plot for genetic correlation results between HSM2 at age 14 and a range of traits.....	224
Figure 7.13 Volcano plot for genetic correlation results between HSM5 at age 14 and a range of traits.....	225
Figure 7.14 Volcano plot for genetic correlation results between HSM8 at age 14 and a range of traits.....	226
Figure 7.15 Volcano plot for genetic correlation results between HSM9 at age 14 and a range of traits.....	227
Figure 7.16 Volcano plot for genetic correlation results between HSM1 at age 18 and a range of traits.....	228
Figure 7.17 Volcano plot for genetic correlation results between HSM2 at age 18 and a range of traits.....	229
Figure 7.18 Volcano plot for genetic correlation results between HSM3 at age 18 and a range of traits.....	230
Figure 7.19 Volcano plot for genetic correlation results between HSM5 at age 18 and a range of traits.....	231
Figure 7.20 Volcano plot for genetic correlation results between HSM7 at age 18 and a range of traits.....	232
Figure 7.21 Volcano plot for genetic correlation results between HSM8 at age 18 and a range of traits.....	233

List of abbreviations

Abbreviation	In full
2SLS	Two-stage least squares
AD	Acetabular dysplasia
ADAMTS	A disintegrin and metalloproteinase with thrombospondin-like motifs
ALSPAC	Avon Longitudinal Study of Parents and Children
aPHV	Age at peak height velocity
BMD	Bone mineral density
BMI	Body mass index
BML	Bone marrow lesion
BMP	Bone morphogenetic protein
BRU	Bone remodelling unit
CEA	Centre edge angle
CI	Confidence interval
DDH	Developmental dysplasia of the hip
DXA	Dual-energy X-ray absorptiometry
ECM	Extracellular matrix
EO	Endochondral ossification
FAI	Femoroacetabular impingement
FGF	Fibroblast growth factor
FMI	Fat mass index
FN	Femoral neck
FNW	Femoral neck width
FoM	Focus on Mothers clinic
FRAX	Fracture risk assessment tool
GIANT	Genetic Investigation of Anthropometric Traits
GWAS	Genome-wide association study
HSA	Hip Structural Analysis
HAL	Hip axis length
HBM	High Bone Mass
HSM	Hip Shape Mode
HWE	Hardy-Weinberg equilibrium
IBD	Identical by Descent
Ihh	Indian hedgehog
IL	Interleukin
IV	Instrumental variable
IVW	Inverse-variance-weighted
JSN	Joint space narrowing
KL	Kellgren and Lawrence

LCPD	Legg–Calvé–Perthes' disease
LD	Linkage disequilibrium
LS	Lumbar spine
MAF	Minor allele frequency
MEF2C	Myocyte enhancer factor-2
MMP	Matrix metalloproteinase
MR	Mendelian randomization
MrOS	Osteoporotic fractures in men study
MSC	Mesenchymal stem cell
NJR	National Joint Registry for England, Wales, Northern Ireland and the Isle of Man
NSA	Neck-shaft angle
NSAIDs	Non-steroidal anti-inflammatory drugs
NSHD	National Survey of Health and Development
OA	Osteoarthritis
OARSI	Osteoarthritis Research Society International
OI	Osteoarthritis Initiative
OP	Osteoporosis
PA	Physical activity
PCA	Principal Component Analysis
PTHrP	Parathyroid hormone-related peptide
RANKL	Receptor activator of nuclear factor kappa B ligand
RHOA	Radiographic hip osteoarthritis
RKOA	Radiographic knee osteoarthritis
SCFE	Slipped capital femoral epiphysis
SD	Standard deviation
SE	Standard error
SITAR	SuperImposition by Translation and Rotation
SNP	Single nucleotide polymorphism
SOF	Study for Osteoporotic Fractures
SSGAC	Social Science Genetic Association Consortium
SSM	Statistical Shape Model
TB	Total body
TF	Teen Focus clinic
TGF β	Transforming growth factor β
THR	Total hip replacement
TNF	Tumour necrosis factor
TRAP	Tartrate-resistant acid phosphatase

CHAPTER 1. INTRODUCTION AND AIMS OF THIS PhD

In this introductory chapter I will describe the structure and function of bone, and the process of bone development and maintenance (sections 1.1 -1.3). I will give an overview of joints and joint tissues and describe the anatomy of hip joint (sections 1.4 and 1.5). Sections 1.6 and 1.7 will consider osteoarthritis and osteoporosis, including their definitions, epidemiology and pathogenesis, followed by current evidence concerning the relationship between bone mineral density and osteoarthritis. Section 1.9 will describe the application of statistical shape modelling in studies. Finally, section 1.10 will outline the aims to be addressed in this thesis.

1.1. Structure and function of bone

The human skeleton comprises about 20% of total body weight (White, 2005) and can be divided into the axial skeleton (vertebrae, ribs, sternum and skull) and appendicular skeleton (limbs and pelvis) (Drake et al., 2015). The skeletal system consists of cartilage and bone. Bone, which forms the majority of the skeleton, is a specialised type of living connective tissue with mineralized extracellular matrix (ECM). Bone serves a number of important functions such as protection and support of organs and soft tissues, and acts as an anchor for muscles, tendons and ligaments thus facilitating movement. In addition, bone stores fat and minerals and is the primary site of haematopoiesis (White, 2005).

Bone consists of an organic phase (mainly type I collagen) and inorganic phase (hydroxyapatite - insoluble salt of calcium and phosphorus). Morphologically, it can be divided into compact bone (cortical) and trabecular bone (cancellous, spongy) (Figure 1.1). The latter consists of a network of interconnecting rods and plates (trabeculae) separated by spaces filled with bone marrow. Cortical bone, which surrounds trabecular bone, is much denser in structure and consists of closely packed osteons. Each osteon comprises Haversian canal which is surrounded by lamellae (sheets) of bone (White, 2005).

Image removed due to copyright reasons.

Figure 1.1 Compact and spongy bone.

Reproduced from image publicly available at

<https://training.seer.cancer.gov/anatomy/skeletal/tissue.html>

Bone is able to repair itself and it contains a number of distinct cell types which are responsible for its formation and maintenance. The inner (endosteum) and outer (periosteum) layers of bone contain bone lining cells, which are quiescent flat-shaped osteoblasts (Florencio-Silva et al., 2015). These cells are derived from mesenchymal stem cells (MSCs) and are mainly responsible for bone formation (Capulli et al., 2014). Osteoblasts lay down the osteoid, primarily made of collagen type I, which then becomes mineralized to form a new bone (Florencio-Silva et al., 2015). Once new bone has been formed, osteoblasts can differentiate into lining cells, surround themselves with matrix and develop into osteocytes or undergo apoptosis (Florencio-Silva et al., 2015; Marks Jr & Popoff, 1988). Osteocytes are mature osteoblasts trapped within the bone matrix comprising 90-95% of total bone cells (Florencio-Silva et al., 2015). They connect with nearby cells via branching cytoplasmic projections which extend through canaliculi and travel throughout the mineralized bone matrix. Osteocytes act as mechanosensors, responding to stress and stimuli and regulating osteoclast and osteoblast activity accordingly (Bonewald, 2011; Florencio-Silva et al., 2015; Marks Jr & Popoff, 1988). Osteoclasts are large, multinucleated cells involved in bone resorption (breaking down and removal of bone) which are derived from hematopoietic stem cells (Charles & Aliprantis, 2014). Osteoclasts reside on bone surfaces and in order to degrade bone matrix, they lower the pH at bone resorption sites and then secrete cathepsin, matrix metalloproteinase 9 (MMP9), and tartrate-resistant acid phosphatase (TRAP) (Buckwalter et al., 1996; Florencio-Silva et al., 2015).

1.2. Bone development

The process of bone formation is initiated when embryonic MSCs migrate to the sites of future bones where they form condensations of cells outlining the size and shape of future bones. Within these condensations, MSCs differentiate to either chondrocytes which form cartilage scaffolds which are eventually replaced by mineralized bone (in a process of endochondral ossification (EO)) or differentiate into osteoblasts (to form bone via intramembranous ossification) (Berendsen & Olsen, 2015).

Intramembranous ossification

Flat bones (such as skull, mandible or clavicles) are formed via intramembranous ossification. During this process MSCs condensate and proliferate to form dense ossification centres and become either capillaries or osteoprogenitor cells which differentiate further into pre-osteoblasts and subsequently into osteoblasts (Ornitz & Marie, 2002). Osteoblasts secrete osteoid, which consists of collagen-proteoglycan matrix and binds calcium salts enabling the matrix to become calcified to form woven bone trabeculae. Following mineralization, osteoblasts either become trapped in the ECM and transform into osteocytes or undergo apoptosis. Surrounding osteogenic cells differentiate into new osteoblasts which lay more osteoid resulting in the formation of trabeculae matrix and periosteum (Betts et al., 2013; Gilbert, 2000). Cells in the periosteum contribute towards appositional growth and form dense bone around the trabecular bone (pre-cortical bone) which eventually becomes replaced with cortical bone (Rauch, 2005; Roberts et al., 2015).

Endochondral ossification

During embryological development, all long bones develop via EO (see Figure 1.2 for schematic representation of EO). This process involves the initial development of a cartilage template which serves as a scaffold to be later replaced with bone (in a process called ossification). This template is formed by mesenchymal progenitor cells which then differentiate into chondrocytes. Chondrocytes proliferate, undergo hypertrophy and secrete ECM which then becomes mineralized, forming the primary centre of ossification (the metaphysis). Hypertrophic chondrocytes attract blood vessels, bringing osteoclasts, bone forming cells (precursors of osteoclasts) and bone marrow cells. As hypertrophic chondrocytes die, the remaining cartilage matrix is removed by osteoclasts and used as a scaffold for osteoblasts to lay new bone (Firestein et al., 2016; Kronenberg, 2003; Mackie et al., 2008).

Chondrocyte proliferation drives bone elongation and as bone enlarges further secondary centres of ossification are formed at one or both ends of the bone. Primary and secondary centres of ossification are divided by the growth plate (also known as the

epiphyseal plate). EO is responsible for longitudinal bone growth and is most active during growth, resulting in greater height (Berendsen & Olsen, 2015; Mackie et al., 2008), however this process ceases following the closure of the growth plate (i.e. fusion of metaphysis and epiphysis) around the time of puberty (Shim, 2015). Interestingly, processes involved in osteoarthritis (OA) pathogenesis are thought to resemble that of EO (Dreier, 2010; Rosen, 2013).

EO is tightly regulated and is influenced by a number of locally derived factors (such as bone morphogenetic proteins (BMPs), fibroblast growth factors (FGFs), transforming growth factor β (TGF β), Wnts, Indian hedgehog (Ihh), parathyroid hormone-related peptide (PTHrP) and retinoids) and systemic factors (such as growth hormone and thyroid hormone) (Dreier, 2010). Transcription factors (Runx2, Sox9), myocyte enhancer factor-2 (MEF2C) and proteases also play an important role in EO (Dreier, 2010; Mackie et al., 2008).

While longitudinal bone growth stops around puberty, bones continue to grow in width by periosteal expansion whereby new bone forms on already existing bone (Boskey & Coleman, 2010).

Image removed due to copyright reasons.

Figure 1.2 Steps involved in endochondral ossification. Image publicly available at www.orthobullets.com

1.3. Bone maintenance

EO and intramembranous ossification yield immature bone which undergoes further resorption and formation in order to maintain its structure and shape (and thus withstand the loads placed upon it) during the process of bone modelling and remodelling. Bone modelling begins in foetal life and continues into adulthood. During this process bone is resorbed and formed at distinct locations which results in large increases in size and changes in shape of bone (WHO, 2003). While most active during periods of active growth, bone modelling has also been shown to occur in adult life by contributing to periosteal bone formation which enables bones to enlarge circumferentially (Betts et al., 2013). Bone modelling occurs in response to physical activity (PA) as demonstrated in tennis players by higher bone mass in the arm used to play (Kontulainen et al., 2003). Other factors likely to play a role in bone modelling include genetic, environmental and hormonal factors (Langdahl et al., 2016).

The adult skeleton is thought to be renewed every 10 years (Langdahl et al., 2016). During growth, more bone is formed than resorbed, whereas between the ages of 30–50 years, the amount of formed and resorbed bone is approximately equal. In women, after the menopause, bone resorption significantly exceeds the amount of bone formed, while in men this occurs slightly later (WHO, 2003). Any imbalance in bone resorption and formation due to sex hormone deficiency, primary hyperparathyroidism or excess exposure to glucocorticoids, as well as age-related increase in bone resorption and decrease in bone formation (Langdahl et al., 2016), leads to irreversible bone loss and consequently osteoporosis (OP) (WHO, 2003). Throughout life, in order to maintain bone mass and skeletal strength, the bone undergoes remodelling whereby old bone is replaced with new bone. This process involves sequential resorption and formation of bone at the same bone remodelling units (BRUs). Remodelling is initiated by activation of osteoclasts which then resorb bone and subsequently undergo apoptosis. This is followed by recruitment of osteoblasts which lay down new bone which later becomes mineralized. Bone remodelling is regulated by locally secreted and systemic cytokines (Langdahl et al., 2016; WHO, 2003).

1.4. Joints

1.4.1. Types of joints

A joint is a site where two bones connect together and, according to structure, can be classified into three groups: fibrous, cartilaginous or synovial (Drake et al., 2015). Synovial joints (also known as diarthrodial joints) constitute the most common type of joint in the body and can be further divided into six types: hinge, ball and socket (e.g. the hip), pivot, saddle, condyloid and plane. All of these joints share the same basic features including joint cavity, articular cartilage which covers the ends of articulating bones and fibrous joint capsule which encloses the joint and is lined with synovial membrane. One of the essential components secreted by the synovial membrane is the synovial fluid which lubricates the joint and reduces friction during motion. Synovial joints not only facilitate articulation and thus free movement of the bones that they join, but also have the ability to withstand very large loads. For example, previous

studies estimated that during running the compressive forces placed upon patellofemoral joint can range between 4.3 to 7.6 times of body weight (Flynn & Soutas-Little, 1995).

1.4.2. Joint tissues

Synovium and joint capsule

The joint capsule surrounds the joint and attaches to bone via the attachment zone (Ralphs & Benjamin, 1994). This highly innervated fibrous structure brings nutrients via blood vessels and drains waste products via lymphatic vessels (Ralphs & Benjamin, 1994). The joint capsule is lined with the synovial membrane (synovium), which covers all articular joint surfaces except the articular cartilage. The synovium comprises two cell types: type A and B synovial cells. The former is a macrophage-like cell responsible for combatting infections and maintaining an aseptic environment within the joint. The underlying cell, type B synovial cell, is a fibroblastic cell and its main function is to lubricate the joint and support joint articulation by synthesis and secretion of hyaluronan and lubricin (A. R. Poole, 2010).

One of the roles of synovium is to produce synovial fluid which enables provision of nutrients to the joint and articular cartilage, and also lubricates the joint owing to production of lubricin. It also contains high concentrations of hyaluronic acid which provides the fluid with high viscosity (Firestein et al., 2016; Tamer, 2013).

Articular cartilage

Unlike most tissues, articular cartilage lacks blood vessels, lymphatics and nerves. It is between 2 to 4 mm thick and covers the articulating ends of long bones. Along with synovial fluid, it allows a smooth, lubricated surface for articulation, absorbs impacts and dissipates loads to the subchondral bone (Martel-Pelletier et al., 2008; A. R. Poole, 2010). The only type of cell that is present in the articular cartilage is the chondrocyte, which is responsible for the maintenance and synthesis of a dense ECM. In addition, chondrocytes are able to respond to external stimuli via mechanosensors and primary cilia located on its surface (Archer & Francis-West, 2003; Martel-Pelletier et al., 2016).

The ECM predominantly contains collagens and proteoglycans (aggrecan) with non-collagenous proteins, smaller proteoglycans, glycoproteins, lipids and phospholipids present in smaller amounts. The most abundant cartilage protein is type II collagen which represents between 90 to 98% of the collagen ECM. It accumulates into fibrils which aggregate to fibres knotted with proteoglycan aggregates. This fibril network is formed and supported by collagen types I, IV, V, VI, IX and XI. All collagen molecules contain a region with three polypeptide chains and are twisted into a triple helix which stabilizes the matrix. The most abundant proteoglycan in cartilage is aggrecan which consists of a hyaluronic acid strand with multiple monomers attached to it. The bond between each monomer and the hyaluronate is stabilized by a low-molecular-weight link protein. These proteoglycan aggregates occupy the interfibrillar space of the cartilage ECM and provide the osmotic properties necessary for cartilage to withstand compressive loads (Martel-Pelletier et al., 2008). Together, collagens and proteoglycans account for articular cartilage dry weight while water contributes between 65% (found in the deep zone) to 80% (found near the cartilage surface) of tissue wet weight (Fox et al., 2009; Martel-Pelletier et al., 2008).

Articular cartilage can be separated into four zones (superficial, middle, deep and calcified cartilage zone, see Figure 1.3 for schematic representation and histological section of articular cartilage zones) which differ in their function. The superficial zone, which is in contact with synovial fluid, consist of collagen fibrils, has low proteoglycan content and elongated chondrocytes. Its main function is to resist the compressive forces imposed during articulating movements. The middle zone, representing 40-60% of the total cartilage thickness, consists of thicker collagen fibrils and proteoglycans. Here, the chondrocytes have a round shape and are at low density. The deep zone contains the highest aggrecan content and the largest collagen fibrils. Chondrocytes are similar in shape to those in the middle zone, have lower density and lie perpendicular to the articular surface. The calcified cartilage has a scarce cell population and hypertrophic chondrocytes. It is separated from the deep zone via the tidemark and is mainly responsible for anchoring the cartilage to the subchondral bone via penetration of collagen fibrils from deep to calcified cartilage (Martel-Pelletier et al., 2008).

Throughout the life course chondrocytes maintain and repair cartilage environment, however with increasing age and in OA this ability declines (Martel-Pelletier et al., 2016).



Figure 1.3 Schematic diagram and histological section of articular cartilage zones.

Image publicly available at www.orthobullets.com

Subchondral bone

Situated below the articular cartilage is a layer of bone referred to as subchondral bone. It can be divided into distinct regions which differ in their structure and composition.

Closest to the articular cartilage is a layer of calcified cartilage and these structures are separated by the tidemark (Burr, 2004). Subchondral bone plate is located directly underneath the calcified cartilage. It is composed of lamellar bone, is poorly vascularised and has low porosity (Burr, 2004; G. Li et al., 2013). Arising from subchondral bone plate is subchondral trabecular bone, which is more vascular, more porous and less stiff compared with the subchondral bone plate. It provides support and has important shock absorbing functions in healthy joints and is important for the provision of nutrients to the cartilage (Burr, 2004; G. Li et al., 2013). Subchondral bone can dissipate about 30% of the load placed upon joints compared with only 1-3% of load attenuated by cartilage (Madry et al., 2010). Previous research suggests that subchondral bone plays a key part in initiation and progression of OA (Castañeda et al., 2012).

Ligaments, tendons and muscles

Muscles attach to bones via tendons and the contraction of muscles across joints produces movement. Ligaments are strong elastic bands of connective tissue, mainly type I collagen fibres, attached to bones at their ends. They support the joints by holding the bones together and resisting excessive loads or movements. Tendons, which facilitate attachment of muscles to bone, are similar in structure to ligaments (Betts et al., 2013).

1.5. Development and anatomy of the hip joint

1.5.1. Development of the hip joint

The majority of tissues in the developing limb arise from MSCs which differentiate into various articular tissues, except neural elements and blood vessels (Walker, 1991). The majority of joint differentiation is thought to be completed between the 4th and 8th week of embryonic development (Lee & Ebersson, 2006). The acetabulum forms around 6 weeks of gestation, as a shallow depression, proximal to the femoral head (Lee & Ebersson, 2006). Both, the hip joint and acetabulum arise from a cleft formed in the pre-cartilaginous cells, and by 11th week of gestation the hip joint is fully formed with spherical femoral head, short femoral neck, primitive greater trochanter, joint capsule, acetabular labrum and transverse acetabular ligament all visible macroscopically (Lee & Ebersson, 2006; Weinstein & Dolan, 2018). When first formed, the acetabulum is deep and almost completely surrounding the femoral head, however as it continues to grow throughout the intrauterine life its depth increases at much slower rate compared with the rate of increase in the acetabular and femoral head diameters (as a result, the acetabulum becomes shallower and femoral head becomes more hemi-spherical) (Giorgi et al., 2015; Walker, 1991). In the early postnatal period and during early childhood, movement and muscle loading play an important role in shaping of the proximal femur and acetabulum (Ford et al., 2017). The expansion of the acetabulum occurs via appositional growth of articular cartilage and interstitial growth of triradiate cartilage, whereas the longitudinal growth plate, the trochanteric growth plate and the

femoral neck isthmus contribute to the appositional growth of the femoral head and greater trochanter (White, 2005). The triradiate cartilage (situated where the pubis, ischium and ilium meet) begins to ossify between the ages of 15 and 18 years and its fusion is completed by the age of 20 to 25 years. The fusion of proximal femoral epiphyses occurs by the age of 18 years and the fusion of trochanteric growth plate occurs between 16 and 18 years of age (Bonewald, 2011; Marks Jr & Popoff, 1988).

1.5.2. Anatomy of the hip joint

The hip joint (Figure 1.4) is a ball and socket which consists of acetabulum (located on the pelvis) and femoral head. The femoral head is spherical and articulates with the cup-shaped acetabulum. The articulating parts of the acetabulum and femoral head are covered with articular cartilage (with the exception of the attachments of the ligamentum teres). The femoral head joins to the femoral shaft via the femoral neck (FN). Greater and lesser trochanters, which reside on the upper part of the shaft serve as points for muscle attachment that move the hip joint. The range of movement permitted by hip joint include flexion and extension, abduction and adduction, and rotation (Drake et al., 2015; Ombregt, 2013).

Image removed due to copyright reasons.

Figure 1.4 Anatomy of hip joint.

Reproduced from publicly available image at www.orthobullets.com

1.6. Osteoarthritis

1.6.1. Definition of OA

Osteoarthritis (OA) is the most common form of arthritis worldwide (Martel-Pelletier et al., 2016) and can be defined by clinical symptoms, structural joint changes or a combination of both (Nigel K Arden & Nevitt, 2006). Pathologically it is characterized by loss of articular cartilage, presence of osteophytes and subchondral sclerosis, and clinically by pain, stiffness and restricted movement (Nigel K Arden & Nevitt, 2006).

While traditionally regarded as a disease of the articular cartilage it is now recognized as a disease of the whole joint.

Defining OA is challenging, and various definitions have been proposed. For example, in the 'Global burden of osteoarthritis in the year 2000' by Symmons et al. (Symmons et al., 2003) OA was defined as:

"...complex disease entity that is difficult to diagnose and define. The Subcommittee on Osteoarthritis of the American College of Rheumatology Diagnostic and Therapeutic Criteria Committee defined osteoarthritis (OA) as "A heterogeneous group of conditions that lead to joint symptoms and signs which are associated with defective integrity of articular cartilage, in addition to related changes in the underlying bone at the joint margins". Clinically, the condition is characterized by joint pain, tenderness, limitation of movement, crepitus, occasional effusion, and variable degrees of local inflammation."

In their 2015 review, Kraus et al. highlighted the need for the development of standardized definitions of OA in order to aid communication across the field and facilitate the development of new therapeutics by achieving a global consensus on OA definition and classification (Kraus et al., 2015). As a result, the draft definition proposed by the Osteoarthritis Research Society International (OARSI) is as follows (Kraus et al., 2015):

"Osteoarthritis is a disorder involving movable joints characterized by cell stress and extracellular matrix degradation initiated by micro- and macro-injury that activates maladaptive repair responses including pro-inflammatory pathways of innate immunity. The disease manifests first as a molecular derangement (abnormal joint tissue metabolism) followed by anatomic, and/or physiologic derangements (characterized by cartilage degradation, bone remodelling, osteophyte formation, joint inflammation and loss of normal joint function), that can culminate in illness."

In a clinical setting, OA diagnosis is primarily based on symptoms, whereas in a research setting, a number of grading systems have been developed in an attempt to quantify disease severity. Although a number of radiographic grading systems have been proposed, the most commonly used is Kellgren and Lawrence (KL) scoring system, which

scores OA at various sites based on severity and is divided into five grades: no OA (0), doubtful (1), minimal (2), moderate (3) and severe (4) (Kellgren & Lawrence, 1957).

1.6.2. Classification of OA

Traditionally OA has been stratified into primary (no known cause) and secondary (due to known causes such as metabolic – e.g. ochronosis, anatomic – e.g. slipped femoral epiphysis, traumatic or inflammatory) (Nigel K Arden & Nevitt, 2006). However, more than a decade ago, Dieppe and Kirwan argued that this classification is not adequate given that OA is either the result of local biomechanical influences or systemic factors (Dieppe & Kirwan, 1994). Furthermore, in their 2009 commentary, Brandt et al. argued that all OA is secondary (Brandt et al., 2009).

While OA can affect any joint, the most commonly affected joints include knees, hips, hands, spine and feet (Johnson & Hunter, 2014). OA seldom affects a single joint and individuals with OA in one joint often have OA in other joints, a finding which cannot be explained by chance or age alone (Nigel K Arden & Nevitt, 2006). For example, Hirsch et al. found a strong association between hand and knee OA in the Baltimore Longitudinal Study of Aging (Hirsch et al., 1996). According to other studies OA most commonly co-occurs in the hands, neck, lower back and knees, whereas multiple joint involvement in hip OA is less common (Günther et al., 1998; Lawrence, 1969; Ledingham et al., 1992). Although multiple joint involvement (or polyarticular OA) has been described previously and referred to as ‘generalized OA’ throughout the literature (Nigel K Arden & Nevitt, 2006), in their 2014 systematic review Nelson et al. concluded that this term has been used inconsistently and highlighted the need for standardised definition of generalized OA (Nelson et al., 2014).

OA can also be classified based on the appearance of the affected joints. In the case of hip OA, it is frequently defined radiographically by the presence of joint space narrowing (JSN) and osteophyte formation, however both features do not always occur together (Castaño-Betancourt et al., 2013a). Based on these observations, it has been sub-

classified into: normotrophic (both JSN and osteophytes are present), hypertrophic (presence of osteophytes) and atrophic (presence of JSN) (Castaño-Betancourt et al., 2013a; Ishidou et al., 2017; Panoutsopoulou et al., 2016; Solomon, 1976).

1.6.3. Burden of OA

OA is associated with a significant economic burden and its prevalence is increasing with increasing age and the obesity epidemic. It is thought that OA associated pain and loss of function account for ~1% to 2.5 % of gross domestic product in the western world (Woolf & Pfleger, 2003). Currently no disease-modifying treatment is available, other than pain relief and joint replacement for end-stage disease. As highlighted in the OARSI white paper (OARSI, 2016), 'Osteoarthritis: A Serious Disease', submitted to the U.S. Food and Drug Administration, and previously highlighted by Nüesch et al. (Nüesch et al., 2011), individuals with OA are at increased risk of death highlighting the need to develop successful therapies to delay disease progression and manage symptoms such as pain. According to the Global Burden of Disease 2010 study, OA was the 11th highest contributor to disability amongst nearly 300 diseases studied (Cross et al., 2014).

1.6.4. OA diagnosis

Despite its high prevalence, OA can be very difficult to diagnose (Martel-Pelletier et al., 2016) especially in its early stages. Clinical diagnosis of OA is based on history and symptoms; pain being the most common reason for which patients seek medical attention (Glyn-Jones et al., 2015). Specific diagnostic criteria have been developed for the knee (Altman et al., 1986; Wu et al., 2005), hand (Altman et al., 1990) and hip (Altman et al., 1991) OA. While no specific diagnostic criteria have been developed for other sites affected with OA, such as spine or big toe, diagnosis is usually based on symptoms and imaging (Martel-Pelletier et al., 2016).

Pain is the primary reason for patients to seek medical attention, however, it usually develops in advanced stages of the disease which offers little room for targeted prevention (Glyn-Jones et al., 2015). Interestingly, in a large number of patients experiencing pain radiological changes are not always present and conversely

radiological changes are not commonly accompanied by pain (Litwic et al., 2013; Nieuwenhuijse & Nelissen, 2015). This poor correlation could be explained by lack of nociceptive innervation in some of the joint structures or simply due to variability in pain response which is very complex and individual-specific (Litwic et al., 2013). It is also possible that plain radiographs are not sensitive enough to detect all relevant changes associated with OA.

1.6.5. OA pathogenesis

Historically, OA was considered a disease of articular cartilage, however it is now recognized as a disease of the whole joint, affecting all of its tissues and subsequently leading to joint failure (Martel-Pelletier et al., 2016; Van Der Kraan et al., 2016). The pathogenesis of OA is due to multiple risk factors, with biomechanics, inflammation, biochemical mediators and bone response all contributing to this process (Birrell et al., 2011).

In sections to follow I will describe the key changes in cartilage, subchondral bone and synovium observed in OA.

Cartilage

Damage to articular cartilage is one of the key features of OA. In healthy joints the composition and architecture of cartilage is successfully maintained by chondrocytes, however in joints affected by OA the cartilage matrix undergoes substantial alterations (Martel-Pelletier et al., 2016). Histologically cartilage appears rough owing to the development of fibrillations and fissures on its surface. As OA progresses, cartilage becomes fragmented exposing the underlying bone. In addition, the zone of calcified cartilage extends and the tidemark (which separates articular from underlying calcified cartilage) duplicates. These changes are accompanied by vascular invasion of the bone and calcified cartilage. As a result, new bone is formed in a process resembling that of EO (Glyn-Jones et al., 2015; Martel-Pelletier et al., 2016) (as described previously in section 1.2).

During OA, both anabolic and catabolic activities in cartilage are increased. In early disease stages, chondrocytes proliferate and synthesise matrix molecules in order to preserve matrix integrity. With time, the ECM becomes disrupted and proteoglycans depleted leading to erosion which marks irreversible damage to the cartilage. This makes the cartilage particularly susceptible to external insults and stimuli (Man & Mologhianu, 2014; Martel-Pelletier et al., 2016).

In healthy joints chondrocytes are metabolically inactive and their activity is limited to low-turnover repair, however during OA they become metabolically active (Goldring & Otero, 2011). In OA cartilage chondrocytes proliferate and become hypertrophic, form clusters and produce inflammatory response proteins including cytokines (i.e. interleukin (IL) 1, IL-6, IL-15 and tumour necrosis factor (TNF)) and matrix degrading enzymes (such as metalloproteinases and a disintegrin and metalloproteinase with thrombospondin-like motifs 4 (ADAMTS4), ADAMTS5, MMP1, MMP3, MMP13) (Goldring & Otero, 2011; Man & Mologhianu, 2014; Martel-Pelletier et al., 2016).

Subchondral bone

Substantial changes affecting the cortical bone plate and the trabecular bone which lies underneath are also seen in OA. These include changes to the cortical plate (increase in volume and thickness), changes in the architecture of trabecular bone, changes in bone mass, development of bone cysts and osteophytes and presence of bone marrow lesions (BMLs). These changes are thought to be the result of an imbalance between osteoclast and osteoblast activity. Increased matrix production is thought to result in thickening of the subchondral bone plate. BMLs, which can be imaged using MRI, are thought to localise in regions with severe cartilage damage. Subchondral bone cysts are thought to develop in regions previously occupied by BMLs and form by a process of EO. Osteophytes are bony outgrowths on the margins of joints and are thought to support joint stability rather than contribute to OA progression (Loeser, 2010; Man & Mologhianu, 2014; Martel-Pelletier et al., 2016).

Synovium

Inflammation of the synovium (also known as synovitis) is another feature of OA and can be present even in early disease stages. It is characterised by synovial hyperplasia, fibrosis and release of inflammatory mediators and degrading enzymes by synoviocytes (Loeser, 2010; Man & Mologhianu, 2014; Martel-Pelletier et al., 2016). The degree of synovitis varies between patients and disease stage and previous studies found that the presence of synovitis in early OA was associated with disease progression (Loeser, 2010).

1.6.6. OA epidemiology

1.6.6.1. Prevalence and incidence

OA is the most common form of arthritis affecting 10% of men and 18% of women over the age of 60 years and an estimated 240 million people worldwide (Nelson, 2018). The prevalence of OA increases with age in both men and women (Martel-Pelletier et al., 2016) and the risk of hand, hip and knee OA is higher in women compared with men (Lanyon et al., 2003; Oliveria et al., 1995; Palazzo et al., 2016) with similar prevalence reported in European and American data (Martel-Pelletier et al., 2016). Hand OA is less frequent in Native Americans and African-Americans compared with white Americans and the prevalence of primary RHOA in studies from Europe and North America is higher than the prevalence reported in studies from Asia and Africa (Johnson & Hunter, 2014) which could be explained by differences in pelvic morphology (Martel-Pelletier et al., 2016).

The incidence of OA at all sites declines approximately at the age of 80 years, a finding consistently reported in previous studies (Oliveria et al., 1995; Prieto-Alhambra et al., 2014). Some discrepancies in reported prevalence and incidence rates of OA exist which are likely due to high variability in case definition (i.e. radiographic or symptomatic OA) and specific joints involved (Palazzo et al., 2016; Pereira et al., 2011).

1.6.6.2. OA risk factors

A number of risk factors for OA have been identified and these will be discussed in more detail below. These include modifiable and non-modifiable risk factors, some of which act through altered or increased biomechanical stress (such as altered hip shape).

Age and sex

Age is a well-recognized risk factor for OA, however the exact mechanisms underlying the relationship between age and OA risk remain to be fully elucidated. The likely contributors include oxidative stress, decrease in cartilage volume and sarcopenia. Moreover, the ability to respond to stress and injury declines with age resulting in tissue damage (Jordan et al., 2007; Litwic et al., 2013).

The risk of hand, hip and knee OA is higher in women with significant increase around the time of menopause (Litwic et al., 2013) suggesting a potential role of oestrogen in the development of OA, however the evidence from clinical and epidemiological studies is inconclusive (Johnson & Hunter, 2014; Litwic et al., 2013).

Obesity

Obesity represents one of the strongest and most-recognised risk factors for OA (Johnson & Hunter, 2014; Vina & Kwok, 2018) and using a Mendelian randomization (MR) approach, a recent study of the UK Biobank confirmed the causal role of increased body mass index (BMI) and other obesity related traits on the risk of OA (Zengini et al., 2018). In 2012, in a meta-analysis of observational studies, Jiang et al. reported a clear dose-response relationship between BMI and knee OA with 35% increase in knee OA risk for every 5-unit increase in BMI (Jiang et al., 2012). Conversely, in the Framingham study, a reduction in body weight was associated with a decreased risk of knee OA development (Felson et al., 1992), a finding also supported by a 2007 meta-analysis of randomised controlled trials (Christensen et al., 2007).

While the relationship between obesity and knee OA is much stronger than that for hip OA, the evidence supports the role of excess weight in the risk of both (Johnson &

Hunter, 2014; Vina & Kwoh, 2018) and a recent prospective study from Spain reported increased risk of knee, hip, and hand OA in obese subjects (Reyes et al., 2016).

Nutritional factors

Previous studies explored the relationship between a number of nutritional factors and OA. The role of vitamin D, known for its role in cartilage and bone metabolism, is conflicting. Previous studies reported an association between low/moderate levels of vitamin D and increased risk of incident hip OA and progression of knee OA (Johnson & Hunter, 2014). However, in a previous randomized placebo-controlled, double-blind clinical trial, 2 year supplementation with vitamin D in patients with symptomatic knee OA did not impact on pain or cartilage volume loss (McAlindon et al., 2013). In the Osteoarthritis Initiative (OI) study, total dietary fibre intake was associated with reduced risk of symptomatic knee OA, but not with radiographic knee OA (RKOA) (Dai et al., 2017). In terms of antioxidant intake, Li et al. found no evidence of an association between carotenoid, vitamin E, and selenium intake with the prevalence of RKOA (H. Li et al., 2016). Similarly, in The Malmö Diet and Cancer cohort, a prospective population-based study, dietary intake of vitamin E and β -carotene had no protective effect on severe knee and hip OA (Engstrom et al., 2009).

Occupation and physical activity

Physically demanding occupations, especially those involving repetitive activities, have been found to be associated with an increased risk of OA. For example, individuals with occupations requiring squatting or kneeling have been found to be at an increased risk of knee OA compared with individuals in non-manual occupations (Johnson & Hunter, 2014; Vina & Kwoh, 2018). Moreover, individuals in occupations involving prolonged standing (Johnson & Hunter, 2014) and heavy lifting (Bergmann et al., 2017) have been found to have increased risk of hip OA.

The evidence regarding physical activity (PA) and risk of OA is conflicting. On one hand, previous studies showed a relationship between recreational running and decreased risk of knee and hip OA (Alentorn-Geli et al., 2017), on the other hand others found

increased prevalence of knee OA (Driban et al., 2017) and increased incidence of hip OA (Vigdorichik et al., 2017) in footballers. While it appears that the type and intensity of PA is important, the underlying joint health also needs to be considered. For example, previous study in patients with established OA found association between vigorous PA and increased risk of knee replacement surgery (Y. Wang et al., 2010), whereas study in healthy individuals showed beneficial effect of vigorous PA on knee cartilage (Racunica et al., 2007).

It appears that habitual levels of PA do not increase the risk of radiographic or symptomatic OA, as opposed to high levels of PA (Neogi & Zhang, 2013). Overall, the evidence suggests beneficial effect of PA in reducing the risk of OA (particularly in the absence of injury (Litwic et al., 2013)), however clear relationship between elite impact sports and future risk of both hip and knee OA have been shown, which might be explained by higher risk of injury which is common in high impact and elite sports (Vina & Kwoh, 2018).

Joint injury

The knee is one of the most commonly injured joints. Rupture of the anterior cruciate ligament, meniscal tears and damage to the articular cartilage following injury have been found to be associated with increased risk of knee OA, OA changes and functional impairment present as early as 10 years following the injury (Vina & Kwoh, 2018). Moreover, in a population-based case-control study in England, previous hip injury (sustained as a result of a fall, road traffic accident or sports injury) was found to be associated with a 4-fold increase in the risk of hip OA (Cyrus Cooper et al., 1998).

Muscle strength/ weakness

Previous observational evidence showed a relationship between muscle weakness and OA. However, it is possible that muscle weakness might occur as a result of OA itself, which often leads to limited daily activities due to pain (Neogi & Zhang, 2013).

Leg-length inequality

Leg-length inequality (LLI) which leads to altered joint mechanics and results in abnormal joint loading is also thought to contribute to increased risk of OA (Murray & Azari, 2015). In the Johnston County OA Project, individuals with LLI ($\geq 2\text{cm}$) were found to be at increased risk of prevalent RKOA (Golightly et al., 2007). Similarly, Harvey et al. reported association between LLI ($\geq 1\text{cm}$) and higher risk of prevalent radiographic and symptomatic knee OA (Harvey et al., 2010). Likewise, in the Multicentre Osteoarthritis Study and the OI study, LLI was found to be associated with increased odds of radiographic hip OA (RHOA) (Kim et al., 2018).

1.6.7. Hip morphology and OA

As demonstrated, OA is a complex disorder with many risk factors contributing to its development. It has been suggested that hip shape, which forms the primary focus of this thesis, is one of the most important risk factors for the development of hip OA (Murphy et al., 2016). While severe hip abnormalities have been linked to early onset hip OA, more subtle changes in hip morphology are also thought to play an important role in the pathogenesis of hip OA (Murphy et al., 2016). Hip shape abnormalities such as acetabular dysplasia (AD), and pincer- and cam-type femoroacetabular impingement (FAI) deformities are thought to contribute to altered joint biomechanics and thus abnormal distribution of loads within the hip joint leading to excessive contact stress on the cartilage, its degeneration and consequently hip OA (Harris-Hayes & Royer, 2011). As well as alterations in joint shape, soft tissue changes can also contribute to altered biomechanics suggesting that ligament laxity precedes bone and cartilage changes (Quasnichka et al., 2006). It is important to bear in mind that as well as being associated with the development of hip OA, changes in hip morphology can also be the result of the OA process itself (Faber et al., 2017; Resnick, 1976) making it difficult to distinguish changes causing OA from those resulting from it.

1.6.7.1. Acetabular dysplasia

The most striking evidence, confirming the role of altered joint shape in OA development, comes from studies in individuals with developmental dysplasia of the hip (DDH), one of the most common developmental skeletal disorders. DDH is characterized by insufficient acetabular coverage of the femoral head with varying degrees of severity ranging from mild dysplastic acetabular change to complete hip dislocation (Hatzikotoulas et al., 2018). It is most commonly diagnosed in the first few months of life and if left untreated is thought to be the most common cause of early onset hip OA (Khanna & Beaulé, 2014; Pun, 2016). The incidence of DDH ranges between 1 (Lee & Ebersson, 2006) to 3.6 (Hatzikotoulas et al., 2018) per 1000 live births, with higher incidence observed for female gender, positive family history or breech presentation (Abbassi, 1998) illustrating both, strong genetic and environmental components in DDH development. In a recent genome-wide association study (GWAS), Hatzikotoulas et al. identified a robustly replicating association between genetic locus at *GDF5* and DDH case status (Hatzikotoulas et al., 2018). In addition, *GDF5* is known to be associated with OA risk (Zengini et al., 2016).

While DDH can result in severe hip abnormalities, the relationship between milder forms of AD and risk of hip OA have also been explored. It is important to bear in mind that while DDH represents AD most commonly diagnosed in early life, adolescent onset dysplasia has also been reported in the literature. While this could simply represent delayed diagnosis of DDH, AD can develop without prior history of DDH (Pun, 2016) and is thought to develop due to delayed and insufficient ossification at the acetabular socket (Pun, 2016). According to previous studies, of patients with hip OA, between 25-40% cases can be attributed to subtle AD (Khanna & Beaulé, 2014). OA is thought to develop as a result of unequal distribution of shear forces in the hip joint due to decreased femoroacetabular contact surface in shallow acetabulum. With time, both the acetabular labrum and articular cartilage degenerate eventually leading to joint failure (Murphy et al., 2016). The most common measurement used to assess AD in studies is the lateral centre edge angle (CEA) of Wiberg (Chaganti & Lane, 2011). The thresholds defining dysplasia reported in studies vary, with values ranging from $\leq 20^\circ$ to $\leq 30^\circ$ (Harris-Hayes & Royer, 2011; Khanna & Beaulé, 2014).

1.6.7.2. Femoroacetabular impingement

Previous studies in adults have reported an association between FAI and hip OA (Resnick, 1976). Childhood hip disorders, such as Legg–Calvé–Perthes' disease (LCPD) and slipped capital femoral epiphysis (SCFE), which are associated with FAI, are also thought to contribute to hip OA in later life (Froberg et al., 2011; Harris-Hayes & Royer, 2011; Khanna & Beaulé, 2014). In general, two patterns of FAI can be distinguished: cam and pincer FAI (Figure 1.5). Pincer FAI represents a deepened acetabulum and excessive acetabular coverage resulting in abnormal contact between the femoral head-neck junction and the acetabular labrum (Khanna & Beaulé, 2014). It is often quantified using CEA with different thresholds being reported in studies (CEA $\geq 40^\circ$ (Chung et al., 2010), CEA $\geq 45^\circ$ (Gosvig et al., 2010) or no defined cut off value (Ecker et al., 2007)). Other methods used to assess pincer FAI reported in the literature include the crossover sign, coxa profunda (both assessed on radiographs) or global acetabular retroversion (assessed on CT scans) (Harris-Hayes & Royer, 2011). In a previous population-based survey in individuals from the Copenhagen Osteoarthritis Substudy, Gosvig et al. reported a risk ratio of 2.4 for the development of hip OA in individuals with a deepened acetabulum (Gosvig et al., 2010). Cam FAI, also referred to as pistol grip deformity, can be characterized by aspherical femoral head and additional bone growth at the anterolateral aspect of the femoral-head neck junction (Khanna & Beaulé, 2014; Murphy et al., 2016). Unlike pincer FAI, which is more common in women, cam FAI is five times more likely to be found in men (Khanna & Beaulé, 2014). Assessment of cam FAI in studies commonly relies on the alpha angle, with varying thresholds being reported ($>50^\circ$ (Ecker et al., 2007) or $>62.5^\circ$ (Pollard et al., 2013)), while other measures include anterior offset ratios (Pollard et al., 2013) or visual inspection (Harris-Hayes & Royer, 2011). A number of studies have found an association between cam deformity and hip OA (Doherty et al., 2008; Khanna & Beaulé, 2014; Pollard et al., 2013). For example, Doherty et al. reported that cases with symptomatic RHOA were nearly seven times more likely to have a pistol grip deformity compared with controls (Doherty et al., 2008).

Image removed due to copyright reasons.

Figure 1.5 Schematic diagram showing pincer and cam femoroacetabular impingement.

Image publicly available at

<https://www.orthobullets.com>

1.6.8. Genetics of OA

OA is a complex disease with a strong genetic component, inherited in non-Mendelian fashion (Salter et al., 2014; Warner & Valdes, 2016). According to previous studies, between 30-65% of OA risk is determined genetically (Vina & Kwoh, 2018). The evidence for genetic influences on OA comes from family and twin studies, linkage and candidate gene studies and most recently large scale GWASes. These studies enabled identification of several variants, implicated in OA development and progression, each exerting a modest effect on disease risk.

1.6.8.1. Heritability

The earliest evidence for genetic involvement in OA was reported in 1940s by Stecher (Stecher, 1941) who studied familial clustering of Heberden's nodes in hands. A number of studies followed and confirmed clustering of hand, knee, hip and spine OA within families (Spector & MacGregor, 2004). Classic twin studies (where concordance between identical and non-identical twin-pairs are compared) were then used to estimate heritability of OA, defined as the proportion of the total variability in a trait that is explained by the genetic variation. Based on these studies, heritability estimates for

radiographic hand and knee OA range between 39% and 65%, and ~60% for RHOA (Salter et al., 2014).

1.6.8.2. Candidate gene studies, linkage studies, GWAS studies

In order to improve our understanding of the genetic architecture of OA, further approaches have been undertaken to identify novel genetic variants associated with this trait. Linkage studies scan large number of genetic markers in the genome to firstly, identify the patterns that they are inherited in families and secondly, to localize disease loci on the genome. Previous studies implicated several chromosomal regions with linkages to OA, such as 2q31-32, 4q 12-21, 6p/6q, 14q32.11, 16p and Col 9A1 amongst others (Loughlin et al., 2000; Mustafa et al., 2000; Spector & MacGregor, 2004; Valdes & Spector, 2010).

Candidate gene studies, which take a hypothesis-driven approach and test the associations between biologically relevant variants and the disease of interest, identified important loci for OA susceptibility in genes including *GDF5*, *ASPN*, *FRZB* and *PTGS2* (Warner & Valdes, 2016). However, one of the limitations of this approach is the fact that only a small portion of the genome can be studied at any time, thus other important genes are likely to be overlooked. Moreover, this approach requires good prior knowledge and many findings failed to be replicated because the initial evidence was weak (Panoutsopoulou & Zeggini, 2013). Nevertheless, rs143383 in *GDF5* is an example of successfully identified and replicated locus, which was found to be strongly associated with hip OA in Asians and knee OA in Europeans (Panoutsopoulou & Zeggini, 2013). *GDF5* is a member of the transforming growth factor β (TNF- β) superfamily and plays an important role in the development, maintenance and repair of bone and cartilage (Cornelis et al., 2011; Panoutsopoulou & Zeggini, 2013).

A more recent method used to identify genetic variants associated with OA includes GWAS which offer a hypothesis-free approach and simultaneously tests for associations between millions of single nucleotide polymorphisms (SNPs) with a trait of interest. Previous GWAS studies identified 21 loci associated with hand, hip and/or knee OA (defined radiographically, on self-report or as end-stage disease requiring joint replacement) (Cibrián Uhalte et al., 2017) and a recent GWAS in the UK Biobank in

30,727 OA cases identified a further nine novel loci, which together account for 26% of variance in OA (Zeggini et al., 2018). Despite large collaborative efforts only modest number of loci, with moderate-to small effects, have been identified (compared with other complex traits, i.e. ~70 GWAS loci have been identified to date for type 2 diabetes (X. Sun et al., 2014)). This could be partially explained by OA heterogeneity and variation in case definition amongst studies (ranging from self-reported to radiographically defined OA). Nevertheless, these studies support the complex and heterogenous nature of OA with identified SNPs being site-specific and sex-specific. For example, an intronic SNP rs4836732 within the *ASTN2* gene has been found to be strongly associated with THR in females (Zeggini et al., 2012). Another variant, rs12982744 in *DOT1L*, showed stronger association with hip OA in males, compared with females (Castaño-Betancourt et al., 2012). A number of other potentially relevant SNPs have been identified and previously reviewed in the literature, and these include variants involved in the Wnt signalling pathway, synthesis and remodelling of ECM components, or regulation of proteins involved in inflammatory and immune responses (Panoutsopoulou & Zeggini, 2013).

1.6.8.3. OA-associated endophenotypes and genetics of hip shape

Although previous GWASes of OA have identified a number of important variants associated with OA, these studies have largely focused on radiographic, severe OA as defined by joint replacement or self-reported OA. It has been recognized that studying OA-related endophenotypes is likely to increase the power of genetic studies and further improve our understanding of OA pathogenesis (Kerkhof et al., 2011).

One of the first successful examples of genetic discovery when studying OA endophenotypes was the *DOT1L* locus found to be associated with radiographic joint space width (which was used as a proxy for cartilage thickness) and this finding was subsequently replicated in a large hip OA case-control study (Panoutsopoulou & Zeggini, 2013). Other studies identified associations between variants in the *LRCH1* and maximal joint space narrowing (JSN) (Panoutsopoulou et al., 2016), whereas Castaño-Betancourt reported associations between four novel variants (*TGFA*, *PIK3R1*, *FGFR3* and *TREH*) and minimal JSN (Castaño-Betancourt et al., 2016). Furthermore, using

Statistical Shape Modelling (SSM), Linder et al. (Lindner et al., 2015) and Baird et al. (Baird et al., 2018) reported associations between previously established OA loci and the shape of the proximal femur.

1.6.9. OA management

There are currently no disease modifying interventions for OA, but number of treatments are available to manage symptoms. The primary reason for which patients with OA seek medical attention is pain which constitutes the primary target of treatment. OA should be managed on a case by case basis and management will often consist of a combination of non-pharmacological and pharmacological interventions (David J Hunter & Felson, 2006). In the following sections I will describe the non-pharmacological and pharmacological strategies for the management of OA along with its surgical management.

Non-pharmacological interventions

Weight loss, in overweight and obese individuals, comprises one of the most important interventions for OA. While it is thought to reduce the risk of developing OA, by as much as 50% in case of knee OA (Felson et al., 1992), in already established knee OA, weight loss is strongly associated with reduction in pain and improved function (D J Hunter et al., 2015). Although not as robust as for knee OA, there is some evidence suggesting benefit in patients with hip OA, as demonstrated by improvement in self-reported physical function in patients involved in exercise and weight loss programmes (Paans et al., 2013). Nevertheless, both NICE (NICE, 2008) and OARSI (W. Zhang et al., 2008) guidelines recommend weight loss in patients with both hip and knee OA. Alongside weight loss, interventions such as health education, self-management, exercise (low impact sports such as swimming, cycling, rowing) and strength training are often recommended in the management of both knee and hip OA (Aresti et al., 2016; Bennell et al., 2012; Martel-Pelletier et al., 2016).

Pharmacological interventions

There are currently no pharmaceutical therapies that can prevent, reverse or slow down the progression of OA. In terms of pain management, a number of topical, oral and injectable pharmacological treatments are available. Paracetamol and non-steroidal anti-inflammatory drugs (NSAIDs) are often recommended as the first-line treatment options (Martel-Pelletier et al., 2016). However, many patients still suffer with persistent pain despite being on treatment (Martel-Pelletier et al., 2016). Second-line treatment options include opioids (when paracetamol and NSAIDs are either ineffective or contraindicated) or intra-articular injections. While opioids are associated with a number of side effects (including considerable toxicity), intra-articular injections are thought to offer only short-term benefit in both, knee and hip OA (Aresti et al., 2016; Bennell et al., 2012).

Joint surgery

While a combination of pharmacological and non-pharmacological interventions forms the mainstay of OA management, knee and hip replacement surgery is often considered in patients with severe disease characterized by persistent moderate to severe pain, limited function and reduced quality of life, provided conservative management is ineffective and radiographic disease is present (Aresti et al., 2016; Bennell et al., 2012; Litwic et al., 2013).

Total hip replacement (THR) is a commonly performed and successful procedure worldwide (Aresti et al., 2016) and according to the National Joint Registry for England, Wales, Northern Ireland and the Isle of Man (NJR) data, the probability of hip revision at 14 years is 7.27% . The reason for revision depends on the period of follow up; revisions due to aseptic loosening of the prosthesis become the most common reason at longer follow up (Aresti et al., 2016; Kandala et al., 2015) and smoking and obesity are associated with increased postoperative and prosthesis related complications (Aresti et al., 2016).

Although not as common as hip replacement, knee replacement surgery is also thought to be highly successful with about 80% of patients reporting reduction in pain (Bennell et al., 2012). In younger patients, with predominantly unicompartmental OA, knee

osteotomy may be used in order to re-align tibia and correct abnormal joint biomechanics (Katz et al., 2010).

Novel/emerging therapies

Several candidate pathways and processes have been identified as potential treatment targets. These include chondrocyte autophagy, reduction of reactive oxygen species production, modulation of growth factor signalling to prevent cartilage anabolism and degradation, and nociceptive signalling (M. M.-G. Sun et al., 2017). In addition, gene therapy targeting knee OA, which has been approved in South Korea, is due to undergo phase III clinical trials in the USA (C. H. Evans et al., 2018a, 2018b).

1.7. Osteoporosis

The inverse relationship between osteoporosis (OP) and OA is well-recognized (Jan Dequeker et al., 2003; Im & Kim, 2014). While they are different diseases in terms of risk factors and genetics, it is thought that bone metabolism plays a crucial role in the pathophysiology of both (Geusens & van den Bergh, 2016). Furthermore, hip shape is related to both disorders, having previously been found to be associated with hip fracture (Alonso et al., 2000; Gnudi et al., 1999) and the development of hip OA (Baker-LePain & Lane, 2010).

1.7.1. Definition and burden of OP

OP is a complex age-related disease characterized by low BMD and deterioration of bone microarchitecture leading to increased bone fragility and increased risk of fracture (Consensus Development Conference, 1993). OP usually arises due to imbalance between bone formation and resorption. It is often asymptomatic and does not manifest clinically until fracture occurs. It affects almost 1 in 2 women and 1 in 5 men over the age of 50 years (Curtis et al., 2015).

Osteoporotic fractures most commonly affect the hip, forearm and spine with the highest mortality, morbidity and economic burden attributed to hip fractures. Following

hip fracture, in previously independent individuals, about half require long-term care and assistance with day to day living (WHO, 2003). In the UK, the estimated cost associated with osteoporotic fracture is approximately £3 billion per year (Curtis et al., 2015) and about 90% of hospital costs associated with osteoporotic fracture are due to those of hip (WHO, 2003).

1.7.2. OP diagnosis

OP has no warning signs and is most commonly diagnosed when patients present with low trauma fracture. Low BMD (with a T-score of ≤ -2.5), one of the strongest risk factors for fracture, is also indicative of OP. Dual energy x-ray absorptiometry (DXA) of either lumbar spine (LS) or proximal femur is used clinically in the assessment of BMD (Schuiling et al., 2011). An online fracture risk assessment tool (FRAX), which uses combination of risk factors for OP (described in detail in section 1.7.4.1) with or without BMD measurement, is often used to estimate 10-year probability of major osteoporotic or hip fracture in men and women (Kanis et al., 2008).

1.7.3. OP pathogenesis

OP is a multifactorial disease with complex pathogenesis. Low BMD is one of the key contributors to osteoporotic fracture and factors contributing to OP pathogenesis include those influencing the attainment of peak bone mass in early adulthood and factors accelerating bone loss in later life. Factors negatively affecting peak bone mass gain, which largely determines BMD in later life, include poor nutrition, physical inactivity and paediatric disorders (e.g. growth hormone deficiency). Once peak bone mass has been achieved it begins to gradually decline with age, with considerable bone loss observed around the age of 65 and 50 years in men and women, respectively (Rizzoli & Bonjour, 1999; WHO, 2003). At menopause, bone turnover increases, due to oestrogen deficiency, causing imbalance between bone formation and resorption. Mechanisms involved include release of cytokines (such as TNFs and ILs) which stimulate osteoclast activity. In men, the likely contributors to OP are low rates of bone formation (due to decline in the levels of gonadal hormone) rather than increase in bone resorption (WHO, 2003).

While the inverse relationship between BMD and fracture is well-established, reduced bone strength at macro- and microarchitectural levels is also thought to influence fracture susceptibility. As described below (section 1.7.4.1, hip morphology and geometry), a range of measures of hip geometry derived from hip DXA scans have been found to be related to hip fracture risk (Gregory & Aspden, 2008). Furthermore, techniques assessing bone strength such as finite element analysis on DXA scans (Luo et al., 2011) and cortical thickness mapping applied to CT scans (K. E. S. Poole et al., 2012) are examples of other tools used in fracture prediction.

1.7.4. OP epidemiology

1.7.4.1. Risk factors

Clinical risk factors

Several risk factors for OP have been identified and these include low BMI, prior history of low trauma fracture, parental history of hip fracture, use of oral glucocorticoids, rheumatoid arthritis, diabetes, untreated hyperthyroidism, hypogonadism or premature menopause (before the age of 45 years), chronic liver disease, current smoking and alcohol intake of 3 or more units per day (Curtis et al., 2015; WHO, 2003).

Bone mineral density

Previous studies have shown consistent inverse associations between BMD and fracture with a 1.5 to 3-fold increase in fracture risk for each SD decrease in BMD. For example, a meta-analysis showed a 2.6-fold increase in hip fracture risk for every 1 SD decrease in hip BMD (Holroyd et al., 2008). BMD is one of the best predictors of osteoporotic fracture and peak bone mass, which is achieved in adolescence, is the main predictor of BMD in later life (Lane, 2006). However, it is important to bear in mind that fractures do occur in individuals with BMD above the osteoporotic threshold and conversely in individuals with low BMD, fractures are more likely but might not occur (Nguyen et al., 2007), suggesting that factors other than BMD play an important role in fracture pathogenesis.

Hip morphology and geometry

While BMD is one of the most important predictors of fracture, a number of geometrical measures to assess hip morphology have been used in studies in relation to fracture. These include femoral neck width (FNW), Hip Axis Length (HAL) and NSA (Boese et al., 2016; Leslie et al., 2015).

Previous studies found greater NSA in both men and women with fracture, association between higher NSA with hip fracture risk, and a number of studies reported relationship between wider FNW in men and women with fracture, although some studies found the opposite reporting associations with narrower FNW and fracture (for a review of studies please refer to (Gregory & Aspden, 2008)). Similarly, in a recent meta-analysis higher HAL, NSA and FNW were associated with the risk of FN fractures (Fajar et al., 2018).

Hip geometrical measurements can be obtained using hip structural analysis (HSA), a standardized software applied to hip DXA scans (Beck, 2007). The advantage of HSA includes the automated generation of hip geometrical indices; however, these parameters are often correlated with each other (therefore not independent) and with measures of body size (Gregory et al., 2004; Michelotti & Clark, 1999).

1.7.5. Genetics of OP

As previously mentioned, genetic factors play an important role in OP and fracture risk and between 50-85% of variance in BMD, which comprises one of the strongest predictors of fracture, is thought to be determined genetically (Estrada et al., 2012). In addition to BMD, previous studies exploring genetic influences on bone phenotypes looked at hip geometry (Hsu & Kiel, 2012), bone ultrasound measures (Kemp et al., 2017) and fracture risk (Tran et al., 2013). Previous studies reported significant heritability of fractures with 2-fold increase in fracture risk (independent of BMD) in those individuals with a parental history of hip fracture (Zmuda et al., 2006). Both candidate gene and genome-wide searches have been performed and here, I will focus on the findings from the most recent GWASes.

The largest to date meta-analysis of DXA derived phenotypes, based on 17 GWASes, identified 56 loci associated with FN and LS BMD (Estrada et al., 2012). These included variants implicated in pathways with relevance to bone such as Wnt, MSC differentiation, EO and RANK-RANKL-OPG pathways. In addition, 14 BMD-associated loci were also found to be associated with fracture risk. In a recent GWAS of BMD, estimated by quantitative heel ultrasound, in 142,487 participants from the UK Biobank study, 153 novel loci explaining 12% of phenotypic variance in BMD have been identified of which several were rare variants with large effects (Kemp et al., 2017). In addition, this study provided evidence for the causal role of *GPC6* locus (which encodes glypican 6 protein) in BMD and the pathophysiology of OP, a potential novel drug target for OP.

1.7.6. OP management

Non-pharmacological interventions in the management of OP consist of falls prevention, which are important in the pathogenesis of fracture, and lifestyle interventions such as adequate calcium intake and vitamin D levels, regular exercise, smoking cessation and reducing alcohol intake (K. E. S. Poole & Compston, 2006).

A wide range of pharmacological interventions for OP are currently available.

Bisphosphonates, which deactivate osteoclasts and thus inhibit bone resorption, are commonly prescribed to treat glucocorticoid induced or postmenopausal OP (Curtis et al., 2015; K. E. S. Poole & Compston, 2006). Denosumab is a human monoclonal antibody which binds to receptor activator of nuclear factor kappa B ligand (RANKL) expressed on the surface of osteoblasts. By binding to RANKL, denosumab blocks the formation and activation of bone resorbing osteoclasts and previous studies have showed a substantial reduction in vertebral and hip fractures following treatment with denosumab. Teriparatide which is a parathyroid hormone analogue, increases bone formation and has been shown to substantially reduce the incidence of new vertebral fractures. Other treatments such as strontium ranelate, which increases bone strength, and raloxifene (selective oestrogen receptor modulator), which has antiresorptive effects on bone, are also available (Curtis et al., 2015).

1.8. Relationship between osteoporosis and osteoarthritis

OA and OP rarely coexist and the inverse relationship between OP and OA was first reported by Foss and Byers in 1972 (Foss & Byers, 1972) who studied patients with osteoporotic fractures and noted that OA was almost never present in individuals with upper femoral fractures, and patients with hip OA had higher than normal BMD. Since then, a number of epidemiological studies reported inverse relationship between OP (defined as low FN BMD) and radiographically defined OA (C Cooper et al., 1991) as well as an association between higher BMD and increased risk of incident and prevalent OA (Allen & Golightly, 2015; Hardcastle et al., 2015a; Vina & Kwoh, 2018). In terms of the relationship between fracture risk and OA the evidence is conflicting and likely reflects heterogeneity in OA case definition. Previous studies reported either protective effect of self-reported (J Dequeker & Johnell, 1993) and physician diagnosed (Vestergaard et al., 2009) OA on fracture risk, while others reported no association between OA (radiographic and self-reported) and vertebral, nonvertebral or hip fractures (Nigel K Arden et al., 1999; G. Jones et al., 1995). Others yet reported an increased risk of fracture in cases with RHOA compared with controls (N K Arden et al., 1996) and an association between self-reported OA and increased risk of fracture in postmenopausal women (Prieto-Alhambra et al., 2013), a finding likely to be explained by increased risk of falls (Lane & Nevitt, 2002; Prieto-Alhambra et al., 2013). Finally, studies in individuals with extremely high bone mass showed higher prevalence of joint replacement (Hardcastle et al., 2013) and radiographic knee and hip OA (Hardcastle et al., 2015a; Hardcastle et al., 2014) in these individuals compared with general population controls. The exact mechanisms underlying the OA-OP relationship are not fully understood. However, the likely mechanisms contributing to this relationship include a shared relationship with hip shape (Baker-LePain & Lane, 2010) or increased bone remodelling and bone loss in early stages of OA as well as slow remodelling and subchondral sclerosis in the late stages of OA which could both contribute to OA pathogenesis (Burr & Gallant, 2012). Important signalling pathways potentially implicated in OA include Wnt and bone morphogenetic proteins (Lories & Luyten, 2011).

While there is strong epidemiological evidence of an inverse relationship between OP and OA and a clear relationship between higher BMD and OA, the mechanisms underlying this relationship are not fully understood. One explanation for this relationship could be due to shared genetic factors. Previous studies showed 30% overlap between genes involved in bone metabolism and those influencing OA (Williams & Spector, 2006). For example, previous studies reported associations between BMD SNPs with knee (Yerges-Armstrong et al., 2014) and hip OA (Yerges-Armstrong et al., 2014). In addition, Hackinger et al. undertook the first systematic overlap analysis of OA and BMD and identified 143 variants associated with OA and BMD, a number of which had known relevance to bone (Hackinger et al., 2017).

1.9. Statistical Shape Model (SSM)

As discussed above, altered hip shape plays an important role in both, hip fracture and hip OA (Baker-LePain & Lane, 2010; Gregory et al., 2004), possibly via altered biomechanics. While the majority of studies investigating relationships with hip shape relied on individual geometrical measures, given the limitations associated with these measures, Gregory et al. (Gregory et al., 2004) were the first to introduce SSM as a means of capturing the global shape of the proximal femur using Principal Component Analysis (PCA). Since then this method has been applied to radiographs to investigate associations with incident hip fracture (Baker-LePain et al., 2011), incident RHOA (An et al., 2016) and to predict THR in OA cases as shown by Gregory et al. (Gregory et al., 2007) and Agricola (Agricola et al., 2015).

Despite lower resolution, when compared with standard radiographs, DXA images have been successfully used to quantify hip shape with SSM in previous studies (Faber et al., 2017; Pavlova et al., 2017). For example, to investigate the relationships with prevalent RHOA and symptomatic hip OA in MrOS (Faber et al., 2017) and to describe the variation in hip shape and its correlations with spine shape in the MRC National Survey of Health and Development (NSHD) cohort (Pavlova et al., 2017). In the largest SSM study to date, nearly 20,000 DXA images were used to identify novel genetic determinants of hip shape (D. A. Baird et al., 2017) and a previous study which also used SSM, explored

relationships between known OA loci and hip shape (Baird et al., 2018). It is worth noting that compared with radiographs, DXA images are quick to perform and produce very low doses of radiation and are thus readily available. As well as being widely available, hip DXA scans were successfully used in previous studies which explored the relationship between hip shape (derived from SSM) and radiographic and clinical hip OA (Faber et al., 2017; Waarsing et al., 2010). Whilst older DXA devices may produce images of lower resolution, making it difficult to identify specific OA features, such as osteophytes, the resolution of images obtained with newer DXA scanners is comparable to radiographs (Yoshida et al., 2015). Given the many advantages of SSM this method was used to quantify hip shape in this thesis and the method will be described in more detail in Chapter 2.

1.10. Hypotheses and aims to be addressed in thesis

OA is a complex disorder with several risk factors contributing to its development. Abnormal hip morphology has been recognized as an important risk factor for hip OA. Alongside severe skeletal disorders such as DDH, a growing body of evidence suggests that more subtle changes in joint morphology play important role in the development of hip OA (Baker-LePain & Lane, 2010). Whereas hip geometry is known to be related to hip fracture, proximal femur shape measured with SSM is also thought to contribute (Baker-LePain et al., 2011) and this in turn may contribute to the known reciprocal relationship between OA and osteoporotic fracture.

With the majority of studies investigating the association between joint shape and OA in older adults and the lack of longitudinal data with sufficient follow up, it is difficult to distinguish shape changes that are the direct result of OA from those that lead to OA development. While it is clear that joint shape can be altered by OA processes (Resnick, 1976), as discussed in section 1.6.7, it has been recognized that abnormalities in hip morphology can also cause hip OA. While on one extreme DDH is known to be associated with early-onset OA it is being increasingly recognized that subtle changes in hip structure and geometry are present in up to 90% of cases with primary hip OA (Khanna & Beaulé, 2014). For example, Lynch et al. reported that variation in hip shape

at baseline (as measured by SSM) was associated with incident RHOA after 8 years follow up in elderly women (Lynch et al., 2009). While it is likely that variation in hip shape contributed to the development of hip OA in this cohort, little is known when these changes develop and how variation in hip morphology is shaped throughout life. Despite the great body of evidence suggesting that subtle architectural changes in hip morphology predate the onset of hip OA, the development of hip shape and factors influencing this process remain poorly understood (Khanna & Beaulé, 2014).

1.10.1. Knowledge gaps to be addressed in this thesis

Despite the well-established relationship between hip shape and OA, little is known about how hip shape develops in childhood and adolescence, which I aim to address by describing sex differences in hip shape at age 14 and 18 (Chapter 3), and its associations with pubertal timing (Chapter 4).

While the inverse relationship between hip fracture and hip OA may in part reflect associations with BMD, relationships with hip shape could also contribute. In addition, BMD and hip shape could be influenced by common pathways, as supported by findings from the recent hip shape GWAS which identified a number of loci previously found to be related to BMD (D. A. Baird et al., 2017). Therefore, a further aim of my thesis is to explore previously unknown relationships between BMD and hip shape (Chapters 5 and 6). Given the genetic influences on BMD which are well recognised, this opens up the possibility of using methods such as MR to explore shared genetic mechanisms between BMD and hip shape, which I also aimed to apply.

In terms of genetic influences on hip shape, previous studies explored the effect of hip morphology in mediating the risk of OA (Lindner et al., 2015), and one previous study explored genetic influences on hip shape in adult cohorts (D. A. Baird et al., 2017). So far, however, no research has been found that explored the genetic influences on hip shape, as quantified by SSM, in adolescents and Chapter 7 will aim to fill this knowledge gap.

1.10.2. Summary and aims of this PhD

Despite many studies investigating the role of hip morphology in the development of OA many questions remain unanswered. Little is known about the development of hip shape in adolescence and it is not clear what factors influence this process. This thesis aims to provide the first characterisation of hip shape development across adolescence as assessed by SSM, based on application to hip DXA scans obtained from ALSPAC offspring at age 14 and 18.

This thesis is composed of eight chapters. The first Chapter introduces the background and aims of this thesis. The second Chapter is concerned with the methodology, whereas Chapters 3 – 7 are the main results chapters (see Figure 1.6 for overview of relationships to be explored during this PhD). The final Chapter draws upon the entire thesis summarizing the key findings, discussing the strengths and limitations of this research and considerations for future.

The specific aims of my research are

- To apply previously developed SSM methodology and adult reference SSM template to hip DXA scans obtained in adolescents at age 14 and 18 (Chapter 2)
- To examine differences in hip shape between age 14 and 18 and describe sex differences in hip shape at these time points. Also, to determine whether sex differences at age 14 and 18 are explained by those in body size (Chapter 3)
- To examine the relationship between pubertal timing (using measures of height tempo) and hip shape at age 14 and 18 (Chapter 4)
- To investigate cross-sectional associations between hip BMD and hip shape in adolescents, and to explore the extent to which common genetic pathways underlie both BMD and hip shape in this group (Chapter 5)
- To investigate cross-sectional associations between hip BMD and hip shape in adult women, and to explore the extent to which common genetic pathways underlie both BMD and hip shape in this group (Chapter 6)

- To identify genetic variants associated with hip shape in adolescents and to determine if genetic variants associated with adult hip shape have similar effects on hip shape in adolescence. Finally, to determine if OA associated variants are also associated with hip shape in adolescents (Chapter 7).

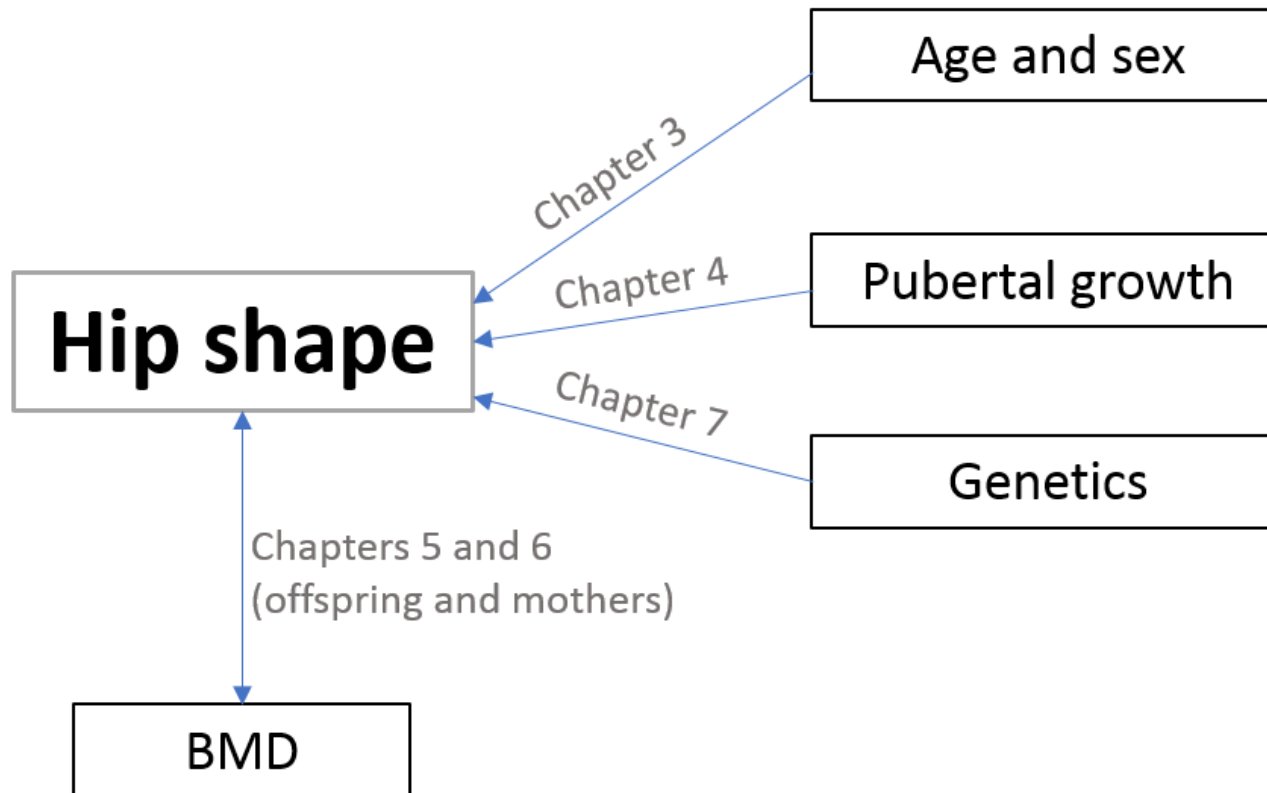


Figure 1.6 Overview of PhD content indicating relationships to be explored during this PhD. Abbreviations: BMD (bone mineral density).

CHAPTER 2. METHODS

In this chapter, I will describe the data and methodology that were used to quantify the shape of proximal femur. Sections 2.1 and 2.2 will describe ALSPAC cohort and data used throughout this thesis. Section 2.3 of this chapter will introduce Statistical Shape Modelling and the technical steps involved in this process. Section 2.4 will describe steps undertaken to apply Statistical Shape Model (SSM) to data from ALSPAC adolescents and model checking. Section 2.5 will describe how external adult reference SSM was applied to ALSPAC data. Finally, Section 2.6 will describe the statistical methods that were used throughout this thesis.

2.1. Cohort description

2.1.1. ALSPAC cohort

The Avon Longitudinal Study of Parents and Children (ALSPAC) is a birth cohort which was initially established to investigate factors influencing child health and development. All pregnant women resident in the county of Avon, South West of England, with expected delivery date between 1st April 1991 and 31st December 1992 were eligible to participate. A total of 14,541 pregnancies were initially enrolled (for details see www.alspac.bris.ac.uk), of these 68 have no known birth outcome, 195 were twin, 3 were triplet and 1 was quadruplet; accounting for 14,676 known foetuses. This resulted in 14,062 live births of whom 13,988 were alive at 1 year of age.

In addition to the initial enrolment that took place between 1991 and 1992, further recruitment took place when the children were on average 7 years old, and another from age 8 onwards to which eligible children and those not initially enrolled were also invited. This resulted in a total of 15,247 pregnancies enrolled (Boyd et al., 2012). Since recruitment these children have been followed up at regular intervals; questionnaire and clinical assessment data have been collected. Moreover, additional data on siblings, mothers and their partners, have also been collected.

The ALSPAC cohort provides a unique opportunity to investigate the environmental and genetic influences on hip shape in adolescence due to the wide range of data which has been collected, including genome-wide genotyping data. Since recruitment these children underwent repeated DXA scans, which enabled me to quantify hip shape at two time points and investigate a range of environmental and genetic influences on hip shape in adolescence.

2.1.2. Ethical approval

Written informed consent was collected for all participants in line with the Declaration of Helsinki (Rickham, 1964). Ethical approval for the study was obtained from the ALSPAC Ethics and Law Committee and the Local Research Ethics Committees (North Somerset & South Bristol Research Ethics Committee: 08/H0106/96). The current project, B2325, has been approved by the ALSPAC executive committee.

2.2. Data

2.2.1. Outcome – hip shape

2.2.1.1. ALSPAC offspring

The majority of data that contribute to this thesis were collected during two separate assessment clinics. These included Teen Focus (TF) 2 and TF 4 clinics. TF 2 was carried out between January 2005 and September 2006. The target age for attendance was 13.5 years (mean age at attendance was 13.8 years, range 12.5 – 15.1 years). Of 11,351 individuals invited to TF 2 clinic, 6,147 attended. TF 4 clinic started in December 2008 and was completed by early to mid-2011. The target age for attendance was 17.5 years (mean age at attendance was 17.8 years, range 16.2 – 19.8 years). Of 10,101 individuals invited to TF 4 clinic, 5,217 attended.

In order to quantify the shape of proximal femur all hip DXA images collected during these clinics were securely sent to collaborators in Aberdeen for image processing and subsequent upload in Shape software (University of Aberdeen, UK). Data generated in Shape was then linked with other ALSPAC variables and all analyses were performed in singletons. The section below describes the data that were available to quantify hip shape at each time point.

1. Hip shape at age 13.8 years

A total of 6,162 images were available to align in Shape (please note that some participants underwent repeat DXA scans to assess data precision, hence the number of images that were uploaded into Shape is higher than the number of participants who attended the clinic). Of those, 268 were excluded due to poor image quality, 171 were duplicate scans (either from twins, siblings or repeat scans) and 1,255 were not aligned due to time constraints (data restricted to include individuals who had both, genetic data and DXA image acquired at TF 4 clinic) (see Table 2.1 for more details). The final dataset, and hence final Statistical Shape Model (SSM) was based on 4,468 images.

2. Hip shape at age 17.8 years

A total of 4,746 images were available to align in Shape (Table 2.2). Of those, 333 were excluded; 218 due to image anomalies, 115 were duplicate scans (either from twins, siblings or repeat scans). The final dataset was based on 4,413 images.

2.2.1.2. ALSPAC mothers'

Hip DXA data were also collected during the Focus on Mothers 1 (FoM1) research clinic. This clinic was held between 2008 and 2011, ~16 – 20 years postpartum. All eligible women (i.e., still engaged with the study; alive with known contact details and who had not withdrawn their consent) were invited to take part. Of 11,264 women invited, 4,834 attended.

A total of 4,631 hip DXA images were available for marking up in Shape and of those 28 were excluded due to image anomalies leaving a total of 4,603 images available for subsequent analysis (Table 2.3). Hip morphology was quantified in the same way as adolescent images (see section 2.3 of this chapter) and adult reference SSM (described in Chapter 2, section 2.5) was then applied to enable direct comparison between adolescent and adult results.

Table 2.1; ALSPAC offspring hip shape data at age 14

Description	N
Total number of images uploaded in shape	6,162
Excluded twins, sibs and re-invites	171
Excluded images without genetic or TF4 data	1,255*
Excluded images due to poor image quality	268
Total hips aligned	4,468
Of those, with genetic data	3,929
Of those, with TF4 data	3,188

*Due to delay in image acquisition and given the time constrains, half way through image alignment it was decided to restrict alignment of the remaining images to those who had both, genetic data and DXA image acquired at TF 4 clinic.

Table 2.2; ALSPAC offspring hip shape data at age 18

Description	N
Total number of images uploaded in shape	4,746
Excluded twins, sibs and re-invites	115
Excluded images due to poor image quality	218
Total hips aligned	4,413
Of those, with genetic data	3,198

Table 2.3; ALSPAC mothers' hip shape data

Description	N
Total number of images uploaded in shape	4,631
Excluded images due to poor image quality	28
Total hips aligned	4,603
Of those, with genetic data	3,111

2.2.2. Exposure and covariate data

2.2.2.1. ALSPAC offspring

Age at clinic attendance

Participant age was calculated as the difference between the date of attendance and date of birth for both TF2 and TF4.

Sex

Data on sex were obtained from hospital birth records.

Anthropometry

Total body (TB) lean and fat mass (kg) along with total hip and femoral neck (FN) bone mineral density (BMD) (g/cm^2) were measured using DXA scans, performed using a GE Lunar Prodigy (Madison, WI, USA). Scans were analysed according to the manufacturers' standard scanning and positioning protocols.

Height was assessed at the time of the DXA scan. It was measured to the nearest 0.1 cm using a Harpenden stadiometer with shoes removed.

Age at peak height velocity (aPHV)

aPHV was estimated from serial height measurements collected during assessment clinics (from age 5 to 20 years). These clinics encompassed 'children in focus clinics' (CIF) to which a random 10% subsample of children were invited between the age 2 and 5

years annual clinics in late childhood (between age 7 and 13 years), three further assessment clinics in adolescence (ages 13, 15 and 17 years). This method is described in more detail in Chapter 4.

Tanner stage assessment

Pubertal status in ALSPAC offspring has been assessed via sex-specific questionnaires, which were repeatedly sent out to participants (between ages 8 - 17 years). See Table 2.4 for details regarding the frequency at which Tanner questionnaires were sent out and the frequency of responses. These questionnaires consisted of a set of line drawings representative of the Tanner stages, as described by Marshall and Tanner (Marshall & Tanner, 1969, 1970), for breast size (sent to females only), genitalia (sent to males only) and pubic hair development (sent to both, males and females). Tanner stage categories are on a scale 1 to 5, with 1 indicating pre-adolescent stage prior to puberty onset, and stage 5 indicating mature adult stage.

During the course of pubertal assessment an issue with genital stage assessment in males was noticed, whereby males went backwards in genital stage when the data was assessed longitudinally. Therefore, pubertal status based on pubic hair development only was used in this thesis in order to aid comparability between males and females.

Table 2.4; Number of puberty questionnaires sent to ALSPAC participants and number of questionnaires returned

Target age (years)	Sent questionnaires	Returned questionnaires
	N	N
8	11,414	6,192
9	11,000	7,020
10	10,450	6,348
11	10,312	6,054
13	10,143	5,801
14	9,947	4,938
15	5,149*	4,637
16	9,534	4,553
17	9,357	4,177

*please note that the questionnaires were only sent to study children who made an appointment for Teen Focus 3 and Teen Focus Express assessment clinics

2.2.2.2. ALSPAC mothers

Age at clinic attendance

Mothers' age was calculated as the difference between the date of clinic attendance and date of birth.

Anthropometry

Total body (TB) lean and fat mass (kg) along with total hip and femoral neck (FN) BMD (g/cm²) were measured using DXA scans, performed using a GE Lunar Prodigy (Madison, WI, USA). Scans were analysed according to the manufacturers' standard scanning and positioning protocols.

Height was assessed at a time of the DXA scan. It was measured to the nearest 0.1 cm using a Harpenden stadiometer with shoes removed.

2.2.3. Genotyping and imputation

Information regarding genotyping and imputation was taken from the ALSPAC data description as previously referred to in other studies (H. J. Jones et al., 2016; Taylor et al., 2018).

A total of 9,912 ALSPAC children were genotyped using the Illumina HumanHap550 quad genome-wide SNP genotyping platform (Illumina Inc., San Diego, CA, USA) by 23andMe subcontracting the Wellcome Trust Sanger Institute, Cambridge, UK and the Laboratory Corporation of America, Burlington, NC, USA. PLINK v1.07 was used for quality control (Purcell et al., 2007) and individuals were excluded on the basis of gender mismatches, minimal or excessive heterozygosity, disproportionate levels of individual missingness (>3%), evidence of cryptic relatedness (>10% of alleles identical by descent (IBD)), and being of non-European ancestry (assessed by multidimensional scaling analysis seeded with HapMap2 individuals). SNPs with a minor allele frequency of <1% and call rate of <95% were removed and only SNPs that passed an exact test of Hardy–Weinberg equilibrium (HWE) ($P > 5 \times 10^{-7}$) were included in the analysis.

ALSPAC mothers were genotyped using the Illumina human660W-quad array at Centre National de Génotypage (CNG) and genotypes were called with Illumina GenomeStudio. PLINK (v1.07) was used to carry out quality control measures on an initial set of 10,015 subjects and 557,124 directly genotyped SNPs. SNPs were removed if they displayed more than 5% missingness or a Hardy-Weinberg equilibrium p value of less than 1.0×10^{-6} . Additionally, SNPs with a minor allele frequency of less than 1% were removed. Samples were excluded if they displayed more than 5% missingness, had indeterminate X chromosome heterozygosity or extreme autosomal heterozygosity. Samples showing evidence of population stratification were identified by multidimensional scaling of genome-wide identity by state pairwise distances using the four HapMap populations as a reference, and then excluded. Cryptic relatedness was assessed using an IBD estimate of more than 0.125 which is expected to correspond to roughly 12.5% alleles shared IBD or a relatedness at the first cousin level. Related subjects that passed all other quality control thresholds were retained during subsequent phasing and imputation. 9,048 subjects and 526,688 SNPs passed these quality control filters.

A total of 477,482 SNP genotypes in common between the sample of ALPSAC mothers and children were combined. SNPs with genotype missingness >1% were removed. Data imputation was performed using Impute2 v2.2.2 software against the 1000 genomes reference panel (phase 1, version 3) using 2186 haplotypes from all populations (haplotype release date Dec 2013), which resulted in 28,699,419 SNPs available for analysis. A total of 8,237 unrelated children and 8,196 mothers with available genotype data were available for analysis.

2.3. Defining and quantifying proximal femur shape

2.3.1. Statistical Shape Modelling

Bones are complex objects with considerable variation observed between individuals which can be attributed to anatomical differences, environmental and genetic influences or be a consequence of a disease process. Traditionally these differences have been assessed by measuring lengths and angles e.g. femoral neck width or neck-shaft angle, which have been described in more detail in the previous chapter (Chapter 1, section 1.7.4.1). However, it has been recognized that single geometrical measurements are often correlated with measures of body size and often highly correlated with other geometrical indices. On the other hand, Statistical Shape Analysis provides the means for capturing global shape of an object as opposed to a single geometrical measurement and can often represent a combination of several different aspects of proximal femur shape (such as variation in femoral neck along with variation in femoral head). It uses a set of landmark points to describe an outline of an object. This concept was validated by Cootes et al. (Cootes et al., 1995) who built on previous work by Kass et al. (Kass et al., 1988). This approach is used to study, describe and compare variations in anatomical shapes within and across different groups and it has been successfully applied to quantify variation in proximal femur shape and predict risk of fracture (Baker-LePain et al., 2011) and progression to THR (Gregory et al., 2007) as described in Chapter 1, section 1.9.

2.3.2. Definition of shape

According to Dryden & Mardia (Dryden & Mardia, 1998) shape can be defined as "all the geometrical information that remains when location, scale and rotational effects are filtered out from an object". In other words, an objects' shape is invariant under Euclidean transformation which preserves its angles and distances. In order to precisely describe shape, a set of points (referred to as landmarks) are identified and located around the object. A landmark can be defined as "a point of correspondence on each object that matches between and within populations" (Dryden & Mardia, 1998). These consist of points that are placed at easily identifiable anatomical features of an object at biologically meaningful locations (anatomical landmarks), points with mathematical or geometrical properties i.e. at a point of high curvature (mathematical landmarks), and the remaining points which are placed between anatomical or mathematical landmarks (pseudo-landmarks) (Dryden & Mardia, 1998; Stegmann & Gomez, 2002).

2.3.3. Analytical steps involved in Statistical Shape Modelling

Figure 2.1 shows all landmark points that were used to mark up each hip DXA image in Shape software (University of Aberdeen). Shape mapped points to each image, and these were then manually re-aligned where necessary. The initial model consisted of 58 landmark points to outline the shape of proximal femur including the acetabular sourcil and lesser trochanter. Key landmark points, shown in red, were placed at easily identifiable features and the remaining points, were evenly spaced between them (Figure 2.1). Table 2.5 describes the anatomical positions of each of the key landmark points which are shown in Figure 2.2.

Following placement of landmark points, Procrustes analysis was used to estimate the mean shape. The aim of this step is to first, remove any translational, rotational and scaling information and then align each image as closely as possible. After completing the alignment, PCA was performed to build the Statistical Shape Model (SSM). PCA, which was first introduced by Hotelling in 1933 (Hotelling, 1933), is a method for data dimensionality reduction, producing a set of orthogonal modes of variation known as principal components. Principal components of hip shape, generated by SSM, are referred to as hip shape modes (HSMs) throughout this thesis, which together explain

100% of variance in the data set. The modes are ordered according to the amount of variance explained: the first mode accounts for the largest amount of variance with subsequent modes accounting for less. Each HSM has a mean of zero and unit standard deviation (SD), and each image and consequently individual is assigned a set of values for each HSM which describes the number of SDs away from the mean shape.

Images of poor quality and those with missing key anatomical features (i.e. features required for placement of all landmark points, as shown in Figure 2.1) were excluded from the analysis. Any outliers (images with scores above or below 4 SDs) were checked, re-aligned where necessary and Procrustes analysis and PCA were then repeated. For more details on Procrustes analysis and PCA please refer to Dryden and Mardia (Dryden & Mardia, 1998).

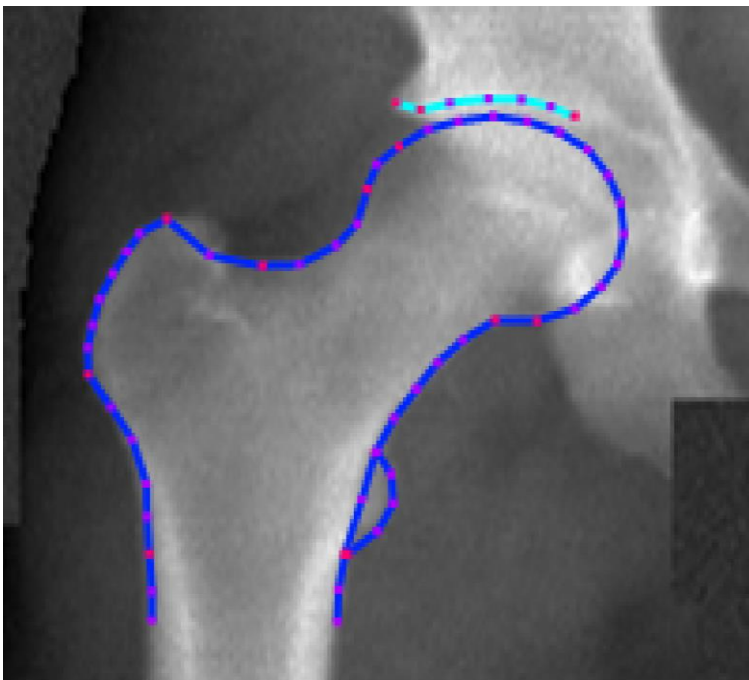


Figure 2.1 Outline of proximal femur shape and point positions

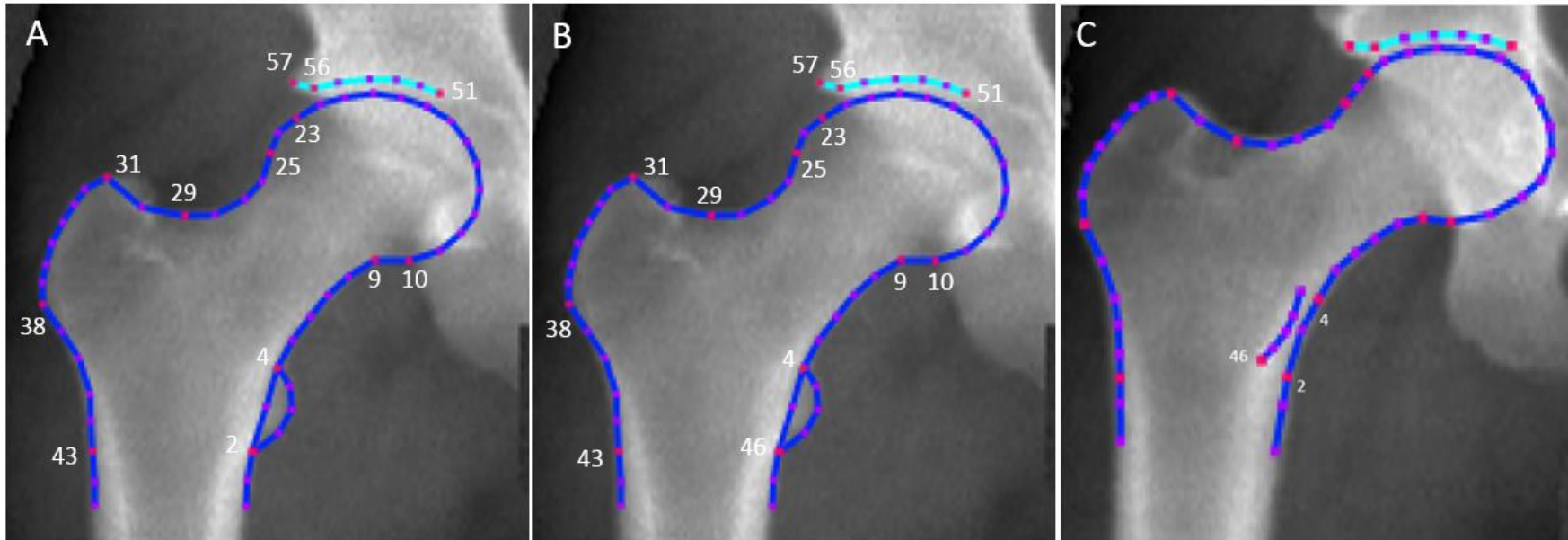


Figure 2.2 Key landmark points. Please note that point 2 (placed on femoral shaft; image A) often maps to point 46 (indicating inferior lesser trochanter; image B). By modelling points 2 and 46 separately, the overlap between the femoral shaft and the lesser trochanter can be visualized as well as the differences between greater and lesser trochanter that can overlap the shaft on 2D images as exemplified on image C.

Table 2.5; Description of the key landmark points shown in red in Figure 2.2

Point number	Anatomical feature
2	Medial femoral shaft meets inferior lesser trochanter (often maps to same position as point 46, depending on orientation)
4	Medial femoral shaft meets superior lesser trochanter
9	Change in curvature: lateral inferior curvature of femoral head at point where it meets femoral neck
10	Change in curvature: medial inferior curvature of the femoral head
23	Change in curvature: superior lateral femoral head curvature
25	Change in curvature: inferior lateral femoral head where meets the superior femoral neck
29	Inferior greater trochanter slope where it meets superior femoral neck
31	Medial superior greater trochanter
38	Inferior lateral greater trochanter
43	Lateral femoral shaft
46	Inferior lesser trochanter (often maps to point 2)
51	Acetabular sourcil medial end (end of brightest line)
56	Acetabular sourcil lateral end
57	Acetabular overhang/osteophyte

2.4. Building the Statistical Shape Model in ALSPAC children

All images uploaded in Shape were aligned by a single person (MF) followed by Procrustes analysis and PCA. Initial model checking (as described in section 2.4.1) and reproducibility (section 2.4.2) were then performed.

2.4.1. Model checking (effect of hip abduction and adduction on hip shape mode scores)

During hip shape alignment, it became apparent that numerous hip DXA images had a degree of abduction and adduction (see Figure 2.3 and Figure 2.4 for examples). It has been suggested that positioning errors during DXA image acquisition may introduce small bias with regards to BMD measurement. For example, a previous study by Lekamwasam et al. reported that external leg rotation by 10° compared with standardized positioning was associated with an increase in femoral neck, trochanter and Ward's area BMD. Whereas, 10° internal leg rotation was associated with a decrease in BMD measurements (Lekamwasam et al., 2003). On the other hand, Ozer et al. found no effect of subtle abduction or adduction on the measurement of BMD (Ozer et al., 2010). However, it is unlikely that positioning errors that were observed in ALSPAC would bias hip shape results as these should be accounted for during Procrustes analysis.

To assess the impact of the positioning errors on the overall model performance and further inform image exclusion criteria when building the final SSM model, abduction and adduction errors were assessed. These errors were assessed visually, based on the assumption that DXA images were acquired according to the manufacturer's standard scanning and positioning protocols. During DXA scan acquisition, the body of a scanned participant should be positioned straight and centered on the scanning table. Subject's leg is rotated inward, and the foot is placed against a positioning device and secured with a strap. If necessary, the leg is adjusted so that the shaft of the femur is parallel to the edge of the table. If these steps are followed correctly, femoral shaft on the DXA image will appear parallel to the edge of the image. Following visual assessment, each image was marked for abduction/adduction. It needs to be noted that the assessment

was subjective (an approach used previously when examining the effect of positioning errors on BMD measurements (McKiernan & Washington, 2005)) and could therefore be less accurate compared with a quantitative assessment of abduction/adduction. Each image was coded in Shape according to the positioning error (see Figure 2.3 and Figure 2.4 for examples of incorrectly vs. correctly (Figure 2.5) positioned hips). The codes were as follows: 1a – slight abduction, 1b – severe abduction, 2a – slight adduction, 2b – severe adduction. All coded images were then excluded to check the impact on model performance and two SSMs were built. The first SSM was based on all DXA images (only excluding images with poor image quality or missing hip components as outlined in section 2.2.1.1 of this chapter). The second SSM excluded images as outlined above and all abducted and adducted hips regardless of the degree of rotation. Scores for the top ten HSMs from each model were cross-correlated.

The proportion of images with positioning errors was 19% and 12% for images collected during TF 2 and TF 4 clinics, respectively (Table 2.6). Variance explained by the first ten HSMs (based on TF 4 data) in the model based on all images vs model based on exclusions was very similar, 83.6 vs 82.2% respectively (Table 2.7).

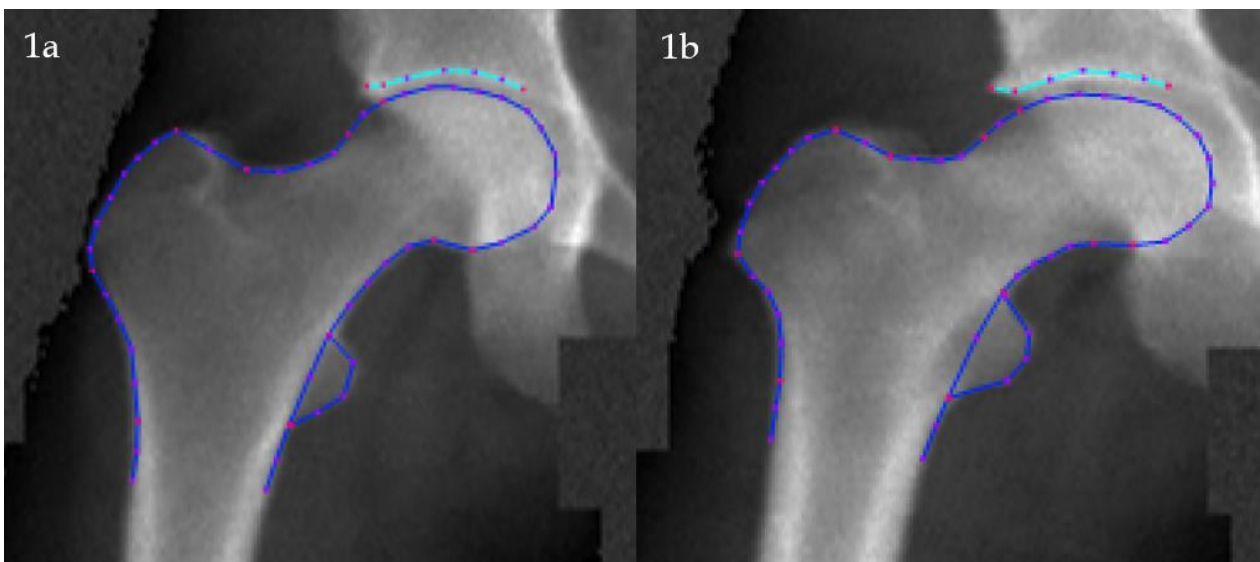


Figure 2.3 Example of hip abduction on DXA images. Left hand side represents lower degree of abduction. Right hand side represents higher degree of abduction

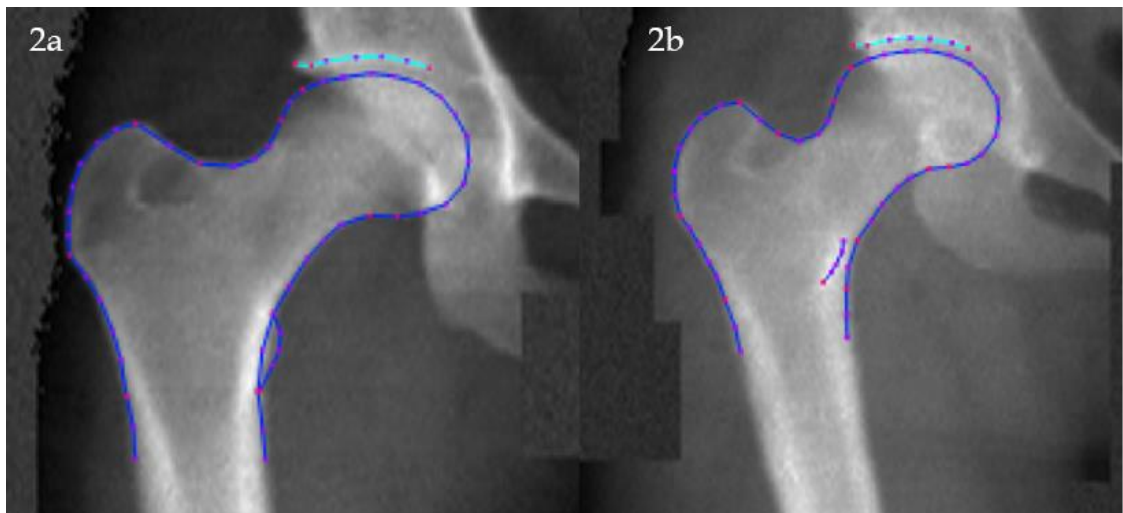


Figure 2.4 Example of hip adduction on DXA image. Left hand side represents lower degree of adduction. Right hand side represents higher degree of adduction

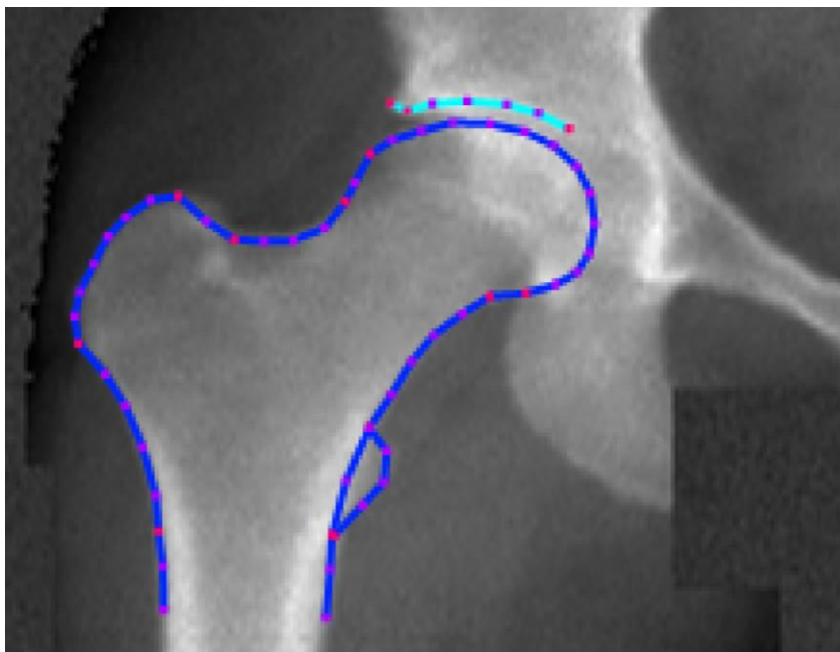


Figure 2.5 Example of correctly positioned hip

Table 2.8 shows cross-correlations between the top ten HSMs for SSM based on all images vs. SSM with exclusions. As demonstrated, correlations for the first eight HSMs were very high (correlation coefficient ≥ 0.95). HSM10 from the model based on all images correlated well with HSM9 based on model with exclusions. Correlations between HSM10 based on SSM with all images vs. HSM10 based on SSM with exclusions

was very weak (correlation coefficient = 0.36). It appears that the variation in HSM10 based on SSM with exclusions is captured by both HSM9 and HSM10 based on SSM with all images included. It is worth noting that variance explained by the latter modes, from mode 9 onwards, is very small (less than 3%). These results are in-keeping with a previous study where the effect of rotation on hip shape measurement was assessed and the authors concluded that rotation not exceeding a few degrees had little impact on variation in hip shape measurement (Pavlova et al., 2017).

Given the high concordance between HSM scores based on these two SSMs, only scans with anomalies (such as poor image quality or missing features from the image) were subsequently excluded when building SSMs. Consequently, the impact of subtle positioning errors was not assessed in mothers' data.

Table 2.6; Number of hips with positioning errors

	Age 14 (TF 2)	% of total images (N=4,468)	Age 18 (TF 4)	% of total images* (N= 4,528)
No. of images with slightly abducted hip (1a)	331	7.4	206	4.5
No. of images with severely abducted hip (1b)	345	7.7	109	2.4
No. of images with slightly adducted hip (2a)	154	3.4	172	3.8
No. of images with severely adducted hip (2b)	39	0.9	44	0.9
Total	869	19	531	11.7

* Number of images after excluding images of poor quality only (N= 218)

Table 2.7; Percentage of hip shape variation at age 18 (TF 4) explained by the top 10 HSMs in SSMs based on all images vs. SSM which excluded hips with positioning errors

	SSM based on all images	SSM with exclusions
HSM	% variance	
1	29.7	29.3
2	16.5	16.5
3	10.0	9.3
4	7.3	7.4
5	5.1	4.8
6	3.8	4.2
7	3.5	3.2
8	3.0	2.7
9	2.6	2.5
10	2.2	2.4
Total variance	83.6	82.2

Table 2.8; Cross-correlations between the top ten HSMs based on SSM built on all images vs. SSM built after excluding images with positioning errors

	HSM1_ex	HSM2_ex	HSM3_ex	HSM4_ex	HSM5_ex	HSM6_ex	HSM7_ex	HSM8_ex	HSM9_ex	HSM10_ex
HSM1	1	-0.01	0	-0.01	0.01	0	0	0	0	0
HSM2	0.02	1	0	0.02	0	0	0	0	0	0
HSM3	0	0.01	-0.98	-0.21	0.04	0.03	-0.01	0	0.01	0
HSM4	0.04	-0.04	-0.27	0.95	-0.1	-0.03	0.02	0	-0.01	0.01
HSM5	-0.03	0	0.03	0.17	0.98	-0.02	0.01	-0.01	0.02	-0.03
HSM6	-0.04	0.01	0.07	0.09	0.03	0.97	-0.07	-0.02	0.05	0.05
HSM7	0	0.01	-0.01	-0.06	-0.01	0.11	0.99	-0.03	-0.07	0.02
HSM8	0.01	0	-0.01	0.01	0.02	0.08	0.01	0.99	-0.09	-0.04
HSM9	-0.04	0.02	0.02	0	0.01	-0.31	0.13	0.2	0.63	0.35
HSM10	-0.01	0	-0.01	-0.04	0.08	-0.13	-0.05	0.01	-0.82	0.36

2.4.2. Repeatability and reproducibility of point placement

Data from the TF4 (which I aligned in Shape first) was used to assess repeatability and reproducibility of point placement as part of the SSM method described above.

From a total of 4,746 hip DXA scans collected during TF 4 clinic which were available in Shape, a set of 100 images were randomly selected and marked 2 months after completing the initial point placement. The same set of images was also marked by a second marker (DB). Intra- (within-) and inter-observer (between-observer) repeatability of manual point placement was measured as the difference in pixels between coordinates of 58 points using Matlab version R2015a. The intra- and inter-observer reliability assessed by mean point-to-point repeatability was 1.22 and 1.78 pixels, respectively. Compared with results from another study using High Bone Mass cohort based on radiographic images, the mean inter-observer reliability (images marked by AJ and DB) was 1.56 pixels. Given the higher resolution of X-ray images, the inter-rater error was comparable with our result (based on DXA images). A cut off median point-to-point difference of less than or equal to 3 has previously been considered as accurate (Faber et al., 2017) .

The mean intra-observer point-to-point repeatability values ranged from 0.61 to 2.18 pixels (Figure 2.6). The highest values: 2.18, 1.97 and 1.65 were recorded for points 51, 52 and 53 respectively, which are placed at the medial end of acetabular sourcil. The mean inter-observer repeatability values ranged from 0.96 to 2.92 pixels. Figure 2.7 shows points with inter-observer repeatability scores higher than 2 pixels (points 0, 21, 24 -27, 31, 32, 42 -46), of those majority were pseudo-landmarks which are placed between key landmark points.

The above results are based on the 58-point model that was available at the beginning of my PhD. However, this was subsequently modified by the Aberdeen group to a 53-point model due to high variability in points placed at the acetabular overhang (point 57), and medial and lateral femoral shaft (points 0, 1, 44 and 45), which also scored high when assessing inter-observer repeatability for TF 4 images. My subsequent analyses were also based on this modified 53-point model.

Before alignment of the offspring data, I marked up a set of 100 hip images (not from ALSPAC cohort) to ensure that accuracy of point placement was maintained. Please note that subsequent repeatability and reproducibility of point placement was only performed using adolescent images from the TF4 assessment clinic, as described above.

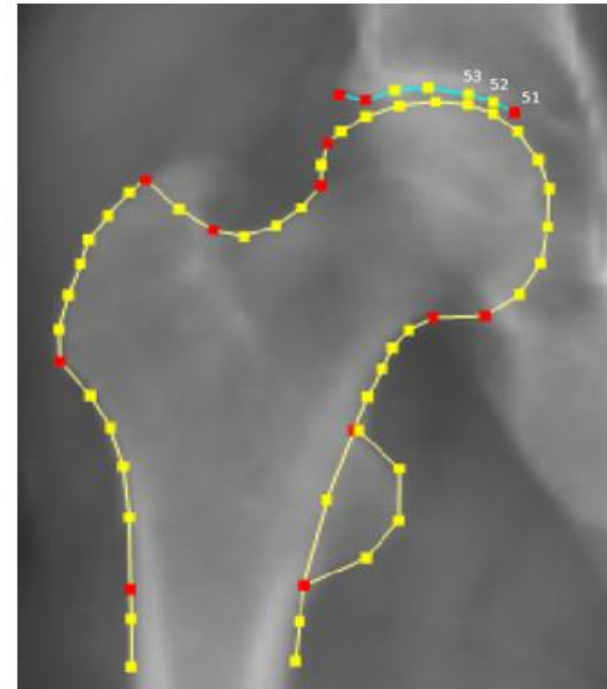
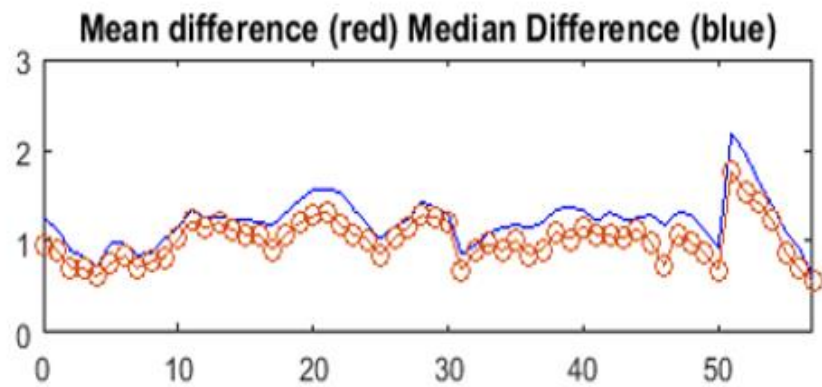


Figure 2.6 Intra-observer repeatability assessed by mean point-to-point repeatability showing mean and median differences in pixels for each point and right-hand figure showing points with the highest intra-observer repeatability error values

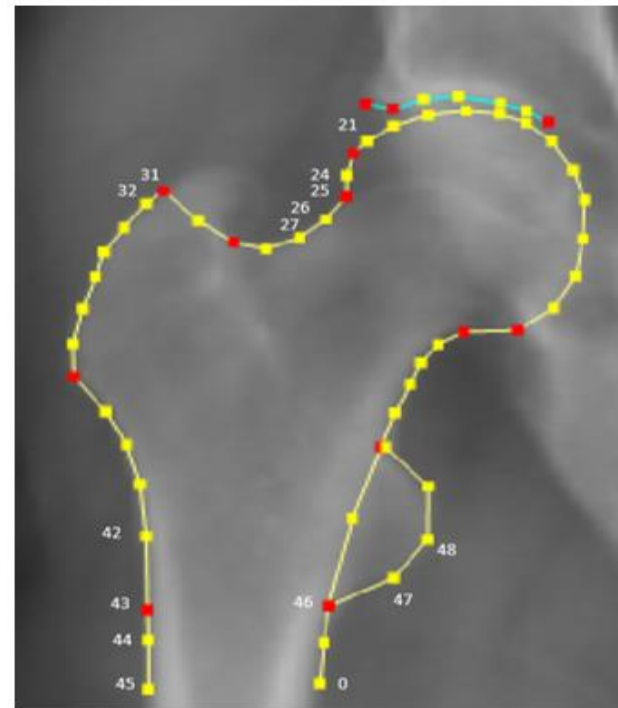
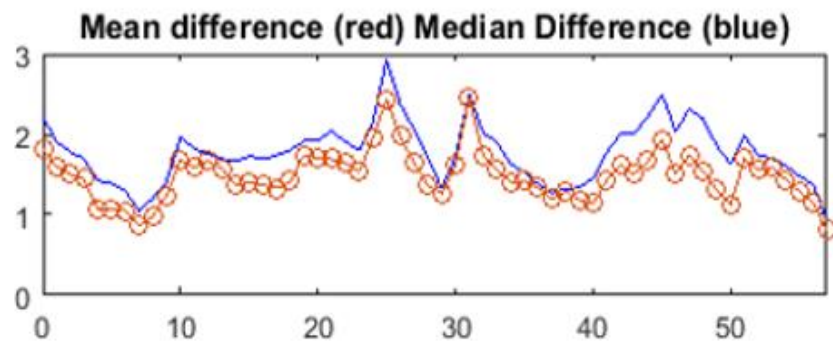


Figure 2.7 Inter-observer repeatability assessed by mean point-to-point repeatability showing mean and median differences in pixels for each point and right-hand figure showing points with the highest intra-observer repeatability error values (>2 pixels)

2.4.3. SSMs in ALSPAC offspring

Initially, I generated HSMs using the included data as its own reference which gives modes with mean = 0 and SD = 1. Similarly to previously published literature (Baird et al., 2018; Faber et al., 2017; Pavlova et al., 2017) the first 10 modes, which together explained 85% and 84% of variance at age 14 and 18 respectively, were selected. In addition, higher modes (>10) can often be regarded as noise as each subsequent mode explained less than 2% of variance at both time points.

Figure 2.8 and Figure 2.9 show variation in hip shape described by the top ten HSMs based on images collected at age 14.

Figure 2.10 and Figure 2.11 show variation in hip shape described by the top ten HSMs based on images collected at age 18.

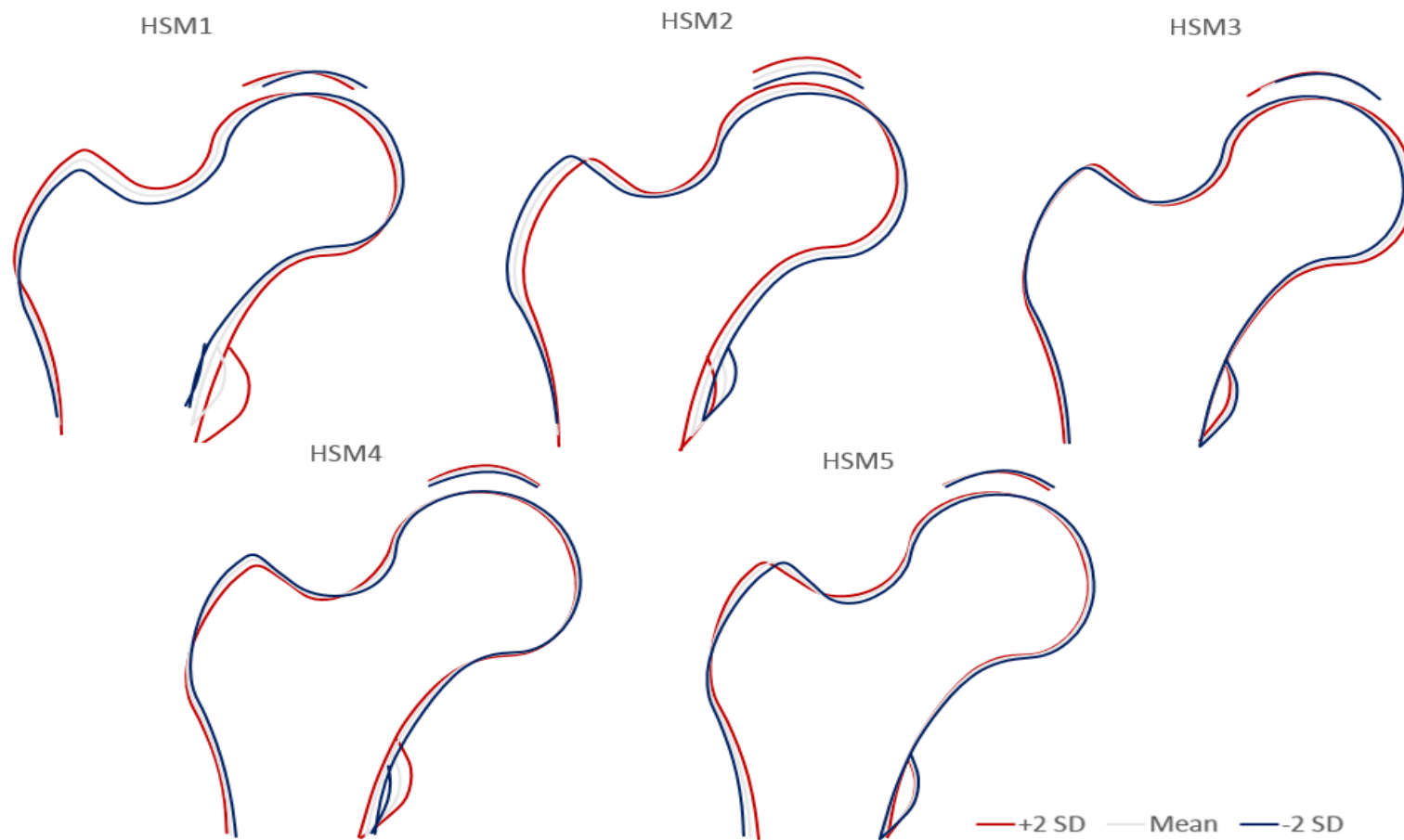


Figure 2.8 Variation in hip shape described by modes 1 - 5 at age 14 (SSM based on age 14 images)

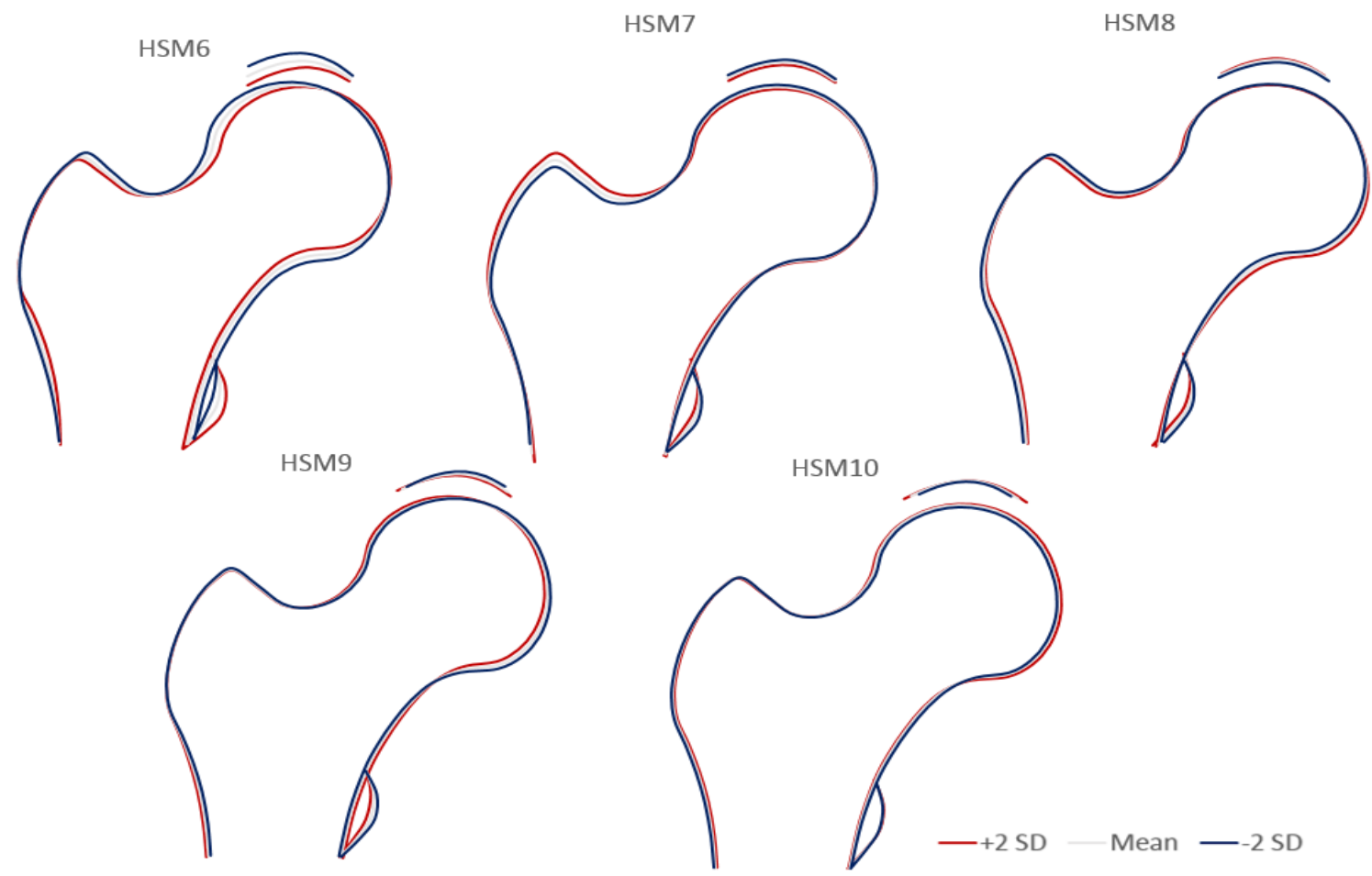


Figure 2.9 Variation in hip shape described by modes 6 -10 at age 14 (SSM based on age 14 images)

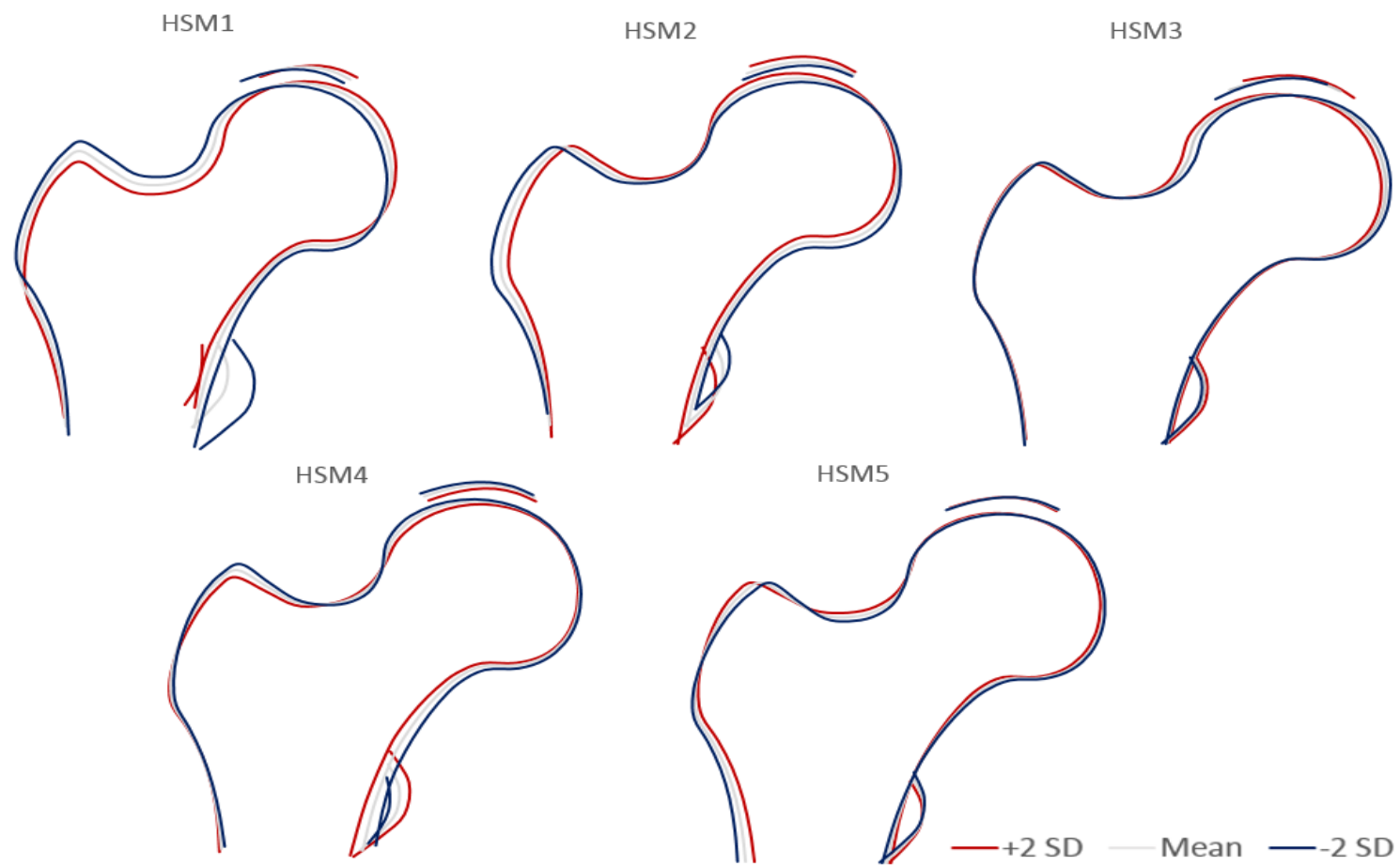


Figure 2.10 Variation in hip shape described by modes 1 - 5 at age 18 (SSM based on age 18 images)

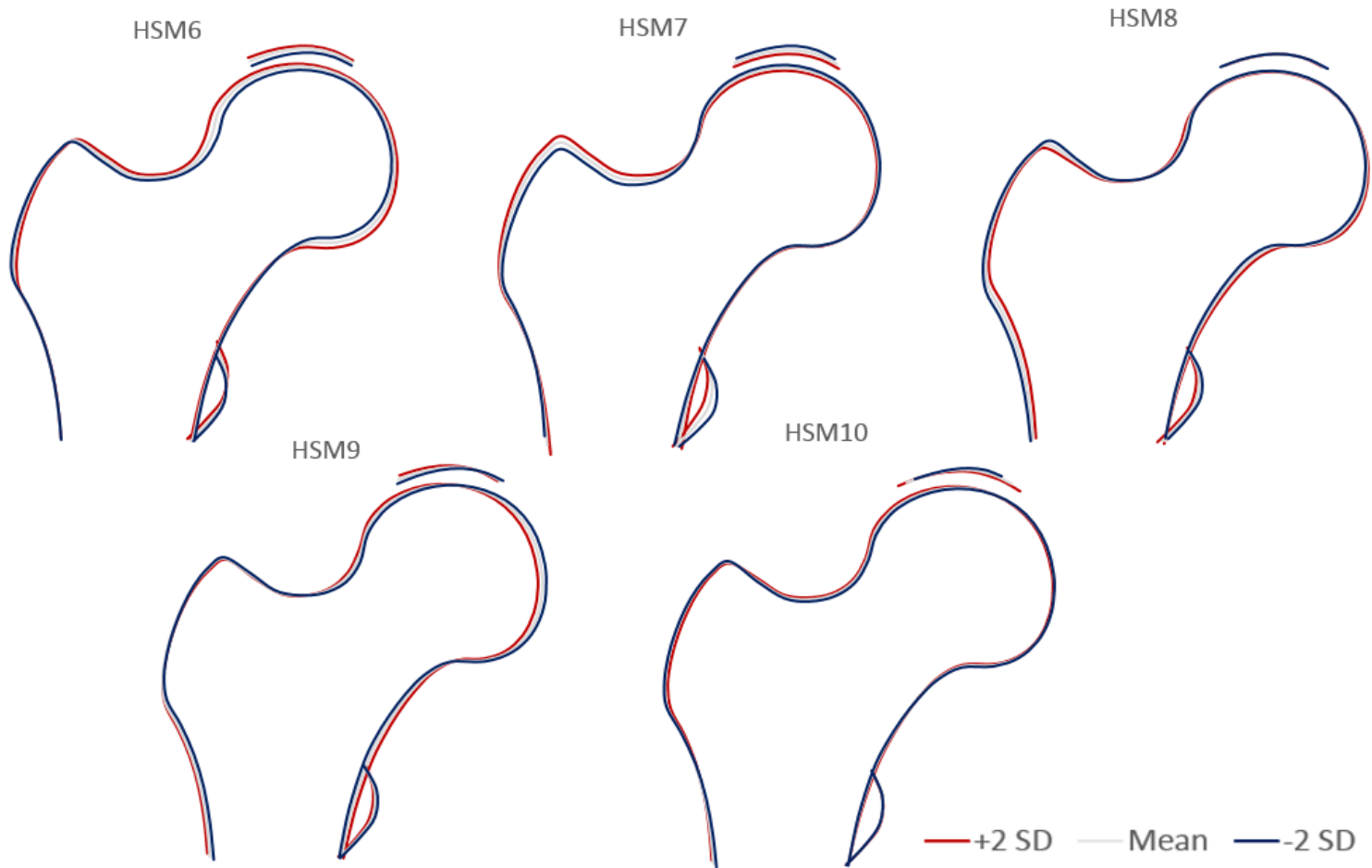


Figure 2.11 Variation in hip shape described by modes 6 - 10 at age 18 (SSM based on age 18 images)

2.5. Applying external reference SSM to adolescent HSMs

2.5.1. Building and applying scores from adult reference Statistical Shape Model

One of the limitations of SSM is the lack of comparability of HSMs with other cohorts, since each SSM is unique to that particular set of images. This issue is relevant to my research where I intend to compare hip shape between adolescents of different ages, and adolescent hip shape to that of adults. One way of overcoming this limitation is to apply a set of pre-defined HSMs, previously obtained from a reference population. I decided to apply this approach, based on a reference set generated from a GWAS meta-analysis of hip shape from five cohorts, derived from the same points template to that used to examine adolescent hip shape as part of my thesis. This included the ALSPAC mothers' cohort (Fraser et al., 2013), Framingham (Hannan et al., 2000), Osteoporotic fractures in men study (MrOS) (Blank et al., 2005), the study of Osteoporotic Fractures (SOF) (Cummings et al., 1990) and Twins UK (Moayyeri et al., 2013; Spector & Williams, 2006) resulting in a total of 19,379 images (Table 2.9). These were aligned in Shape and SSM was built as described previously, in section 2.3.3. Briefly, the reference model was built using PCA which allows any new image (set of points) to be used and (after Procrustes analysis) the eigen vectors can be used to calculate the mode scores for any model (without adding the new image to the reference model or changing it in any way).

Table 2.9; Cohorts contributing to the adult reference Statistical Shape Model

Cohort	N	Gender	Mean age (SD) of participants
ALSPAC mothers	4,603	Females	47.9 (4.3)
Framingham	3,088	Males and females	63.3 (11.0)
MrOS	5,924	Males	74.0 (6.0)
SOF	1,715	Females	72.8 (4.6)
Twins UK	4,049	Males and females	52.5 (13.5)
Total	19,379		

Abbreviations: ALSPAC (Avon Longitudinal Study of Parents and Children), MrOS (Osteoporotic fractures in men study), SOF (Study of Osteoporotic Fractures).

2.5.2. Comparing adolescent HSM scores with HSM scores based on adult reference SSM

In order to compare the current SSM based on adolescent images (included as its own reference) with the SSM after applying scores from the combined adult reference model, the first ten HSMs were cross-correlated and means and SDs were calculated.

Mean HSM scores

Compared to mean = 0 and SD = 1 when using the data as its own reference, when using the combined adult reference, means for the first ten HSMs ranged from -1.14 to 2.26 at age 14 and from -1.5 to 2.42 at age 18, whereas SDs ranged from 0.42 to 0.97 at age 14 and from 0.41 to 0.91 at age 18 (Table 2.10). When the adult reference SSM was applied to ALSPAC mothers' images, means for modes 2-9 were close to 0 (ranging from -0.35 to 0.34) and SDs were close to 1 (ranging from 0.8 to 1), whereas mean and SD HSM1 score were 1.45 and 0.5 respectively. These differences, in means and SDs, could be due to sex and/or age differences (i.e. mothers were on average 48 years old, therefore much closely resembling the ages of cohorts included in the reference model as opposed to ALSPAC offspring). The deviation away from the mean was particularly noted for HSM1, in the case of both ALSPAC offspring and mothers, which is likely to reflect scanner differences between ALSPAC and other cohorts in the adult reference set. Different pixel spacing in the Lunar Prodigy scanner (used to acquire DXA scans in ALSPAC) relative to other scanners alters the aspect ratio (ratio between image height and width) and therefore HSM1 reflects these differences. An attempt was made to correct for these differences; however some residual differences still remain. What is more, compared with the other modes, SD for HSM1 appears to be artefactually lowered as the contribution of scanner differences is excluded when looking at a single cohort. In addition, whilst using adult reference SSM is an added advantage, the source of data for limitations of positioning for DXA needs to be carefully considered. For example, to what extent the variation in lesser trochanter size and position represents anatomical variation as opposed to subject positioning during image acquisition, is currently unknown. Whilst in adolescents, rotation of lesser trochanter might reflect a tendency towards joint hypermobility, in older adults, particularly those with hip pain, the degree of hip rotation required for DXA positioning may be limited.

When using adolescent data as its own reference, the percentage of variance explained by the first ten HSMs was 85% and 84% at age 14 and 18, respectively and 81% in ALSPAC mothers (Table 2.11). The variance explained by the first ten modes in the adult reference model was 86%. It is important to note that one limitation of this approach is the fact that I was unable to calculate the exact variance explained in the adolescent and mothers' data after applying the adult reference SSM (also discussed in Chapter 8, section 8.4).

Cross-correlations

The majority of modes based on age 14 images correlated well with HSM scores based on the reference SSM (Table 2.12). For example, HSM1 scores based on the adolescent dataset correlated well with HSM2 scores based on the reference dataset. Variation in shape at age 14 described by the top ten modes is presented in Figure 2.8 and Figure 2.9, and the variation in shape after applying the adult reference model at both time points is presented in Figure 2.12 and Figure 2.13. Although the modes do not directly correlate with each other (i.e. HSM1 does not strongly correlate with HSM1 based on adult reference SSM; HSM2 does not strongly correlate with HSM2 based on the adult reference set and so on), both HSM1 and HSM2 based on the reference SSM describe variation in the same aspects of hip shape, namely greater and lesser trochanters, FNW and femoral head size (especially in the inferior aspect proximal to lesser trochanter). Furthermore, HSM2 correlated well with HSM1 based on the reference SSM and both modes describe variation in femoral head (particularly at the superior aspect proximal to greater trochanter), greater and lesser trochanters and FNW. Table 2.14 shows the summary of key morphological features described by the top ten HSMs based on the combined adult reference model.

At age 18, the majority of modes correlated well with the adult reference HSM scores, except modes 6 and 10 (Table 2.13). Variation in shape at age 18 described by the top ten modes is presented in Figure 2.10 and Figure 2.11, and Figure 2.12 and Figure 2.13 show the variation in shape after applying adult reference model scores. In terms of correlations, HSM1 correlated well with HSM2 based on the reference SSM. HSM3 (Figure 2.10) correlated with both HSM3 and HSM4 based on the reference SSM (Figure 2.12); the common variation described by HSM3 and HSM4 based on the reference SSM

included variation in lesser trochanter and acetabular coverage, while the common variation between HSM3 and HSM4 based on the reference SSM was clearly related to superolateral aspect of femoral head.

As expected, slight differences between the mean adolescent shape and adult shape were observed (i.e. particularly with regards to the shape of greater trochanter as it appeared more pointed in the children compared with adults, and the inferior lateral greater trochanter which was more pronounced in adults compared with adolescents). However, the majority of modes correlated well with HSM scores based on the adult reference SSM and the modes which correlated well with each other described variation in the same aspects of shape.

In addition, when referring to mode scores based on adult reference SSM, the features described by each HSM are the same at both adolescent time points and in ALSPAC mothers (please refer to Supplementary Table 10.1.1 in Appendix 1 for detailed description of the variation described by the top ten HSMs based on the adult reference SSM). This is important particularly when comparing the influence of various exposures on specific aspects of shape across different time points. Therefore, HSM scores based on the reference SSM will be used throughout this thesis.

Table 2.10; Mean HSM scores for the top ten HSMs based on ALSPAC adolescent and mothers' images, after applying adult reference model (compared with mean=0 and SD=1 when data from each time point included as its own reference)

	Age 14	Age 18	Mothers
HSM	Mean (SD)	Mean (SD)	Mean (SD)
1	2.26 (0.42)	2.42 (0.41)	1.45 (0.53)
2	0.57 (0.76)	0.23 (0.85)	-0.01 (0.90)
3	-0.19 (0.68)	0.10 (0.66)	-0.31 (0.92)
4	0.87 (0.68)	0.36 (0.73)	0.32 (0.77)
5	-1.14 (0.79)	-1.50 (0.84)	-0.35 (0.94)
6	0.27 (0.68)	0.27 (0.86)	-0.01 (1.00)
7	-0.25 (0.63)	0.02 (0.70)	-0.14 (0.87)
8	0.39 (0.97)	0.02 (0.91)	0.06 (0.95)
9	0.22 (0.76)	-0.21 (0.91)	0.34 (0.95)
10	-1.09 (0.59)	-1.04 (0.77)	0.11 (0.92)

Table 2.11; Percentage of variance explained by the first ten HSMs by different SSMs

	% variance explained			
HSM	Age 14	Age 18	Mothers	Adult reference SSM
1	28.9	29.7	25.2	42.1
2	19.1	16.5	15.5	13.4
3	9.2	10.0	12.5	8.5
4	7.1	7.3	6.8	6.1
5	6.3	5.1	5.0	4.1
6	5.9	3.8	4.7	3.4
7	2.9	3.5	3.8	2.6
8	2.4	3.0	3.2	2.5
9	1.8	2.6	2.3	1.8
10	1.8	2.2	1.8	1.5
total	85.4	83.6	80.7	86.1

Table 2.12; Correlations between first ten HSMs at age 14 vs. the adult reference model

	HSM1_14	HSM2_14	HSM3_14	HSM4_14	HSM5_14	HSM6_14	HSM7_14	HSM8_14	HSM9_14	HSM10_14
ref_HSM1_14	-0.62	-0.76	0.09	0.14	0.03	0.09	-0.03	0.01	0.02	0.02
ref_HSM2_14	-0.85	0.43	-0.27	-0.01	-0.09	0.08	-0.10	0.03	0.00	0.00
ref_HSM3_14	-0.50	0.46	0.50	0.22	0.48	-0.09	0.05	-0.07	0.01	-0.06
ref_HSM4_14	-0.22	0.15	0.67	-0.43	-0.37	0.39	0.05	-0.03	0.01	-0.03
ref_HSM5_14	-0.63	-0.20	0.06	-0.05	-0.34	-0.56	0.32	-0.02	-0.06	0.00
ref_HSM6_14	0.11	0.25	-0.34	0.42	-0.02	0.45	0.60	0.12	0.14	-0.04
ref_HSM7_14	-0.18	-0.09	0.20	-0.42	0.37	0.17	0.20	0.59	-0.25	0.18
ref_HSM8_14	0.22	0.33	0.43	0.60	-0.47	-0.06	-0.15	0.19	0.00	0.04
ref_HSM9_14	-0.26	0.36	0.09	-0.57	0.06	-0.42	0.07	0.21	0.25	0.12
ref_HSM10_14	0.21	-0.02	-0.14	0.08	0.004	-0.15	-0.12	0.07	-0.70	0.08

Abbreviations: HSM (Hip shape Mode), ref_HSM (Hip Shape Mode, based on SSM to which scores from an adult reference model have been applied)

Table 2.13; Correlations between top ten HSMs at age 18 vs. the adult reference model

	HSM1_18	HSM2_18	HSM3_18	HSM4_18	HSM5_18	HSM6_18	HSM7_18	HSM8_18	HSM9_18	HSM10_18
ref_HSM1_18	0.50	-0.85	-0.01	0.16	-0.04	-0.04	-0.02	0.07	-0.04	0.02
ref_HSM2_18	0.89	0.38	0.20	0.13	-0.02	-0.04	-0.07	0.05	-0.01	0.02
ref_HSM3_18	0.57	0.05	-0.65	0.13	0.36	0.22	0.03	-0.10	0.21	-0.03
ref_HSM4_18	0.31	0.20	-0.77	-0.13	-0.29	-0.35	0.10	0.03	-0.16	0.00
ref_HSM5_18	0.66	-0.26	0.18	-0.31	-0.33	0.28	0.32	-0.20	0.04	-0.11
ref_HSM6_18	-0.33	0.24	0.12	0.73	-0.11	-0.04	0.49	0.05	-0.02	-0.07
ref_HSM7_18	0.20	0.03	-0.27	-0.16	0.38	0.25	0.21	0.57	-0.35	-0.19
ref_HSM8_18	-0.27	0.14	-0.37	0.27	-0.63	0.35	-0.33	0.12	0.09	-0.06
ref_HSM9_18	0.33	0.29	0.07	-0.65	-0.08	0.19	0.24	0.27	-0.01	0.11
ref_HSM10_18	-0.11	-0.03	0.14	0.07	0.07	0.38	-0.33	-0.06	-0.61	-0.36

Abbreviations: HSM (Hip shape Mode), ref_HSM (standardized Hip Shape Mode, based on SSM to which scores from an adult reference model have been applied)

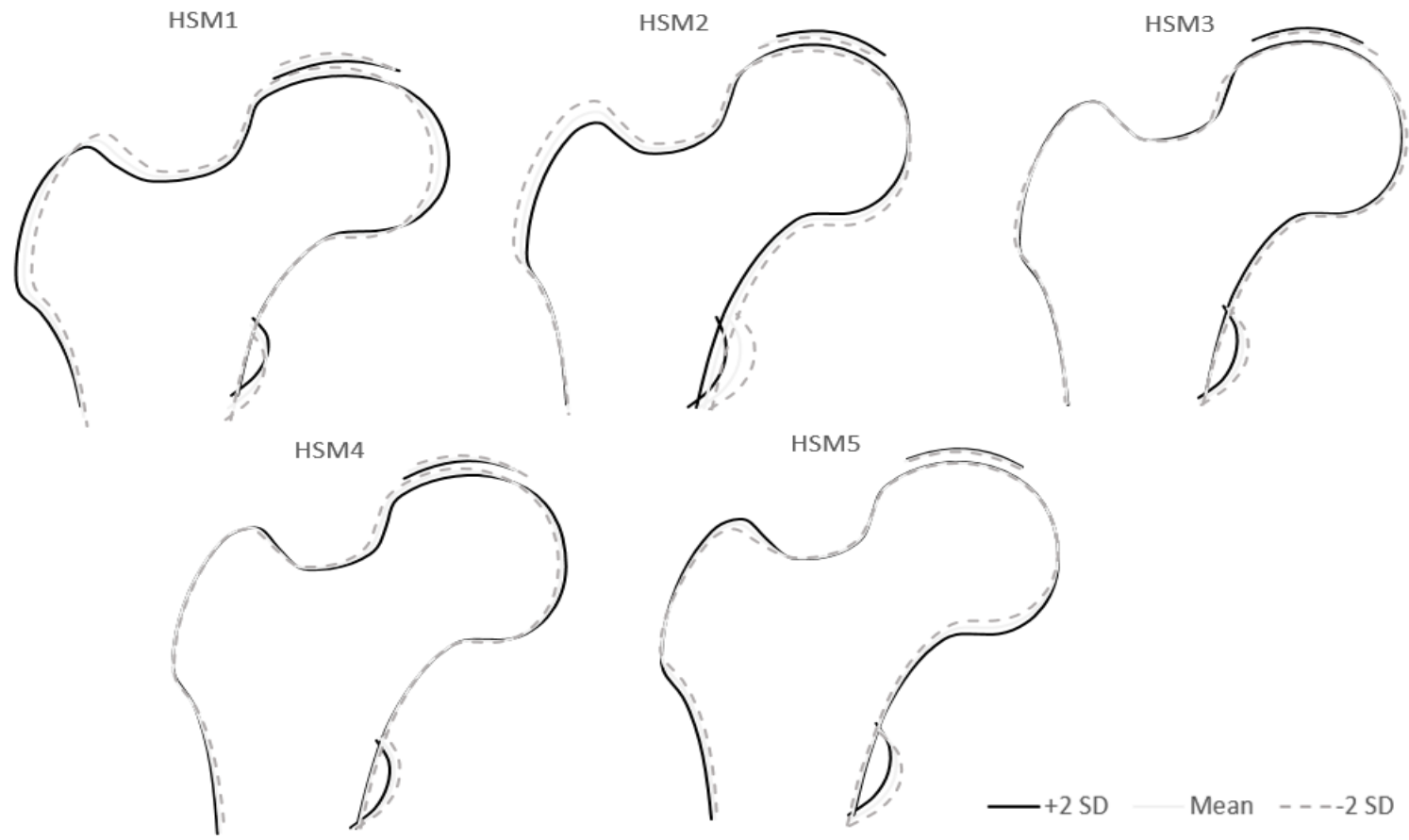


Figure 2.12 Variation in hip shape at ages 14 and 18 described by modes 1 - 5, based on adult reference SSM

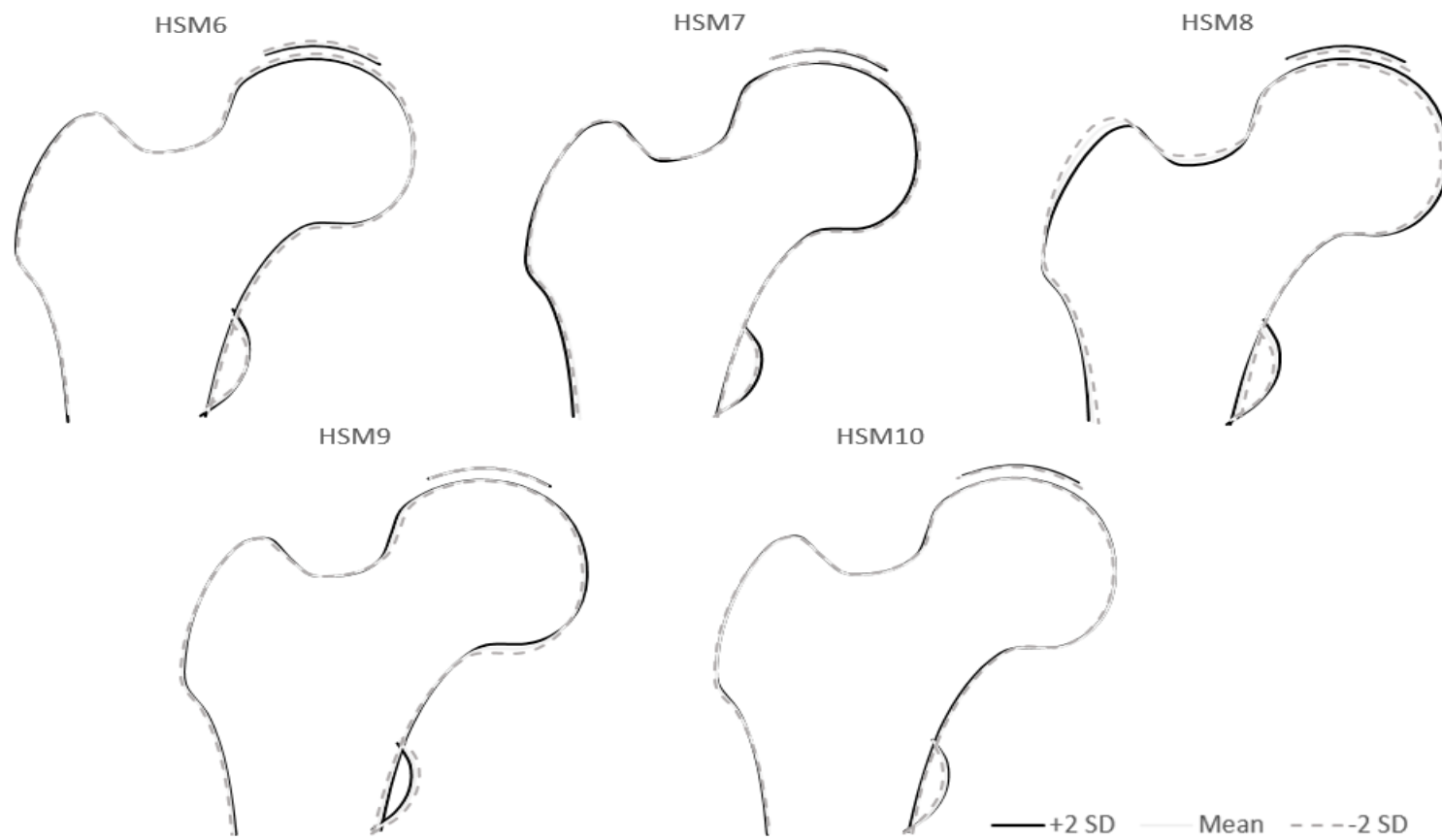


Figure 2.13 Variation in hip shape at ages 14 and 18 described by modes 6 -10, based on adult reference SSM

Table 2.14; Summary of the key morphological features described by the top ten HSMs based on combined adult reference model

HSM	Variation described by each mode
1	Femoral head (most pronounced in the medial aspect, also superolateral and inferolateral aspects), FNW, greater and lesser trochanters
2	Femoral head (inferolateral and superior aspects), FNW, greater and lesser trochanters, neck-shaft angle
3	Femoral head (inferolateral aspect, cam-type deformity), FNW, lesser trochanter
4	Femoral head (superolateral and medial aspects), FNW, lesser trochanter
5	Femoral head (inferolateral aspect), FNW, greater and lesser trochanters, femoral shaft width
6	Femoral head (superior aspect), FNW
7	Femoral head (medial and inferolateral aspect), femoral shaft width and lesser trochanter
8	Femoral head (superior and medial aspects), FNW, greater and lesser trochanters, femoral shaft width
9	Femoral head (superolateral and inferolateral aspects), lesser trochanter
10	Lesser trochanter

Abbreviations: HSM (Hip shape Mode), FNW (femoral neck width)

2.5.3. Checking independence of standardized HSMs

One of the potential issues that may arise after applying an external reference data set to another set of data is that previously independent HSMs might no longer be independent of each other. The greater the differences between the original data and the reference dataset, including different scanners used to acquire the data or differences in age between the cohorts, the greater the potential for modes not being independent of one another. To explore if this is likely to have an important impact on the results, I aimed to quantify the extent of this loss of independence. After applying SSM based on the combined adult reference model to adolescent data Matrix Spectral Decomposition was performed using the matSpD tool (<https://gump.qimr.edu.au/general/daleN/matSpD/>) to compute the number of independent modes.

The top ten HSMs based on adult reference SSM at both time points were first correlated (Table 2.15 and Table 2.16) and tested for the number of independent variables (HSMs) using matSpD. The results showed close to ten (9.6) independent variables for both time points suggesting that the loss of independence is unlikely to materially affect the results. Therefore, given the advantages of using an external reference model (such as direct comparison between time points, as discussed previously in section 2.5.1), I decided to use the results generated for the top ten HSMs using the adult reference template, to use as outcomes throughout this thesis.

Table 2.15; Correlation matrix for the top ten standardized HSM scores at age 14 to assess the number of independent variables using matrix Spectral Decomposition (matSpD) which showed strong evidence for nearly all variables (9.6) to be independent

	HSM1	HSM2	HSM3	HSM4	HSM5	HSM6	HSM7	HSM8	HSM9	HSM10
HSM1	1	0.1853	0.0371	0.0375	0.4698	-0.198	0.1578	-0.272	-0.2019	-0.1227
HSM2	0.1853	1	0.4216	0.131	0.3872	0.0883	0.054	-0.118	0.3098	-0.1471
HSM3	0.0371	0.4216	1	0.2081	0.1451	-0.0381	0.1772	0.144	0.2597	-0.1564
HSM4	0.0375	0.131	0.2081	1	0.0924	-0.1778	0.248	0.1602	0.2208	-0.2277
HSM5	0.4698	0.3872	0.1451	0.0924	1	-0.2271	0.0095	-0.0648	0.3164	-0.0647
HSM6	-0.198	0.0883	-0.0381	-0.1778	-0.2271	1	-0.0972	0.1324	-0.2759	-0.0347
HSM7	0.1578	0.054	0.1772	0.248	0.0095	-0.0972	1	-0.3302	0.2572	0.0019
HSM8	-0.272	-0.118	0.144	0.1602	-0.0648	0.1324	-0.3302	1	-0.191	0.0862
HSM9	-0.2019	0.3098	0.2597	0.2208	0.3164	-0.2759	0.2572	-0.191	1	-0.1126
HSM10	-0.1227	-0.1471	-0.1564	-0.2277	-0.0647	-0.0347	0.0019	0.0862	-0.1126	1

Table 2.16; Correlation matrix for the top ten standardized HSM scores at age 18 to assess the number of independent variables using matrix Spectral Decomposition (matSpD) which showed strong evidence for nearly all variables (9.6) to be independent

	HSM1	HSM2	HSM3	HSM4	HSM5	HSM6	HSM7	HSM8	HSM9	HSM10
HSM1	1	0.141	0.2264	-0.0047	0.4621	-0.2515	0.0537	-0.1779	-0.1618	-0.0226
HSM2	0.141	1	0.3793	0.1983	0.4458	-0.1167	0.1083	-0.1985	0.3159	-0.0712
HSM3	0.2264	0.3793	1	0.4535	0.1827	-0.1872	0.3169	-0.0169	0.0756	-0.1303
HSM4	-0.0047	0.1983	0.4535	1	0.0864	-0.1524	0.1849	0.204	0.1695	-0.2213
HSM5	0.4621	0.4458	0.1827	0.0864	1	-0.3191	0.0347	-0.1862	0.4001	-0.0575
HSM6	-0.2515	-0.1167	-0.1872	-0.1524	-0.3191	1	-0.1257	0.1897	-0.3383	-0.0189
HSM7	0.0537	0.1083	0.3169	0.1849	0.0347	-0.1257	1	-0.1477	0.2756	0.1138
HSM8	-0.1779	-0.1985	-0.0169	0.204	-0.1862	0.1897	-0.1477	1	-0.1628	0.1194
HSM9	-0.1618	0.3159	0.0756	0.1695	0.4001	-0.3383	0.2756	-0.1628	1	-0.0967
HSM10	-0.0226	-0.0712	-0.1303	-0.2213	-0.0575	-0.0189	0.1138	0.1194	-0.0967	1

2.6. Statistical methods

This section describes general statistical methods used in several chapters, more detailed methods description, where necessary, are included in relevant chapters. All analyses were carried out in Stata versions 14.0 and 15.0 (StataCorp, College Station, TX, USA), unless otherwise stated.

2.6.1. Data checking and descriptive statistics

Although ALSPAC data was cleaned and checked prior to data release, each variable was checked for plausibility, for example by checking minimum and maximum values, with any implausible values set to missing. Distributions of continuous variables were assessed by plotting histograms. Descriptive statistics are presented as means and SDs. Frequency statistics for categorical variables are presented as percentages.

2.6.2. Regression analysis

Observational associations between exposures of interest and the top ten HSMs were investigated using linear regression. As discussed below, adjustment for confounders was based on previous literature. For a variable to be a confounder it must be associated with the outcome and with the exposure, in addition it must not lie on the causal path from the exposure to outcome (Suttorp et al., 2014). While possible to assess statistically, these assumptions should be based on prior knowledge rather than the strength of statistical associations. Age, height, lean and fat mass were considered to be *a priori* confounders for analyses carried out in Chapters 3, 5 and 6, whereas analysis in Chapter 4 adjusted for fat mass index (FMI). Given the sex differences in hip shape described in Chapter 3, analyses in Chapters 4-6 were additionally adjusted for sex.

Age is an important determinant of hip shape and a previous study describing femoral morphology in Spanish adolescents showed that the size and shape of the femur varied with age in both, males and females (Pujol et al., 2014; Pujol et al., 2016). Therefore, age was also adjusted for except in studies of puberty effects as described in Chapter 4. The role of mechanical loading in the developing skeleton is well-recognized (Frost,

1987; Moro et al., 1996) and body size, in particular higher body weight, is thought to increase the strain placed on the bone thus stimulating bone remodelling (Timpson et al., 2009). Previous studies showed that adjustment for height and weight partially explained differences in hip geometry in individuals over 20 years of age (Looker et al., 2001), and higher BMI was associated with femoral morphology (as measured by alpha angle, head-neck offset, tilt angle, epiphyseal angle, and epiphyseal extension on CT images) in adolescents aged 15 +/- 1.95 years (Novais et al., 2018). While body size (weight and height) is thought to influence the development of the skeleton, the effects of body weight are more accurately explored by examining distinct influences of fat and lean mass (Ho-Pham et al., 2014) and previous studies reported that sex differences in hip geometry attenuated following adjustment for height, lean and fat mass (Forwood et al., 2004; Sayers et al., 2010).

Previous studies suggest that fat mass or BMI affect the onset of puberty in males and females (Kaplowitz, 2008), therefore analyses in Chapter 4 adjusted for FMI (independent of height) (for more details please refer to Chapter 4, section 4.2.2.3).

All analyses were restricted to individuals who had complete data on the outcome, exposure and covariates. Overall, children attending TF 2 and TF 4 clinics were more likely to be white and of female sex compared with those who did not attend (Table 2.17 and Table 2.18). Please note that the number of individuals included in each of the analyses in the results chapters varies. This is due to sources of data available for each participant. For example, in Chapter 4, which looked at the relationship between age at peak height velocity (aPHV) and hip shape, fewer participants had complete data on the exposure as estimation of aPHV required repeated height measurements compared with i.e. BMD measurement which was assessed at a time of a DXA scan. Figure 2.14 shows participants included in the ALSPAC study and numbers of participants which were included in the analyses in the results chapters.

The first ten HSMs were used as outcomes in all analyses.

Table 2.17; A comparison of characteristics between adolescents who did and did not participate in the TF 2 assessment clinic

Characteristic	Category	Mean (SD) for continuous variables and prevalence n(%) for categorical variables				
		Subjects with no data available N = 8,551		Attended TF 2 clinic N = 6,133		P-val ¹
		N	N(%)	N	N(%)	
Child sex	Male	8,551	4,525 (52.9)	6,133	3,011 (49.1)	<0.001
Child ethnicity	White	6,507	6,114 (93.7)	5,570	5,354 (96.1)	<0.001

¹Chi-square test for categorical variables to assess the null hypothesis of no difference in those who did ad those who did not attend the follow-up clinic.

Table 2.18; A comparison of characteristics between adolescents who did and did not participate in the TF 4 assessment clinic

Characteristic	Category	Mean (SD) for continuous variables and prevalence n(%) for categorical variables				
		Subjects with no data available N = 9,469		Attended TF 4 clinic N = 5,215		P-val ¹
		N	N(%)	N	N(%)	
Child sex	Male	9,469	5,260 (55.6)	5,215	2,276 (43.6)	<0.001
Child ethnicity	White	7,446	7,041 (94.6)	4,631	4,427 (95.6)	0.012

¹Chi-square test for categorical variables to assess the null hypothesis of no difference in those who did ad those who did not attend the follow-up clinic.

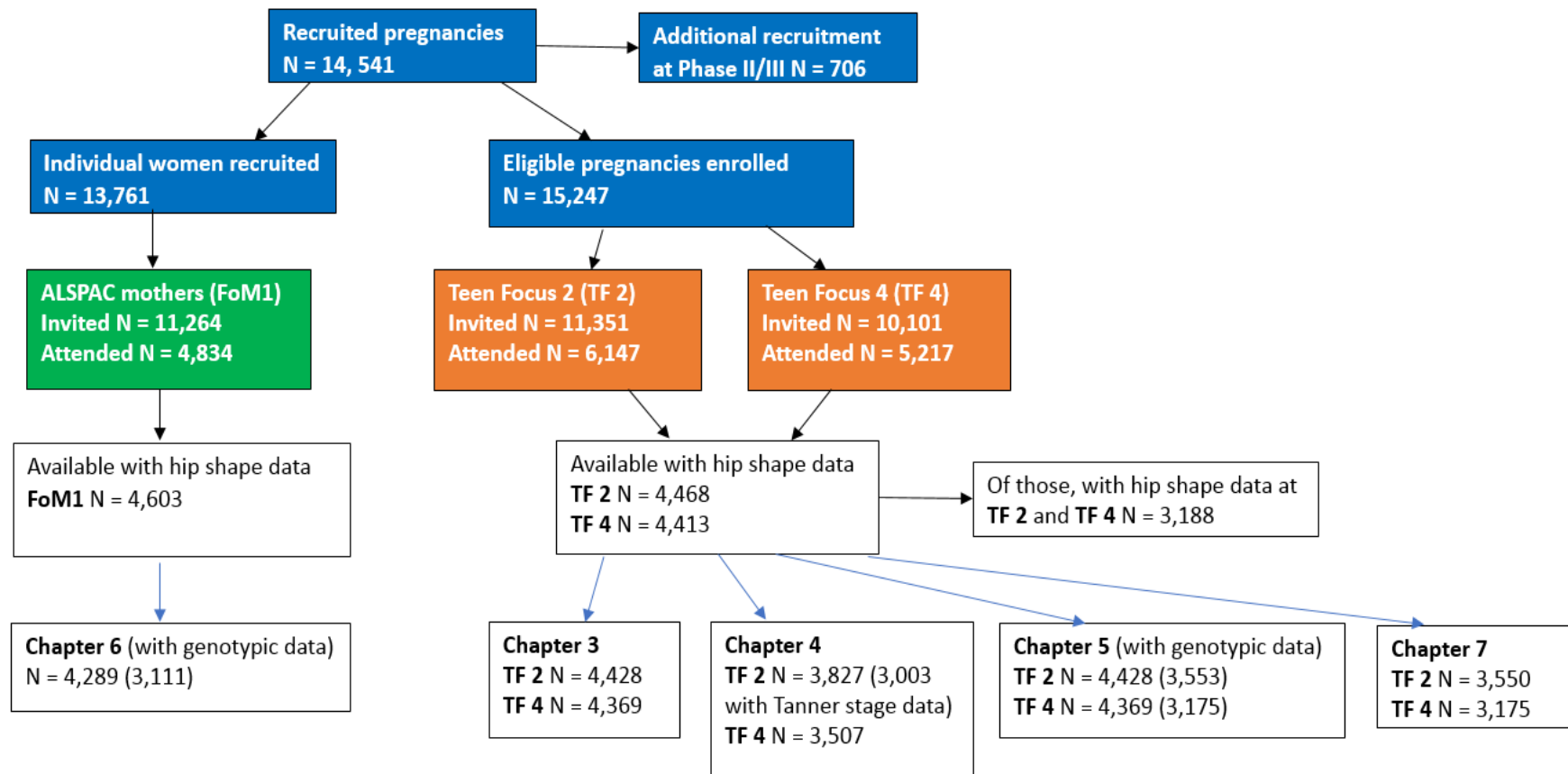


Figure 2.14 Flow chart of participants included in the ALSPAC study and number of participants included in each analysis chapter

2.6.3. Testing for interaction

The likelihood-ratio test was used to test for interaction with sex (in Chapters 4 and 5) and if there was evidence of an interaction, the analysis was further stratified by sex.

2.6.4. P value threshold

A Bonferroni corrected p value threshold of 0.005 (0.05/10 outcomes) was applied to all cross-sectional results.

2.6.5. Mendelian randomization (MR) analysis

MR is an instrumental variable (IV) analysis which uses genetic variants to infer causality between a given exposure (X) and an outcome (Y), as illustrated in Figure 2.15 (Davey Smith & Ebrahim, 2003; Davey Smith & Hemani, 2014; Lawlor et al., 2008; Wehby et al., 2008). The MR concept relies on the fact that genetic variants are randomly distributed in the population and are inherited independently of potential environmental confounders and other genetic variants. MR is often compared to randomized controlled trials where participants are divided into groups to which treatment is randomly allocated thus ensuring balanced distribution of known and unknown confounders between these groups which therefore limits the issues of confounding and reverse causality (Davey Smith & Hemani, 2014; Lawlor et al., 2008). In the MR setting, to be a valid IV, a genetic variant must satisfy the following assumptions:

- 1) it must be associated with the exposure,
- 2) it must not be associated with any confounders, and
- 3) it must not directly influence the outcome, except through the exposure of interest.

An exposure refers to any risk factor which can influence an outcome such as a biomarker, an anthropometric measure or any other risk factor, whereas the outcome is most commonly disease (Burgess & Thompson, 2015; Davey Smith & Ebrahim, 2003).

MR is most commonly used to assess a causal effect of a modifiable exposure on an outcome and thus inform disease prevention strategies. In cases where IV assumptions are not plausible, a MR framework can be used to test if similar causal mechanisms underlie two different traits (as described previously by Burgess et al. (Burgess et al.,

2016a)). In this thesis, MR analysis was used in the latter context, i.e. to investigate the extent to which BMD and hip shape share genetic influences. One-sample MR (whereby data on exposure, outcome and the genetic instrument all come from one sample (D. M. Evans & Davey Smith, 2015)) was used in ALSPAC offspring (Chapter 5) and a two-sample MR approach (which relies on summary statistics data from two independent, and often publicly available, GWASes (D. M. Evans & Davey Smith, 2015)) was used in ALSPAC mothers (Chapter 6).

Conventionally, MR uses instruments constructed from SNPs reaching genome-wide significance. Given that for many complex traits, the heritability (defined as the proportion of variance in a trait explained by the genetic variation (Mayhew & Meyre, 2017)) is distributed across many variants with small effects, utilising information on all SNPs (including those not reaching genome-wide significance) can also be used to explore shared genetic basis of complex traits (B. Bulik-Sullivan et al., 2015). For example, LD score regression, can be used for the estimation of SNP-based heritability and genetic correlation between different phenotypes (Visscher et al., 2017; Zheng et al., 2017). However, methods to estimate SNP-based heritability require larger sample size (B. Bulik-Sullivan et al., 2015) compared with methods which utilise individual level data (as in one-sample MR).

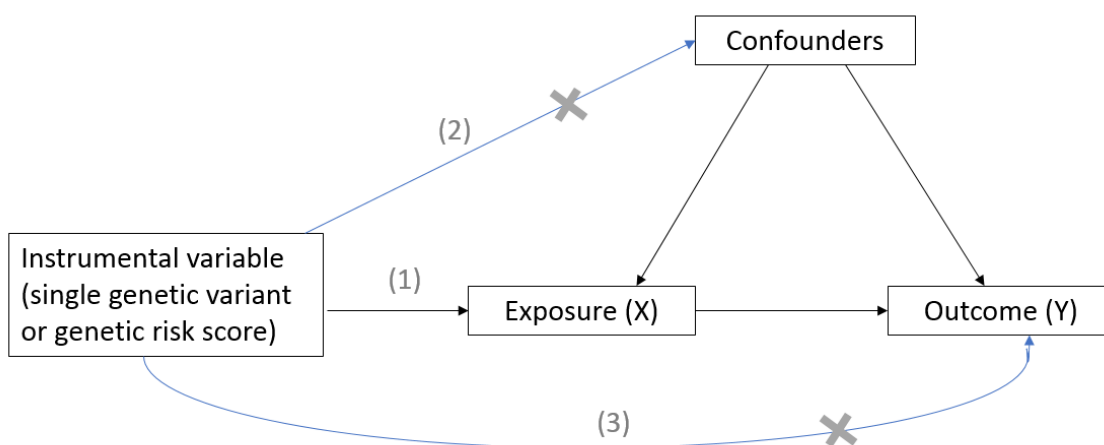


Figure 2.15 Directed acyclic graph illustrating Mendelian randomization and its underlying assumptions.

2.6.6. Composite hip shape figures

After association analysis, in order to illustrate the overall effect of a particular exposure on hip shape, composite HSM figures were plotted to represent an overall contribution to hip shape variation by all modes showing evidence of an association with that exposure. As summarised in Table 2.14, the first nine modes all describe variation in the shape of the femoral head (Figure 2.12 and Figure 2.13) (although different aspects of femoral head such as superolateral, inferomedial or superior) coupled with variation in either greater and lesser trochanters and/or FNW. For factors like age, which affects multiple HSMs, interpretation of the results can be challenging. Therefore, I aimed to model the overall effect on hip shape by combining all modes associated with a given exposure. This was achieved by simultaneously entering coefficients from the linear regression analysis into Shape software, for all modes showing evidence for an association with that exposure, thus combining the effect of a single exposure across hip shape components.

In order to aid visualisation of the overall effect on hip shape, all coefficients entered into Shape were multiplied by a factor of 2 (as in Chapter 3), or where necessary due to small effect sizes, by a factor of 10 (Chapter 5 and Chapter 6). Figure 2.16 shows example of hip shape features referred to throughout this thesis.

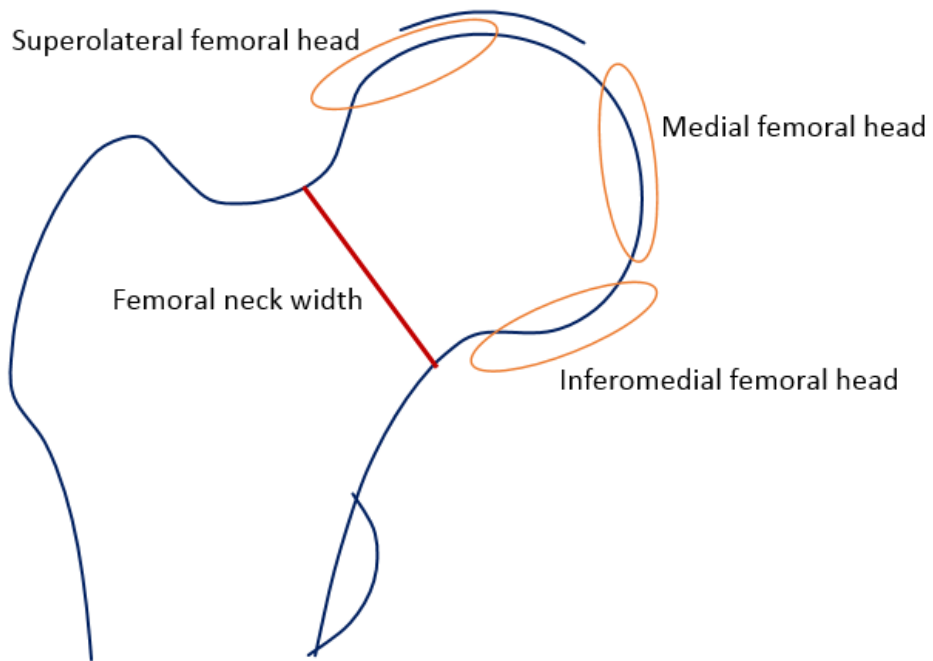


Figure 2.16 Example hip shape features referred to throughout this thesis.

CHAPTER 3. AGE AND SEX

DIFFERENCES IN HIP SHAPE

3.1. Introduction and chapter aims

In general, the incidence of hand, hip and knee OA is higher in women compared with men, especially after the age of 50 years (Litwic et al., 2013; Prieto-Alhambra et al., 2014). One explanation for this could be due to varying levels of hormones, in particular the rapid decrease of oestrogen around the time of menopause in women (Nevitt et al., 1996; Wluka et al., 2000). Another explanation for the differences in OA incidence might be due to differences in anatomical features including those present earlier in life. For example, one study, investigating joint space changes according to age and sex in asymptomatic hip joints (free from pain), found that minimum hip joint space is smaller in women compared with men (Lanyon et al., 2003). As described in the introduction chapter, as well as being risk factors for OA, age and gender are also related to hip fracture. It has been estimated that almost one in two women and one in five men over the age of 50 years are at risk of fracture (Curtis et al., 2016). Previous research has indicated that variation in hip morphology established early in life, including hip geometrical indices, could account for these differences (Hind et al., 2012; F. Zhang et al., 2010).

Previous studies suggest that sexual dimorphism in hip geometry emerge around the time of puberty (Sayers et al., 2010). However, certain limitations when investigating relationships with individual geometrical measurements must be considered, such as high correlations with other geometrical indices and body size measurements (Gregory & Aspden, 2008). Therefore, in this chapter, I will characterise sex differences in hip shape, quantified by SSM, in peri-pubertal children and adolescents from the ALSPAC cohort, including whether any differences observed are independent of those in body size.

The aims of this chapter are

- (i) To examine differences in hip shape between age 14 and 18
- (ii) To explore sex differences in hip shape at ages 14 and 18
- (iii) To determine whether sex differences at age 14 and 18 are explained by those in body size.

3.2. Methods

3.2.1. Subjects

Data were obtained from TF 2 and TF 4 clinics when the participants were on average 14 and 18 years old, respectively. The study population for the current analyses comprised individuals with complete outcome and covariate data from each assessment clinic. For more details regarding data collection and cleaning, please refer to the methods chapter (Chapter 2).

3.2.2. Measures

3.2.2.1. Outcome

To quantify the shape of proximal femur, DXA images collected at TF 2 and TF 4 clinics were used. Images were analysed in Shape and to allow comparison between the time points, scores from a consistent external adult reference SSM were applied to each data set (see Chapter 2 for details). The first ten HSMs were used as outcomes.

3.2.2.2. Exposure and covariate data

Age was calculated as the difference between the date of clinic attendance and date of birth. Sex was available from hospital records. As previously described in Chapter 2, section 2.6.2, age, height, lean and fat mass, were considered as potential confounders.

3.2.3. Statistical analysis

The differences in mean HSM scores between age 14 and 18 were assessed by paired t-test (results expressed as mean difference in HSM scores (SD)). Linear regression was used to explore sex differences in the top ten HSMs at each time point. The differences

in mean HSM scores between males and females were explored in unadjusted analysis (model 1), and in adjusted analysis controlling for age at clinic attendance, height, lean and fat mass (model 2).

I hypothesised that age and body size might confound the relationship between sex and hip shape, hence univariate associations between each confounder and the top ten HSMs were also explored.

To illustrate the overall sex differences in hip shape at each time point, coefficients from linear regression were simultaneously entered into Shape software, for all modes showing evidence for sex differences ($p < 0.005$).

3.3. Results

3.3.1. Participant characteristics

Of 11,351 children invited to the TF 2 clinic, 6,147 attended, and of those 4,428 had complete data on outcome and covariates. Participant recruitment has been described previously (Chapter 2, section 2.2.1.1). Table 3.1 shows the characteristics of TF 2 participants. Their mean (SD) age was 13.8 (0.2) years. Boys were taller and had more lean mass compared with girls, whereas girls had higher fat mass compared with boys.

A total of 10,101 individuals were invited to the TF 4 clinic, of whom 5,217 attended and of those 4,369 individuals had complete data on outcome and covariates. Table 3.1 shows participant characteristics. Mean (SD) age at clinic attendance was 17.8 (0.4) years, and similarly to TF 2 boys were taller and had more lean mass, while girls had more fat mass compared with boys.

Table 3.1; Characteristics of participants who attended TF 2 and TF 4 assessment clinics

		Age 14			Age 18		
		N	Mean (SD)	p for sex diff*	N	Mean (SD)	p for sex diff*
Age	Combined	4,428	13.8 (0.2)	0.36	4,369	17.8 (0.4)	0.59
	Male	2,117	13.8 (0.2)		1,931	17.8 (0.4)	
	Female	2,311	13.8 (0.2)		2,438	17.8 (0.4)	
Height (cm)	Combined	4,428	163.4 (7.6)	<0.0001	4,369	171.2 (9.2)	<0.0001
	Male	2,117	165.0 (8.7)		1,931	178.7 (6.6)	
	Female	2,311	162.0 (6.2)		2,438	165.2 (6.2)	
Fat mass (kg)	Combined	4,428	13.9 (8.0)	<0.0001	4,369	18.4 (10.5)	<0.0001
	Male	2,117	11.2 (7.7)		1,931	14.1 (10.0)	
	Female	2,311	16.4 (7.5)		2,438	21.8 (9.6)	
Lean mass (kg)	Combined	4,428	38.0 (6.4)	<0.0001	4,369	45.7 (9.9)	<0.0001
	Male	2,117	41.0 (7.2)		1,931	55.2 (6.1)	
	Female	2,311	35.2 (4.0)		2,438	38.1 (4.3)	

*Unpaired t-test to assess the null hypothesis of no difference in distributions between males and females at each time point

3.3.2. Differences in hip shape between age 14 and 18

A total of 3,188 individuals had complete outcome data available for both time points. In gender combined analysis, all HSMs, except HSM6, showed differences in mean HSMs scores between age 14 and 18 (Table 3.2). Whereas in sex stratified analysis, the results showed strong evidence for differences in mean HSM scores between the time points for all modes tested, with slightly weaker evidence for HSM10 (Table 3.3). In males, the largest difference was seen for HSM2, HSM5, HSM8 and HSM9 (with mean differences in mode scores ranging between 0.57 – 0.67 SDs between age 14 and 18). In females, the largest difference was seen for HSM4 scores, with a decrease of 0.55 SDs between the time points. The direction of change in HSM scores was consistent in both sexes, except for HSM6 which increased with age in males (representing narrower FNW and smaller femoral head) but decreased in females (representing wider FNW and larger femoral head). As highlighted in the methods chapter (section 2.5.2, Table 2.14), the first nine modes all reflect variation in femoral head (with each mode describing variation in different aspects of femoral head) along with a combination of either variation in greater and lesser trochanters, femoral shaft or changes in FNW which makes interpretation of these results challenging given the number of modes affected.

Table 3.2; Differences in mean HSM scores, between age 14 and 18, for the top ten HSMs based on adolescent images, after applying the combined adult reference model (N= 3,188)

	AGE 14	Age 18	AGE 18 – AGE 14	
Mode (% of variation)	Mean (SD)	Mean (SD)	Mean diff. (SD)	*P
1 (42%)	2.26 (0.41)	2.41 (0.42)	0.15 (0.27)	< 0.001
2 (13%)	0.58 (0.75)	0.24 (0.84)	-0.34 (0.57)	< 0.001
3 (8.5%)	-0.22 (0.69)	0.10 (0.65)	0.32 (0.74)	< 0.001
4 (6.1%)	0.87 (0.68)	0.36 (0.72)	-0.52 (0.66)	< 0.001
5 (4.1%)	-1.14 (0.79)	-1.50 (0.85)	-0.36 (0.72)	< 0.001
6 (3.4%)	0.25 (0.67)	0.26 (0.86)	0.01 (0.80)	0.533
7 (2.6%)	-0.25 (0.62)	0.03 (0.69)	0.28 (0.65)	< 0.001
8 (2.5%)	0.36 (0.96)	0.00 (0.91)	-0.35 (0.89)	< 0.001
9 (1.8%)	0.23 (0.77)	-0.21 (0.90)	-0.44 (0.88)	< 0.001
10 (1.5%)	-1.09 (0.58)	-1.04 (0.78)	0.06 (0.82)	< 0.001
Total = 85.5%				

*Paired t-test to assess the null hypothesis of no difference in mean HSM scores between each time point

Table 3.3; Differences in mean HSM scores between age 14 and age 18 after applying the combined adult reference model, stratified by sex

	Males N = 1,426				Females N=1,762			
	Age 14	Age 18	Age 18 – Age 14		Age 14	Age 18	Age 18 – Age 14	
HSM	Mean (SD)	Mean (SD)	Mean diff (SD)	*p	Mean (SD)	Mean (SD)	Mean diff (SD)	*p
1	2.20 (0.43)	2.40 (0.44)	0.21 (0.28)	6.15x10 ⁻¹³⁶	2.32 (0.39)	2.42 (0.40)	0.10 (0.25)	6.74x10 ⁻⁶⁰
2	0.55 (0.76)	-0.02 (0.78)	-0.57 (0.57)	2.77x10 ⁻²²⁰	0.60 (0.75)	0.46 (0.83)	-0.14 (0.50)	1.64x10 ⁻³²
3	-0.12 (0.70)	0.02 (0.64)	0.14 (0.75)	1.14x10 ⁻¹¹	-0.30 (0.67)	0.16 (0.66)	0.46 (0.69)	5.06x10 ⁻¹⁴⁵
4	0.74 (0.69)	0.27 (0.71)	-0.47 (0.68)	1.71x10 ⁻¹²²	0.98 (0.65)	0.43 (0.73)	-0.55 (0.65)	5.04x10 ⁻²¹²
5	-1.05 (0.80)	-1.72 (0.77)	-0.67 (0.69)	2.05x10 ⁻²⁰⁶	-1.21 (0.78)	-1.33 (0.87)	-0.12 (0.65)	1.89x10 ⁻¹⁴
6	0.33 (0.71)	0.60 (0.84)	0.27 (0.78)	8.1x10 ⁻³⁷	0.19 (0.62)	-0.01 (0.77)	-0.20 (0.75)	4.86x10 ⁻²⁸
7	-0.34 (0.61)	0.02 (0.64)	0.36 (0.66)	4.71x10 ⁻⁸³	-0.18 (0.62)	0.03 (0.73)	0.21 (0.64)	1.69x10 ⁻⁴¹
8	0.73 (0.94)	0.13 (0.92)	-0.60 (0.98)	5.49x10 ⁻¹⁰⁰	0.05 (0.86)	-0.10 (0.88)	-0.15 (0.76)	4.29x10 ⁻¹⁷
9	0.16 (0.76)	-0.48 (0.76)	-0.64 (0.84)	2.09x10 ⁻¹⁴⁵	0.29 (0.77)	0.02 (0.94)	-0.27 (0.89)	5.61x10 ⁻³⁶
10	-1.08 (0.58)	-1.01 (0.77)	0.07 (0.83)	0.001	-1.10 (0.57)	-1.06 (0.79)	0.05 (0.81)	0.015

*Paired t-test to assess the null hypothesis of no difference in mean HSM scores between each time point, in males and females

3.3.3. Univariate associations between confounders and hip shape

Supplementary Table 10.2.1 in Appendix 2 shows associations between age at clinic attendance and the top ten HSMs at both time points. At age 14, there was strong evidence for associations between age and HSM1 and HSM8, and weaker evidence for associations with HSM3, HSM6 and HSM7. At age 18, there was strong evidence for an association with HSM6 and no evidence to suggest associations with other modes.

Supplementary Table 10.2.2 in Appendix 2 shows associations between height and the top ten HSMs. At age 14, there was strong evidence for associations with all modes except HSM6. Whereas, by age 18 there was evidence for associations with HSM2, HSM4, HSM5, HSM6 and HSM9, with consistent direction of effect across the time points.

There was strong evidence for an association between lean mass and hip shape with the majority of modes, except for little evidence of an association with HSM7 at age 14, and HSM1 at age 18. The direction of effect was consistent across the time points, apart from mode 8 which was positively related to lean mass at age 14 and negatively at age 18 (Supplementary Table 10.2.3 in Appendix 2).

Finally, fat mass was associated with most modes across the time points, other than little evidence for associations with HSM5, HSM7 and HSM9 at age 14 and HSM4 at age 18. The direction of effect was consistent across time points (Supplementary Table 10.2.4 in Appendix 2).

3.3.4. Sex differences in hip shape

Age 14

In unadjusted analysis, all modes, except HSM10, showed some evidence for sex differences (Table 3.4). Following adjustment for age, height, lean and fat mass associations with HSM4 and HSM7 remained unchanged, HSM2 and HSM6 results were attenuated towards the null (and there was no longer evidence of an association), while several associations (HSM1, HSM3, HSM5 and HSM8) were strengthened. Interestingly, in unadjusted analysis the difference between mean male and female HSM9 scores was 0.12 (positive coefficient indicating higher mean score in females compared with males).

Following adjustment for age and body size (model 2), the difference in mean HSM9 score switched to negative (mean score in females being now lower than that in males) (Table 3.4).

The proportion of variance explained in HSMs by sex alone ranged from <0.5 – 14%, while the variance in HSMs predicted from sex, age, height, lean and fat mass ranged from 3 – 22%, with the largest variance accounted for in HSM8 ($R^2= 0.22$, models 2 and 3).

The combined effect of sex on hip shape at age 14 is shown in Figure 3.1. In the unadjusted model, females had smaller femoral heads (in the superolateral and inferomedial aspects) and lesser trochanter compared with males. In addition, differences in femoral neck length and greater trochanter size were also observed. After controlling for age and body size differences in femoral head size became more pronounced (smaller femoral head in females in the superolateral and inferomedial aspects), while the differences in the size of lesser trochanter were less marked. Moreover, the difference in femoral neck length and greater trochanter size also became more pronounced.

Age 18

In unadjusted analysis, there was strong evidence for sex differences in all modes except HSM1 and HSM7 (Table 3.5). Following adjustment for age, height, lean and fat mass (model 2) associations of sex with HSM2, HSM5, HSM6 and HSM9 were partially attenuated, while the association with HSM10 was strengthened. Adjustment for age and body size had little or no impact on HSM3, HSM4 and HSM8 results.

Compared with age 14 results, sex along with other covariates explained less variance in hip shape. Sex alone explained between <1 -12% of variance and the addition of further predictors slightly increased the strength of the association which ranged between <1-13% (model 2). The highest proportion of variance in hip shape explained by sex along with the predictors was observed for HSM2 ($R^2=0.13$) and HSM6 ($R^2=13$).

The combined effect of sex on hip shape at age 18 is shown in Figure 3.2. In unadjusted model, females had narrower FNW, smaller lesser trochanters and wider femoral shafts.

In addition, the medial part of the femoral head appeared larger in females compared with males. Following adjustment for age and body size, differences in the femoral head and femoral shaft were considerably attenuated, whilst smaller lesser trochanters and slightly narrower FNW in females were still present.

Table 3.4; Differences in hip shape mode scores between males and females (age 14)

HSM	Model 1			Model 2		
	β (95% CI)	p	R ²	β (95% CI)	p	R ²
1	0.13 (0.11,0.15)	3.7x10 ⁻²⁵	0.02	0.19 (0.16,0.22)	1.1x10 ⁻³²	0.05
2	0.06 (0.01,0.10)	0.013	1.4 x10 ⁻³	-0.04 (-0.09,0.02)	0.163	0.09
3	-0.19 (-0.23,-0.15)	1.7x10 ⁻²¹	0.02	-0.35 (-0.40,-0.30)	5.6x10 ⁻⁴⁶	0.11
4	0.22 (0.18,0.26)	4.8x10 ⁻²⁸	0.03	0.18 (0.13,0.23)	1.1x10 ⁻¹²	0.03
5	-0.18 (-0.23,-0.14)	6.1x10 ⁻¹⁵	0.01	-0.34 (-0.39,-0.28)	4.5x10 ⁻³⁰	0.06
6	-0.14 (-0.18,-0.10)	9.8x10 ⁻¹²	0.01	-0.03 (-0.08,0.02)	0.210	0.03
7	0.18 (0.15,0.22)	3.3x10 ⁻²²	0.02	0.23 (0.19,0.28)	2.2x10 ⁻²³	0.05
8	-0.73 (-0.78,-0.67)	7.2x10 ⁻¹⁴⁸	0.14	-0.87 (-0.93,-0.80)	2.3x10 ⁻¹⁴⁵	0.22
9	0.12 (0.08,0.17)	1.5x10 ⁻⁷	0.01	-0.08 (-0.14,-0.03)	0.004	0.05
10	-0.01 (-0.04,0.03)	0.737	2.6 x10 ⁻⁵	-0.02 (-0.06,0.03)	0.478	0.03

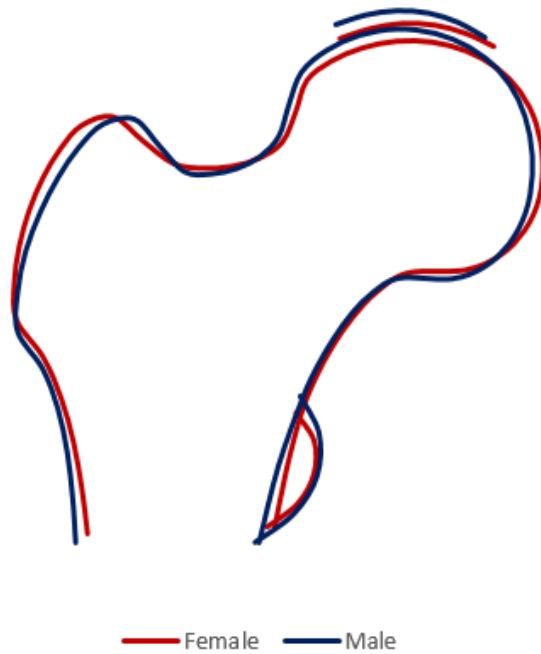
Abbreviations: HSM (hip shape mode), CI (confidence interval). Table shows mean difference in HSM scores between males and females (N=4,428) and 95% CIs, p value and r squared (R²). Positive beta coefficients indicate higher mean HSM scores in females, compared with males. Model 1: unadjusted, model 2: adjusted for age, height, lean and fat mass.

Table 3.5; Differences in hip shape mode scores between males and females (age 18)

HSM	Model 1			Model 2		
	β (95% CI)	p	R ²	β (95% CI)	p	R ²
1	0.02 (-0.003,0.05)	0.084	0.001	0.09 (0.03,0.14)	0.001	0.005
2	0.48 (0.43,0.52)	1.4x10 ⁻⁷⁸	0.08	0.41 (0.31,0.51)	3.8x10 ⁻¹⁶	0.13
3	0.13 (0.09,0.17)	5.1x10 ⁻¹¹	0.01	0.17 (0.09,0.25)	4.6x10 ⁻⁵	0.05
4	0.15 (0.11,0.20)	5.1x10 ⁻¹²	0.01	0.19 (0.10,0.28)	5.7x10 ⁻⁵	0.01
5	0.39 (0.34,0.44)	5.7x10 ⁻⁵³	0.05	0.29 (0.19,0.39)	3.4x10 ⁻⁸	0.06
6	-0.60 (-0.65,-0.55)	6.9x10 ⁻¹²⁴	0.12	-0.53 (-0.63,-0.43)	1.2x10 ⁻²⁴	0.13
7	0.003 (-0.04,0.04)	0.872	0	-0.09 (-0.18,-0.01)	0.036	0.04
8	-0.25 (-0.31,-0.20)	7.4x10 ⁻²⁰	0.02	-0.31 (-0.42,-0.20)	4.5x10 ⁻⁸	0.05
9	0.49 (0.43,0.54)	2.0x10 ⁻⁷²	0.07	0.33 (0.22,0.44)	4.8x10 ⁻⁹	0.08
10	-0.07 (-0.11,-0.02)	0.004	0.002	-0.16 (-0.25,-0.06)	0.001	0.06

Abbreviations: HSM (hip shape mode), CI (confidence interval). Table shows mean difference in HSM scores between males and females (N=4,369) and 95% CIs, p value and r squared (R²). Positive beta coefficients indicate higher mean HSM scores in females, compared with males. Model 1: unadjusted, model 2: adjusted for age, height, lean and fat mass.

Unadjusted sex differences at age 14



Adjusted sex differences at age 14

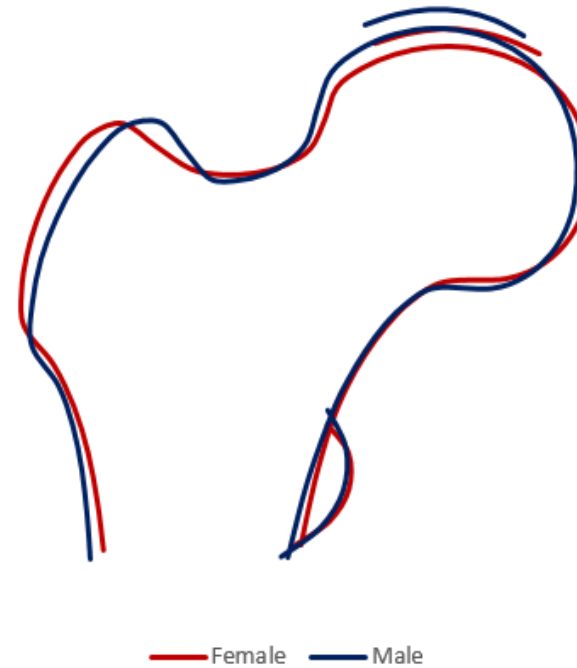
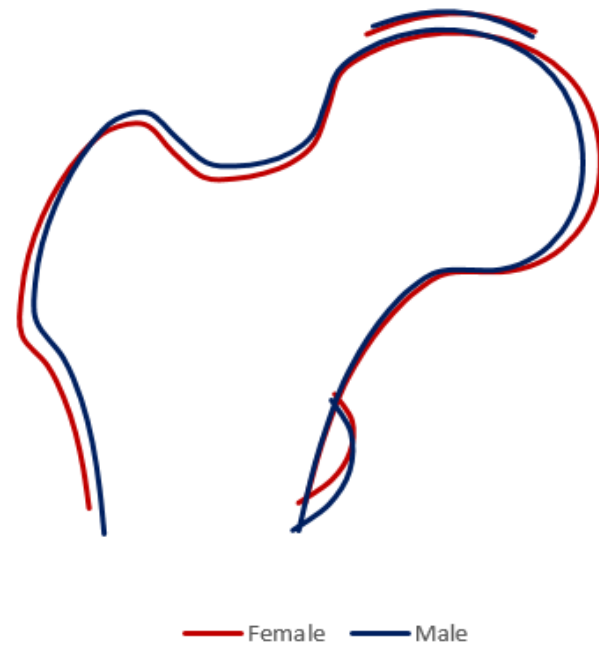


Figure 3.1 Sex differences in hip shape at age 14 based on the difference in mean HSM scores. Sex beta coefficients (for all modes with $p < 0.005$) magnified 4-fold were modelled in Shape to represent the average overall hip shape between males and females.

Unadjusted sex differences at age 18



Adjusted sex differences at age 18

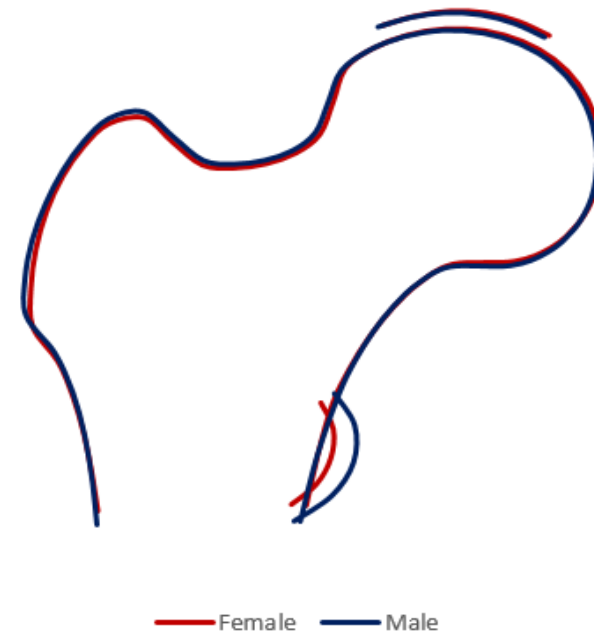


Figure 3.2 Sex differences in hip shape at age 18 based on the difference in mean HSM scores. Sex beta coefficients (for all modes with $p < 0.005$) magnified 4-fold were modelled in Shape to represent the average overall hip shape between males and females.

3.4. Discussion

In this chapter, I examined age and sex differences in hip shape in a cohort of ALSPAC adolescents. In gender stratified analysis, there was strong evidence for differences in mean HSM scores between age 14 and 18 for several HSMs with consistent effects observed across sexes, except HSM6 (which reflects variation in femoral head size and FNW) which increased with age in boys but decreased with age in girls. It needs to be noted that the observed differences are unlikely to represent longitudinal change at the individual patient level. Previous evidence suggests that skeletal maturation is related to changes in hip morphology and the following chapter will further explore the effect of the pubertal growth marker of tempo on hip shape.

Having described the differences in HSM scores between age 14 and 18, I went on to explore sex differences at each time point. Several modes showed evidence for sex differences. Previous studies revealed sex differences in various aspects of hip morphology, including greater FNW (Sayers et al., 2010) and hip joint space in boys (Wegener et al., 2017). However, it has been suggested that sexual dimorphism in hip morphology can be largely explained by the differences in body size, due to high correlations between hip geometric indices and those of body size (Arsuaga & Carretero, 1994). Employing SSM enables identification of independent hip shape components which can be related to either exposures of interest or relevant disease outcomes.

At age 14, the majority of modes showed strong evidence for sex differences. Of the modes which were associated with sex following age and body size adjustment, the majority represent variation in femoral head along with other morphological features of the hip. As highlighted previously (Chapter 2, section 2.6.6), this is challenging to interpret, and therefore the combined effect of sex on hip shape was modelled. As expected, females had smaller femoral head and lesser trochanter compared with males. In addition, differences in femoral neck length and greater trochanter were also observed. Following adjustment for age and body size these differences became more pronounced, indicating that age and body size may confound these associations. At age 18, several associations between sex and HSMs were also observed and the

majority of these were attenuated following adjustment for age and body size. What is more, the combined effect of sex on hip shape was mainly reflected by narrower FNW, smaller lesser trochanter, wider femoral shaft and larger femoral head in the medial aspect in females compared with males. Most of these differences attenuated following adjustment for age and body size, however differences in FNW and lesser trochanter remained.

This is the first time SSM has been applied to describe variation in hip shape in a cohort of adolescents. One previous cross-sectional study in adults from the Medical Research Council (MRC) National Survey of Health and Development (NSHD) (mean age 63 years), which also used SSM, reported sex differences in hip shape in older adults (Pavlova et al., 2017). Consistent with the findings at age 18, men in the NSHD cohort had greater FNW compared with women. The authors also observed flattening of femoral head and greater acetabular coverage in women, a finding which was not observed in this study. Both increased acetabular coverage (Harris-Hayes & Royer, 2011) and flattening of femoral head (Doherty et al., 2008) have been previously found to be risk factors for OA. Given the average age of study participants it is likely that some of the shape features identified in the NSHD cohort might be the result of OA associated changes.

The relationship between FNW with hip OA and fracture have been investigated previously. In a previous prospective population-based study investigating the role of hip geometry in prediction of RHOA, a wider femoral neck was associated with higher risk of incident hip OA (Castaño-Betancourt et al., 2013b). In terms of the associations with hip fracture, the evidence is conflicting. While some studies reported associations between wider neck and hip fracture in males and females (Alonso et al., 2000; Karlsson et al., 1996), others reported the opposite in men (Ego Seeman et al., 2001) and women (Ahlborg et al., 2005). Others yet, found that the association between femoral neck diameter and trochanteric hip fracture fully attenuated following adjustment for age, height, weight and BMD (Duboeuf et al., 1997).

The relationship between femoral head morphology and hip OA has been widely investigated (Baker-LePain & Lane, 2010). For example, pistol grip deformity (Doherty et al., 2008) as well as cam-type deformities (Heijboer et al., 2012) are both well-established risk factors for hip OA. In this study, sex differences in hip shape observed at

age 14, amongst other features, reflect variation in femoral head size. Interestingly boys had a larger femoral head in the superolateral and inferomedial aspects, which may contribute to risk of hip OA in later life. For example, a previous study investigating radiographic patterns of OA in older men and women (mean age 66 years) found clear associations of male gender with superolateral osteoarthritis while females showed a tendency to more medial patterns (Ledingham et al., 1992).

Standardization of HSM scores, by applying adult reference SSM, allows comparison between time points and will enable future comparisons with other cohorts. Although sex differences observed here were relatively small, SSM enables global assessment of hip morphology and might be more sensitive at picking up subtle anatomical variations, compared with more traditional approaches.

Conclusions

In summary, several aspects of hip shape were related to age and sex. In terms of sex differences assessed at age 14, these mainly comprised of smaller femoral head and lesser trochanter in females and variation in femoral neck length and greater trochanter and these differences became more pronounced after adjustment for age and body size. At age 18, the differences in femoral head and femoral shaft were explained by those in body size, while differences including narrower FNW and lesser trochanter in females compared with males remained. These results demonstrate that sex differences in several components of hip shape can be discerned in childhood and adolescence. These are largely independent of sex differences in body size and could play a yet unrecognized role in predisposing to hip OA or fracture in later life.

In this chapter I found evidence for differences in mean HSM scores between age 14 and 18 years and sex differences in hip shape at both time points, however to what extent these differences could be explained by other factors, such as timing of pubertal growth will be explored in Chapter 4. In addition, having observed age and sex differences in hip shape, analyses in subsequent chapters will be adjusted for age and sex along with other potential confounders (as discussed in Chapter 2, section 2.6.2).

CHAPTER 4. INFLUENCE OF PUBERTAL GROWTH ON HIP SHAPE

4.1. Introduction and chapter aims

This chapter builds on the previous chapter which examined age and sex differences in hip shape. Having found differences in hip shape between age 14 and 18, this chapter will explore the relationship between pubertal timing and hip shape.

Puberty is described as a period of rapid growth and is thought to be a critical period for bone development (Kuh et al., 2016; Q. Wang et al., 2015). Furthermore, the timing of puberty has been linked to a number of important health outcomes later in life (Day et al., 2015). For example, in the UK Biobank study, early menarche was associated with an increased risk of OA and reduced risk of OP (Day et al., 2015). On the other hand, in the MRC NSHD cohort later puberty was associated with lower aBMD at the hip and spine in men and women, which in turn confers the risk of fracture (Kuh et al., 2016). However, the exact mechanisms contributing to the risk of OA and OP in later life are not fully understood. While the relationship between hip shape and risk of hip fracture and OA are well-established, factors influencing hip shape including critical periods for shape development remain to be elucidated. Previous studies suggest that sex differences in bone geometry emerge around the time of puberty (Sayers et al., 2010). However, it is unclear whether other aspects of hip structure, including hip shape, are also related to puberty.

Pubertal assessment

One of the hallmarks of puberty onset is a rapid growth spurt accompanied by the development of secondary sexual characteristics (Rogol et al., 2002). Various methods

to assess an individuals' pubertal status exist and these include recalled age at menarche or age at voice breaking, Tanner staging assessment (most commonly assessed via questionnaire), age at take-off or aPHV (J. Baird et al., 2017; Dhiman et al., 2015; Sherar et al., 2010). Due to its complexity, puberty assessment is challenging, and the assessment methods suffer from a number of limitations. While age at menarche or age at voice breaking are easy and relatively cheap to assess they are prone to recall bias (Kindblom et al., 2006). The agreement between self-reported vs. clinically assessed Tanner stage can range from as little as 43% to 81% (J. Baird et al., 2017). Age at take-off (indicating the start of pubertal growth spurt (Di Giovanni et al., 2017)) and aPHV provide objective assessment of pubertal timing, and are free from recall bias, but require frequent height measurements. An added advantage of using aPHV is that it enables alignment of individuals on the same developmental scale (Kuh et al., 2016) which is important when comparing pubertal effects between males and females (Bundak et al., 2007; Demirjian et al., 1985; Dhiman et al., 2015; Granados et al., 2015). Given the limitations of conventional methods and high frequency of height measurements available in ALSPAC, height tempo (which corresponds to aPHV) was estimated, in order to explore the relationship between puberty and hip shape. The aim of this chapter was:

- i) to examine the relationship between pubertal timing (using measures of height tempo) and hip shape at age 14 and 18 in ALSPAC cohort

4.2. Methods

4.2.1. Subjects

Data were obtained from ALSPAC TF 2 and TF 4 clinics when the participants were on average 14 and 18 years old, respectively. The study population for current analyses comprised individuals with complete outcome and covariate data from each assessment clinic. Details regarding data collection have been described in more detail in Chapter 2.

4.2.2. Measures

4.2.2.1. Outcome

To quantify the shape of proximal femur, DXA images collected at TF 2 and TF 4 clinics were used. Images were analysed in Shape and to allow comparison between the time points scores from a consistent external adult reference SSM were applied to each data set (see Chapter 2 for details). Top ten HSMs were used as outcomes, for details see Chapter 2.

4.2.2.2. Exposures

Growth tempo (equivalent to age at peak height velocity)

Age at peak height velocity (aPHV) was estimated using SuperImposition by Translation and Rotation (SITAR) mixed effects growth curve analysis. This is a shape-invariant growth curve model consisting of a mean growth curve along with three transformations (size, tempo and velocity) to describe how each individual differs from the mean curve (see Figure 4.1 for model illustration). The three SITAR parameters are size, reflecting up/down shift relative to height; tempo (corresponding to aPHV), reflecting left/right shift (on the age scale) (with negative values indicating early puberty and positive late puberty), and velocity reflecting stretching/shrinking of the age scale and hence describing differences in the rate at which individuals pass through puberty. Size (cm) is a random intercept relative to the spline curve intercept, tempo (years) reflects the timing of the growth process and corresponds to aPHV, and velocity (years) reflects the rate at which 'time' passes for individuals. Details describing the method have been described previously (Cole et al., 2010).

While aPHV and tempo both measure the timing of pubertal growth spurt (Pearson's correlation coefficient between tempo and aPHV was 0.9946 and 0.9971 in males and females, respectively), aPHV is measured from individual growth curves whereas tempo, is a random effect from a single analysis and much easier to estimate (Cole et al., 2010). Given the range of estimates for aPHV (10.8 – 16.6 years in males and 9.0 – 14.6 years in females) and tempo (-2.7 – 2.7 in males and -3.0 – 3.0 in females) and considering the age at TF 2 attendance (mean age was 13.8 years), for a substantial number of boys,

aPHV occurred after attending this clinic, therefore tempo, instead of aPHV, was used in all analyses to indicate the relative timing of puberty.

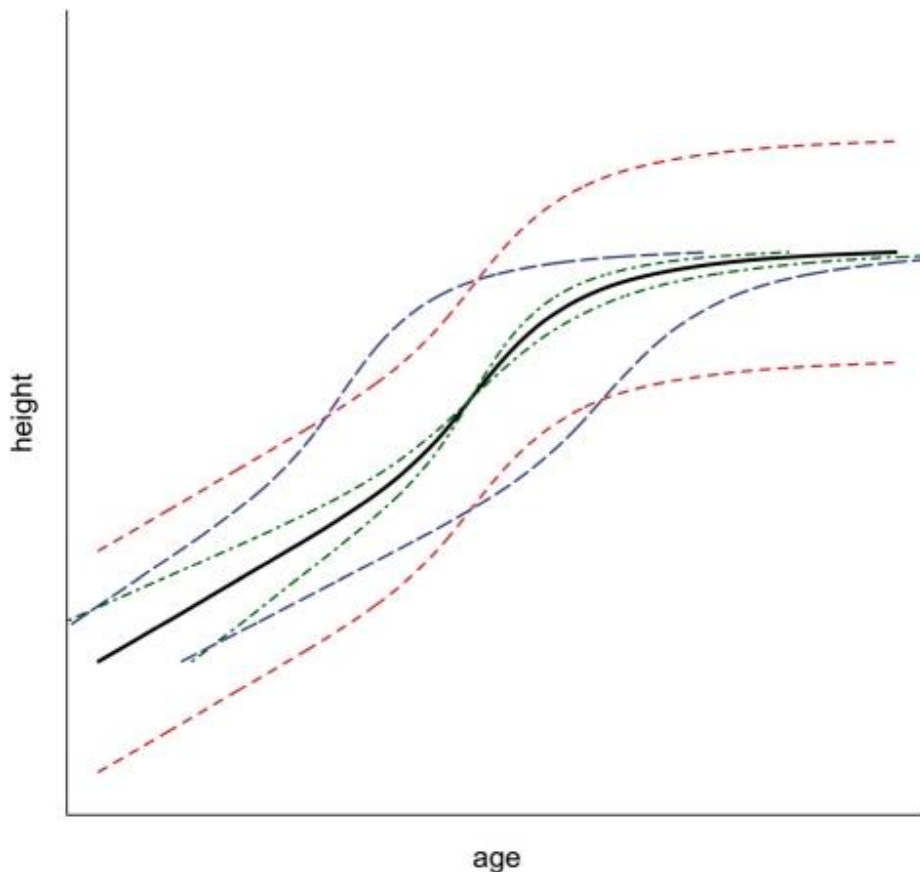


Figure 4.1 Illustration of the SITAR model for height in puberty. The solid line is the mean growth curve; size (α) corresponds to vertical or height shift in the curve (the short-dashed lines in red); tempo (β) corresponds to a horizontal or age shift (the long-dashed lines in purple) and velocity (γ) corresponds to a shrinking–stretching of the age scale (the dot-dashed line in green).

Figure credit to (Cole et al., 2010).

Data sources

Height measurements collected during assessment clinics between age 5 and 20 years (measurements taken by trained field workers) were used to estimate SITAR parameters.

These included

- (i) Children in Focus data – 10% sample were measured regularly in a clinic setting at 10 equally spaced intervals from 4 months to 61 months of age (for this analysis measurements were restricted to those taken from age 5 onwards),
- (ii) assessment clinics in childhood (around age 7, 8, 9, 10, 11 and 12 years),
- (iii) assessment clinics in adolescence (ages 13, 15 and 17 years).

These data were further restricted to only include individuals with at least one measurement for the following time periods: 5 to 10 years, 10 to 15 years and 15 to 20 years.

Data analysis

The height data was analysed for males and females separately using SITAR model with 5 degrees of freedom (Cole et al., 2010). Optimal degrees of freedom value, which indicates the number of parameters that are free to vary in the model, was chosen to minimise the Bayesian Information Criterion (BIC)(Schwarz, 1978). The model was fitted using sitar package in R version 3.4.1.

After fitting the initial model, the data were checked and points with velocity exceeding 4 SDs and standardized residuals exceeding 4 in absolute value were removed.

For details regarding estimation of aPHV in ALSPAC please refer to a data note (available in Appendix 3 and published online (Frysz et al., 2018)).

Tanner stage

Self-reported Tanner stage assessed when the children were approximately 13 years old was used in this analysis. To aid comparability between the sexes only data relating to pubic hair development was used. Tanner stages were combined to indicate early/pre-pubertal (Tanner stage I+II), mid- (Tanner III), and advanced (Tanner IV+V) pubertal stages. For more details regarding data collection and pubertal assessment please refer to Chapter 2.

4.2.2.3. Confounding variables

Previous studies suggest that fat mass or BMI affect the onset of puberty in males and females (Kaplowitz, 2008). To adjust for the effect of fat mass, fat mass index (FMI) (independent of height) was calculated for each time point, as described previously (Wells & Cole, 2002). Briefly, fat mass and height were log transformed. Log transformed fat mass was then regressed on log height, separately for males and females. Subsequently fat mass was regressed on height raised to the appropriate power (value corresponding to regression coefficient of log fat mass on log height) and the residuals were used to adjust for FMI in the following analyses. In addition, to estimate the relationship between tempo and hip shape independent of sex and the remaining SITAR parameters (size and velocity), an additional model adjusting for these covariates was run.

4.2.3. Statistical analysis

SITAR parameters (estimated in R) were exported into Stata and merged with outcome and covariate data. Multivariable linear regression was used to examine cross-sectional associations between growth tempo and the top ten HSMs at age 14 and 18, adjusting for sex (model 1) and additionally for FMI (model 2). Sensitivity analyses additionally adjusting for the remaining SITAR parameters, size and velocity of height, were also performed (model 3). In addition, associations between Tanner stage and the top ten HSMs at age 14 were explored and compared with tempo results. Sex differences were explored by comparing regression coefficients and their 95% CIs in gender stratified analysis and by formally testing for evidence of statistical interaction using likelihood-ratio tests.

Given the strong association between tempo and hip shape at age 14 (but not at age 18), tempo was further split into quintiles to explore the relationships between tempo quintiles and hip shape in males and females separately. Tempo was sorted in ascending order and split into five equal groups using `xtile` command in Stata version 14.0.

To illustrate the overall relationship between pubertal timing and hip shape at each time point, sex-stratified coefficients from adjusted linear regression models corresponding to 10th and 90th percentiles of tempo (each beta coefficient was multiplied by a value

corresponding to 10th and 90th percentile of tempo to represent the differences between early vs. late maturers) were simultaneously entered into Shape software, for all modes showing evidence of an association with growth tempo ($p < 0.005$).

4.3. Results

4.3.1. Assessment of puberty

SITAR results

A total of 18,095 height measurements for 2,688 males, and 21,942 measurements for 3,019 females were available for analysis. Mean (SD) aPHV was 13.5 (0.9) years for males and 11.8 (0.8) years for females (see Supplementary Figure 10.3.1 and Supplementary Figure 10.3.2 in Appendix 3). The SITAR model explained 98.5% and 98.7% of variance in the height data set in males and females, respectively.

Tanner stage

The Tanner stage questionnaire was completed at an average age of 13.2 years. Complete outcome, Tanner stage and confounder data were available for 3,003 individuals (1,364 were male and 1,639 were female). Table 4.4 shows age distribution by Tanner stage. Compared with males, females were more advanced in puberty as demonstrated by a higher proportion of females in advanced pubertal stages and a small proportion of females in pre-pubertal stages (i.e. 35%, 28% and 38% of males vs. 16%, 23% and 60.5% of females in early, mid and late pubertal stages, respectively).

4.3.2. Study participant characteristics

Of individuals who attended the TF 2 clinic (mean age at attendance 13.8 years), complete outcome and covariate data were available for 1,797 males and 2,030 females. Males who attended the assessment clinic were taller, had higher total body lean mass and lower total body fat mass compared with females (Table 4.1).

Of those who attended the TF 4 clinic (mean age at attendance 17.8 years), a total of 1,597 males and 1,910 females had complete data. Similarly, to TF 2 results, males were

taller and heavier, had higher lean mass content and lower fat mass content compared with females (Table 4.1).

The target age for TF 2 clinic recruitment was 13.5 years. Although there was no difference with regards to the age at clinic attendance (males and females attended at a mean age of 13.8 years) it is clear that males and females were at distinct pubertal stages, as reflected by the differences in mean aPHV (Table 4.1), time since achieving PHV when attending the clinic (Table 4.2) and Tanner stage category distributions (Table 4.4). As shown in Table 4.2, based on sex, tempo quintiles 1 and 2 indicate early maturers (they reached their aPHV earlier compared with the mean aPHV), quintile 3 indicates average maturers (those around mean aPHV) and quintiles 4 and 5 indicate late maturers (they reached their aPHV later compared with the mean aPHV). For example, females in the first quintile of tempo achieved their PHV at least 3 years prior to attending the clinic compared with an average of 1.5 years for males in this quintile. In addition, 729 males achieved their PHV after attending the clinic compared with only 22 females.

At the time of TF 4 clinic attendance (the target age for attendance was 17.5 years) similar differences in terms of time since achieving PHV were observed for males and females (Table 4.3). For example, females in the first quintile of tempo achieved their PHV an average 7 years prior to attending the clinic compared with an average of 5.4 years in males.

Table 4.1; Descriptive statistics of ALSPAC study participants

		Age 14 (TF 2)			Age 18 (TF 4)		
		N	Mean (SD)	p for sex diff*	N	Mean (SD)	p for sex diff*
Age at clinic attendance	M&F	3,827	13.8 (0.2)	0.077	3,507	17.7 (0.4)	0.612
	M	1,797	13.8 (0.2)		1,597	17.7 (0.4)	
	F	2,030	13.8 (0.2)		1,910	17.7 (0.4)	
Height (cm)	M&F	3,827	163.6 (7.5)	<0.0001	3,507	171.6 (9.2)	<0.001
	M	1,797	165.0 (8.5)		1,597	178.8 (6.5)	
	F	2,030	162.0 (6.2)		1,910	165.5 (6.1)	
Weight (kg)	M&F	3,827	54.6 (10.9)	0.675	3,507	67.1 (13.4)	<0.001
	M	1,797	54.8 (11.5)		1,597	72.5 (13.3)	
	F	2,030	54.5 (10.4)		1,910	62.5 (11.7)	
Lean mass (kg)	M&F	3,827	38.1 (6.4)	<0.0001	3,507	45.9 (9.9)	<0.001
	M	1,797	41.2 (7.1)		1,597	55.2 (6.1)	
	F	2,030	35.3 (4.1)		1,910	38.1 (4.0)	
Fat mass (kg)	M&F	3,827	13.9 (8.0)	<0.0001	3,507	18.0 (10.3)	<0.001
	M	1,797	11.1 (7.6)		1,597	14.1 (10.1)	
	F	2,030	16.3 (7.5)		1,910	21.3 (9.2)	
**Tempo (years)	M&F	3,827	0.03 (0.8)	0.999	3,507	0.01 (0.8)	0.999
	M	1,797	0.02 (0.8)		1,597	-0.02 (0.8)	
	F	2,030	0.04 (0.9)		1,910	0.03 (0.9)	
aPHV (years)	M&F	3,827	12.6 (1.2)	<0.0001	3,507	12.6 (1.2)	<0.001
	M	1797	13.5 (0.9)		1597	13.5 (0.9)	
	F	2030	11.8 (0.8)		1910	11.8 (0.8)	

* Unpaired t-test to assess the null hypothesis of no difference in distributions between males and females at each time point. **Tempo corresponds to the timing of pubertal growth spurt (and thus aPHV) in each individual compared with the mean. Geometrically it indicates subject-specific left-right shift or translation in the spline curve. Negative values indicate early puberty, and positive values indicate late puberty. Abbreviations: M (males), F (females), aPHV (age at peak height velocity).

Table 4.2; Mean aPHV and years since aPHV by quintiles of tempo stratified by gender, in children who attended TF 2 clinic (mean age at attendance 13.8 years)

	Males (N= 1,797)			Females (N=2,030)		
		aPHV	years since aPHV		aPHV	years since aPHV
Tempo quintile	N	Mean (SD)	Mean (SD)	N	Mean (SD)	Mean (SD)
1	360	12.4 (0.38)	1.5 (0.42)	406	10.7 (0.35)	3.1 (0.38)
2	359	13.1 (0.17)	0.8 (0.24)	406	11.4 (0.14)	2.4 (0.24)
3	360	13.6 (0.17)	0.2 (0.25)	406	11.8 (0.14)	2.0 (0.23)
4	359	14.0 (0.16)	-0.2 (0.27)	406	12.3 (0.16)	1.6 (0.29)
5	359	14.8 (0.47)	-0.9 (0.51)	406	13.0 (0.39)	0.8 (0.43)

Abbreviations: aPHV (age at peak height velocity), years since aPHV (difference between age at peak height velocity and age at clinic attendance)

Table 4.3; Mean aPHV and years since aPHV by quintiles of tempo stratified by gender, in children who attended TF 4 clinic (mean age at attendance 17.7 years)

	Males (N=1,597)			Females (N=1,910)		
		aPHV	years since aPHV		aPHV	years since aPHV
Tempo quintile	N	Mean(SD)	Mean(SD)	N	Mean(SD)	Mean(SD)
1	320	12.3 (0.37)	5.4 (0.49)	382	10.7 (0.35)	7.1 (0.49)
2	319	13.0 (0.17)	4.7 (0.40)	382	11.4 (0.14)	6.4 (0.39)
3	320	13.5 (0.17)	4.2 (0.40)	382	11.8 (0.14)	5.9 (0.33)
4	319	13.9 (0.16)	3.8 (0.39)	382	12.3 (0.16)	5.5 (0.41)
5	319	14.7 (0.52)	3.0 (0.63)	382	13.0 (0.39)	4.8 (0.55)

Abbreviations: aPHV (age at peak height velocity), years since aPHV (difference between age at peak height velocity and age at clinic attendance)

Table 4.4; Age distribution by pubertal status for 3,003 individuals with complete outcome, Tanner stage and covariate data at age 14

Tanner stage	Males (N= 1,367)		Females (N=1,639)	
	N (%)	Mean age (SD)	N (%)	Mean age (SD)
I + II	472 (34.6)	13.8 (0.19)	269 (16.4)	13.8 (0.19)
III	378 (27.7)	13.8 (0.18)	379 (23.1)	13.8 (0.20)
IV + V	514 (37.7)	13.8 (0.19)	991 (60.5)	13.8 (0.18)

Results shown for individuals with complete outcome, covariate and Tanner stage data

Table 4.5; Number of individuals in each Tanner stage category (assessed at a mean age of 13.2 years) per quintile of tempo

		Males (N= 1,226)				Females (N= 1,495)			
		Tanner stage				Tanner stage			
Tempo quintiles		I + II	III	IV + V	N	I + II	III	IV + V	N
1	N (%)	18 (7.2)	33 (13.2)	199 (79.6)	250	3 (1.0)	22 (7.1)	284 (91.9)	309
2	N (%)	38 (15.6)	62 (25.4)	144 (59.0)	244	6 (2.5)	49 (20.5)	238 (99.6)	293
3	N (%)	66 (26.6)	107 (43.1)	75 (30.2)	246	13 (4.2)	89 (28.7)	208 (67.1)	310
4	N (%)	134 (55.1)	85 (35.0)	24 (9.9)	243	46 (16.3)	108 (38.3)	128 (45.4)	282
5	N (%)	168 (71.8)	56 (23.9)	10 (4.3)	243	174 (57.8)	82 (27.2)	45 (15.0)	301

* number of individuals in each tempo quintile restricted to individuals with complete hip shape data age 14, SITAR parameters and Tanner stage data assessed at mean age of 13.2 years.

4.3.3. Relationship between tempo and hip shape

4.3.3.1. Age 14

In gender combined analysis (model 1), tempo was associated with the majority of HSMs, except for HSM4 (Table 4.6). Following adjustment for FMI (model 2), associations were essentially unchanged. After further adjustment for the remaining SITAR parameters (size and velocity of growth) (model 3), the results remained essentially unchanged, except for the association with HSM6 which attenuated. There was strong evidence of interaction by sex (consistent across the models) for all modes except HSM6 (Table 4.6).

In males, in unadjusted analysis there was strong evidence of association of tempo with all modes, and some evidence of an association with HSM6 (model 1), and these results were essentially unchanged following FMI adjustment (model 2) (Table 4.7). Following further adjustment for size and velocity of growth (model 3), HSM4 result attenuated slightly and the evidence of an association was weak, while the remaining results were unchanged (Table 4.7).

Compared with males, associations between tempo and HSMs in females were generally weaker. There was evidence for an association with a number of modes, including HSM2, HSM3, HSM6, HSM8, HSM9 and HSM10 (model 1, Table 4.8). Following adjustment for FMI (model 2) associations with HSM2, HSM3 and HSM10 attenuated towards the null and there was no longer evidence of an association, the association with HSM6 was strengthened, whereas HSM8 and HSM9 results remained unchanged (Table 4.8). After additional adjustment for size and velocity of growth (model 3), HSM6 and HSM8 results remained unchanged, whereas the HSM9 association was strengthened, and associations with HSM3 and HSM5 emerged (Table 4.8).

The overall relationship between tempo (early vs. late) and hip shape, independent of FMI, was modelled separately for males and females and is shown in Figure 4.2. In males, the overall change in hip shape associated with later timing of puberty was reflected by slight narrowing of FNW, smaller lesser and greater trochanters and larger

femoral head in the superolateral aspect. In females, the overall relationship between pubertal timing and hip shape was harder to discern.

To explore possible non-linear relationship between pubertal timing and hip shape, tempo was divided into quintiles; with quintiles 1 and 2 indicating early maturers, quintile 3 indicating average maturers (those around mean aPHV) and quintiles 4 and 5 indicating late maturers. Unadjusted mean HSM scores and their 95% CIs were plotted per each quintile of tempo in males and females separately (Figure 4.3 - Figure 4.7).

In males, the strongest associations were seen for modes HSM2, HSM3, HSM5, HSM8 and HSM9 and these results were reflected when modelling the relationship between tempo quintiles with these modes, i.e. there was a clear increase in mean HSM scores with each quintile of tempo and clear differences in mean HSM scores were particularly noted between 1st and 5th (early vs. late maturers) quintiles of tempo as reflected by non-overlapping CIs.

In females, the relationship between tempo and HSM scores was much weaker compared with that in males. The strongest association with tempo was observed for HSM8, however when looking at the relationship with tempo quintiles no clear pattern of change in mean HSM scores per quintile of tempo emerged, and this was similar for other modes showing evidence of an association with tempo.

Tempo vs. Tanner stage results

Compared with tempo results, the associations between Tanner stage and HSMs were broadly similar. It is important to bear in mind that the direction of beta coefficients was in the opposite direction representing the differences in coding of tempo and Tanner stage variables. Negative tempo (quintiles 1 and 2) indicates early timing of puberty and roughly corresponds to Tanner stages IV and V (with majority of individuals in tempo quintiles 1 and 2 being in Tanner stages IV and V, as shown in Table 4.5). On the other hand, Tanner stages I and II correspond to the pre-pubertal stage (and thus could represent late maturers i.e. individuals who enter puberty later compared with those already in Tanner stages IV and V) and, as shown in Table 4.5, the majority of individuals in tempo quintile 5 are in Tanner stages I and II.

In gender combined analysis, in minimally adjusted model there was evidence for an association between Tanner stage and all modes, apart from HSM4 and these results were essentially unchanged following adjustment for FMI (model 2) (Table 4.9). As with tempo results, there was strong evidence of sex interaction.

In males, there was evidence for an association between the Tanner stage and the majority of modes, apart from HSM6, and adjustment for FMI made little difference to these results (Table 4.10). These findings were consistent with those observed for tempo, however associations between Tanner stage and hip shape (models 1 and 2) were generally weaker.

In females, similarly to tempo results, the association between Tanner stage and hip shape were weaker compared with the results in males. There was some evidence of association between Tanner stage with most modes (apart from HSM2, HSM3 and HSM4) and following adjustment for FMI, associations with HSM1 and HSM7 were attenuated towards the null and there was no longer evidence of an association, association with HSM8 was slightly attenuated whereas the remaining results remained unchanged (Table 4.11). In contrast to tempo results, there was some evidence to suggest association between Tanner stage with HSM5 and HSM10 independent of FMI.

Table 4.6; Associations between tempo and the top ten HSMs in ALSPAC adolescents at age 14 (N=3,827)

HSM	Model 1			Model 2			Model 3		
	β (95% CI)	p	p for sex-int	β (95% CI)	p	p for sex-int	β (95% CI)	p	p for sex-int
1	-0.04 (-0.06,-0.03)	1.4x10 ⁻⁸	5.3x10 ⁻⁵	-0.04 (-0.06, -0.03)	3.8x10 ⁻⁸	2.6x10 ⁻⁵	-0.03 (-0.05, -0.00)	0.015	3.8x10 ⁻⁶
2	0.15 (0.12, 0.18)	4.5x10 ⁻²⁵	6.8x10 ⁻⁹	0.13 (0.10, 0.15)	2.6x10 ⁻¹⁸	9.7x10 ⁻¹⁵	0.14 (0.10, 0.17)	6.7x10 ⁻¹³	4.3x10 ⁻¹⁶
3	0.14 (0.12, 0.17)	9.2x10 ⁻²⁸	2x10 ⁻¹³	0.12 (0.10, 0.15)	7.4x10 ⁻²²	5.0x10 ⁻¹⁹	0.16 (0.12, 0.19)	2.9x10 ⁻²⁰	5.3x10 ⁻¹⁹
4	0.02 (-0.00, 0.05)	0.073	0.001	0.02 (-0.00, 0.05)	0.093	0.001	0.02 (-0.02, 0.05)	0.333	2.7x10 ⁻⁴
5	0.14 (0.11, 0.17)	1.1x10 ⁻²¹	1.9x10 ⁻²¹	0.15 (0.12, 0.18)	4.8x10 ⁻²⁴	3.2x10 ⁻¹⁹	0.19 (0.15, 0.23)	3.9x10 ⁻²¹	3.7x10 ⁻²⁰
6	-0.04 (-0.07,-0.02)	0.001	0.758	-0.06 (-0.08, -0.03)	6.4x10 ⁻⁶	0.385	-0.07 (-0.10, -0.04)	4.0x10 ⁻⁵	0.232
7	-0.06 (-0.08,-0.03)	2.4x10 ⁻⁶	1.6x10 ⁻¹⁴	-0.07 (-0.09, -0.04)	1.6x10 ⁻⁸	1.2x10 ⁻¹¹	-0.03 (-0.06, 0.00)	0.082	1.2x10 ⁻¹³
8	0.25 (0.21, 0.28)	7.8x10 ⁻⁴⁸	8.7x10 ⁻¹⁴	0.23 (0.20, 0.27)	5.3x10 ⁻⁴³	1.1x10 ⁻¹⁶	0.26 (0.21, 0.30)	2.6x10 ⁻³¹	5.2x10 ⁻¹⁹
9	0.12 (0.09, 0.15)	7.2x10 ⁻¹⁶	8.6x10 ⁻⁸	0.12 (0.09, 0.15)	2.0x10 ⁻¹⁶	2.5x10 ⁻⁷	0.16 (0.12, 0.19)	7.7x10 ⁻¹⁶	1.5x10 ⁻⁷
10	0.06 (0.04, 0.08)	6.4x10 ⁻⁸	0.038	0.05 (0.03, 0.07)	1.7x10 ⁻⁵	0.001	0.05 (0.02, 0.08)	4.9x10 ⁻⁴	6.7x10 ⁻⁴

Abbreviations: HSM (hip shape mode), CI (confidence interval). Table shows results of linear regression analysis between tempo and the top ten HSMs in male and female adolescents. Regression coefficients represent SD change in HSM per one-year increase in growth tempo, 95% CIs and p value. Model 1: adjusted for sex; model 2: model 1 + fat mass index; model 3: model 2 + size and velocity.

Table 4.7; Associations between tempo and the top ten HSMs in ALSPAC males at age 14 (N=1,797)

HSM	Model 1		Model 2		Model 3	
	β (95% CI)	p	β (95% CI)	p	β (95% CI)	p
1	-0.08 (-0.10, -0.06)	1.2×10^{-10}	-0.08 (-0.10, -0.06)	1.1×10^{-10}	-0.06 (-0.09, -0.02)	4.0×10^{-4}
2	0.24 (0.20, 0.28)	2.8×10^{-29}	0.24 (0.20, 0.28)	9.8×10^{-31}	0.24 (0.19, 0.30)	4.3×10^{-20}
3	0.24 (0.21, 0.28)	1.6×10^{-36}	0.25 (0.21, 0.28)	9.2×10^{-38}	0.24 (0.19, 0.29)	1.4×10^{-23}
4	0.07 (0.03, 0.11)	4.2×10^{-4}	0.07 (0.03, 0.11)	4.4×10^{-4}	0.05 (0.00, 0.10)	0.045
5	0.30 (0.26, 0.34)	3.0×10^{-41}	0.30 (0.26, 0.34)	3.4×10^{-41}	0.30 (0.25, 0.36)	8.6×10^{-28}
6	-0.05 (-0.09, -0.01)	0.020	-0.05 (-0.09, -0.01)	0.025	-0.07 (-0.12, -0.01)	0.013
7	-0.16 (-0.19, -0.12)	3.0×10^{-19}	-0.15 (-0.19, -0.12)	4.3×10^{-19}	-0.10 (-0.14, -0.06)	1.9×10^{-6}
8	0.38 (0.33, 0.43)	1.6×10^{-49}	0.38 (0.33, 0.43)	4.1×10^{-50}	0.36 (0.30, 0.42)	9.0×10^{-30}
9	0.20 (0.16, 0.24)	1.2×10^{-21}	0.20 (0.16, 0.24)	1.2×10^{-21}	0.21 (0.16, 0.26)	5.4×10^{-15}
10	0.09 (0.05, 0.12)	4.4×10^{-7}	0.09 (0.06, 0.12)	2.0×10^{-7}	0.10 (0.05, 0.14)	7.6×10^{-6}

Abbreviations: HSM (hip shape mode), CI (confidence interval). Table shows results of linear regression analysis between tempo and the top ten HSMs in male adolescents. Results are SD change in HSM per one-year increase in growth tempo, 95% CIs and p value. Model 1: unadjusted; model 2: adjusted for fat mass index; model 3: model 2 + size and velocity.

Table 4.8; Associations between tempo and the top ten HSMs in ALSPAC females at age 14 (N=2,030)

HSM	Model 1		Model 2		Model 3	
	β (95% CI)	p	β (95% CI)	p	β (95% CI)	p
1	-0.02 (-0.04, 0.00)	0.109	-0.01 (-0.03, 0.01)	0.196	0.00 (-0.03, 0.03)	0.898
2	0.07 (0.04, 0.11)	1.2x10 ⁻⁴	0.01 (-0.02, 0.05)	0.476	0.03 (-0.02, 0.09)	0.208
3	0.06 (0.02, 0.09)	0.001	0.01 (-0.02, 0.05)	0.498	0.08 (0.03, 0.12)	0.001
4	-0.01 (-0.05, 0.02)	0.379	-0.03 (-0.06, 0.01)	0.126	-0.02 (-0.07, 0.02)	0.338
5	0.02 (-0.02, 0.06)	0.416	0.04 (-0.00, 0.08)	0.052	0.09 (0.04, 0.15)	8.8x10 ⁻⁴
6	-0.04 (-0.07, -0.01)	0.012	-0.07 (-0.10, -0.03)	6.1x10 ⁻⁵	-0.08 (-0.13, -0.04)	3.1x10 ⁻⁴
7	0.03 (-0.01, 0.06)	0.109	0.01 (-0.02, 0.04)	0.498	0.04 (-0.01, 0.08)	0.085
8	0.13 (0.09, 0.18)	1.3x10 ⁻⁹	0.10 (0.05, 0.14)	1.6x10 ⁻⁵	0.17 (0.11, 0.23)	6.0x10 ⁻⁸
9	0.05 (0.01, 0.09)	0.017	0.06 (0.02, 0.10)	0.006	0.12 (0.07, 0.18)	1.1x10 ⁻⁵
10	0.04 (0.01, 0.07)	0.007	0.02 (-0.01, 0.05)	0.303	0.01 (-0.03, 0.05)	0.614

Abbreviations: HSM (hip shape mode), CI (confidence interval). Table shows results of linear regression analysis between tempo and the top ten HSMs in female adolescents. Results are unit change in HSM per one-year increase in growth tempo, 95% CIs and p value. Model 1: unadjusted; model 2: adjusted for fat mass index; model 3: model 2 + size and velocity.

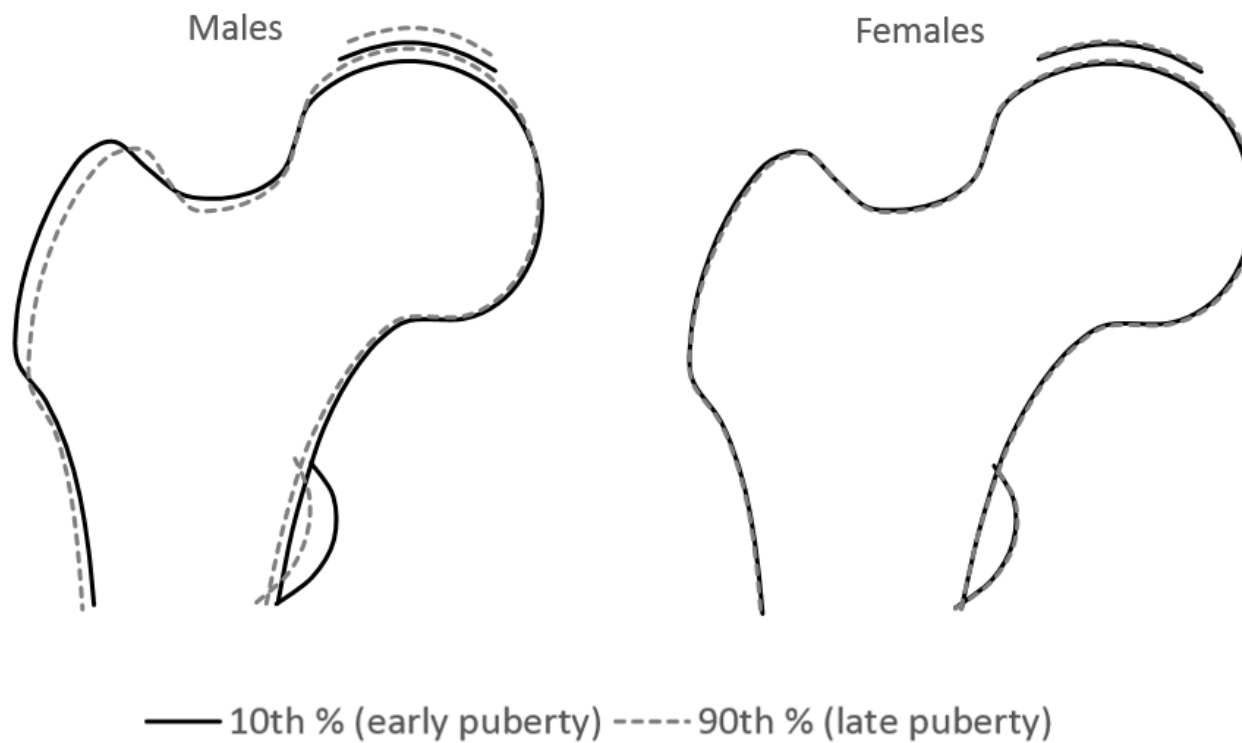


Figure 4.2 The overall difference in hip shape at age 14 between early vs. late maturers (changes in hip shape associated with unit change in tempo) based on adjusted beta coefficients. Beta coefficients were scaled to reflect changes in early maturers (10th percentile of tempo) vs. late maturers (90th percentile of tempo).

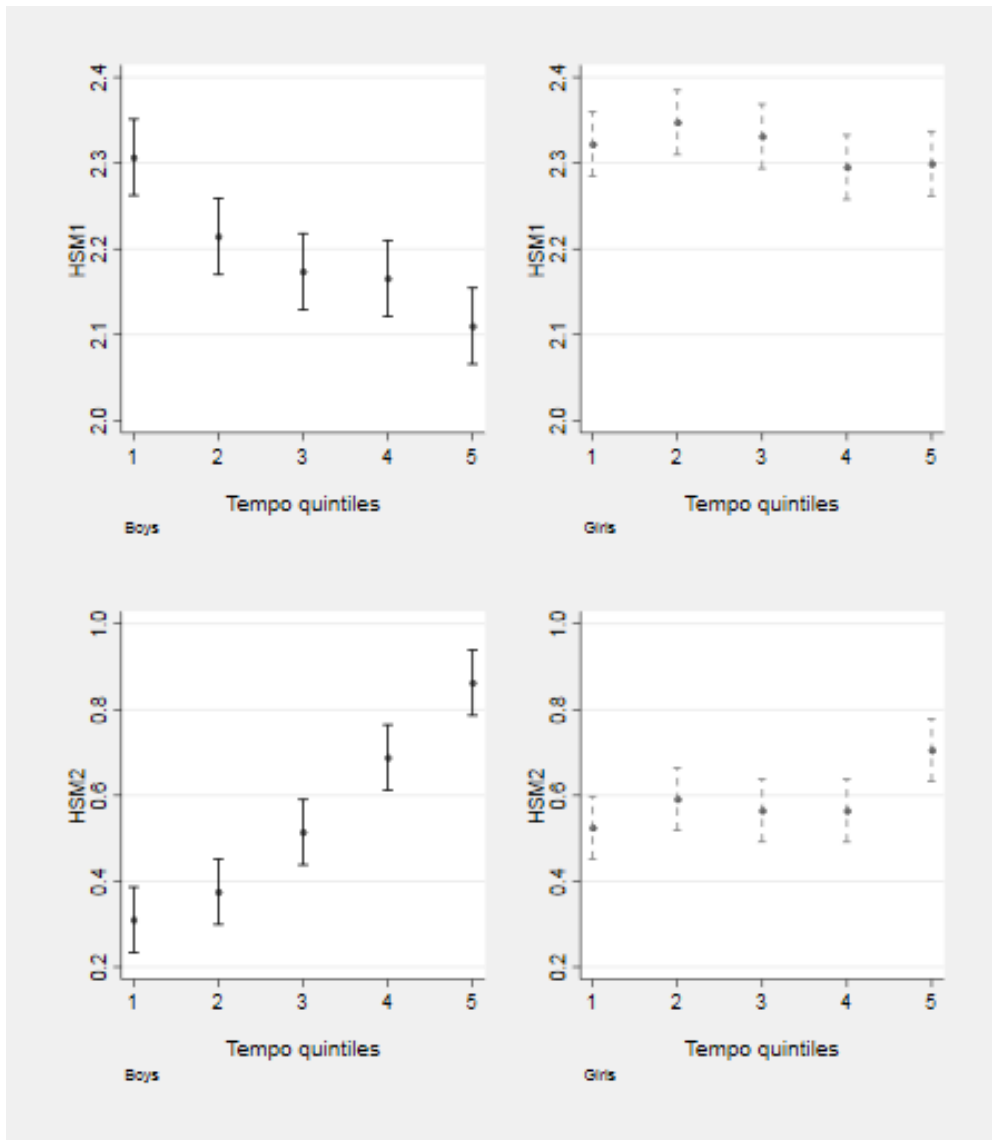


Figure 4.3 Unadjusted mean (and 95% CIs) HSM1 and HSM2 scores per quintile of tempo in males and females. Tempo quintiles 1 and 2 indicate those maturing early (earlier aPHV), quintile 3 indicates those around mean aPHV and quintiles 4 and 5 indicate those maturing later (later aPHV).

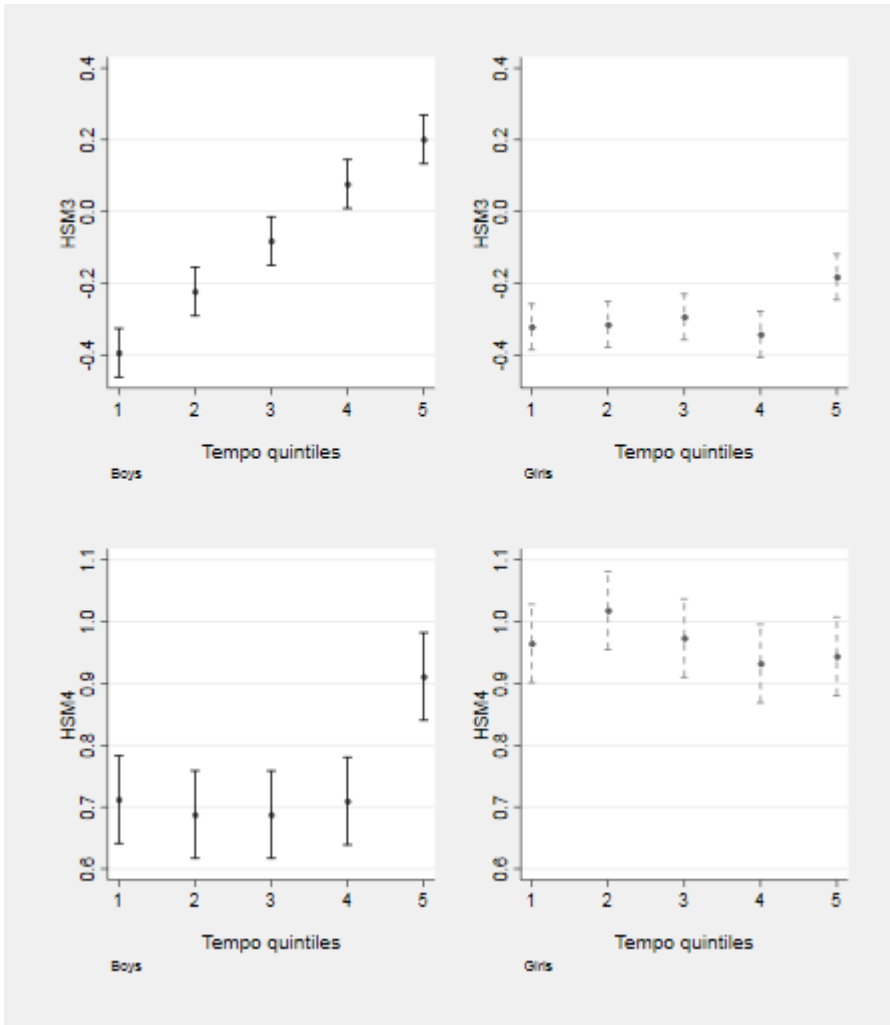


Figure 4.4 Unadjusted mean (and 95% CIs) HSM3 and HSM4 scores per quintile of tempo in males and females. Tempo quintiles 1 and 2 indicate those maturing early (earlier aPHV), quintile 3 indicates those around mean aPHV and quintiles 4 and 5 indicate those maturing later (later aPHV).

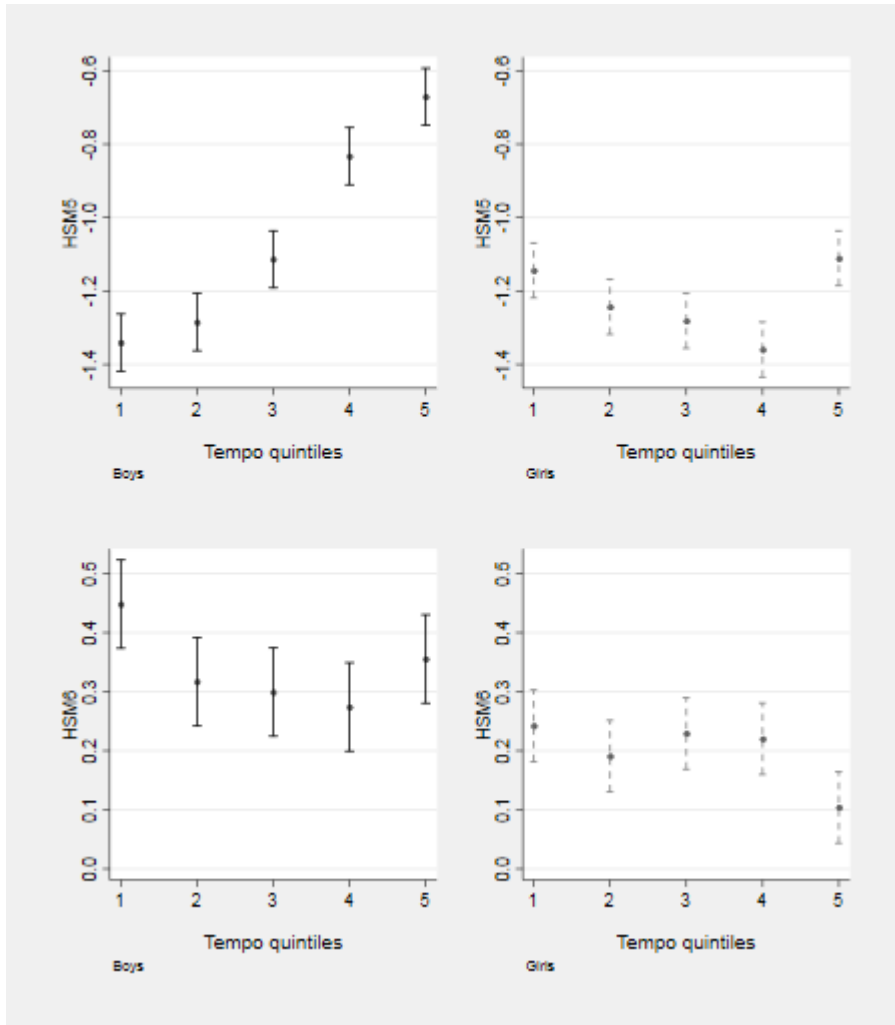


Figure 4.5 Unadjusted mean (and 95% CIs) HSM5 and HSM6 scores per quintile of tempo in males and females. Tempo quintiles 1 and 2 indicate those maturing early (earlier aPHV), quintile 3 indicates those around mean aPHV and quintiles 4 and 5 indicate those maturing later (later aPHV).

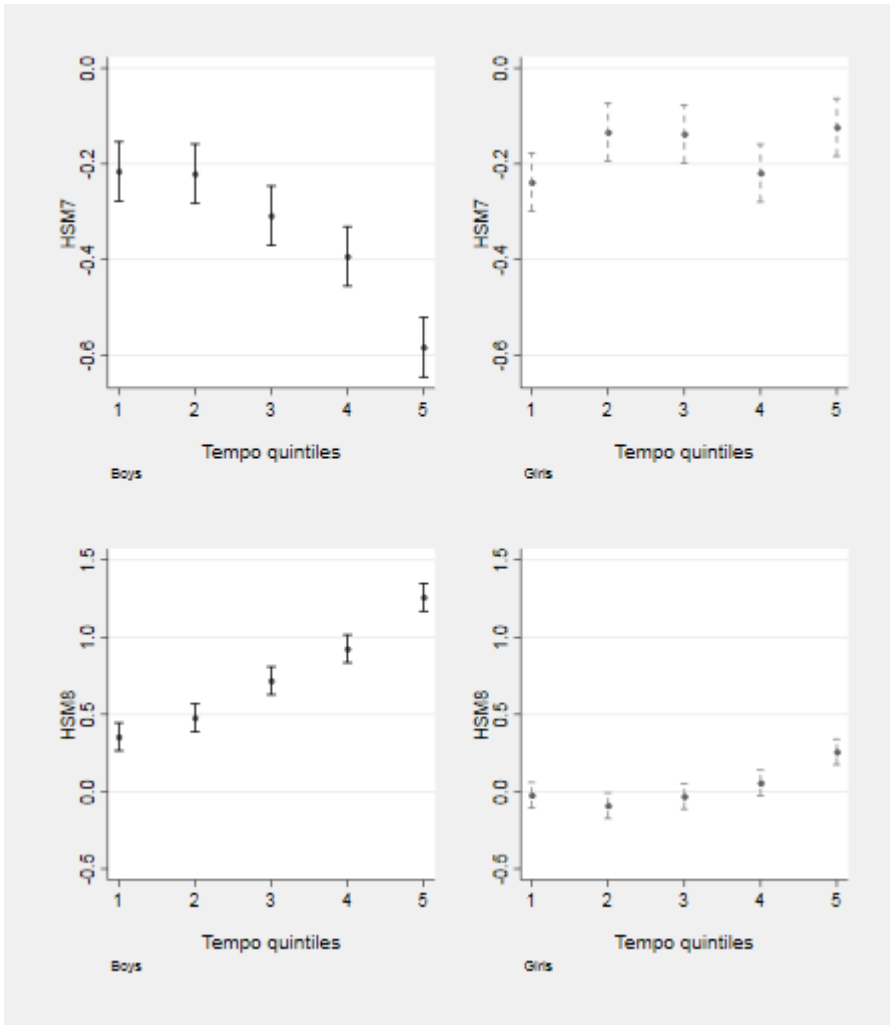


Figure 4.6 Unadjusted mean (and 95% CIs) HSM7 and HSM8 scores per quintile of tempo in males and females. Tempo quintiles 1 and 2 indicate those maturing early (earlier aPHV), quintile 3 indicates those around mean aPHV and quintiles 4 and 5 indicate those maturing later (later aPHV).

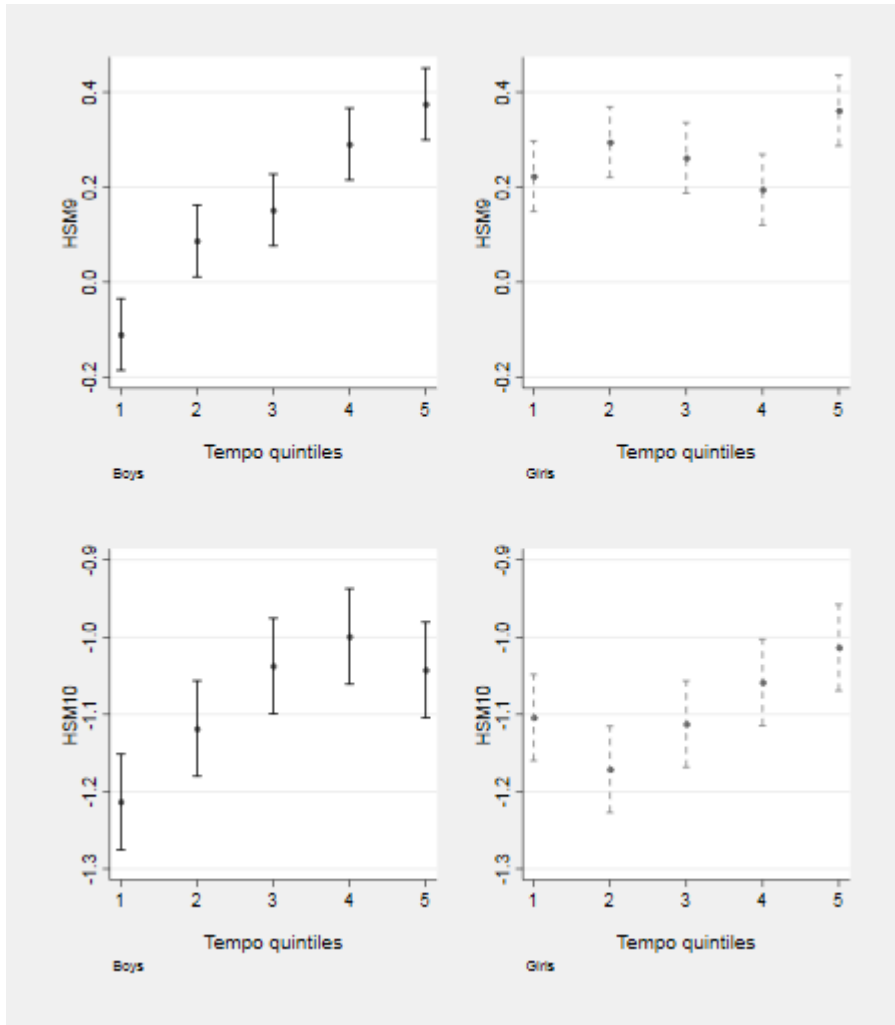


Figure 4.7 Unadjusted mean (and 95% CIs) HSM9 and HSM10 scores per quintile of tempo in males and females. Tempo quintiles 1 and 2 indicate those maturing early (earlier aPHV), quintile 3 indicates those around mean aPHV and quintiles 4 and 5 indicate those maturing later (later aPHV).

Table 4.9; Test for linear trend between Tanner stages and the top ten HSMs in ALSPAC adolescents at age 14 (N=3,003)

HSM	Model 1			Model 2		
	β (95% CI)	p	p for sex-int	β (95% CI)	p	p for sex-int
1	0.05 (0.03,0.07)	1.1×10^{-8}	0.007	0.05 (0.03,0.07)	1.3×10^{-8}	0.003
2	-0.10 (-0.14,-0.07)	3.0×10^{-9}	0.001	-0.10 (-0.13,-0.07)	4.4×10^{-9}	5.1×10^{-7}
3	-0.11 (-0.14,-0.08)	7.8×10^{-13}	5.6×10^{-6}	-0.11 (-0.14,-0.08)	1.1×10^{-12}	6.5×10^{-9}
4	-0.02 (-0.05,0.01)	0.158	0.064	-0.02 (-0.05,0.01)	0.159	0.059
5	-0.14 (-0.17,-0.11)	2.5×10^{-15}	4.2×10^{-5}	-0.14 (-0.18,-0.11)	1.8×10^{-15}	<0.0001
6	0.04 (0.01,0.08)	0.003	0.362	0.05 (0.02,0.08)	0.003	0.091
7	0.05 (0.03,0.08)	1.4×10^{-4}	1.1×10^{-11}	0.05 (0.03,0.08)	9.0×10^{-5}	9.2×10^{-10}
8	-0.23 (-0.27,-0.19)	8.4×10^{-30}	4.8×10^{-8}	-0.23 (-0.27,-0.19)	1.2×10^{-29}	1.6×10^{-10}
9	-0.12 (-0.15,-0.08)	7.9×10^{-12}	0.114	-0.12 (-0.15,-0.08)	8.1×10^{-12}	0.107
10	-0.06 (-0.09,-0.03)	4.9×10^{-6}	0.414	-0.06 (-0.09,-0.03)	6.9×10^{-6}	0.940

Abbreviations: HSM (hip shape mode), CI (confidence interval). Table shows regression coefficients with 95% CIs for linear trend test between Tanner stage and the top ten HSMs at age 14 in ALSPAC adolescents. Model 1: adjusted for sex, model 2: adjusted for sex and fat mass index. Analysis based on three Tanner stage categories (I+II, III, IV +V) based on self-reported pubic hair development.

Table 4.10; Test for linear trend between Tanner stages and the top ten HSMs in ALSPAC males at age 14 (N=1,364)

HSM	Model 1		Model 2	
	β (95% CI)	p	β (95% CI)	p
1	0.08 (0.05,0.10)	1.4×10^{-8}	0.08 (0.05,0.11)	5.6×10^{-9}
2	-0.16 (-0.21,-0.11)	5.8×10^{-11}	-0.18 (-0.23,-0.13)	1.4×10^{-13}
3	-0.18 (-0.22,-0.13)	2.7×10^{-16}	-0.19 (-0.23,-0.15)	3.3×10^{-19}
4	-0.05 (-0.09,-0.01)	0.025	-0.05 (-0.09,0.00)	0.031
5	-0.21 (-0.26,-0.16)	3.7×10^{-17}	-0.21 (-0.26,-0.16)	3.5×10^{-17}
6	0.03 (-0.01,0.08)	0.177	0.02 (-0.03,0.06)	0.402
7	0.14 (0.11,0.18)	3.3×10^{-14}	0.14 (0.10,0.17)	9.1×10^{-13}
8	-0.33 (-0.39,-0.28)	5.1×10^{-31}	-0.35 (-0.40,-0.29)	6.7×10^{-33}
9	-0.14 (-0.19,-0.10)	1.1×10^{-9}	-0.15 (-0.19,-0.10)	5.2×10^{-10}
10	-0.05 (-0.09,-0.01)	0.007	-0.06 (-0.10,-0.02)	0.001

Abbreviations: HSM (hip shape mode), CI (confidence interval). Table shows regression coefficients with 95% CIs for linear trend test between Tanner stage and the top ten HSMs at age 14 in ALSPAC males. Model 1: unadjusted, model 2: adjusted for fat mass index. Analysis based on three Tanner stage categories (I+II, III, IV +V) based on self-reported pubic hair development.

Table 4.11; Test for linear trend between Tanner stages and the top ten HSMs in ALSPAC females at age 14 (N=1,639)

HSM	Model 1		Model 2	
	β (95% CI)	p	β (95% CI)	p
1	0.03 (0.00,0.05)	0.03	0.02 (0.00,0.05)	0.053
2	-0.04 (-0.09,0.01)	0.087	-0.01 (-0.06,0.04)	0.725
3	-0.04 (-0.08,0.00)	0.071	-0.02 (-0.06,0.02)	0.426
4	0.01 (-0.03,0.05)	0.731	0.01 (-0.03,0.05)	0.612
5	-0.07 (-0.12,-0.02)	0.008	-0.08 (-0.13,-0.03)	0.002
6	0.06 (0.02,0.10)	0.004	0.07 (0.03,0.11)	0.001
7	-0.04 (-0.08,0.00)	0.031	-0.03 (-0.07,0.01)	0.096
8	-0.12 (-0.17,-0.06)	2.9×10^{-5}	-0.09 (-0.15,-0.04)	0.001
9	-0.09 (-0.14,-0.04)	3.1×10^{-4}	-0.09 (-0.14,-0.04)	2.3×10^{-4}
10	-0.07 (-0.11,-0.03)	1.6×10^{-4}	-0.06 (-0.10,-0.02)	0.002

Abbreviations: HSM (hip shape mode), CI (confidence interval). Table shows regression coefficients with 95% CIs for linear trend test between Tanner stage and the top ten HSMs at age 14 in ALSPAC females. Model 1: unadjusted, model 2: adjusted for fat mass index. Analysis based on three Tanner stage categories (I+II, III, IV +V) based on self-reported pubic hair development.

4.3.3.2. Age 18

Compared with age 14 results, the associations between tempo and hip shape at age 18 were much weaker. Although there was some evidence to suggest association between tempo and hip shape, the magnitude of effect was much weaker (across all models tested) compared with the results at age 14, with coefficients ranging from -0.08 to 0.08.

In gender combined analysis, in the minimally adjusted model there was evidence to suggest association between tempo with HSM1, HSM2, HSM5, HSM9 and HSM10 and following adjustment for FMI (model 2) these results remained unchanged except association with HSM2 which fully attenuated (Table 4.12). In addition, the association of tempo with HSM10 attenuated slightly, and an association with HSM8 emerged although the evidence was weak. After further adjustment for the remaining SITAR parameters (model 3), the association with HSM5 attenuated towards the null and there was no longer evidence of an association, associations with HSM1 and HSM10 were strengthened, the association with HSM9 attenuated slightly, whereas the association with HSM8 switched to positive, however the evidence was weak (Table 4.12).

While there was no evidence to suggest interaction by sex, some differences in the effect estimates were observed in gender stratified analysis. There was consistent evidence for an association between tempo and HSM9 in both males (Table 4.13) and females (Table 4.14) across the models tested, however following full adjustment (model 3) the association fully attenuated in females, whereas there was still evidence of an association in males. With regards to the remaining modes, different patterns of associations were observed between the sexes. There was evidence to suggest an association between tempo and HSM10 (model 1) in both sexes, but these results were attenuated following adjustment for FMI and there was no longer evidence of an association (Table 4.13 and Table 4.14), however while the results were unchanged following further adjustment for size and velocity of growth (model 3) in males, an association emerged in females.

In females, additional unadjusted associations between tempo with HSM2 and HSM5 were seen (model 1) (Table 4.14). Following adjustment for FMI (model 2), the

association with HSM2 was attenuated and there was no longer evidence of an association, whereas the HSM5 association was strengthened, but the latter was fully attenuated following further adjustment for size and velocity (model 3) (Table 4.14).

When modelling the overall relationship between pubertal timing and hip shape, the differences between early vs. late maturers were hard to discern in both sexes (Figure 4.8).

Table 4.12; Associations between tempo (continuous measure) and the top ten HSMs in ALSPAC adolescents at age 18 (N=3,507)

HSM	Model 1			Model 2			Model 3		
	β (95% CI)	p	p for sex-int	β (95% CI)	p	p for sex-int	β (95% CI)	p	p for sex-int
1	0.02 (0.00, 0.03)	0.031	0.756	0.02 (0.00, 0.04)	0.014	0.762	0.03 (0.01, 0.05)	0.009	0.784
2	0.05 (0.02, 0.08)	0.003	0.186	0.00 (-0.03, 0.04)	0.789	0.197	0.03 (-0.01, 0.08)	0.106	0.263
3	0.00 (-0.02, 0.03)	0.823	0.178	-0.02 (-0.05, 0.00)	0.092	0.159	-0.01 (-0.05, 0.02)	0.413	0.258
4	-0.00 (-0.03, 0.03)	0.889	0.172	-0.01 (-0.04, 0.02)	0.523	0.168	0.00 (-0.04, 0.04)	0.915	0.176
5	-0.06 (-0.09, -0.03)	2.6x10 ⁻⁴	0.149	-0.06 (-0.09, -0.03)	2.7x10 ⁻⁴	0.148	-0.00 (-0.05, 0.04)	0.877	0.111
6	-0.01 (-0.04, 0.02)	0.488	0.670	-0.02 (-0.05, 0.01)	0.235	0.679	-0.04 (-0.08, 0.00)	0.065	0.789
7	0.01 (-0.01, 0.04)	0.306	0.880	-0.01 (-0.04, 0.02)	0.490	0.847	-0.01 (-0.04, 0.03)	0.784	0.924
8	-0.01 (-0.04, 0.03)	0.650	0.079	-0.04 (-0.08, -0.01)	0.021	0.068	0.05 (0.00, 0.10)	0.033	0.035
9	-0.08 (-0.11, -0.05)	3.9x10 ⁻⁶	0.766	-0.07 (-0.11, -0.04)	2.4x10 ⁻⁵	0.761	-0.06 (-0.11, -0.02)	0.008	0.731
10	0.07 (0.04, 0.10)	5.3x10 ⁻⁶	0.677	0.03 (0.00, 0.06)	0.038	0.627	0.07 (0.03, 0.11)	0.001	0.491

Abbreviations: HSM (hip shape mode), CI (confidence interval). Table shows results of linear regression analysis between tempo and the top ten HSMs in male and female adolescents. Regression coefficients represent unit change in HSM per one-year increase in growth tempo, 95% CIs and p value. Model 1: adjusted for sex; model 2: model 1 + fat mass index; model 3: model 2 + size and velocity.

Table 4.13; Associations between tempo (continuous measure) and the top ten hip shape modes in ALSPAC males (N=1,597)

HSM	Model 1		Model 2		Model 3	
	β (95% CI)	p	β (95% CI)	p	β (95% CI)	p
1	0.02 (-0.01, 0.05)	0.119	0.02 (-0.00, 0.05)	0.080	0.03 (-0.00, 0.07)	0.067
2	0.02 (-0.02, 0.07)	0.333	-0.01 (-0.06, 0.03)	0.613	0.03 (-0.03, 0.09)	0.357
3	0.02 (-0.02, 0.06)	0.235	0.00 (-0.03, 0.04)	0.831	0.03 (-0.02, 0.08)	0.223
4	0.02 (-0.02, 0.06)	0.342	0.02 (-0.02, 0.06)	0.352	0.02 (-0.03, 0.08)	0.436
5	-0.03 (-0.08, 0.01)	0.163	-0.03 (-0.08, 0.01)	0.167	0.03 (-0.03, 0.08)	0.410
6	-0.02 (-0.07, 0.03)	0.455	-0.03 (-0.08, 0.02)	0.303	-0.01 (-0.08, 0.05)	0.701
7	0.02 (-0.02, 0.05)	0.396	-0.00 (-0.04, 0.03)	0.841	-0.01 (-0.06, 0.04)	0.740
8	0.03 (-0.03, 0.08)	0.314	-0.01 (-0.06, 0.05)	0.770	0.10 (0.03, 0.17)	0.005
9	-0.09 (-0.13, -0.04)	2.4x10 ⁻⁴	-0.08 (-0.13, -0.03)	7.7x10 ⁻⁴	-0.11 (-0.17, -0.05)	5.2x10 ⁻⁴
10	0.08 (0.03, 0.12)	8.8x10 ⁻⁴	0.04 (-0.01, 0.08)	0.118	0.04 (-0.02, 0.10)	0.219

Abbreviations: HSM (hip shape mode), CI (confidence interval). Table shows results of linear regression analysis between tempo and the top ten HSMs in male adolescents. Results are unit change in HSM per unit increase in exposure, 95% CIs and p value. Model 1: unadjusted; model 2: adjusted for fat mass index; model 3: model 2 + size and velocity.

Table 4.14; Association between tempo and the top ten HSMs in ALSPAC females at age 18 (N=1,910)

HSM	Model 1		Model 2		Model 3	
	β (95% CI)	p	β (95% CI)	p	β (95% CI)	p
1	0.02 (-0.00, 0.04)	0.131	0.02 (-0.00, 0.04)	0.087	0.03 (-0.00, 0.05)	0.074
2	0.07 (0.02, 0.11)	0.002	0.01 (-0.03, 0.06)	0.513	0.04 (-0.02, 0.09)	0.207
3	-0.01 (-0.05, 0.02)	0.482	-0.04 (-0.08, -0.01)	0.013	-0.05 (-0.10, -0.01)	0.023
4	-0.02 (-0.06, 0.02)	0.320	-0.03 (-0.07, 0.00)	0.080	-0.02 (-0.07, 0.03)	0.521
5	-0.08 (-0.12, -0.04)	4.2x10 ⁻⁴	-0.08 (-0.13, -0.04)	4.2x10 ⁻⁴	-0.02 (-0.08, 0.04)	0.540
6	-0.01 (-0.05, 0.04)	0.801	-0.01 (-0.06, 0.03)	0.501	-0.07 (-0.13, -0.02)	0.010
7	0.01 (-0.03, 0.05)	0.524	-0.01 (-0.05, 0.02)	0.450	0.00 (-0.05, 0.05)	0.914
8	-0.04 (-0.08, 0.01)	0.128	-0.07 (-0.11, -0.02)	0.005	0.01 (-0.05, 0.07)	0.736
9	-0.08 (-0.12, -0.03)	0.002	-0.07 (-0.12, -0.02)	0.006	-0.01 (-0.08, 0.05)	0.718
10	0.07 (0.02, 0.11)	0.002	0.03 (-0.01, 0.07)	0.144	0.10 (0.04, 0.15)	5.9x10 ⁻⁴

Abbreviations: HSM (hip shape mode), CI (confidence interval). Table shows results of linear regression analysis between tempo and the top ten HSMs in female adolescents. Results are unit change in HSM per unit increase in exposure, 95% CIs and p value. Model 1: unadjusted; model 2: adjusted for fat mass index; model 3: model 2 + size and velocity.

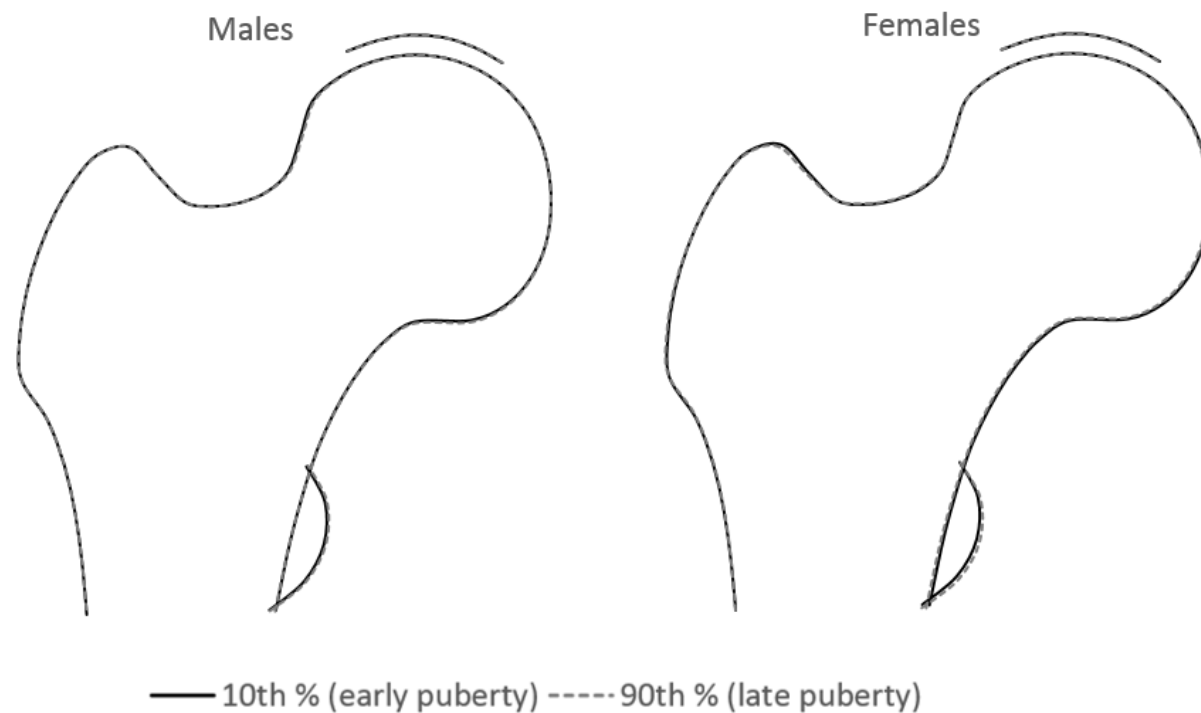


Figure 4.8 The overall difference in hip shape at age 18 between early vs. late matures (changes in hip shape associated with unit change in tempo) based on adjusted beta coefficients. Beta coefficients were scaled to reflect changes in early maturers (10th percentile of tempo) vs. late maturers (90th percentile of tempo).

4.4. Discussion

Summary of findings

In this chapter, I examined the association between pubertal timing (as reflected by tempo) and hip shape in ALSPAC adolescents. At age 14, several associations between tempo and hip shape were observed, and these were stronger in males compared with females. In males, several modes were associated with tempo (unadjusted analysis) and clear patterns of association were also observed when modelling the relationship between tempo quintiles and hip shape (i.e. relationships appeared to be linear). Further adjustment for FMI, size and velocity made little difference to these results. In contrast, the associations between tempo and HSMs in females were weaker in terms of both strength and magnitude of the effect and no distinct patterns of relationship were observed when modelling the relationship between tempo quintiles and hip shape. The strongest association was observed for HSM8, and adjustment for FMI, size and velocity made little difference to these results. When the overall relationship between pubertal timing (early vs. late) and hip shape was modelled, clear differences between males and females were observed. In males, later puberty was associated with narrower FNW, smaller lesser trochanter and larger superolateral femoral head. Whereas in females, the overall relationship between tempo and hip shape was hard to detect.

At age 18, associations between pubertal timing and hip shape were much weaker compared with age 14 results. Tempo was associated with HSM9 in males and this association was independent of FMI, size and velocity of growth, while in females there was some evidence of an association with HSM2, HSM5 and HSM9, however these results were fully attenuated following adjustment for either FMI and/or additional adjustment for size and velocity. Interestingly, there was evidence of an association with HSM10 which attenuated following FMI adjustment in both males and females, and additional adjustment for size and velocity made little difference to these results in males, whereas in females these results were strengthened and there was evidence for an association. As expected, when modelling the overall relationship between early vs. late pubertal timing and hip shape the differences were hard to discern in both males

and females. Taken together these results suggest that pubertal timing might not exert lasting effects on hip shape.

Differences between males and females

In this chapter, a number of strong relationships between tempo and hip shape at age 14 were seen in males, but not in females. A possible explanation for these results may be due to differences in pubertal stages between males and females during scan acquisition. For example, of females in tempo quintile 1 (early maturers) only 3 were in Tanner stages I and II while over 90% were in Tanner stages IV and V (Table 4.5). In males, the reverse was observed, whereby only 4.3% of individuals in tempo quintile 5 were in advanced Tanner stages (stages IV and V) (Table 4.5). Given the fact that the majority of females had already entered puberty at the time of TF 2 clinic attendance (compared with males), part of the effect of pubertal timing on hip shape in females may have been missed. While it is well recognized that there is a considerable degree of variation in maturity at any specific (chronological) age, this is true both within and between the sexes (Cameron, 2015). For example, a previous study estimated mean aPHV (SD) of 12.4 (0.14) in females (Marshall & Tanner, 1969) and 14.1 (0.14) in males (Marshall & Tanner, 1970), a difference of ~2 years, a finding consistent with estimates reported in this study. Another possible explanation for the differences seen between males and females could be the fact that changes in hip shape in females are established shortly before puberty, consistent with a previous study by Pasco et al., which found no relationship between age at menarche and FNW in a cohort of women aged between 20–30 years (Pasco et al., 1999). Alternatively, changes in hip shape in females might be established during the pubertal growth spurt which is shorter compared to males. According to Seeman, males have longer pre-pubertal growth, greater growth velocity and a much longer duration of pubertal growth spurt compared with females (Ego Seeman, 1999).

In relation to published literature

This is the first study to investigate the relationship between the timing of puberty and hip shape as quantified using SSM. A number of researchers have investigated the relationships between markers of pubertal timing (such as age at menarche, age at voice breaking, Tanner stage or aPHV) and musculoskeletal health. These studies have largely

focused on either hip geometrical indices (Sayers et al., 2010) including measures of bone strength (Šešelj et al., 2012) (which are important predictors for hip OA and/or hip fracture in later life) or measures of bone density (Bonjour & Chevalley, 2014; Kuh et al., 2016). In this study, the overall effect of later puberty on hip shape in males was associated with narrower FNW, smaller lesser trochanter and variation in superolateral aspect of femoral head. One previous study by Pujol et al. in boys aged between 9 and 16 years, found that the size of the femoral head and greater and lesser trochanters increased with age (Pujol et al., 2016). These findings were partially replicated in this study, showing that with maturation (in males post PHV) FNW gets wider and lesser trochanter gets larger. However, in this chapter I was also able to describe changes in the entire contour of the femoral head, femoral shaft and acetabular sourcil which was not explored by the Spanish group due to limitations of their model. In addition, the authors did not specifically explore the effect of pubertal timing on hip morphology, however measurements under investigation were collected during the adolescent growth spurt. While the size of the femoral head and the trochanters increase with age, especially around puberty, it is possible that early or later pubertal timing might exert distinct effects on these aspects of the proximal femur.

On the other hand, rather than specific timing of puberty, the period of pubertal growth might represent a sensitive period for the development of unfavourable bone phenotype leading to increased risk of fracture or OA in later life. As suggested by Bass et al., during periods of fast growth (as in puberty) specific bone regions might be more responsive to genetic and/or environmental stimuli, compared with periods of steady growth or with stages near or at completion of growth (Bass et al., 1999). Consistent with this suggestion, Siebenrock et al. showed that cam-type deformity arises in childhood, often as a result of high impact sporting activity (Siebenrock et al., 2011). In addition, previous study in pre-professional soccer players (mean age 14.4), followed up for a mean period of 2.4 years, noted an increase in cam-type deformities between age 12 and 14 years, which continued to increase from the age of 14 until closure of the growth plate (Agricola et al.). Furthermore, Packer et al. suggested that high impact activities and injuries taking place around critical periods of development can result in cam-type deformities, and the authors found no evidence for increase in cam-deformity

prevalence or severity following the closure of the growth plate (Packer & Safran, 2015). While in this chapter, the overall relationship between pubertal timing and hip shape in males was reflected by larger superolateral femoral heads, there was strong evidence for positive relationship between tempo and HSM9 – a mode possibly representative of cam-type deformity. In females, there was also some evidence of an association with this mode, however the magnitude of effect was weaker. Interestingly, when exploring the relationship between tempo and hip shape at age 18 in males, the strongest association seen was with HSM9 and this association persisted after adjustment for FMI, size and velocity, however the effect was in the opposite direction to that observed at age 14. Taken together, these findings suggest that pubertal growth, particularly in males, may represent a critical period for the development of cam-type deformity.

Changes in puberty in relation to future pathology

Previous research has indicated a relationship between pubertal timing and adverse musculoskeletal outcomes in later life. For example, a study of the UK Biobank reported associations between early menarche and increased risk of OA as well as between increasing age at menarche and risk of OP (Day et al., 2015). What is more, a previous study by Finkelstein et al. found that men with a history of delayed puberty had a lower FN BMD, a factor likely to increase the risk of fracture in later life, compared with men with normal pubertal timing (Finkelstein et al., 1996). What is surprising is that I found no strong evidence to suggest a relationship between pubertal timing and hip shape quantified post puberty, suggesting that pubertal timing may not exert lasting effects on hip shape.

Strengths and limitations

One of the strengths of this study includes non-subjective assessment of pubertal stage based on serial height measurements. Although the associations between Tanner stage and HSMs at age 14 were comparable to the associations between tempo and HSMs, it is important to bear in mind that while some studies found good agreement between PHV and secondary sexual characteristics, such as testicular volume (Bundak et al., 2007) and age at menarche (Demirjian et al., 1985), others reported substantial variability in the timing of PHV across Tanner stages (Granados et al., 2015). For example, according to one study PHV is thought to occur between Tanner breast stages

2 and 3 and between Tanner genitalia stages 4 and 5 (Granados et al., 2015) or, according to Abbassi, between Tanner testis stages 3 and 4 (Abbassi, 1998).

In the present study, clear associations between tempo and hip shape at age 14 were observed in males, while these were much weaker in females. One of the limitations of this study is the fact that by the time baseline hip DXA scans were performed in ALSPAC, the great majority of females had already entered puberty, making it difficult to detect effects on hip shape occurring in early puberty. On the other hand, effects occurring in later puberty should have been detectable had they been present. Finally, if pubertal timing exerted lasting effects on hip shape this would have likely been detected in females at age 14 and both sexes at age 18. Any future studies should consider matching males and females on maturational status in order to directly compare the effect of pubertal timing on hip shape in both sexes.

Conclusions

This study offers some important insights into our understanding of periods critical for hip shape development. At age 14, I found strong evidence of an association between pubertal timing (as measured by growth tempo) and hip shape in males, suggesting this may be a sensitive period for environmental and other influences on hip shape which may ultimately determine the risk of hip OA and fracture in later life.

The sex differences in relationships between pubertal timing and hip shape at age 14 observed in this chapter might be due to variation in maturational status, i.e. compared with males, females were more advanced in terms of skeletal and sexual development as reflected by a higher proportion of females in advanced Tanner stages and the majority achieving PHV prior to TF 2 clinic attendance. However, given the lack of compelling evidence for a relationship between tempo and hip shape at age 14 in females and at age 18 in both sexes, it would seem that age at puberty does not exert lasting effect on hip shape post puberty.

In conclusion, the results of this study indicate that puberty represents a critical period for hip shape development, in particular aspects of shape which may be related to future risk of hip OA and/or fracture. Therefore, stratification of at-risk individuals and

preventative measures early in life might reduce the risk of fracture and/or OA development in later life.

Findings in this chapter suggest that age and sex differences observed in the preceding chapter could be partially attributed to differences in pubertal timing, given the strong associations between growth tempo and hip shape described in this chapter, particularly at age 14. However, weak associations between growth tempo and hip shape observed at age 18 suggest that pubertal timing may not exert lasting effects on hip shape, and thus cannot explain sex differences in hip shape that were observed at age 18.

Moving forward, given the differences in pubertal stages at the time of TF 2 attendance and the fact that females mature quicker than males (as described in this chapter), the design of future studies investigating hip morphology should be carefully considered. In order to fully evaluate relationships with hip shape and related bone phenotypes across all pubertal stages, females should be recruited earlier than males while males should be followed for longer to account for longer period of the pubertal growth spurt, to allow matching of participants on their pubertal stage and thus direct comparison of the effect of pubertal timing on hip shape in both sexes.

CHAPTER 5. INVESTIGATING THE RELATIONSHIP BETWEEN BMD AND HIP SHAPE IN ALSPAC OFFSPRING

5.1. Introduction and chapter aims

OP and OA are both common age-related conditions associated with ill health, morbidity and significant economic burden (Jan Dequeker et al., 2003). While they are different diseases in terms of risk factors and genetics it is thought that bone metabolism plays a crucial role in the pathophysiology of both (Geusens & van den Bergh, 2016). On the one hand, low BMD (T-score of -2.5 or less) is used to diagnose OP and predict individual risk of osteoporotic fracture (Geusens & van den Bergh, 2016) whereas on the other, individuals with OA have been found to have increased BMD especially at weight bearing sites, such as hips and knees (Hardcastle et al., 2015b). As discussed previously, hip shape is also related to both disorders, having previously been found to be associated with hip fracture (Alonso et al., 2000; Gnudi et al., 1999) and the development of hip OA (Baker-LePain & Lane, 2010). Relationships of BMD and hip shape with OP and OA are generally thought to represent independent pathways (see Figure 5.1). However, given the biological pathways common to both conditions, and to different bone phenotypes, hitherto unexplored relationships may also exist between hip shape and BMD.

Shared genetic factors may also contribute to the association between OP and OA, based on observations of significant shared heritability. For example, Antoniadou et al. reported higher hip BMD in twins with hip OA compared with their unaffected cotwins, suggesting a role of shared genetic factors in hip OA and BMD (Antoniades et al., 2000). Consistent with this suggestion, a previous GWAS by Yerges-Armstrong et al. identified

four BMD loci that were associated with knee OA (Yerges-Armstrong et al., 2014), and one variant (rs7217932), located near the *SOX9* gene, to be associated with hip OA (Yerges-Armstrong et al., 2014). More recently, in a GWAS by Hackinger et al. investigating shared aetiology between OA and BMD, 143 variants were found to be associated with OA and BMD, a number of which had known relevance to bone (Hackinger et al., 2017). Although these studies suggest that several BMD SNPs influence OA risk, whether BMD and hip shape share common genetic influences, helping to explain the association between OA and OP, is currently unknown. MR represents a useful framework to explore shared genetic contributions to hip BMD and hip shape. In its traditional sense, MR is used to assess a causal effect of modifiable exposure on an outcome. However, rather than being a cause or outcome, BMD and hip shape develop simultaneously, and are thus likely to be influenced by a common biological pathway (referred to as vertical pleiotropy (Swerdlow et al., 2016)).

Figure 5.1 depicts known associations and pathways related to both OA and OP and the unknown association between BMD and hip shape, to be explored. In this chapter, I investigated whether shared developmental influences on hip BMD and hip shape might contribute to the OA-OP relationship, by firstly (i) investigating cross-sectional associations between hip BMD and the top ten HSMs in ALSPAC adolescents at age 14 and 18; secondly ii) using one-sample MR, I aimed to determine the extent to which common genetic pathways underlie both BMD and hip shape. In the next chapter, I will investigate BMD and hip shape associations in adult women in order to provide better understanding of influences on hip shape, and possibly OA risk.

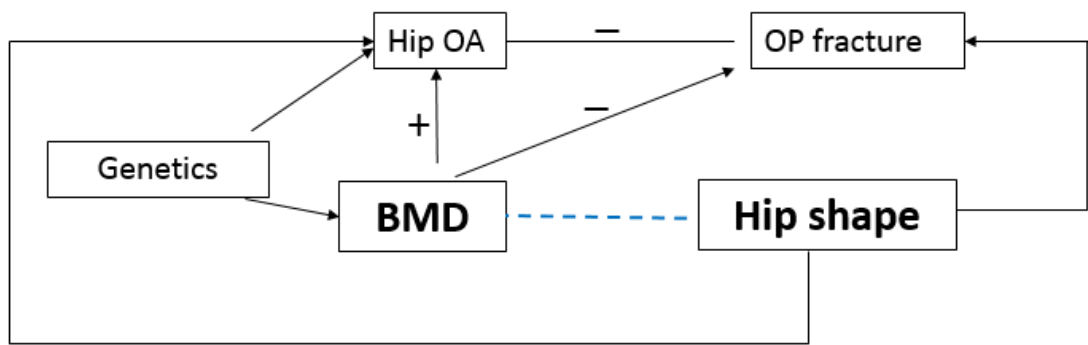


Figure 5.1 Schematic diagram representing relationship to be explored in this chapter (dashed blue line) and known pathways relevant to this analysis (solid black lines). Abbreviations: OA (osteoarthritis), OP (osteoporotic), BMD (bone mineral density).

5.2. Methods

5.2.1. Subjects

Data were obtained from ALSPAC TF 2 and TF 4 clinics when the participants were on average 14 and 18 years old, respectively. The study population for observational analyses comprised individuals with complete data on outcome, exposure and confounders from each assessment clinic, and of those, individuals with genome-wide genetic data, comprised the study sample for MR analyses. For more details regarding data collection and cleaning please refer to the methods chapter (Chapter 2).

5.2.2. Measures

5.2.2.1. Outcome

To quantify the shape of proximal femur, DXA images collected at TF 2 and TF 4 clinics were used. Images were analysed in Shape and to allow comparison between the time points scores from a consistent external adult reference SSM were applied to each data set (see Chapter 2 for details). The top ten HSMs were used as outcomes. For details see Chapter 2.

5.2.2.2. Exposure and covariate data

DXA measured total hip BMD, acquired during TF 2 and TF 4 clinic (at mean ages of 13.8 and 17.8 years, respectively), was used as exposure in the analysis. Age at clinic attendance, sex, height, lean and fat mass were considered potential confounders. For more details see Chapter 2.

5.2.2.3. Genotyping

ALSPAC participants were genotyped using the Illumina HumanHap550 quad genome-wide SNP genotyping platform (Illumina Inc., San Diego, CA, USA). Quality control and exclusion criteria were performed, and data were imputed against the 1000 genomes reference panel (phase 1, version 3). For more details see Chapter 2.

5.2.3. Statistical analysis

5.2.3.1. Observational associations

Cross-sectional associations between total hip BMD and hip shape at age 14 and 18 were assessed using linear regression models. Firstly, age and sex adjusted analysis was performed (model 1) and subsequent model additionally adjusted for height, lean and fat mass (model 2). Sex differences were explored by comparing regression coefficients and their 95% CIs in gender stratified analysis and by formally testing for evidence of statistical interaction using a likelihood-ratio test. As the genetic risk score (GRS) was based on SNPs associated with FN BMD, observational associations between FN BMD and the top ten HSMs were also explored and compared with total hip BMD results.

To provide intuitive visualization of results, the overall relationship between BMD and hip shape at each time point was modelled by simultaneously entering coefficients from linear regression into Shape software, for all modes showing evidence of an association with BMD ($p < 0.005$). In order to aid visualization, coefficients entered into Shape, were multiplied by a factor of 10 and the figures are presented for combined and gender stratified results based on the fully adjusted model.

Having found a number of associations with BMD, I further explored whether sex differences in hip shape (previously described in Chapter 3) could be explained by

differences in BMD. This was explored by further adjusting the model looking at sex differences in hip shape for BMD (model 3: adjusted for age, height, lean and fat mass and total hip BMD).

5.2.3.2. Mendelian randomization

In order to investigate shared genetic influences on BMD and hip shape, I performed one-sample MR analysis. Based on the largest meta-analysis to date of DXA measured LS and FN BMD by Estrada et al. in adults (Estrada et al., 2012), a genetic risk score (GRS) was constructed from 49 independent SNPs (for list of SNPs see Supplementary Table 10.4.5 in Appendix 4) associated with FN BMD at the genome-wide level ($p < 5 \times 10^{-8}$). Given the FN BMD SNPs were identified in adult GWASes, and therefore the published effect sizes might not represent the effect sizes in children, I constructed unweighted GRS. I used two-stage least squares (2SLS) instrumental variable (IV) analysis assuming an additive genetic model, to examine the association between GRS and the top ten HSMs. The strength of the instrument was assessed by examining the F-statistic ($F > 10$ is regarded as a strong instrument (Staiger & Stock, 1997)). Linear regression to explore the strength of an association between the instrument and exposure was also performed. In addition, MR assumes that the instrument is independent of confounders, which was explored by examining associations between the GRS and confounders that were adjusted for in the observational analysis.

5.3. Results

5.3.1. Participant characteristics

Table 5.1 shows the characteristics of study participants.

A total of 4,428 participants (2,117 were male and 2,311 were female) who attended the TF 2 assessment clinic at a mean (SD) age of 13.8 (0.2) years had complete outcome and covariate data. Of those, 3,553 individuals had complete phenotypic and genotypic data.

A total of 4,369 participants (1,931 were male, 2,438 were female) who attended the TF 4 assessment clinic, at a mean (SD) age of 17.8 (0.4) years, had complete outcome and covariate data. Of those, 3,175 individuals had complete phenotypic and genotypic data.

At both time points males were taller, had greater lean mass and total hip BMD compared with females, whereas fat mass was greater in females compared with males.

Table 5.1; Characteristics of participants who attended TF 2 and TF 4 assessment clinics

		TF 2 (Age 14)			TF 4 (Age 18)		
		N	Mean (SD)	p for sex diff*	N	Mean (SD)	p for sex diff*
Age	M + F	4,428	13.8 (0.2)	0.36	4,369	17.8 (0.4)	0.59
	M	2,117	13.8 (0.2)		1,931	17.8 (0.4)	
	F	2,311	13.8 (0.2)		2,438	17.8 (0.4)	
Height (cm)	M + F	4,428	163.4 (7.6)	<0.001	4,369	171.2 (9.2)	<0.001
	M	2,117	165.0 (8.7)		1,931	178.7 (6.6)	
	F	2,311	162.0 (6.2)		2,438	165.2 (6.2)	
Fat mass (kg)	M + F	4,428	13.9 (8.0)	<0.001	4,369	18.4 (10.5)	<0.001
	M	2,117	11.2 (7.7)		1,931	14.1 (10.0)	
	F	2,311	16.4 (7.5)		2,438	21.8 (9.6)	
Lean mass (kg)	M + F	4,428	38.0 (6.4)	<0.001	4,369	45.7 (9.9)	<0.001
	M	2,117	41.0 (7.2)		1,931	55.2 (6.1)	
	F	2,311	35.2 (4.0)		2,438	38.1 (4.3)	
Total hip BMD (g/cm²)	M + F	4,428	1.0 (0.1)	0.006	4,369	1.1 (0.2)	<0.001
	M	2,117	1.0 (0.1)		1,931	1.2 (0.2)	
	F	2,311	0.99 (0.1)		2,438	1.1 (0.1)	
FN BMD (g/cm²)	M + F	4,428	1.0 (0.1)	0.121	4,369	1.1 (0.1)	<0.001
	M	2,117	0.97 (0.1)		1,931	1.14 (0.1)	
	F	2,311	0.98 (0.1)		2,438	1.05 (0.1)	

*Unpaired t-test to assess the null hypothesis of no difference in distributions between males and females. Abbreviations: M (males), F (females) .

5.3.2. Observational associations

5.3.2.1. Age 14

In minimally adjusted analyses adjusted for age and sex (model 1, males and females combined) there was strong evidence for an association between hip BMD and all modes except HSM2 (Figure 5.2). Following further adjustment for height, lean and fat mass (model 2) HSM1, HSM6 and HSM7 results were essentially unchanged, whereas associations with HSM8 and HSM10 were attenuated. In addition, the previously negative association between hip BMD and HSM3 switched to positive, whereas associations with HSM4 and HSM5 were strengthened. Interestingly, a strong positive association with HSM2 now emerged. On examining the association between BMD and HSM1, the adjustment for covariates made little difference to this result and similarly when adjusting for each covariate in turn, the beta coefficients remained broadly similar to the unadjusted estimate (results not shown). On the other hand, on examining the association between BMD and HSM5, when adjusting for each covariate in turn, the biggest change was observed following adjustment for lean mass and height (unadjusted beta 0.06 (0.04,0.09) $p=4.9 \times 10^{-8}$ vs. lean mass adjustment 0.15 (0.12,0.17) $p=3 \times 10^{-27}$; vs. height adjustment 0.13 (0.11,0.16) $p=8.6 \times 10^{-26}$).

Figure 5.3 shows gender stratified results. There was strong evidence for gender interaction for modes 1 ($p=0.002$), 2 ($p=0.005$), 3 ($p=0.001$), 5 ($p=5.8 \times 10^{-8}$), and 9 ($p=2.6 \times 10^{-10}$) (model 1) and HSM1 ($p=0.004$) and HSM9 ($p=0.001$) (model 2). The pattern of associations for modes 1, 2, 3, 4, 5, 8 and 10 were broadly similar (model 1 and 2) between sexes. However, some differences were noted. In particular, following confounder adjustment positive associations with HSM6, HSM7 and HSM9 emerged in females, whereas in males HSM7 and HSM9 results attenuated towards the null and there was no longer evidence of an association.

When looking at the relationship between FN BMD and hip shape, the results were comparable with total hip BMD results (see Supplementary Table 10.4.1 for gender combined and Supplementary Table 10.4.2 for gender stratified results in Appendix 4). In general, associations between FN BMD and HSMs were slightly weaker in terms of the magnitude of effect, but in a consistent direction compared with total hip BMD results.

Figure 5.4 shows the overall relationship between higher hip BMD and hip shape, based on fully adjusted coefficients (model 2). In males and females combined, the total effect of increased hip BMD on hip shape was reflected by narrower FNW and changes in femoral head and greater and lesser trochanters. When the effect was plotted for males and females separately, no striking differences in the overall relationship between higher BMD and hip shape were noted.

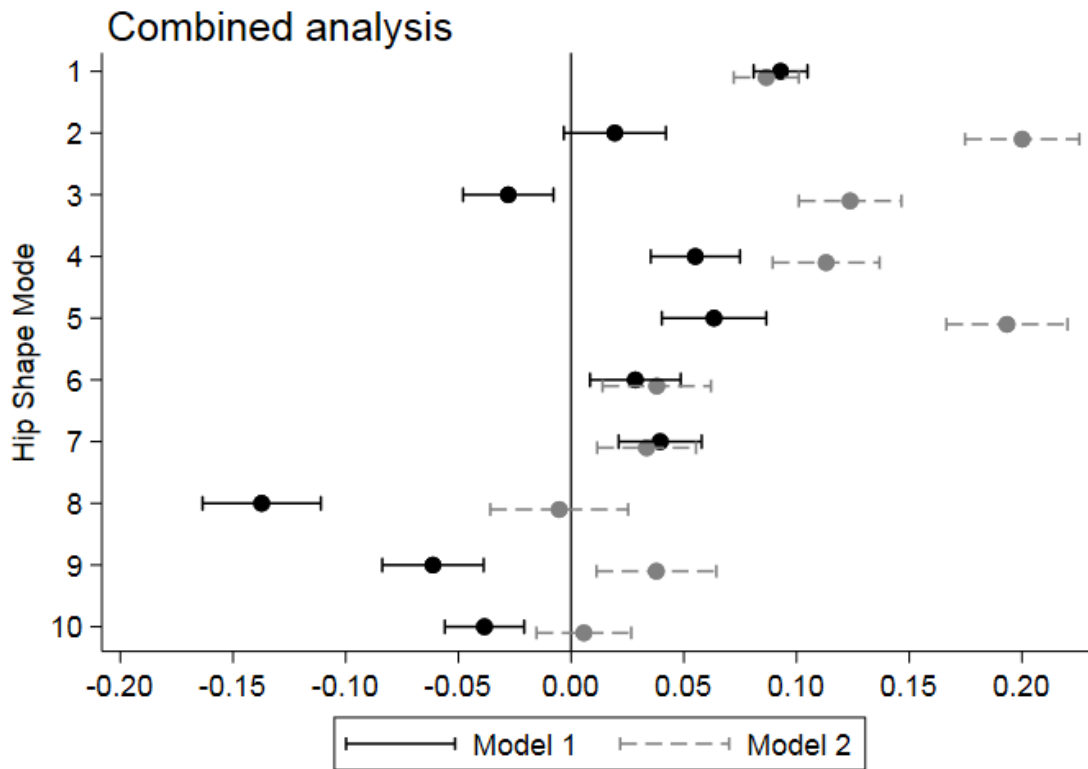
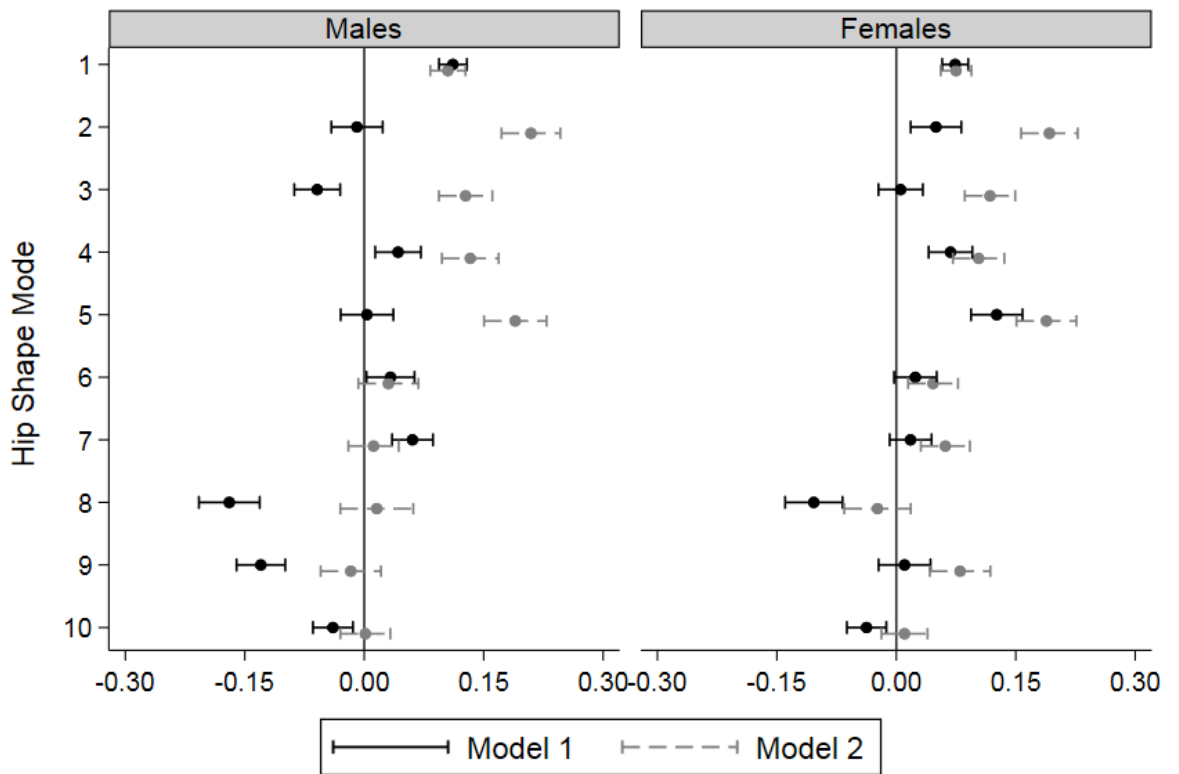


Figure 5.2 Linear regression coefficients with 95% CIs for the association between total hip BMD and the top ten HSMs in ALSPAC adolescents at age 14 (N=4,428). Results show SD change in HSM per SD increase in BMD. Model 1 adjusted for age and gender, model 2 adjusted for age, gender, height, lean and fat mass.



Graphs by gender

Figure 5.3 Linear regression coefficients with 95% CIs for the association between total hip BMD and the top ten HSMs in ALSPAC adolescents at age 14, stratified by gender. Results show SD change in HSM per SD increase in BMD. Model 1 adjusted for age, model 2 adjusted for age, height, lean and fat mass.

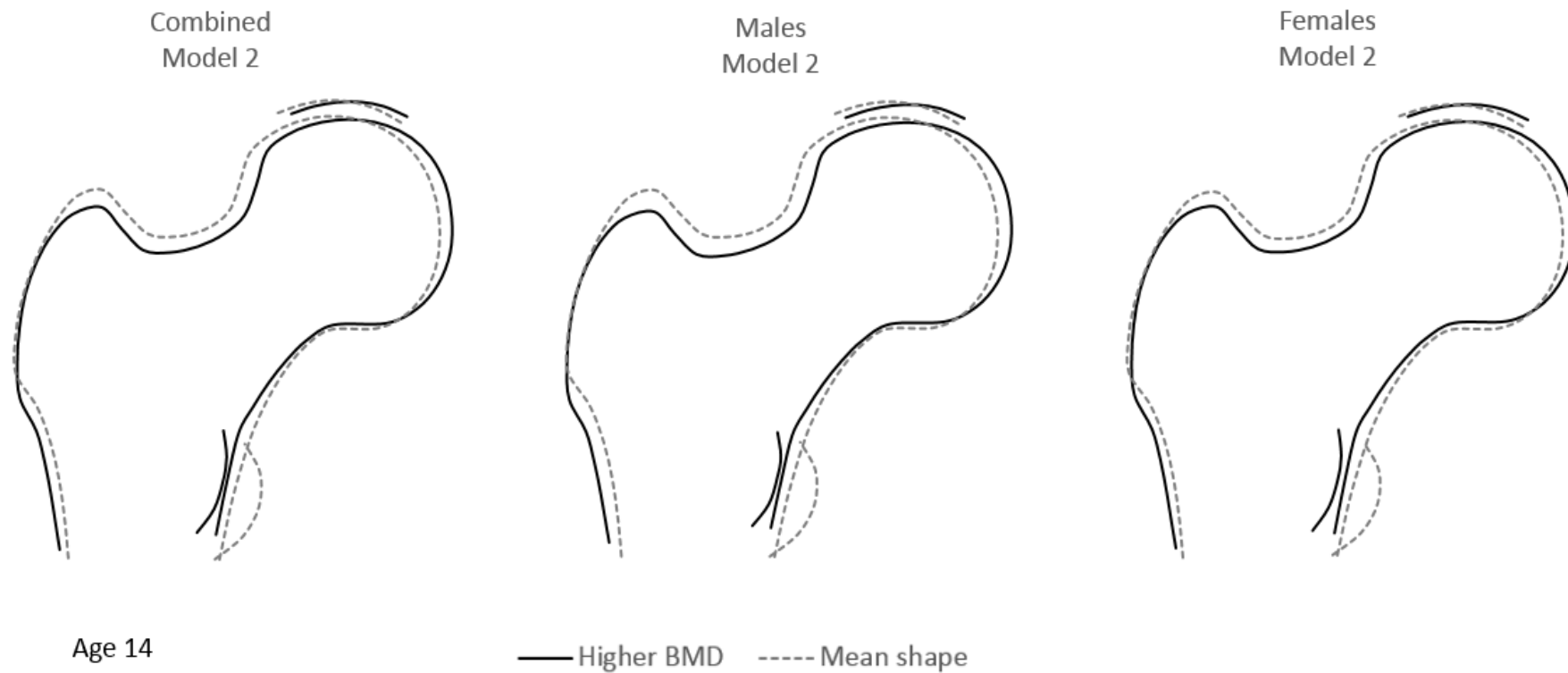


Figure 5.4 Composite hip shape changes associated with higher hip BMD at age 14 based on fully adjusted coefficients (model 2) multiplied by a factor of 10. Dotted line (mean hip shape), solid line (overall change in hip shape per 10 x SD increase in BMD).

5.3.2.2. Age 18

Compared with age 14 results, the associations between hip BMD and HSMs at age 18 (males and females combined) were broadly similar across the models (Figure 5.5). In minimally adjusted analyses (model 1, males and females combined) there was strong evidence for an association between hip BMD and several HSMs and following further adjustment for height, lean and fat mass associations with HSM2, HSM4, HSM5 and HSM9 were strengthened, associations with HSM1 and HSM6 remained unchanged, while association with HSM8 attenuated and there was no longer evidence of an association. Interestingly, associations with HSM3 and HSM7 emerged. Furthermore, the previously negative association with HSM10 switched to positive in the fully adjusted model, and there was evidence of an association in contrast to the fully adjusted result at age 14. There was strong evidence to suggest gender interaction for HSM5 ($p \leq 9 \times 10^{-4}$), HSM7 ($p \leq 5.6 \times 10^{-4}$) and HSM9 ($p \leq 2.8 \times 10^{-5}$) results (consistent for models 1 and 2). Similarly to age 14 results, when the analysis was stratified by gender some differences were observed (Figure 5.6). In males (minimally adjusted model) hip BMD was related to several modes and following full adjustment, there was evidence to suggest associations between hip BMD with the first five modes, and the direction of effect was consistent with age 14 results. However, in contrast with age 14 results, there was strong evidence for an association with HSM6 (both models) and some evidence for an association with HSM10 which emerged following adjustment for confounders. In females, the associations between BMD and hip shape were similar to age 14 results (both models), except there was little evidence for an association with HSM6 at age 18 (both models). The associations between FN BMD and hip shape (males and females combined) were comparable to the associations with total hip BMD (see Supplementary Table 10.4.3 in Appendix 4). Similarly, in gender stratified analysis the associations between FN BMD with HSMs were equivalent to those between total hip BMD (see Supplementary Table 10.4.4 in Appendix 4), except the association between FN BMD and HSM2 which was weaker in males compared with total hip BMD result.

On modelling the relationship between increased hip BMD across all HSMs, based on fully adjusted coefficients (model 2), findings were consistent across both time points (Figure 5.7 shows the effect at age 18). In gender combined analysis, the effect of

greater BMD was mainly reflected by narrower FNW, changes in the femoral head (smaller in superolateral and inferomedial aspects and larger in the medial aspect) and greater and lesser trochanters. When modelled in males and females separately, the effect was broadly similar reflecting narrower FNW and smaller greater trochanter with greater BMD. In addition, higher BMD was reflected by a smaller femoral head (superolateral and inferomedial aspects) in both sexes, and larger femoral head in the medial aspect which was more pronounced in females.

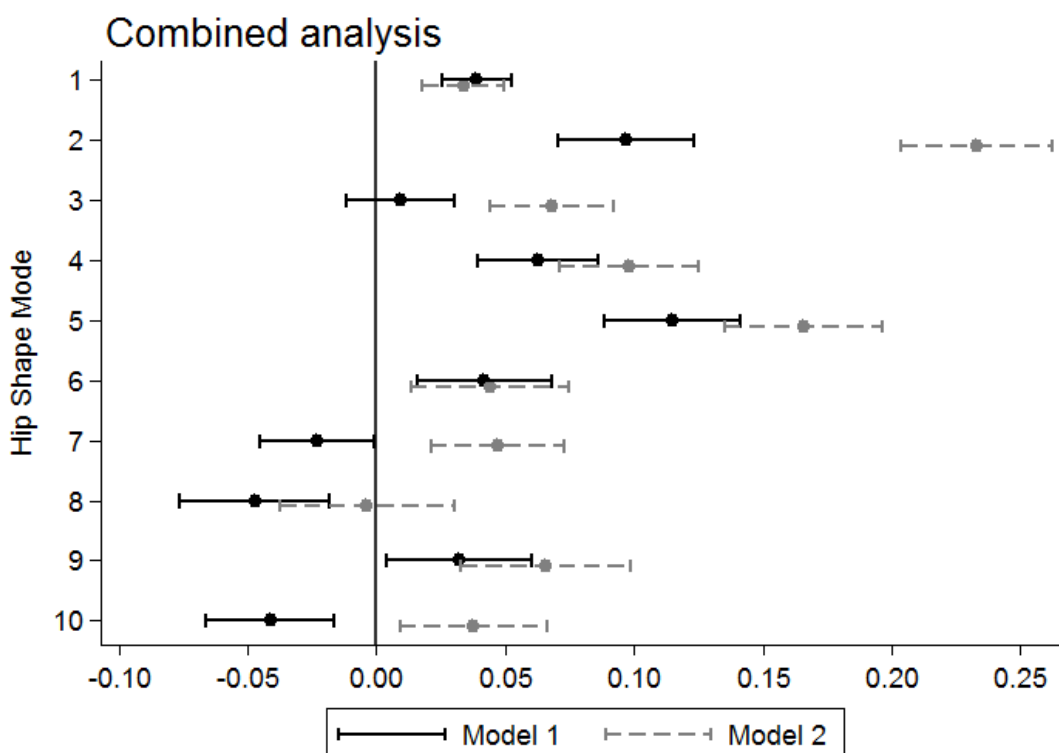
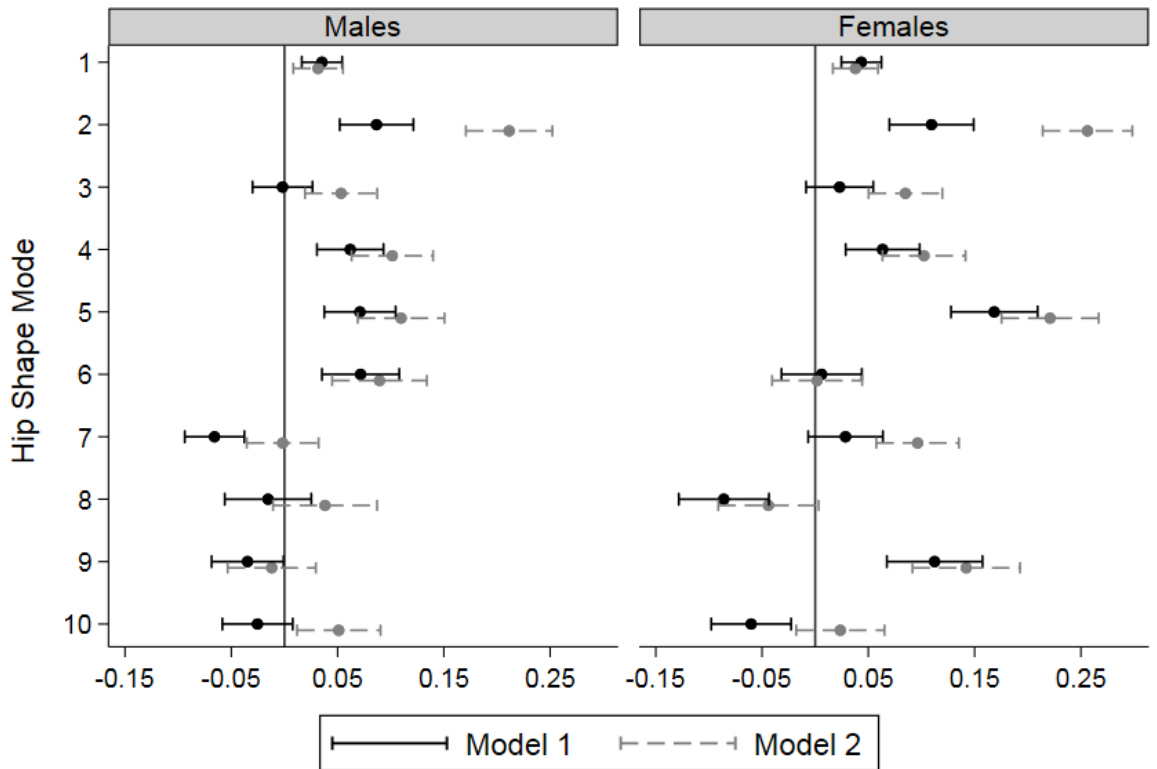


Figure 5.5 Linear regression coefficients with 95% CIs for the association between total hip BMD and the top ten HSMs in ALSPAC adolescents at age 18 (N= 4,369). Results show SD change in HSM per SD increase in BMD. Model 1 adjusted for age and gender, model 2 adjusted for age, gender, height, lean and fat mass.



Graphs by gender

Figure 5.6 Linear regression coefficients with 95% CIs for the association between total hip BMD and the top ten HSMs in ALSPAC adolescents at age 18, stratified by gender. Results show SD change in HSM per SD increase in BMD. Model 1 adjusted for age, model 2 adjusted for age, height, lean and fat mass.

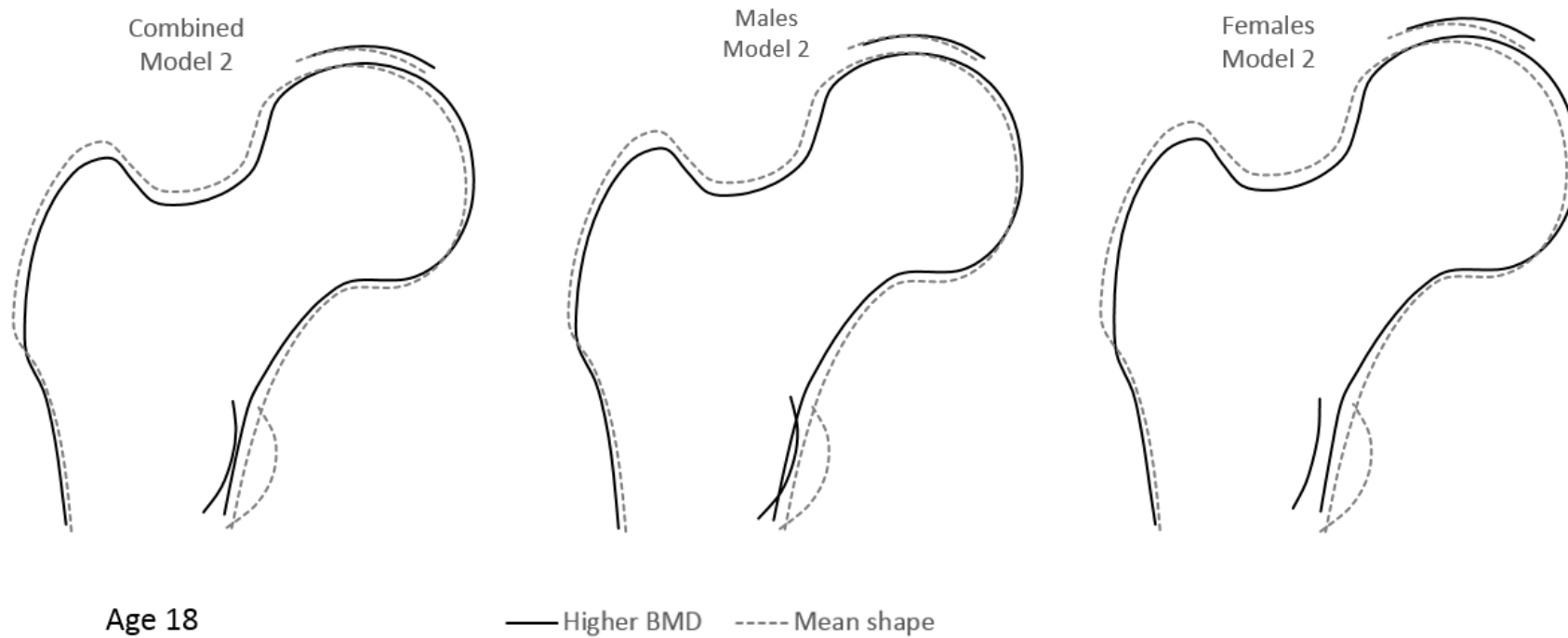


Figure 5.7 Composite hip shape changes associated with higher hip BMD at age 18 based on fully adjusted coefficients (model 2) multiplied by a factor of 10. Dotted line (mean hip shape), solid line (overall change in hip shape per 10 x SD increase in BMD).

5.3.3. Can sex differences in hip shape be explained by differences in BMD

In Chapter 3, I found strong evidence for sex differences in several components of hip shape, independent of body size. Having found a number of relationships between BMD and hip shape, I further explored if sex differences in hip shape could be explained by differences in BMD between the sexes. To explore this, multivariable linear regression exploring the effect of sex on hip shape was further adjusted for BMD.

In Chapter 3, the differences in mean HSM scores between males and females were explored in unadjusted analysis (model 1), and in adjusted analysis controlling for age at clinic attendance, height, lean and fat mass (model 2).

At age 14, further adjustment for hip BMD (Table 5.2, model 3) had little or no effect on the differences in HSM7, HSM8 and HSM9 scores between males and females, while the differences in HSM3 and HSM5 between sexes were strengthened. Interestingly, while there was little or no evidence for gender differences in HSM2 in unadjusted and body size adjusted analyses, respectively, following adjustment for BMD, evidence for gender differences emerged. In addition, following BMD adjustment sex differences in HSM4 attenuated (with 30% decrease in beta coefficient).

At age 18, further adjustment for hip BMD had little or no impact on HSM1, HSM3, HSM6, HSM8, HSM9 and HSM10 scores (Table 5.3, model 3); HSM2, HSM4 and HSM5 results were attenuated (with decrease in beta coefficients of 30% and more); while association with HSM7 was slightly strengthened.

Table 5.2; Differences in hip shape mode scores between males and females (age 14)

HSM	Model 1			Model 2			Model 3		
	β (95% CI)	p	R ²	β (95% CI)	p	R ²	β (95% CI)	p	R ²
1	0.13 (0.11,0.15)	3.7x10 ⁻²⁵	0.02	0.19 (0.16,0.22)	1.1x10 ⁻³²	0.05	0.15 (0.11,0.18)	3.9x10 ⁻²⁰	0.07
2	0.06 (0.01,0.10)	0.013	1.4x10 ⁻⁰³	-0.04 (-0.09,0.02)	0.163	0.09	-0.13 ⁺ (-0.19,-0.08)	1.2x10 ⁻⁶	0.14
3	-0.19 (-0.23,-0.15)	1.7x10 ⁻²¹	0.02	-0.35 (-0.40,-0.30)	5.6x10 ⁻⁴⁶	0.11	-0.41 ⁺ (-0.46,-0.36)	3.6x10 ⁻⁶⁰	0.14
4	0.22 (0.18,0.26)	4.8x10 ⁻²⁸	0.03	0.18 (0.13,0.23)	1.1x10 ⁻¹²	0.03	0.13 ⁻ (0.08,0.18)	8.6x10 ⁻⁷	0.05
5	-0.18 (-0.23,-0.14)	6.1x10 ⁻¹⁵	0.01	-0.34 (-0.39,-0.28)	4.5x10 ⁻³⁰	0.06	-0.43 ⁺ (-0.49,-0.37)	3.7x10 ⁻⁴⁷	0.1
6	-0.14 (-0.18,-0.10)	9.8x10 ⁻¹²	0.01	-0.03 (-0.08,0.02)	0.210	0.03	-0.05 (-0.10,0.00)	0.056	0.03
7	0.18 (0.15,0.22)	3.3x10 ⁻²²	0.02	0.23 (0.19,0.28)	2.2x10 ⁻²³	0.05	0.22 (0.17,0.26)	1.3x10 ⁻¹⁹	0.05
8	-0.73 (-0.78,-0.67)	7.2x10 ⁻¹⁴⁸	0.14	-0.87 (-0.93,-0.80)	2.3x10 ⁻¹⁴⁵	0.22	-0.86 (-0.93,-0.80)	6.8x10 ⁻¹³⁸	0.22
9	0.12 (0.08,0.17)	1.5x10 ⁻⁷	0.01	-0.08 (-0.14,-0.03)	0.004	0.05	-0.10 (-0.16,-0.04)	5.2x10 ⁻⁴	0.05
10	-0.01 (-0.04,0.03)	0.737	2.6x10 ⁻⁰⁵	-0.02 (-0.06,0.03)	0.478	0.03	-0.02 (-0.06,0.03)	0.421	0.03

Abbreviations: HSM (hip shape mode), CI (confidence interval). Table shows mean SD difference in HSM scores between males and females (N=4,428) and 95% CIs, p value and r squared (R²). Model 1: unadjusted, model 2: adjusted for age, height, lean and fat mass, model 3: model 2 + hip BMD. ⁻ represents 30% or higher decrease in beta coefficient, ⁺ represents increase in beta coefficient following adjustment for BMD

Table 5.3; Differences in hip shape mode scores between males and females (age 18)

HSM	Model 1			Model 2			Model 3		
	β (95% CI)	p	R ²	β (95% CI)	p	R ²	β (95% CI)	p	R ²
1	0.02 (-0.003,0.05)	0.084	0.001	0.09 (0.03,0.14)	0.001	0.005	0.07 (0.01,0.12)	0.015	0.01
2	0.48 (0.43,0.52)	1.4x10 ⁻⁷⁸	0.08	0.41 (0.31,0.51)	3.8x10 ⁻¹⁶	0.13	0.28 ⁻ (0.18,0.38)	3.2x10 ⁻⁸	0.18
3	0.13 (0.09,0.17)	5.1x10 ⁻¹¹	0.01	0.17 (0.09,0.25)	4.6x10 ⁻⁵	0.05	0.13 ⁻ (0.05,0.21)	0.002	0.06
4	0.15 (0.11,0.20)	5.1x10 ⁻¹²	0.01	0.19 (0.10,0.28)	5.7x10 ⁻⁵	0.01	0.13 (0.04,0.22)	0.006	0.02
5	0.39 (0.34,0.44)	5.7x10 ⁻⁵³	0.05	0.29 (0.19,0.39)	3.4x10 ⁻⁸	0.06	0.19 ⁻ (0.09,0.30)	2.5x10 ⁻⁴	0.08
6	-0.60 (-0.65,-0.55)	6.9x10 ⁻¹²⁴	0.12	-0.53 (-0.63,-0.43)	1.2x10 ⁻²⁴	0.13	-0.56 (-0.66,-0.45)	3.5x10 ⁻²⁶	0.13
7	0.003 (-0.04,0.04)	0.872	0.00	-0.09 (-0.18,-0.01)	0.036	0.04	-0.12 ⁺ (-0.21,-0.03)	0.007	0.04
8	-0.25 (-0.31,-0.20)	7.4x10 ⁻²⁰	0.02	-0.31 (-0.42,-0.20)	4.5x10 ⁻⁸	0.05	-0.31 (-0.42,-0.20)	8.9x10 ⁻⁸	0.05
9	0.49 (0.43,0.54)	2.0x10 ⁻⁷²	0.07	0.33 (0.22,0.44)	4.8x10 ⁻⁹	0.08	0.29 (0.18,0.40)	3.6x10 ⁻⁷	0.08
10	-0.07 (-0.11,-0.02)	0.004	0.002	-0.16 (-0.25,-0.06)	0.001	0.06	-0.18 (-0.27,-0.08)	2.4x10 ⁻⁴	0.06

Abbreviations: HSM (hip shape mode), CI (confidence interval). Table shows mean difference in HSM scores between males and females (N=4,369) and 95% CIs, p value and r squared (R²). Model 1: unadjusted, model 2: adjusted for age, height, lean and fat mass., model 3: model 2 + hip BMD. ⁻ represents 30% or higher decrease in beta coefficient, ⁺ represents increase in beta coefficient following adjustment for BMD

5.3.4. Mendelian randomization

5.3.4.1. Association between BMD GRS and hip BMD

Since the observational association between BMD and several HSMs persisted following adjustment for potential confounders, this suggests that important causal relationships may exist between BMD and hip shape, reflecting shared biological pathways, which I subsequently examined using a MR approach. There was strong evidence for an association between the BMD GRS derived using SNPs identified in adults, and hip BMD at both time points (Table 5.4), suggesting that despite age differences, this will prove useful for MR analyses of BMD in adolescents. At age 14, GRS explained 3% and 2% of variance in total hip and FN BMD, respectively. At age 18, GRS explained 3% of variance in total hip and FN BMD. This compares with 5.8% of genetic variance in FN BMD explained in adults (Estrada et al., 2012).

5.3.4.2. Association between BMD GRS and confounders

Associations between confounders and GRS are shown in Table 5.5. In general, there was no strong evidence for associations between GRS and confounders, except weak association between GRS and height at age 14 ($p=0.02$). While this could indicate a potential pleiotropic effect, the evidence is somewhat weak when considering the number of tests performed (0.05α threshold corrected for 10 tests (five confounders tested at both time points) = 0.005).

5.3.4.3. Mendelian randomization results

At age 14 (Figure 5.8 and Supplementary Table 10.4.6 in Appendix 4), there was some evidence of positive associations between the hip BMD instrument and HSM1, HSM2 and HSM5 and these results were in a consistent direction and of similar magnitude to the adjusted (for age, gender, height, lean mass and fat mass) observational associations when these analyses were restricted to individuals with complete genotype and phenotype data.

At age 18 (Figure 5.9 and Supplementary Table 10.4.7 in Appendix 4), the MR analysis showed some evidence of positive associations between the hip BMD instrument and HSM2, HSM3 and HSM5. Associations with HSM2 and HSM5 were of similar magnitude

to the fully adjusted observational associations, whereas the magnitude of the effect of BMD on HSM3 was stronger compared with the observational effect.

On comparing findings at both time points, associations with HSM2 and HSM5 were consistent across both time points in terms of the magnitude and direction of the effect. Both, positive HSM2 and HSM5 scores reflect smaller lesser trochanters. In addition, BMD was positively related to HSM1 at age 14, and although little evidence for an effect at age 18 was seen, the direction and magnitude of the effect was consistent with that at age 14. In addition, there was evidence for positive association between BMD and HSM3 at age 18 with comparable effect at age 14 although the evidence was weaker, with CIs overlapping zero. Positive HSM1 scores reflect loss of femoral head curvature and narrower femoral neck whereas positive HSM3 scores reflect narrower FNW and both, HSM1 and HSM3 reflect smaller lesser trochanters.

Table 5.4; Associations between genetic risk score and total hip and FN BMD at age 14 and 18

Outcome	SD change in outcome per 1 SD increase in GRS					
	Age 14 (N= 3,553)			Age 18 (N = 3,175)		
	β (95 % CI)	p	R ²	β (95 % CI)	p	R ²
Hip BMD	0.18 (0.14, 0.21)	2.1x10 ⁻²⁶	0.03	0.16 (0.13, 0.19)	1.6x10 ⁻¹⁹	0.03
FN BMD	0.17 (0.14, 0.20)	9.3x10 ⁻²⁵	0.02	0.17 (0.13, 0.20)	2.8x10 ⁻²¹	0.03

Abbreviations: GRS (genetic risk score), CI (confidence interval). Table shows results of linear regression analysis between standardized unweighted genetic risk score and total hip and FN BMD in ALSPAC adolescents. Results are unit change in outcome per standard deviation increase in exposure, 95% CIs, p value and R².

Table 5.5; Associations between genetic risk score and confounders at age 14 and 18

Outcome	SD change in outcome per 1 SD increase in GRS			
	Age 14 (N= 3,553)		Age 18 (N = 3,175)	
	β (95 % CI)	p	β (95 % CI)	p
Gender	0.01 (-0.01,0.03)	0.27	0.01 (0.00,0.03)	0.13
Age at clinic attendance	0.00 (0.00,0.01)	0.38	0.01 (-0.01,0.02)	0.31
Height	0.29 (0.04,0.54)	0.02	0.24 (-0.08,0.56)	0.15
Lean mass	0.03 (-0.18,0.24)	0.81	-0.12 (-0.46,0.23)	0.51
Fat mass	0.12 (-0.14,0.38)	0.38	0.16 (-0.19,0.52)	0.37

Abbreviations: GRS (genetic risk score), CI (confidence interval). Table shows results of linear regression analysis between standardized unweighted genetic risk score and gender, age, height, lean and fat mass in ALSPAC adolescents. Results are unit change in outcome per standard deviation increase in exposure, 95% CIs and p value.

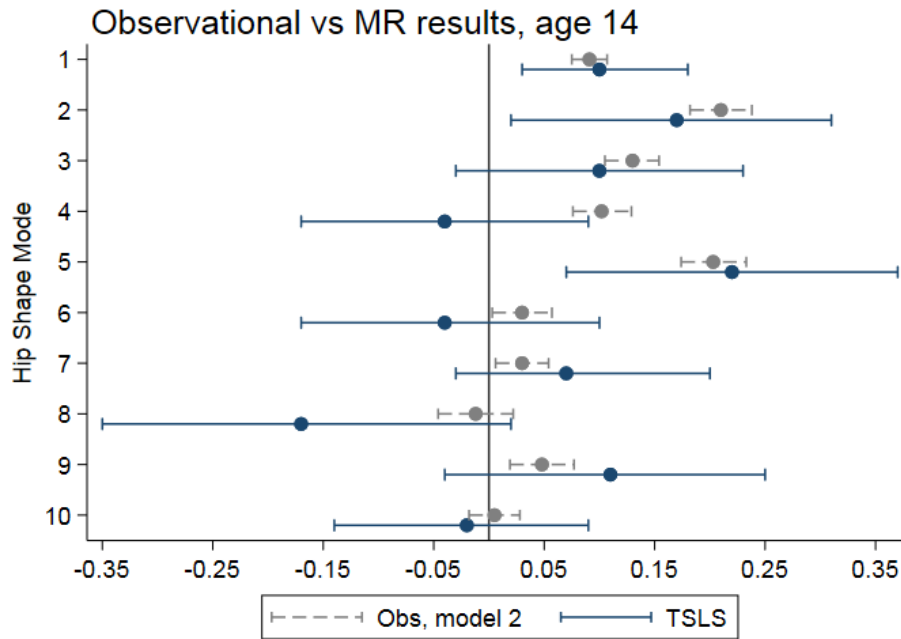


Figure 5.8 Fully adjusted observational (dashed grey line) and MR (solid navy line) estimates and 95% CIs for the association between BMD and hip shape in ALSPAC adolescents at age 14.

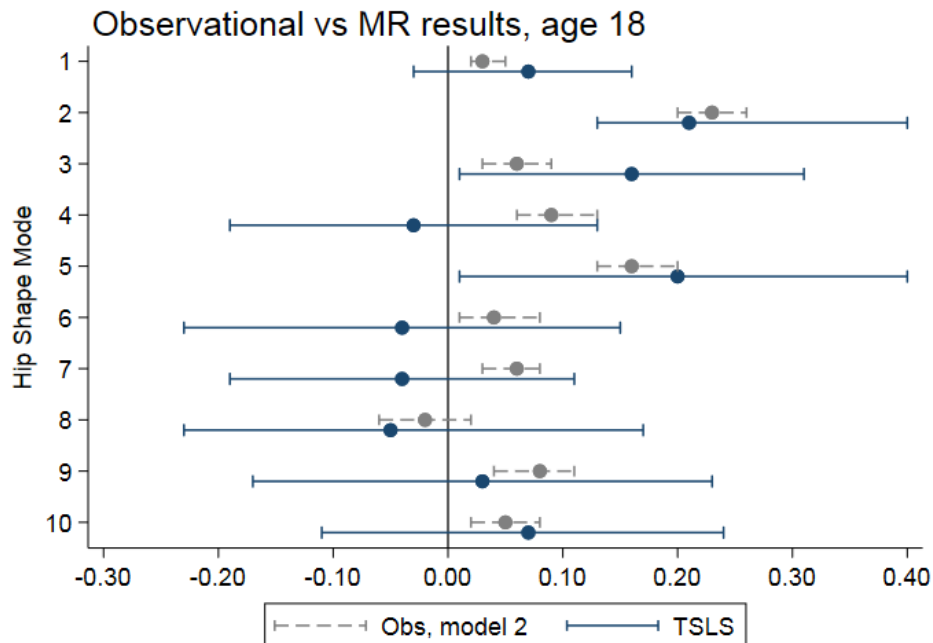


Figure 5.9 Fully adjusted observational (dashed grey line) and MR (solid navy line) estimates and 95% CIs for the association between BMD and hip shape in ALSPAC adolescents at age 18.

5.4. Discussion

The relationship between BMD and hip shape with OA is well-established, however little is known about the relationship between BMD and OA-related endophenotypes. In this chapter, I examined the relationship between BMD and hip shape at age 14 and 18 in a cohort of ALSPAC adolescents and these analyses were followed up with MR approach to investigate shared genetic architecture underlying these relationships.

Summary of observational findings

Observationally, I found strong evidence for associations between hip BMD and a number of HSMs at age 14 and age 18. In males, consistent associations between BMD and the first five modes were observed at both time points. While there was little evidence to suggest association with HSM6 at age 14, by the age of 18 there was robust evidence for an association and the effect was strengthened following confounder adjustment. In females, the effect of BMD on hip shape was consistent across the time points with the majority of modes related to BMD. Following adjustment for age, height, lean and fat mass these associations were strengthened (except HSM8 and HSM10 results which attenuated and there was no longer evidence of an association). While there was evidence to suggest an association between BMD and HSM6 at age 14, there was little evidence for an association at age 18. In terms of the relationship between higher BMD across all HSMs combined, consistent associations were noted in both sexes across the time points, mainly reflecting narrower FNW, smaller greater trochanter and variation in femoral head (which appeared smaller in the superolateral and inferomedial aspects and larger in the medial aspect).

In terms of sex differences in hip shape (previously described in Chapter 3), some associations were partly explained by differences in BMD. For example, sex differences in HSM4 at age 14 and HSM2, HSM4 and HSM5 at age 18 showed partial attenuation after adjustment for BMD. Interestingly, while there was previously no evidence of sex differences in HSM2 at age 14, these differences emerged following adjustment for BMD. One possible explanation for this could be due to opposing direction of effect

between confounder-exposure and confounder-outcome associations. For example, height, lean and fat mass were all negatively related to HSM2 (see Supplementary Table 10.2.2 - Supplementary Table 10.2.4 in Appendix 2) whereas there was strong positive relationship between BMD and HSM2. Another possibility could be due to an artefact or measurement error.

Results in relation to published literature

To my knowledge, this is the first study to explore the relationship between BMD and hip shape as quantified by SSM in a cohort of adolescents. One previous study explored the relationship between BMD and hip shape in a cohort of adults (mean age 63 years) from the MRC NSHD cohort (Pavlova et al., 2017). The authors reported an association between higher hip BMD and HSM3 in women and this mode reflected smaller neck-shaft angle and greater acetabular coverage. This contrasts with findings in this chapter and is likely to reflect changes associated with age and other disease processes given the age of the MRC NSHD participants. The association between BMD and hip shape in this cohort was reflected by narrowing of FNW and variation in superolateral and inferomedial aspects of femoral head in both sexes. Hence, higher BMD was related to larger femoral heads (in the medial aspect). The relationship between FNW with osteoporotic fracture (Ego Seeman et al., 2001) and OA (Castaño-Betancourt et al., 2013b) has been investigated previously. In terms of OA risk, a previous study reported an association between wider FNW and higher risk of incident hip OA (Castaño-Betancourt et al., 2013b), suggesting that BMD-hip shape association is unlikely to explain the relationship between FNW and risk of OA. With regards to the relationship between FNW and hip fracture the evidence is conflicting, with previous studies reporting associations between both, wider and narrower FNW and hip fracture (Ahlborg et al., 2005; Alonso et al., 2000; Karlsson et al., 1996; Ego Seeman et al., 2001). Interestingly, larger femoral heads have been found to predict radiographic hip OA in a cohort of elderly women (Lynch et al., 2009), a feature similar to that observed when modelling the overall relationship between higher BMD and hip shape in adolescents in this study.

Mendelian randomization

Using a MR approach, I found some evidence for shared genetic mechanisms underlying BMD and hip shape. In particular, there was evidence for consistent positive associations between BMD and HSM2 (which observationally showed the strongest effect; fully adjusted betas ≈ 0.2 in both sexes across the time points) and HSM5 at both time points. There was evidence of positive association with HSM1 at age 14 and HSM3 at age 18. While there was little evidence to suggest association with HSM1 at age 18 and HSM3 at age 14, the estimates were consistent between the time points and given the overlap of 95% CIs surrounding these estimates, an effect of BMD on hip shape cannot be ruled out hence follow up in a larger, independent cohort is required. HSM2, HSM3 and HSM5 all reflect variation in inferolateral aspect of femoral head, FNW and greater and lesser trochanters. HSM1 reflects variation in femoral head size and shape (variation is most pronounced in the medial aspect, additional variation in the superolateral and inferolateral aspects) along with FNW and greater and lesser trochanters.

MR, which uses genetic variants as instrumental variables, is generally used to assess causality, which is important from a public health perspective as modifying causal exposures will in turn reduce disease risk or alter its course. However, in this context I used MR to evaluate the contribution of a common genetic pathway to two distinct developmental traits. For MR to be valid, several assumptions need to be met: the genetic instrument i) must be associated with the exposure of interest, ii) must not be associated with any confounders, and iii) must not directly influence the outcome, except through the exposure of interest. In this study, I found strong evidence for an association between GRS and DXA measured FN and total hip BMD (which satisfies the first assumption). When exploring the association between GRS and confounding variables, included in the observational analyses, no evidence for associations was found, except weak evidence for an association between GRS and height measured at age 14. While this could be a chance finding, given the number of tests that were performed, it is possible that this represents a true causal relationship. Consistent with this suggestion, a previous large-scale study in the UK Biobank reported that several loci for heel BMD were also related to height in the Genetic Investigation of Anthropometric

Traits (GIANT) consortium and this was also true for a number of DXA measured BMD loci (Kemp et al., 2017). Given the polygenic nature of genetic variants contributing to complex traits (Sivakumaran et al., 2011), it is possible that SNPs involved in skeletal growth and BMD acquisition also affect other traits. In this study, more than half of the variants included in the GRS were of unknown function to bone biology. While it is likely that some variants will have pleiotropic effects, the issue of horizontal vs. vertical pleiotropy needs to be carefully examined. While the latter (one variant has an effect on two or more traits that both influence the outcome via the same biological pathway) is not an issue for MR analysis, horizontal pleiotropy (one variant is associated with two traits which influence the outcome via independent biological pathways) could invalidate MR results (Yarmolinsky et al., 2018). One way of overcoming issues of horizontal pleiotropy would be to check published literature or GWAS databases for associations between BMD-related SNPs with other traits. This could then be followed up with a sensitivity analysis where only SNPs with known function and relevance are included and estimates between initial vs. restricted analyses are compared. In addition, statistical methods which detect and account for pleiotropy, such as MR-Egger regression and the weighted median estimator (Yarmolinsky et al., 2018), should also be considered.

It is also worth noting that the GRS was based on BMD SNPs discovered in adult cohorts. While these SNPs may be responsible for BMD maintenance and bone loss, different variants might contribute to bone acquisition in adulthood. However, as shown in Table 5.4 the instrument was strongly related to BMD in adolescence in my data and a previous study by Warrington et al. showed that BMD SNPs identified in adults were partly responsible for the rate of bone acquisition in adolescents (Warrington et al., 2015).

Despite strong observational evidence for associations between BMD and a number of HSMs, not all of these results were supported by MR. While the GRS was strongly associated with total hip and FN BMD at both time points and the F statistic (above 10) indicated good instrument strength, wide 95% CIs for the MR results that were observed in this chapter, are indicative of low power. For example, the power to detect an effect of BMD on HSM2, similar in magnitude to the observational estimate, was 72%,

however this would be much lower for the remaining modes which had smaller estimates. For that reason, these results should be followed up in a larger adolescent cohort to increase power and rule out chance finding.

Nevertheless, MR results suggest that biological pathways underlying BMD variation could contribute to aspects of hip shape (such as variation in FNW described by HSM2, HSM3 and HSM5, and variation in femoral head size described by HSM1) which have previously been found to be associated with increased risk of OA (Castaño-Betancourt et al., 2013b; Lynch et al., 2009) and/or fracture (Ego Seeman et al., 2001). In terms of specific pathways underlying BMD and hip shape and thus potential future risk of OA, Wnt pathway genes (associated with BMD in both adults and children) which play an important role in skeletal development and growth (Lodewyckx & Lories, 2009) also have a regulatory role in OA (Lane et al., 2017). In addition, recent hip shape GWAS meta-analysis in older adults (D. A. Baird et al., 2017) (using hip shape mode scores based on the same SSM template used throughout this thesis) found an association between *SOX9* SNP and HSM5 (shape related to total hip BMD in observational and MR analysis), and this signal co-localised with that previously reported for *SOX9* and hip BMD (D. A. Baird et al., 2017; Estrada et al., 2012). Inclusion of *SOX9* in the hip BMD allele score is likely to have contributed to the relationship with HSM5 in MR analyses. Given the role of *SOX9* in endochondral bone formation (Huang et al., 2001), these findings may reflect shared influences of longitudinal growth on hip shape and BMD. In order to identify specific pathways relevant to hip shape development, further analysis investigating the relationship between GRSes based on SNPs belonging to certain genetic pathways, such as Wnt signalling or RANK-RANKL-OPG, (an approach previously employed by Warrington et al. (Warrington et al., 2015)) should be undertaken. It is worth mentioning that although I found evidence for an association between a genetic instrument for BMD and hip shape, given the close relationship between these traits, a direct effect of BMD SNPs on hip shape cannot be ruled out. Therefore, future analysis should also explore the relationship between GRS based on variants with an established functional role with a clear effect on BMD. Furthermore, as our understanding of the genetic architecture underlying BMD (Kemp et al., 2017) and hip shape improves, future analysis could be extended to formally test for an overlap between BMD and hip shape

(Hackinger et al., 2017) enabling identification of additional shared loci and biological pathways common to these traits. If features likely to predict OA develop early in life this provides a window of opportunity for potential stratification of individuals into high risk groups and scope for early prevention.

Conclusions

In this chapter, I explored the relationship between BMD and hip shape in ALSPAC adolescents. Observationally, BMD was related to a number of modes and the composite relationship between higher BMD and hip shape, which was reflected by narrower FNW and variation in femoral head, was consistent between sexes and across the time points. MR results suggested that shared genetic factors, presumably reflecting common biological mechanisms, influence both BMD and hip shape, partly explaining the association between these two traits in observational analyses. Hence, whereas hip shape may contribute to the association between OP and OA indirectly through biomechanical influences on hip shape, the present findings suggest that more direct biological relationship between hip shape and BMD may also play a role. Further studies in a larger sample of adolescents are justified to confirm these findings and identify specific pathways common to BMD variation and hip shape which will in turn help elucidate shared mechanisms related to OA and OP risk.

CHAPTER 6. INVESTIGATING THE RELATIONSHIP BETWEEN BMD AND HIP SHAPE IN MIDDLE-AGED WOMEN

6.1. Introduction chapter aims

In the previous chapter, I found strong evidence for consistent observational associations between BMD and hip shape in ALSPAC adolescents at age 14 and 18. Furthermore, a MR results provided some evidence to suggest that shared genetic factors, influence both BMD and hip shape. Here, I repeated the observational analyses and used MR approach, in adult women from ALSPAC cohort, in order to gain understanding of shared genetic contributions to hip BMD and hip shape in adolescents and adult women.

As described in the previous chapter the inverse relationship between OA and OP, as well as the role of hip shape in the development of hip OA and fracture risk prediction are well-established. In addition, previous studies found evidence for genetic overlap between BMD and OA suggesting shared genetic aetiology of these traits (Antoniades et al., 2000; Hackinger et al., 2017). However, whether BMD and hip shape share common genetic influences which might help explain the mechanisms underlying the OA-OP association, have not been explored previously.

Therefore, the aims of this chapter are to

(i) examine cross-sectional relationships between BMD and proximal femur shape in a cohort of adult women, and (ii) investigate whether shared genetic architecture underlies these relationships using two-sample MR analysis.

6.2. Methods

6.2.1. Study population

Data from ALSPAC mothers who attended the FoM 1 clinic, between 2008 and 2011, were used. The study population for observational analyses comprised mothers with complete data on exposure, outcomes and confounders, and of those, mothers with genome-wide genetic data, contributed to GWAS of hip shape. Summary statistics from hip shape GWAS in ALSPAC mothers (unpublished data) along with summary statistics from previously published GWAS of BMD (Estrada et al., 2012) were used for MR analysis.

6.2.1.1. Outcome

Hip shape in ALSPAC mothers was quantified in the same way as adolescent data (see Chapter 2 for full method description) and all images were aligned in Shape by Ben Faber and Denis Baird. Following shape alignment, Procrustes analysis and PCA were performed and the same adult reference SSM (described in section 2.5, Chapter 2) which was applied to adolescent data, was also applied to mothers' images, allowing for direct comparison of adult and adolescent results. The top ten HSMs were used as outcome variables. For more details regarding hip shape quantification and data collection see Chapter 2.

6.2.1.2. Exposure and covariate data

DXA measured BMD, acquired during FoM 1 research clinic (at mean age of 48 years) was used as exposure. Age at clinic attendance, height, lean and fat mass were considered potential confounders. For more details regarding data collection and cleaning please refer to the methods chapter (Chapter 2, section 2.2.2.2).

6.2.1.3. Genotyping

ALSPAC participants were genotyped using the Illumina HumanHap550 quad genome-wide SNP genotyping platform (Illumina Inc., San Diego, CA, USA). Quality control and exclusion criteria were performed, and data were imputed against the 1000 genomes reference panel (phase 1, version 3). For more details see Chapter 2, section 2.2.3.

6.2.2. Statistical analysis

6.2.2.1. Cross-sectional analysis

Descriptive statistics are expressed as means (SD). While selection of confounders was based on prior knowledge, univariable linear regression was used to assess the strength of statistical evidence of an association between each confounder with exposures and outcomes within this sample. Multivariable linear regression was used to explore the relationship between BMD and the top ten HSMs adjusting for age (model 1), and additionally for height, lean and fat mass (model 2). Results are expressed as regression coefficients (β) with 95% confidence intervals (i.e. SD change in HSM per SD increase in exposure). All cross-sectional analyses were performed in Stata version 14 (StataCorp, College Station, TX, USA). Though the primary analysis is with total hip BMD, the genetic instrument for BMD (see section 6.2.2.2 below) was based on SNPs associated with FN BMD, therefore observational associations between FN BMD and the top ten HSMs were also explored and compared with total hip BMD results.

To provide intuitive visualization of results, the overall relationship between BMD and hip shape at each time point was modelled by entering coefficients from linear regression into Shape software, based on the fully adjusted model, for all modes showing evidence of an association with BMD ($p < 0.005$). In order to aid visualization, all coefficients entered into Shape were multiplied by a factor of 10 (as in the previous chapter).

6.2.2.2. Mendelian randomization

Similarly to the previous chapter, I used a MR approach to investigate shared genetic influences on BMD and hip shape. In this instance, I was able to use a two-sample MR approach given the availability of GWAS results of BMD in adults (Estrada et al., 2012) and hip shape GWAS results in ALSPAC mothers (analysis performed by Denis Baird; unpublished data). In contrast to one-sample MR, this method uses summary statistics data (as opposed to one-sample MR which used person level data) and has the added advantage of increased statistical power. In addition, obtaining BMD and hip shape instruments from non-overlapping samples (as in this chapter) eliminates the issue of ‘winners curse’ which can underestimate effects in one-sample MR setting (Lawlor, 2016).

SNP-exposure effects were based on the largest meta-analysis of DXA-measured FN and LS BMD by Estrada et al. (Estrada et al., 2012). I selected 49 SNPs (the same variants were used for analysis in Chapter 5) that were associated with FN BMD at genome-wide significant level ($P < 5 \times 10^{-8}$). FN BMD effect estimates based on a sample of 83,894 (combined discovery (stage 1) and replication (stage 2) samples) were recorded. These estimates and therefore effect allele frequencies were consequently flipped to represent FN BMD increasing effects (see Supplementary Table 10.5.3 in Appendix 5 for a list of SNPs). To obtain the SNP-outcome effects, FN BMD associated SNPs were then looked up in summary statistics from hip shape GWAS of ALSPAC mothers, and the coefficients along with SEs were recorded. The SNP-exposure and SNP-outcome effects were harmonized (Hartwig et al., 2016) (i.e. variants not sharing the same allele pair between the data sets were identified and either corrected, where possible, or removed) and inverse-variance-weighted (IVW) approach using TwoSampleMR package in R version 3.4.1 was performed to estimate the overall effect of BMD increasing variants on hip shape.

6.3. Results

6.3.1. Sample characteristics

Of 11,264 (82%) women invited to the assessment clinic, 4,834 (43%) attended. A total of 4,289 (89%) who attended the assessment clinic, had complete outcome and covariate data. Of those, a total of 3,111 contributed to hip shape GWAS. In comparison with the 9,511 women excluded because of non-clinic attendance or missing data, those with complete data were older at birth of their child, more likely to have a university degree, own their own property and were less likely to smoke when recruited to the study (Table 6.1). Table 6.2 shows the characteristics of women participating in the study. Their mean age was (SD) 47.9 (4.4) years, and mean BMI was 26.7 (5.6) kg/m².

Table 6.3 shows the means and SDs for the top ten HSMs. Compared to mean=0 and SD=1 when using individual cohort data, when using the combined adult reference SSM means ranged from -0.35 to 1.45 and SDs were in the range of 0.53-1, which most likely

reflects the differences between the scanners used for each cohort included in the adult reference SSM (as described previously in Chapter 2, section 2.5.2).

Table 6.1; Baseline characteristics in women who attended the research clinic, and had data available for exposure, outcome and main confounder variables, and women initially recruited but did not attend the first follow up clinic assessment of mothers

¹Unpaired t-test for continuous variables and chi-square test for categorical variables to

	Mean (SD) for continuous variables and prevalence n (%) for categorical variables				
	Subjects with no data available N = 9,511		Current study population N = 4,289		P value ¹
	Total N	N (%)	Total N	N (%)	
Age at birth of child (years)	9,511	27.2 (5.0)	4,289	29.6 (4.5)	<0.001
Had a university degree at time of index pregnancy [n (%)]	8,085	800 (9.9)	4,175	777 (18.6)	<0.001
Ever smoked [n (%)]	8,691	4,867 (56.0)	4,212	1,700 (40.4)	<0.001
Owned property at time of index pregnancy [n (%)]	8,677	5,828 (67.2)	4,188	3,606 (86.1)	<0.001

assess the null hypothesis of no difference in those who did and those who did not attend the follow-up clinic.

Table 6.2; Characteristics of participating ALSPAC cohort study adult women (N=4,289)

Variable	Mean (SD)
Age (years)	47.9 (4.4)
Height (cm)	164.0 (6.2)
Fat mass (kg)	27.2 (10.9)
Lean mass (kg)	41.3 (5.1)
Total hip BMD (g/cm ²)	1.03(0.14)
Femoral neck BMD (g/cm ²)	0.99 (0.13)
BMI (kg/m ²)	26.7 (5.6)

Abbreviations: SD (standard deviation), BMD (bone mineral density), BMI (body mass index).

Table 6.3; Summary statistics for the top ten HSMs in ALSPAC mothers (N= 4,289) based on the adult reference SSM template

HSM and % var. explained*	Mean HSM score (SD)
1 (42%)	1.45 (0.53)
2 (13%)	-0.01 (0.90)
3 (8.5%)	-0.31 (0.92)
4 (6.1%)	0.32 (0.77)
5 (4.1%)	-0.35 (0.94)
6 (3.4%)	-0.01 (1.00)
7 (2.6%)	-0.14 (0.87)
8 (2.5%)	0.06 (0.95)
9 (1.8%)	0.34 (0.95)
10 (1.5%)	0.11 (0.92)

Abbreviations: HSM (hip shape mode), var (variance).

*Variance explained in the adult reference model.

6.3.2. Cross-sectional associations

6.3.2.1. Confounder- exposure and confounder- outcome associations

Supplementary Table 10.5.6 and Supplementary Table 10.5.7 in Appendix 5 show the associations between confounders and exposures used in the main analysis. As expected, there was strong evidence for associations between all confounders and both, total hip and FN BMD.

Supplementary Table 10.5.8 in Appendix 5 shows associations between each confounder and the top ten HSMs. There was strong evidence for an association between age and HSM3 and HSM4 and very weak evidence for an association with HSM10. There was strong evidence for an association between height and HSM2, HSM5, HSM8 and HSM10. There was strong evidence for an association between both fat and lean mass and the majority of HSMs, except HSM3 (lean mass), HSM4 and HSM6 (lean and fat mass).

6.3.2.2. Total hip BMD and FN BMD associations

In age adjusted analysis, there was strong evidence for an association between total hip BMD and HSM1, HSM3, HSM5, HSM6, HSM7 and HSM9 and weak evidence to suggest an association with HSM2 (model 1, Figure 6.1). Following adjustment for height, lean and fat mass associations with HSM1, HSM3, HSM6 and HSM9 remained unchanged, whereas associations with HSM2, HSM5, and HSM7 were strengthened and an association with HSM10 emerged (model 2, Figure 6.1).

The overall relationship between higher hip BMD and hip shape, independent of age, height, lean and fat mass was reflected by narrower FNW, smaller lesser trochanter, larger femoral head in the medial aspect but smaller in the superolateral aspect (Figure 6.2).

Associations between FN BMD and hip shape were similar to that with total hip BMD results (both age adjusted and fully adjusted models, Supplementary Figure 10.5.1 in Appendix 5), however the magnitude of the effect in FN BMD analyses was generally weaker. In addition, while associations between total hip and FN BMD with HSM4 were

in the same direction, there was strong evidence for FN BMD association and little evidence for total hip BMD association (with confidence intervals overlapping 0).

On modelling the relationship between increased FN BMD across all HSMs based on fully adjusted coefficients, findings were similar to that of total hip BMD (Supplementary Figure 10.5.2 in Appendix 5) with higher FN BMD associated with narrower FNW, smaller lesser trochanter and variation in femoral head (medial and superolateral aspects).

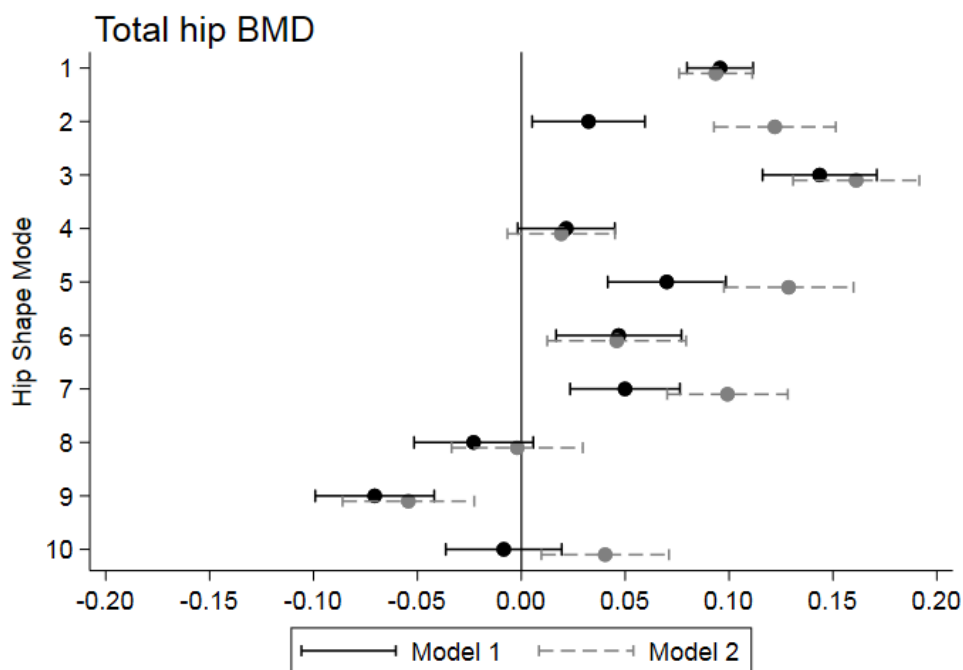


Figure 6.1 Linear regression coefficients (black and dashed grey lines) with 95% CIs for the association between total hip BMD and the top ten HSMs. Results show SD change in HSM per SD increase in BMD. Model 1 adjusted for age, Model 2 additionally adjusted for height, lean and fat mass.

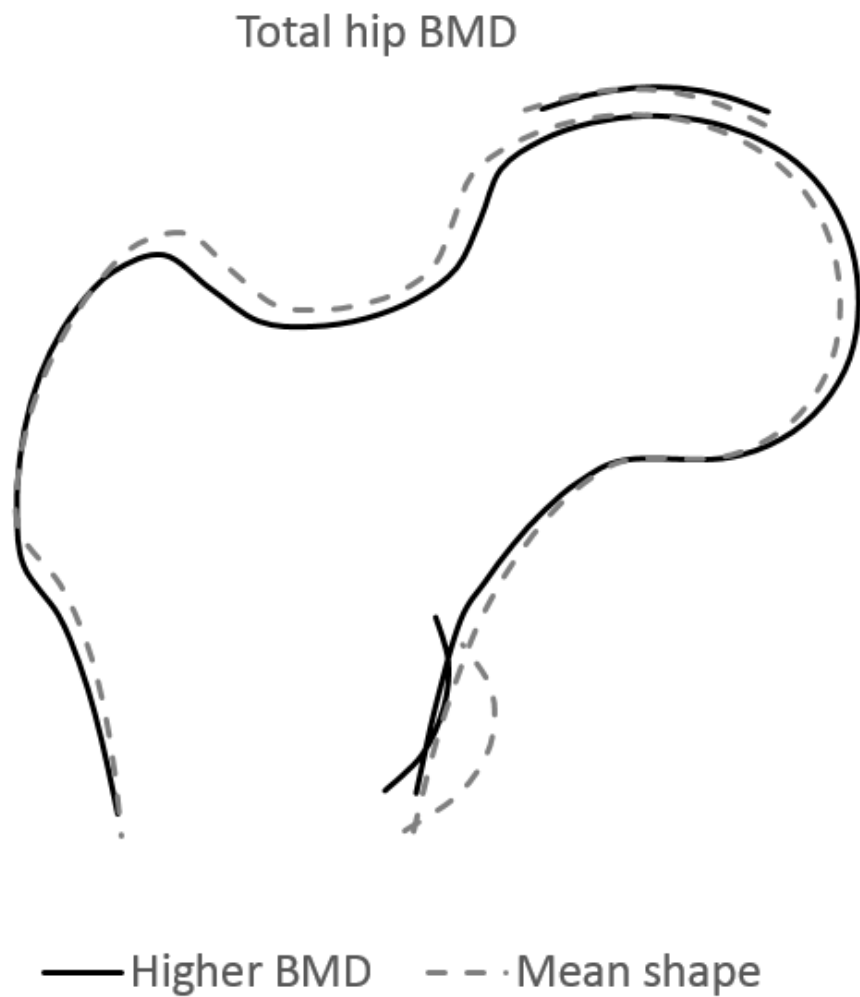


Figure 6.2 Hip shape changes observed per SD increase in total hip BMD based on fully adjusted coefficients (model 2) (to aid visualisation each coefficient was multiplied by a factor of 10). Multiple regression coefficients, showing associations with total hip BMD (see Supplementary Table 10.5.1 in Appendix 2) were entered into Shape software and the combined relationship between total hip BMD and hip shape plotted. Dotted line represents mean hip shape, solid line represents composite change in hip shape per 10 x SD increase in total hip BMD.

6.3.2.3. Adolescent vs. adult results

Compared with fully adjusted observational associations between total hip BMD and hip shape in adolescent females (both time points) and adult women, there was strong evidence to suggest associations with HSM1, HSM2, HSM3, HSM5 and HSM7 in both, adolescent and adult women (Figure 6.3). In terms of the magnitude of the effect, associations with HSM2 and HSM5 were weaker in adult women compared with adolescents, associations with HSM1 and HSM3 were slightly stronger in adult women, whereas associations with HSM7 were similar to age 18 results, with a slightly weaker effect at age 14. Interestingly, while in adolescents' hip BMD was positively related to HSM9 (at both time points) this association was negative in adult women.

The combined relationship between higher hip BMD and hip shape (based on fully adjusted model) in both adolescent and adult women was very similar, with higher hip BMD associated with narrower FNW, smaller lesser trochanter and larger femoral head (medial aspect).

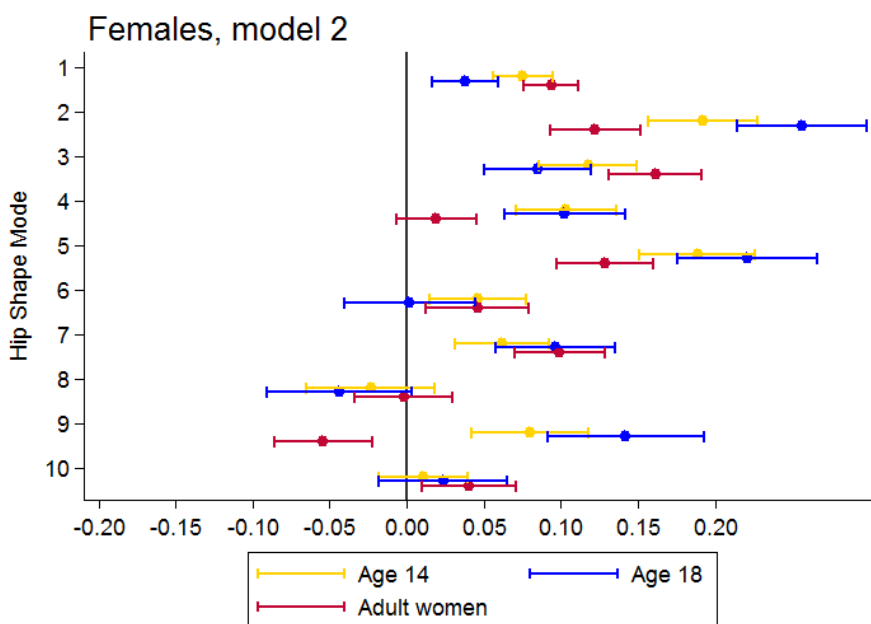


Figure 6.3 Linear regression coefficients with 95% CIs for the association between total hip BMD and the top ten HSMs in adolescent females at age 14 (yellow line) and 18 (blue line) years and adult women (red line). Analysis adjusted for age, height, lean and fat mass (model 2).

6.3.3. Two-sample Mendelian randomization

Having identified strong observational relationships between BMD and a number of HSMs, I followed this up with a two-sample MR approach. FN BMD GWAS identified 49 SNPs at genome-wide level, and these were identified in the outcome GWAS (hip shape GWAS in 3,111 ALSPAC mothers). Of these SNPs, four were removed due to harmonization issues.

Based on a total of 45 SNPs, there was no compelling evidence for an association between BMD and hip shape (Figure 6.4 and Supplementary Table 10.5.5 in Appendix 5). When looking at the relationship between BMD and HSM2 (which, in terms of the magnitude, showed the strongest observational effect), compared with the fully adjusted observational effect (0.13 (0.10, 0.15) $p=5 \times 10^{-20}$) the 2-sample IVW MR estimate was slightly stronger (0.17 (-0.03, 0.37) $p=0.09$), but there was still little evidence of an association. Similarly, the MR estimate for the association between BMD and HSM9 (-0.11 (-0.27, 0.06) $p=0.2$) appeared stronger and in a consistent direction with the observational effect (-0.06 (-0.09, -0.02) $p = 3 \times 10^{-36}$), but again the MR estimate was under-powered, with wide CIs overlapping 0.

It is worth noting that the power to detect an effect of 0.13 with a sample size of 3,111 was 63%, and sample size of $N \sim 4,700$ would be required to detect an effect of 0.13 at 80% power. Therefore, larger samples are required in order to detect smaller effects (for example, to detect an effect of 0.11 with 80% power $N = \sim 13,600$ would be required) (see Appendix 5, section 10.5.2 for details regarding power calculations).

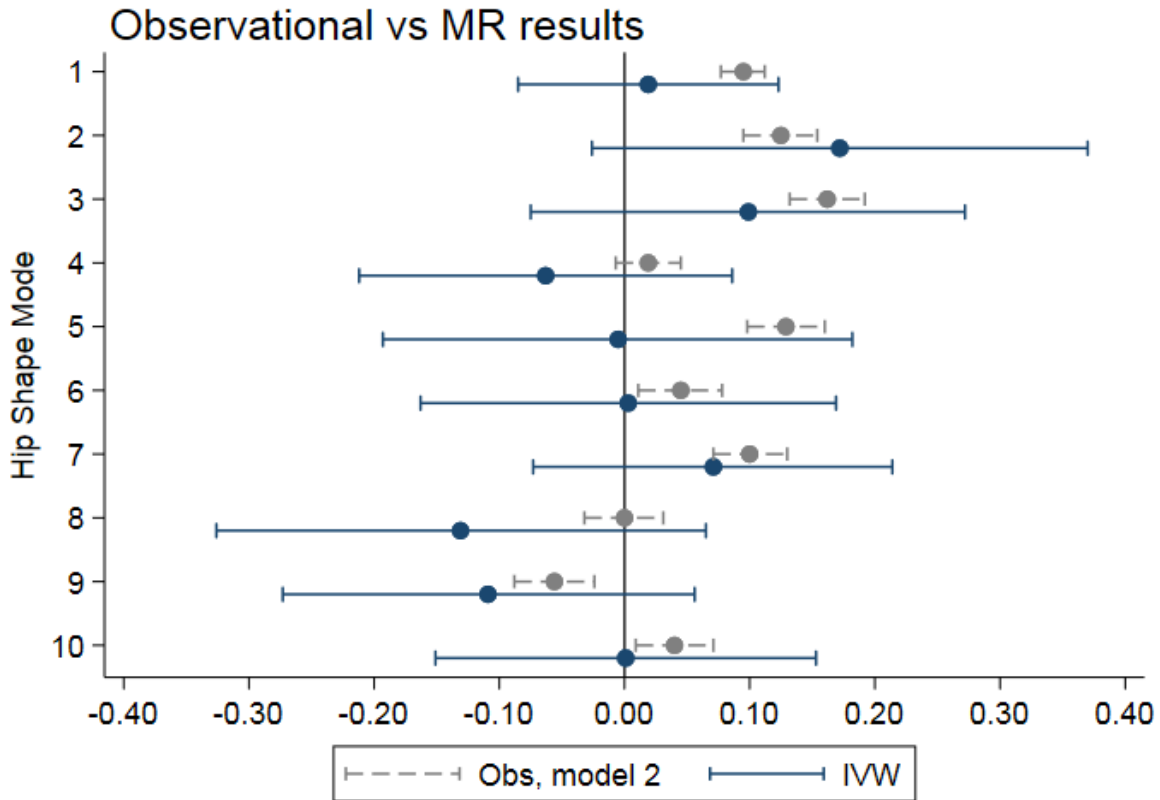


Figure 6.4 Linear regression (dashed grey lines) and Mendelian randomization (using inverse variance weighted method) estimates (solid navy line) between BMD and the top ten HSMs. Results are SD change in HSM per SD increase in BMD. Observational (Obs) associations adjusted for age, height, lean and fat mass and based on N= 4,289.

Adult vs. adolescent results

While there was consistent evidence to suggest associations between BMD with HSM2 and HSM5 at both time points in adolescents (using a one-sample MR approach), there was little evidence for an association between BMD and hip shape in adult women (using a two-sample MR approach). However, IVW estimates for HSM2 in mothers were consistent with the magnitude of effect in adolescents, in particular at age 14 (Figure 6.5) with overlapping 95% CIs. While there was consistent evidence for an association between BMD and HSM5 in adolescents, IVW estimates in mothers were close to the null suggesting little evidence of an association.

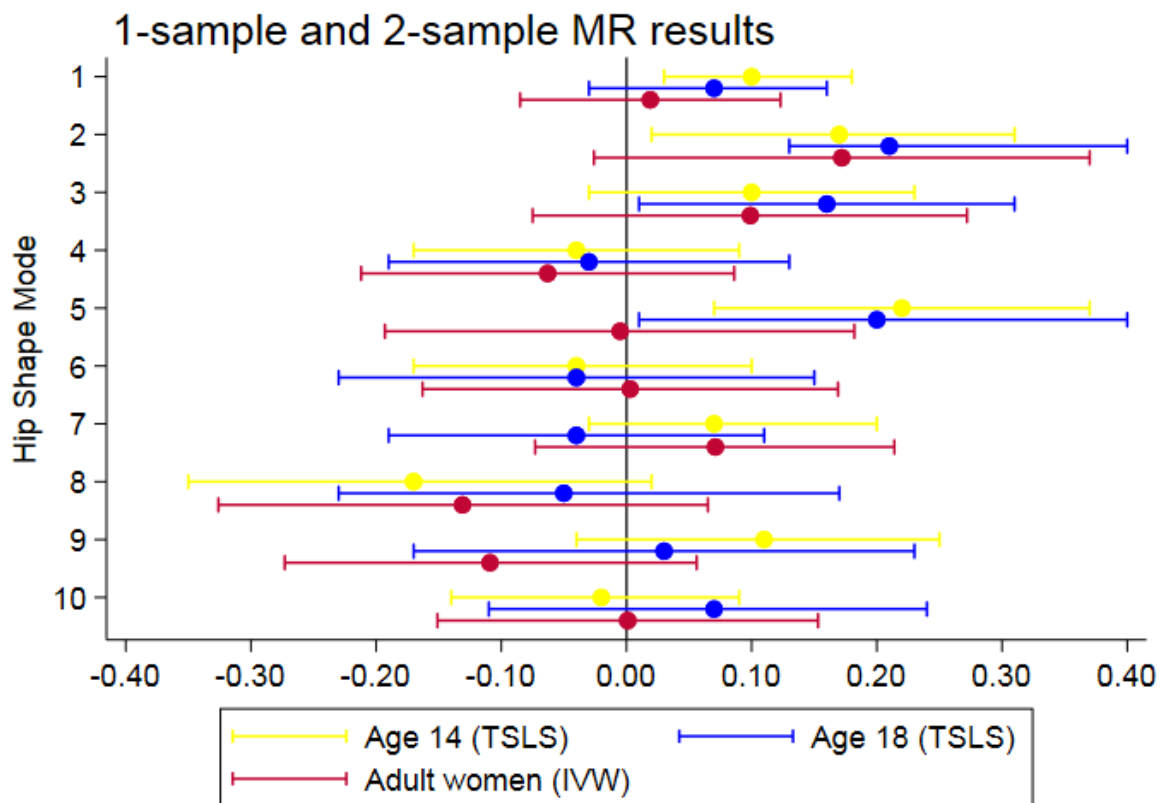


Figure 6.5 One-sample (TSLS) and two-sample (IVW) MR estimates for the association between BMD and hip shape in ALSPAC adolescents at age 14 (yellow line) and 18 (blue line) and ALSPAC mothers (red line). Abbreviations: TSLS (two-stage least squares), IVW (inverse variance-weighted).

6.4. Discussion

In the previous chapter, I found strong evidence of observational associations between BMD and hip shape in ALSPAC adolescents and MR analysis provided evidence for shared genetic aetiology between these traits. In this chapter, I first investigated observational associations between BMD and hip shape in adult women and further explored whether this relationship could be due to shared genetic aetiology.

Summary of observational results

Observationally, there was strong evidence for associations between hip BMD and a number of HSMs. Following adjustment for body size, associations with HSM2, HSM5 and HSM7 were strengthened, while the remaining results were essentially unchanged.

Associations between FN BMD and hip shape were comparable with total hip BMD results; however, the magnitude of FN BMD-hip shape associations was slightly weaker compared with the total hip BMD associations. In addition, while little evidence of an association between FN BMD and HSM2 was observed in the age adjusted model this association was strengthened following adjustment for body. One possible explanation for this could be due to opposing confounder-exposure and confounder-outcome associations, i.e. positive confounder-exposure and negative confounder-outcome associations which were observed in the current analysis. As expected, height, lean and fat mass were all positively associated with FN BMD, while the association with age was negative. With regards to confounder-outcome associations; both lean and fat mass were negatively associated with HSM2, and there was no evidence of an association between age and height with HSM2 (see Supplementary Table 10.5.6 and Supplementary Table 10.5.8 in Appendix 5). Another possibility could be due to artefact or measurement error. Finally, given similar findings when assessing the relationship between total hip BMD and HSM2 this result is likely to represent true underlying relationship between FN BMD and HSM2.

The combined relationship between higher BMD and hip shape was represented by narrower FNW, smaller lesser trochanter and larger femoral head, particularly in the medial aspect.

Adolescent vs. adult results

When comparing adolescent with adult results consistent associations were observed with several modes. In general, the results were in a consistent direction, except the association with HSM9 which was positive in adolescents and negative in mothers. In terms of the magnitude of the effect, associations with HSM1 and HSM3 were stronger and associations with HSM2 and HSM5 were weaker in adult women compared with adolescents. However, when considering the magnitude of estimates, it should be noted that lower modes explain more variance compared with each subsequent mode (with HSM1 explaining the most variance in the dataset). Therefore, smaller effects in lower modes, i.e. 0.10 SD increase in HSM1 per SD increase in BMD observed in this chapter, could be of greater importance than 0.16 SD increase in HSM3 given the difference in variance explained by these modes (42% for HSM1 vs. 8.5% for HSM3). As described in Chapter 2, one of the limitations of SSM is that a model built for a particular dataset is only relevant to that dataset, making comparisons with other studies problematic. In my thesis, I tried to overcome this issue by applying the same SSM template (based on a large adult dataset based on over 19,000 images) to both adolescent and mothers' images enabling direct comparison of each HSM between the time points. However, it needs to be noted that I was unable to calculate the variance explained in the adolescent dataset after applying the adult SSM template, thus making interpretation of the magnitude of beta coefficients in relation to variance explained by each mode difficult. However, similar means and distributions of the top ten modes (as shown in Chapter 2, section 2.5.2) observed in both, adolescents and adult females from ALSPAC, could suggest that the magnitude of effect is comparable. Therefore, the combined effect of higher BMD on hip shape was probably similar in both adolescents and adult women, with higher BMD reflecting narrower FNW and larger femoral heads.

Comparison with published literature

While the relationships between higher BMD and OA (Hardcastle et al., 2015b) and the role of hip shape in OA development (Baker-LePain & Lane, 2010) and increased fracture risk (Gregory et al., 2004) are well-established, the associations between BMD and hip morphology have not been explored in detail. To my knowledge, only one previous study, in adults from the NSHD cohort who were all born in 1946, explored the

association between BMD and hip shape in men and women (Pavlova et al., 2017). In contrast to findings in this chapter, the authors reported an association between higher hip BMD and HSM3 in women and this mode reflected a lower neck-shaft angle and greater acetabular coverage. It is important to bear in mind that the mean (SD) age of women in the current study was 47.9 (4.4) years, compared with 63.3 (1.09) years in the NSHD cohort. As expected, mean (SD) total hip BMD in NSHD women was lower compared with ALSPAC women, 0.87 (0.13) vs. 1.03 (0.14) g/cm², respectively. Due to the properties of SSM, the individual modes from the NSHD cohort cannot be directly compared with those from ALSPAC, although subjective, qualitative comparisons regarding variation described by these modes can be made. For example, HSM6 which was positively associated with BMD in ALSPAC mothers also reflected increased acetabular coverage, although not as pronounced as in the NSHD cohort, likely to be the result of age differences between these cohorts.

The associations between BMD and hip shape, reported in this chapter, could conceivably contribute to the relationship between OP and OA. In a study by Lynch et al., larger femoral heads have been found to predict radiographic hip OA in a cohort of elderly women (Lynch et al., 2009), a feature similar to that observed when modelling the overall relationship between higher BMD and hip shape in adult women and adolescents (as discussed in the previous chapter). Conversely, Castano-Betancourt reported an association between wider FNW and higher risk of incident hip OA (Castaño-Betancourt et al., 2013b), suggesting that BMD-hip shape association is unlikely to explain the relationship between FNW and risk of OA.

In terms of the relationship between FNW and osteoporotic hip fractures, the evidence is inconclusive. While some studies reported associations between wider neck with hip fracture in both males and females (Alonso et al., 2000; Karlsson et al., 1996), others found reduced FNW in men with hip fractures (Ego Seeman et al., 2001) and narrower FNW in women was associated with increased risk of hip fracture (Ahlborg et al., 2005). Others yet, found that the association between femoral neck diameter and trochanteric hip fracture in a study of elderly women, fully attenuated following adjustment for age, height, weight and BMD (Duboeuf et al., 1997). It has been previously recognized that individual geometrical measurements are often highly correlated with those of body size

(Gregory & Aspden, 2008), therefore cannot be interpreted in isolation. More advanced quantification techniques independent of body size, such as SSM will be better suited for such analyses and may offer opportunities for identifying new predictors of hip fracture independent of both, BMD and body size.

Mendelian randomization

In the observational analysis I adjusted for age, height, lean and fat mass, however it is possible that the relationship between BMD and hip shape could be explained by other factors that were either not measured or adjusted for. To avoid such issues and further explore the underlying mechanisms contributing to the BMD-hip shape relationship, the observational analysis was followed up with two-sample MR. There was no strong evidence to suggest association between BMD and hip shape in ALSPAC mothers.

Compared with the adolescent results, HSM2 results were consistent in terms of direction with a slightly weaker magnitude of effect, however there was little evidence either for or against an effect, with wide 95% CIs. Compared with a one-sample approach, which requires person-level data (Chapter 5), a two-sample approach (employed in this chapter) uses summary level data. While the latter offers more power to detect causal effect compared with a one-sample approach, it requires strong instruments based on large non-overlapping samples. Compared with BMD instrument, based on a sample of approximately 84,000 individuals, hip shape GWAS relied on a sample of ~3,000 mothers thus resulting in less precise estimates (as reflected by larger SEs compared with BMD instrument). Therefore, in a two-sample setting any bias arising from a weak instrument is likely to bias the results towards the null (Burgess et al., 2016b; Lawlor, 2016). In order to combat this bias, future analysis should consider using a stronger instrument for hip shape, for example recent results from hip shape GWAS meta-analysis based on approximately 16,000 individuals (D. A. Baird et al., 2017), as well as stronger instruments for BMD such as GWAS in 142,487 individuals from the UK Biobank study (Kemp et al., 2017). GWASes on large samples are likely to identify novel variants associated with BMD and hip shape and in turn are likely to explain larger proportion of variance in these traits thus resulting in better power for future analyses (Burgess et al., 2015).

Conclusions

In this chapter, I found strong observational evidence for associations between BMD and a number of HSMs. The overall relationship between higher BMD and hip shape, which was reflected by narrower FNW and variation in femoral head size was consistent with the results observed in adolescents and this finding may help to explain the inverse relationship between OP and OA. When using a MR approach to investigate shared genetic contributions to BMD and hip shape, there was little evidence of an association between BMD and hip shape in adults, most likely reflecting limited power. The suggestion from my findings that the relationship between BMD and hip shape contributes to the inverse relationship between OP and OA warrants further investigation based on a larger sample.

CHAPTER 7. GENETIC VARIANTS ASSOCIATED WITH HIP SHAPE IN ADOLESCENTS

7.1. Introduction and chapter aims

As highlighted in Chapter 1, OA is a complex disease with an estimated heritability of between 30% and 65% (Warner & Valdes, 2016). Previous studies identified 21 loci associated with hip, knee and hand OA (Cibrián Uhalte et al., 2017) and a recent UK Biobank study identified a further nine loci, which together account for 26% of variance in OA (Zengini et al., 2018). OA is very heterogenous which might explain why a fairly modest number of OA-associated loci (compared with other complex traits such as diabetes) have been identified by GWAS to date. In order to increase power, recent studies have focused on OA-related endophenotypes and this approach is likely to identify genetic variants with functional potential. For example, a recent GWAS of Rotterdam study cohorts identified a number of novel variants associated with OA-related endophenotypes (such as joint space width and JSN) (Boer et al., 2018), which is likely to improve our understanding of underlying disease mechanisms. Another GWAS of 770 cases with DDH and 3,364 healthy controls, in the NJR, identified rs143383 polymorphism in GDF5 to be robustly associated with DDH case status (Hatzikotoulas et al., 2017), and the same variant has previously been reported to be associated with increased OA risk (Chapman et al., 2008). These findings are consistent with the suggestion that OA development is mediated through joint shape and variants associated with hip morphology are likely to mediate this relationship. Thus, studying genetics of hip shape may shed a light on disease pathogenesis and determine how early genetic risk factors for OA influence OA-related traits which might in turn point towards new disease modifying targets.

In this chapter I aim to:

- 1) Identify genetic variants associated with hip shape in adolescents, and additionally
 - a. perform a look-up of any adolescent genome-wide significant variants in an adult cohort,
 - b. check previous literature for associations with other phenotypes and formally test for genetic correlations with other phenotypes.
- 2) Determine if genetic variants associated with adult hip shape have similar effects on hip shape across adolescence.
- 3) Determine if OA associated variants are also associated with hip shape in adolescents.

7.2. Methods

7.2.1. Study population

Data were obtained from ALSPAC TF 2 and TF 4 clinics when the participants were on average 14 and 18 years old, respectively. The study population for current analyses comprised individuals with complete phenotypic and genotypic data. For more details regarding data collection and cleaning please refer to the methods chapter (Chapter 2).

7.2.2. Data

7.2.2.1. Genome- wide genetic data

As described in Chapter 2, ALSPAC offspring were genotyped using Illumina HumanHap550 quad genome-wide SNP genotyping platform and were imputed to 1000 Genomes. A number of quality checks were applied, and the analysis was restricted to individuals of European descent, as described previously.

7.2.2.2. Outcome and covariate data

Hip DXA images collected during TF 2 and TF 4 clinics were used to quantify the shape of the proximal femur. HSMs were generated and scores from a consistent external adult

reference SSM were applied to each data set (as described in Chapter 2). The first ten HSMs were used as outcomes as in previous chapters. Age at clinic attendance and sex were used as covariates in the analysis. For more details on data collection and quantification of hip shape see Chapter 2.

7.2.3. Analysis

7.2.3.1. GWAS analysis

Linear regression analyses to explore the association between each SNP and the top ten HSM scores at age 14 and 18 were performed using SNPTEST v2.5. An additive genetic model was assumed, adjusting for age and sex.

Example code (adapted from Lavinia Paternoster

https://github.com/epxlp/GWAS_scripts) that was used to perform the analysis is available in Appendix 6.

Any SNPs reaching genome wide significance ($P < 5 \times 10^{-8}$), a threshold traditionally applied to GWAS findings (McCarthy et al., 2008), were looked up in MR-Base PheWAS (Hemani et al., 2016) (<http://phewas.mrbase.org/>) to identify other phenotypes that might be associated with these hip shape loci (genome-wide ‘suggestive’ threshold for associations with other traits was set to $P < 5 \times 10^{-5}$).

In order to explore the functional potential of hip shape associated SNPs, a look-up of these SNPs was performed in a summary expression quantitative trait loci (eQTLs) results in order to identify any correlations between these variants and all available tissue-specific gene expression levels using the GTEx portal (<https://www.gtexportal.org/home/>, accessed on 11/05/2018). The tissues that were available include whole blood, skeletal muscle or adipose tissues (for more details, please refer to GTEx portal).

7.2.3.2. Replication

A look-up of genome-wide-significant hits found in adolescents (across the time points) was performed (by Denis Baird) in corresponding HSM results in hip shape GWAS in ALSPAC mothers and meta-analysis of GWASes performed in other cohorts (including

Twins UK, MrOS, SOF, and Framingham). Both adult and adolescent analyses relied on the same SSM template, allowing direct comparison of adolescent and adult results.

7.2.3.3. The effect of adult hip shape variants on adolescent hip shape

Previous meta-analysis of GWAS in adults identified 9 loci associated with hip shape (five SNPs were associated with HSM1, three with HSM2 and one with HSM5) (D. A. Baird et al., 2017) and I looked up these loci within ALSPAC adolescent results in relevant modes at both time points.

7.2.3.4. Look-up of known OA variants in adolescent hip shape

Based on a 2016 review of candidate gene and GWA studies by Zengini et al. (Zengini et al., 2016) and the largest to date OA GWAS in the UK Biobank (Zengini et al., 2018), 17 SNPs associated with hip OA at a genome-wide significant level ($P < 5 \times 10^{-8}$) were selected (of these variants, three were just below the genome-wide significance with $P < 8 \times 10^{-8}$; see Table 7.1 for a list of SNPs) and a look-up of these variants was performed in GWASes of the top ten HSMs at both, age 14 and age 18 results. The 0.05 α threshold was corrected for 340 tests = 1.5×10^{-4} (17 SNPs x 10 outcomes x 2 time points = 340 tests).

Table 7.1; List of SNPs associated with hip OA available from previously published literature

Index variant	Nearest gene	Ethnic group	Joint site	Sex	RA	RAF	Reported OR (95% CI)	Reported P value	Ref.
rs3771501	<i>TGFA</i>	EUR	hip	both	G	0.53	0.94 (0.92–0.96)	1.66×10 ⁻⁸	a
rs6976	<i>GLT8D1</i>	EUR	knee & hip	both	T	0.37	1.12 (1.08 - 1.16)	7.2×10 ⁻¹¹	b
rs10948172	<i>SUPT3H- CDC5L</i>	EUR	knee & hip	M	G	0.29	1.14 (1.09 - 1.20)	7.9×10 ⁻⁸	
rs9350591	<i>FILIP1- SENP6</i>	EUR	hip	both	T	0.11	1.18 (1.12 - 1.25)	2.4×10 ⁻⁹	
rs11780978	<i>PLEC</i>	EUR	hip	both	A	0.39	1.13 (1.08–1.17)	1.98×10 ⁻⁹	a
rs4836732	<i>ASTN2</i>	EUR	hip	F	C	0.47	1.20 (1.13 - 1.27)	6.1×10 ⁻¹⁰	b
rs10492367	<i>KLHDC5- PTHLH</i>	EUR	hip	both	T	0.19	1.14 (1.09 - 1.20)	1.5×10 ⁻⁸	
rs835487	<i>CHST11</i>	EUR	hip	both	G	0.34	1.13 (1.09 - 1.18)	1.6×10 ⁻⁸	
rs11842874	<i>MCF2L</i>	EUR	knee & hip	both	A	0.93	1.17 (1.11 - 1.23)	2.1×10 ⁻⁸	
rs12901071	<i>SMAD3</i>	EUR	knee & hip	both	A	0.68	1.08 (1.05 - 1.11)	3.1×10 ⁻¹⁰	c
rs8044769	<i>FTO</i>	EUR	knee & hip	F	C	0.5	1.11 (1.07 - 1.15)	6.9×10 ⁻⁸	b
rs864839	<i>JPH3</i>	EUR	hip	both	T	0.7	1.08 (1.05–1.11)	2.1×10 ⁻⁸	a
rs2521349	<i>MAP2K6</i>	EUR	hip	both	A	0.37	1.13 (1.09–1.17)	9.95×10 ⁻¹⁰	
rs12982744	<i>DOT1L</i>	EUR	hip	M	C	0.74	1.17 (1.11 - 1.23)	7.8×10 ⁻⁹	b
rs143383*	<i>GDF5</i>	Asian and EUR	knee & hip	both	T	Asian 0.74, EUR N/A	Asian 1.79 (1.53 - 2.09), EUR 1.16 (1.11 - 1.22)	Asian 1.8×10 ⁻¹³ , EUR 8.3×10 ⁻⁹	a, b
rs6094710	<i>NCOA3</i>	EUR	hip	both	A	0.04	1.28 (1.18 - 1.39)	7.9×10 ⁻⁹	b
rs6516886	<i>RWDD2B</i>	EUR	hip	both	T	0.75	1.10 (1.06–1.14)	5.84×10 ⁻⁸	a

*rs143383 was not available in ALSPAC data, instead rs143384 (R²=0.82, D'=0.99) was used as a proxy. Abbreviations: RA (reported risk allele), RAF (reported risk allele frequency), OR (odds ratio), EUR (European), M (males), F (females). Ref. a: (Zengini et al., 2018); b: (Zengini et al., 2016); c: (Hackinger et al., 2017).

7.2.3.5. Genetic correlation between hip shape and other phenotypes

In previous chapters, I investigated shared genetic aetiology between BMD and hip shape using one-sample MR in adolescents (Chapter 5) and two-sample MR in ALSPAC mothers (Chapter 6), however, for many complex traits, the proportion of heritability explained by SNPs reaching genome-wide significance is small, therefore these methods often suffer from low power and weak instrument bias (B. Bulik-Sullivan et al., 2015). In this chapter, I used LD Hub (<http://ldsc.broadinstitute.org/ldhub/>) (accessed 8 -10 May 2018) (Zheng et al., 2017), an online platform for LD score regression (B. K. Bulik-Sullivan et al., 2015), to estimate the shared genetic aetiology between hip shape in adolescence and BMD as well as a range of other phenotypes using all SNPs in the genome, rather than just the genome-wide significant ones. LD Hub contains summary-level GWAS results for over 170 phenotypes from various publicly available data sources and provides an automated LD score regression analysis pipeline. This method (first proposed by Bulik-Sullivan et al. (B. K. Bulik-Sullivan et al., 2015)) relies on SNP correlations, i.e. SNPs in high LD will have higher X^2 values as opposed to SNPs in low LD. To estimate the genetic correlations between two traits, Z-scores (BETA/SE) from each study are calculated and regressed onto the LD score and genetic covariance is then estimated from the slope.

Summary level data for the top ten HSMs from age 14 and age 18 GWASes were uploaded in LD Hub. SNP heritability (h^2) and SE were estimated and used to calculate Z-scores (h^2/SE) in order to inform further analysis. Genetic correlation estimates for traits with heritability Z-scores below 2 are unreliable (Zheng et al., 2017), therefore only HSMs with heritability Z-scores ≥ 2 were selected to perform genetic correlations between hip shape and all traits available in LD Hub (including anthropometric and bone traits, such as FN and LS BMD, amongst other traits).

7.3. Results

7.3.1. Participant characteristics

Complete outcome and genetic data were available from 3,550 and 3,175 individuals at a mean age of 13.8 and 17.8 years respectively. After applying filtering steps 8,310,190 imputed SNPs were available for analysis.

7.3.2. GWAS at age 14, 18 and replication in adult cohort

In adolescents, several SNPs were associated with hip shape at a genome-wide significant level ($p < 5 \times 10^{-8}$). Top hits were then pruned using the SNAP tool (Pers et al., 2014) to select independent loci. QQ and Manhattan plots were generated (see Supplementary Figure 10.6.1 - Supplementary Figure 10.6.20 for Manhattan and QQ plots in Appendix 6) and genomic inflation factors for all HSMs at both time points were close to 1.

At age 14, two SNPs showed associations with hip shape (Table 7.2).

rs8079830, an intergenic variant on chromosome 17 located near *SOX9* (Figure 7.1) was associated with HSM1 (effect allele: C, $\beta = -0.06$, $p = 1.76 \times 10^{-8}$). This variant was also associated with HSM1 in ALSPAC mothers ($\beta = -0.06$, $p = 4.87 \times 10^{-5}$) and adult meta-analysis (which excluded ALSPAC mothers) ($\beta = -0.03$, $p = 1.9 \times 10^{-8}$) and showed weaker evidence of an association with HSM1 at age 18 ($\beta = -0.03$, $p = 0.001$).

rs1827922 an intergenic variant, near *ANKRD50*, on chromosome 4 (Figure 7.2) was associated with HSM3 (effect allele: C, $\beta = 0.10$, $p = 3.69 \times 10^{-8}$) with no robust evidence for an association at age 18 ($\beta = 0.01$, $p = 0.546$) and no evidence of an association in ALSPAC mothers ($\beta = -0.005$, $p = 0.862$), while there was very weak evidence for an association in adult meta-analysis ($\beta = 0.02$, $p = 0.048$).

At age 18, three SNPs were associated with hip shape (Table 7.3).

rs10748285, a non-coding intronic variant in *RP11-114H23.1* located on chromosome 12 (Figure 7.3) was associated with HSM1 (effect allele: T, $\beta = 0.06$, $p = 2.76 \times 10^{-8}$) and there was weak evidence of an effect of this variant on HSM1 at age 14 ($\beta = 0.02$, $p = 0.017$) with little evidence of an association in ALSPAC mothers ($\beta = 0.02$, $p = 0.084$) and adult meta-analysis ($\beta = 0.008$, $p = 0.234$).

rs8111495, residing in an intron of *DUXA* on chromosome 19 (Figure 7.4), was associated with HSM5 at both time points, with weaker magnitude of an effect and weaker evidence for an association at age 14 (effect allele: A, $\beta=0.10$, $p=1.23 \times 10^{-5}$) compared with age 18 result ($\beta=0.15$, $p=2.52 \times 10^{-8}$). There was little evidence to suggest an association of this variant with HSM5 in ALSPAC mothers ($\beta=0.02$, $p=0.480$) and adult meta-analysis ($\beta=0.02$, $p=0.194$).

rs1111767, an intronic SNP in AL391117.1 located on chromosome 9 (Figure 7.5), was associated with HSM6 (effect allele: G, $\beta=-0.13$, $p=2.34 \times 10^{-9}$). The effect of this variant on HSM6 at age 14 was much weaker compared with age 18 effect with little evidence of an association ($\beta=-0.03$, $p=0.091$), similarly no evidence of an effect was observed in ALSPAC mothers ($\beta=0.01$, $p=0.787$) and weak evidence of an association in adult meta-analysis, with the effect being in the opposite direction ($\beta=0.02$, $p=0.038$).

These SNPs were investigated in MR-Base PheWAS to identify potential associations with other traits. rs8079830, associated with HSM1 at age 14, showed association with height and knee pain in the UK Biobank study (Table 7.4). rs8111495, associated with HSM5 at age 18, showed strong relationship with fibroblastic disorders (e.g. Dupuytren's contracture) as well as associations with lower limb and total body mass in the UK Biobank study (Table 7.5). rs1111767, associated with HSM6 at age 18, showed evidence for associations with educational phenotypes in two independent cohorts: UK Biobank and the Social Science Genetic Association Consortium (SSGAC) (Table 7.6).

There was no compelling evidence (no associations below the pre-specified genome wide suggestive threshold) for associations between rs1827922 and rs10748285 (found to be associated with HSM3 at age 14 and HSM1 at age 18, respectively) with other traits. Finally, no significant eQTLs were found for any of the hip shape associated loci.

Table 7.2; Genome-wide significant hits for hip shape at age 14 in ALSPAC adolescents and a look-up of these loci in adolescent and adult GWAS

HSM	SNP	CHR	EA	EAF	Age 14 GWAS* (N= 3,550)			Age 18 GWAS (N=3,175)		ALSPAC mothers (N=3,111)		ADULT meta-analysis (N= 12,823)	
					Beta	SE	P	Beta	P	Beta	P	Beta	P
1	rs8079830	17	C	0.66	-0.06	0.01	1.76x10 ⁻⁸	-0.03	0.001	-0.06	4.87x10 ⁻⁵	-0.03	1.9x10 ⁻⁸
3	rs1827922	4	C	0.28	0.10	0.02	3.69x10 ⁻⁸	0.01	0.546	-0.005	0.862	0.02	0.048

*adjusted for age and sex, adult meta-analysis excluded ALSPAC mothers. Abbreviations: SNP (Single nucleotide polymorphism), CHR (chromosome), EA (effect allele), EAF (effect allele frequency), SE (standard error), P (p value).

Table 7.3; Genome-wide significant hits for hip shape at age 18 in ALSPAC adolescents and a look-up of these loci in adolescent and adult GWAS

HSM	SNP	CHR	EA	EAF	Age 18 GWAS* (N =3,175)			Age 14 GWAS (N= 3,550)		ALSPAC mothers (N=3,111)		ADULT meta-analysis (N= 12,823)	
					Beta	SE	P	Beta	P	Beta	P	Beta	P
1	rs10748285	12	T	0.58	0.06	0.01	2.76x10 ⁻⁸	0.02	0.017	0.02	0.084	0.008	0.234
5	rs8111495	19	A	0.72	0.15	0.03	2.52x10 ⁻⁸	0.10	1.23x10 ⁻⁵	0.02	0.480	0.02	0.194
6	rs1111767	9	G	0.69	-0.13	0.02	2.34x10 ⁻⁹	-0.03	0.091	0.01	0.787	0.02	0.038

*adjusted for age and sex, adult meta-analysis excluded ALSPAC mothers. Abbreviations: SNP (Single nucleotide polymorphism), CHR (chromosome), EA (effect allele), EAF (effect allele frequency), SE (standard error), P (p value).

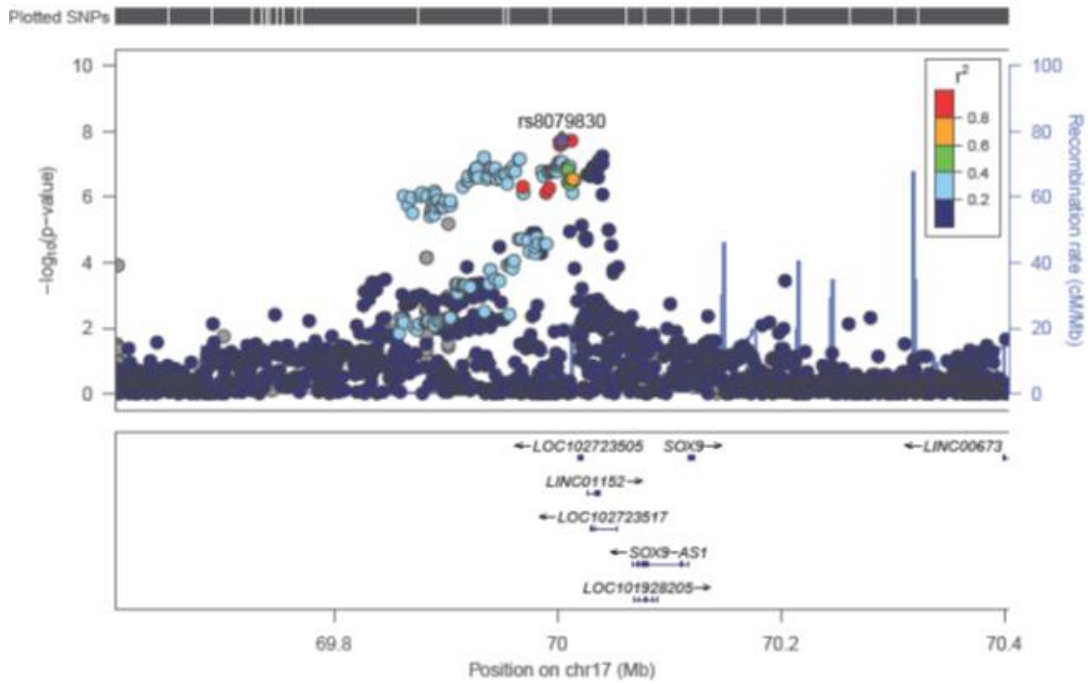


Figure 7.1 Regional association plot for rs8079830 locus associated with HSM1 at age 14. The y axis represents the negative logarithm (base 10) of the variant P value (likelihood ratio test), and the x axis represents the position on the chromosome, with names and location of genes and nearest genes shown at the bottom. Purple diamond represents the variant with the lowest P value and colours of the remaining points correspond to the degree of LD with the top variant.

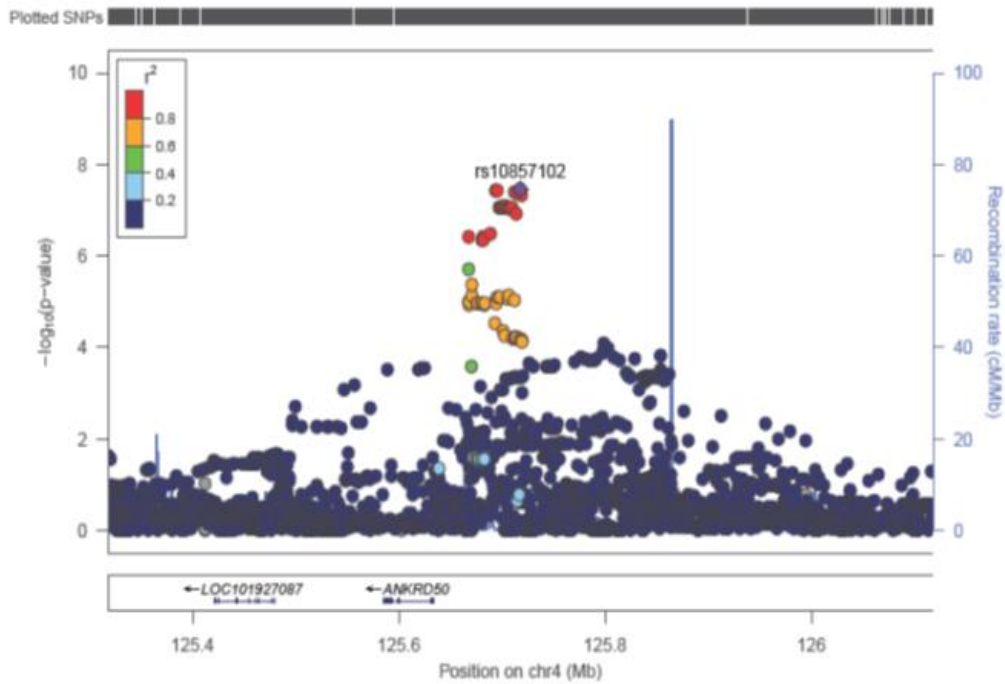


Figure 7.2 Regional association plot for rs10857102 (in high LD >0.8 with rs1827922) locus associated with HSM3 at age 14. The y axis represents the negative logarithm (base 10) of the variant P value (likelihood ratio test), and the x axis represents the position on the chromosome, with names and location of genes and nearest genes shown at the bottom. Purple diamond represents the variant with the lowest P value and colours of the remaining points correspond to the degree of LD with the top variant.

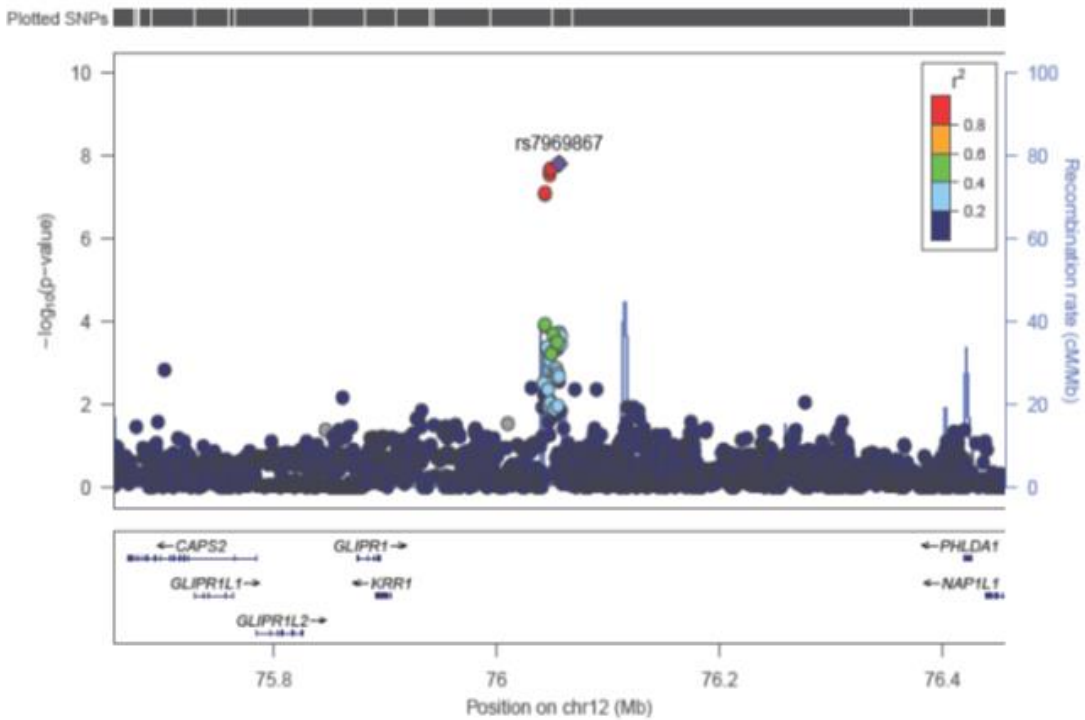


Figure 7.3 Regional association plot for rs7969867 (in high LD >0.8 with rs10748285) locus associated with HSM1 at age 18. The y axis represents the negative logarithm (base 10) of the variant P value (likelihood ratio test), and the x axis represents the position on the chromosome, with names and location of genes and nearest genes shown at the bottom. Purple diamond represents the variant with the lowest P value and colours of the remaining points correspond to the degree of LD with the top variant.

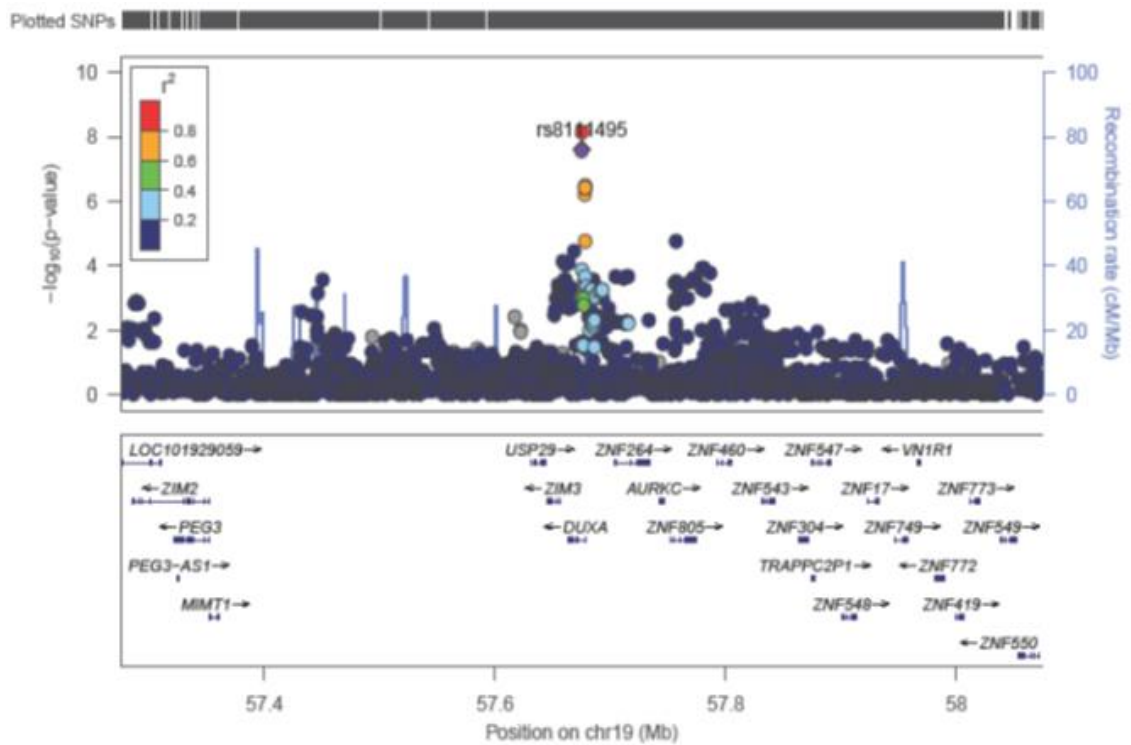


Figure 7.4 Regional association plot for rs8111495 locus associated with HSM5 at age 18. The y axis represents the negative logarithm (base 10) of the variant P value (likelihood ratio test), and the x axis represents the position on the chromosome, with names and location of genes and nearest genes shown at the bottom. Purple diamond represents the variant with the lowest P value and colours of the remaining points correspond to the degree of LD with the top variant.

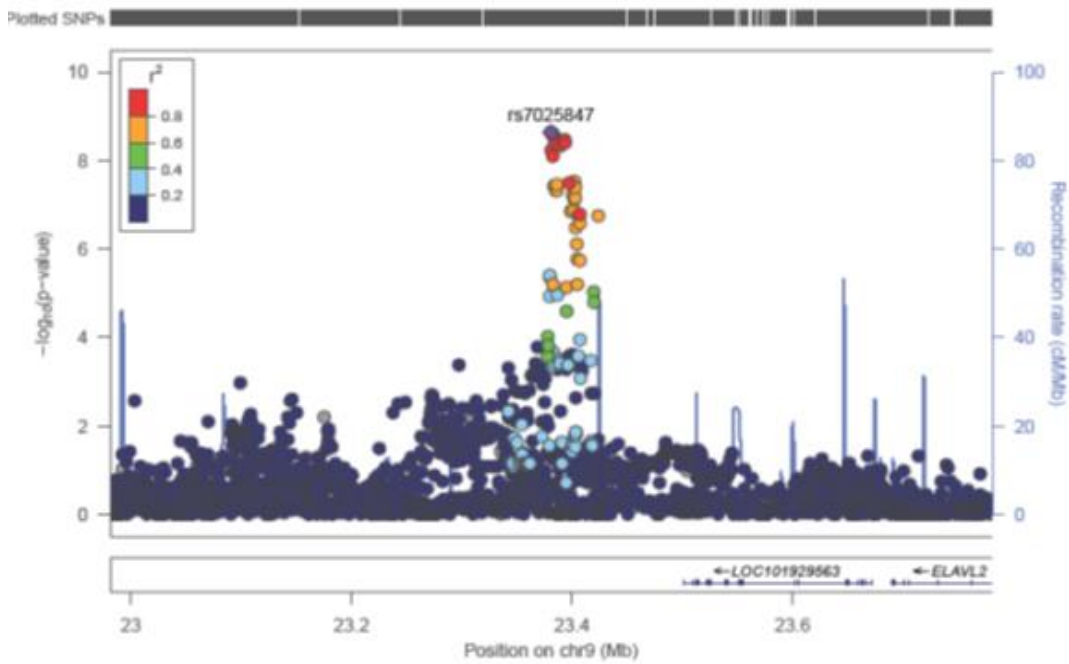


Figure 7.5 Regional association plot for rs7025847 (in high LD >0.8 with rs1111767) locus associated with HSM6 at age 18. The y axis represents the negative logarithm (base 10) of the variant P value (likelihood ratio test), and the x axis represents the position on the chromosome, with names and location of genes and nearest genes shown at the bottom. Purple diamond represents the variant with the lowest P value and colours of the remaining points correspond to the degree of LD with the top variant.

Table 7.4; Look-up of rs8079830 associated with HSM1 at age 14 in MR Base PheWAS showing traits associated with this SNP reaching suggestive genome-wide significance level ($P < 5 \times 10^{-5}$)

Trait	Consortium	Sex	N	EA	OA	Beta	P	SE	Cases	Controls
Standing height	UK Biobank	M & F	336,474	C	T	-0.009	1.6×10^{-7}	0.002	NA	NA
Comparative height size at age 10	UK Biobank	M & F	332,021	C	T	-0.008	1.4×10^{-6}	0.002	NA	NA
Pain type(s) experienced in last month: Knee pain	UK Biobank	M & F	336,650	C	T	-0.004	1.8×10^{-5}	0.001	71,561	265,089

Abbreviations: EA (Effect allele), OA (Other allele), SE (Standard error).

Table 7.5; Look-up of rs8111495, associated with HSM5 at age 18, in MR Base PheWAS showing traits associated with this SNP reaching suggestive ($P < 5 \times 10^{-5}$) and genome-wide significance level ($P < 5 \times 10^{-8}$)

Trait	Consortium	Sex	N	EA	OA	Beta	P	SE	Cases	Controls
Diagnoses - main ICD10: M72 Fibroblastic disorders	UK Biobank	M & F	337,199	A	C	-0.001	2.2×10^{-10}	0.000	1,862	335,337
Leg predicted mass (right)	UK Biobank	M & F	331,285	A	C	0.009	3.1×10^{-6}	0.002	NA	NA
Leg fat-free mass (right)	UK Biobank	M & F	331,285	A	C	0.008	5.1×10^{-6}	0.002	NA	NA
Leg fat-free mass (left)	UK Biobank	M & F	331,258	A	C	0.008	9.2×10^{-6}	0.002	NA	NA
Leg predicted mass (left)	UK Biobank	M & F	331,253	A	C	0.008	1.0×10^{-5}	0.002	NA	NA
Whole body fat-free mass	UK Biobank	M & F	331,291	A	C	0.008	2.5×10^{-5}	0.002	NA	NA
Impedance of leg (right)	UK Biobank	M & F	331,301	A	C	-0.011	2.6×10^{-5}	0.003	NA	NA
Impedance of leg (left)	UK Biobank	M & F	331,296	A	C	-0.010	4.5×10^{-5}	0.003	NA	NA

Abbreviations: EA (Effect allele), OA (Other allele), SE (Standard error).

Table 7.6; Look-up of rs1111767 associated with HSM6 at age 18 in MR Base PheWAS showing traits associated with this SNP reaching suggestive genome-wide significance level ($P < 5 \times 10^{-5}$)

Trait	Consortium	Sex	N	EA	OA	Beta	P	SE	Cases	Controls
Qualifications: College or University degree	UK Biobank	M & F	334,070	G	A	0.006	2.5×10^{-7}	0.001	106,305	227,765
Years of schooling	SSGAC	F	182,286	A	G	-0.017	1.7×10^{-6}	0.004	NA	NA
Years of schooling	SSGAC	M & F	293,723	A	G	-0.013	1.8×10^{-6}	0.003	NA	NA
Neuroticism	SSGAC	M & F	170,911	A	G	0.018	2.4×10^{-6}	0.004	NA	NA

Abbreviations: EA (Effect allele), OA (Other allele), SE (Standard error), SSGAC (Social Science Genetic Association Consortium).

7.3.3. The effect of adult hip shape variants on adolescent hip shape

Table 7.7 shows the SNPs associated with adult hip shape (D. A. Baird et al., 2017) and a look-up of these SNPs in adolescent GWAS at age 14 and 18. Five SNPs were associated with HSM1, two with HSM2 and one with HSM5 and these SNPs were looked up in relevant HSMs in adolescents.

A number of variants affecting hip shape in adults were also found to be associated with hip shape in adolescents, however the evidence for these associations was generally weaker. The strongest associations were seen for two SNPs, rs2158915 (associated with HSM1 in adults) and rs2160442 (associated with HSM5 in adults) (both in complete linkage, $R^2=1.0$), near *SOX9*, and these variants were associated with HSM1 and HSM5 respectively at both time points (consistent with the direction of the effect in adults). There was strong evidence for an association between rs10743612 (associated with HSM1 in adults), an intergenic SNP between *KLHL42* and *PTHLH* and HSM1 at both time points. Furthermore, rs73197346 (between *RUNX1* and *MIR802*; associated with HSM1 in adults) was strongly related to HSM1 at age 14 with consistent direction of an effect at age 18, although much weaker evidence. In addition, rs6537291 SNP (associated with HSM2 in adults) near *HHIP* (associated with height and implicated in endochondral bone formation) was associated with adolescent HSM2 at both time points and the magnitude of the effect was similar to the effect reported in adults. Another variant, rs1966265 (a missense SNP of *FGFR4*, associated with HSM2 in adults) was associated with HSM2 at age 18 and there was some evidence to suggest an association at age 14. Finally, there was weak evidence of an association between intronic SNP, rs1885245 in *ASTN2* (associated with HSM2 in adults), and HSM2 at age 14, but no robust evidence for an association at age 18 was seen.

Table 7.7; Hip shape meta-analysis results (adjusted for age and gender) and look-up in ALSPAC adolescent GWAS (adjusted for age and gender)

HSM	SNP	Locus	Adult meta-analysis N=15,934		Age 18 GWAS N=3,175		Age 14 GWAS N=3,550	
			BETA	P	BETA ¹	P	BETA ²	P
1	rs2158915	<i>SOX9</i>	-0.13	8.47x10 ⁻²⁷	-0.05	3.25 x10 ⁻⁶	-0.05	9.94 x10 ⁻⁸
1	rs1243579	<i>GSC</i>	0.12	2.85x10 ⁻¹⁴	0.02	0.086	0.03	0.01
1	rs10743612	<i>KLHL42-PTHLH</i>	0.09	2.91x10 ⁻¹²	0.04	0.003	0.05	1.13 x10 ⁻⁵
1	rs73197346	<i>RUNX1- MIR802</i>	-0.11	2.52x10 ⁻¹⁰	-0.03	0.026	-0.05	2.38 x10 ⁻⁴
1	rs59341143	<i>NKX3-2</i>	0.098	6.53x10 ⁻¹⁰	0.02	0.093	0.02	0.102
2	rs1966265	<i>FGFR4</i>	0.13	3.73x10 ⁻²⁰	0.07	0.003	0.05	0.018
2	rs6537291	<i>HHIP</i>	-0.07	1.01x10 ⁻⁹	-0.07	0.001	-0.06	0.001
2	rs1885245	<i>ASTN2</i>	0.07	4.95x10 ⁻⁹	0.01	0.545	0.04	0.019
5	rs2160442	<i>SOX9</i>	-0.09	5.18x10 ⁻¹⁴	-0.10	2.83 x10 ⁻⁶	-0.07	1.36 x10 ⁻⁴

Abbreviations: HSM (Hip shape mode), SNP (Single nucleotide polymorphism), P (p value).

¹Results from hip shape GWAS in ALSAPC adolescents (age 18), adjusted for age and gender

²Results from hip shape GWAS in ALSAPC adolescents (age 14), adjusted for age and gender

0.05 α threshold corrected for 18 tests=0.003

7.3.4. Look-up of known OA variants in adolescent hip shape

A look-up of hip OA associated variants, based on previously published literature, was performed in GWAS of adolescent hip shape at both time points (Figure 7.6 - Figure 7.10).

The strongest evidence was seen for an association between rs10492367 (*KLHDC5-PTHLH*) and HSM1 at age 14 (beta= 0.05, $p= 4.0 \times 10^{-5}$) and there was some evidence of an association at age 18 (beta= 0.03, $p=0.01$) (Figure 7.6).

There was some evidence of consistent associations between rs10948172 (*SUPT3H - CDC5L*) and HSM3 (Figure 7.7) at both time points (age 14 beta= 0.05, $p=0.006$; age 18 beta= 0.05, $p=0.002$). Similarly, there was some evidence for consistent associations between the same variant and HSM4 across the time points (age 14 beta= 0.05, $p=0.004$, age 18 beta= 0.06, $p=0.002$) (Figure 7.7). In addition, there was weak evidence of an association between rs11780978 (*PLEC*) and HSM4 at age 18 (beta=-0.05, $p=0.008$), but no robust evidence for an association at age 14 (Figure 7.7).

Two SNPs showed evidence for an association with HSM5 at age 18, rs9350591 (*FILIP1 - SENP6*; beta=-0.09, $p=0.008$) and rs11842874 (*MCF2L*; beta=0.014, $p=5.5 \times 10^{-4}$) (Figure 7.8). While consistent in terms of the direction of effect, the evidence for associations at age 14 was much weaker.

There was some evidence of an association between rs6094710 (*NCOA3*) and HSM8 at age 14 (beta -0.14, $p=0.009$) with little evidence of an association at age 18 (Figure 7.9).

Finally, there was evidence of an association between rs143384 (*GDF5*) and HSM9 at age 18 (beta= 0.08, $p=2.7 \times 10^{-4}$), but no robust evidence at age 14 (Figure 7.10).

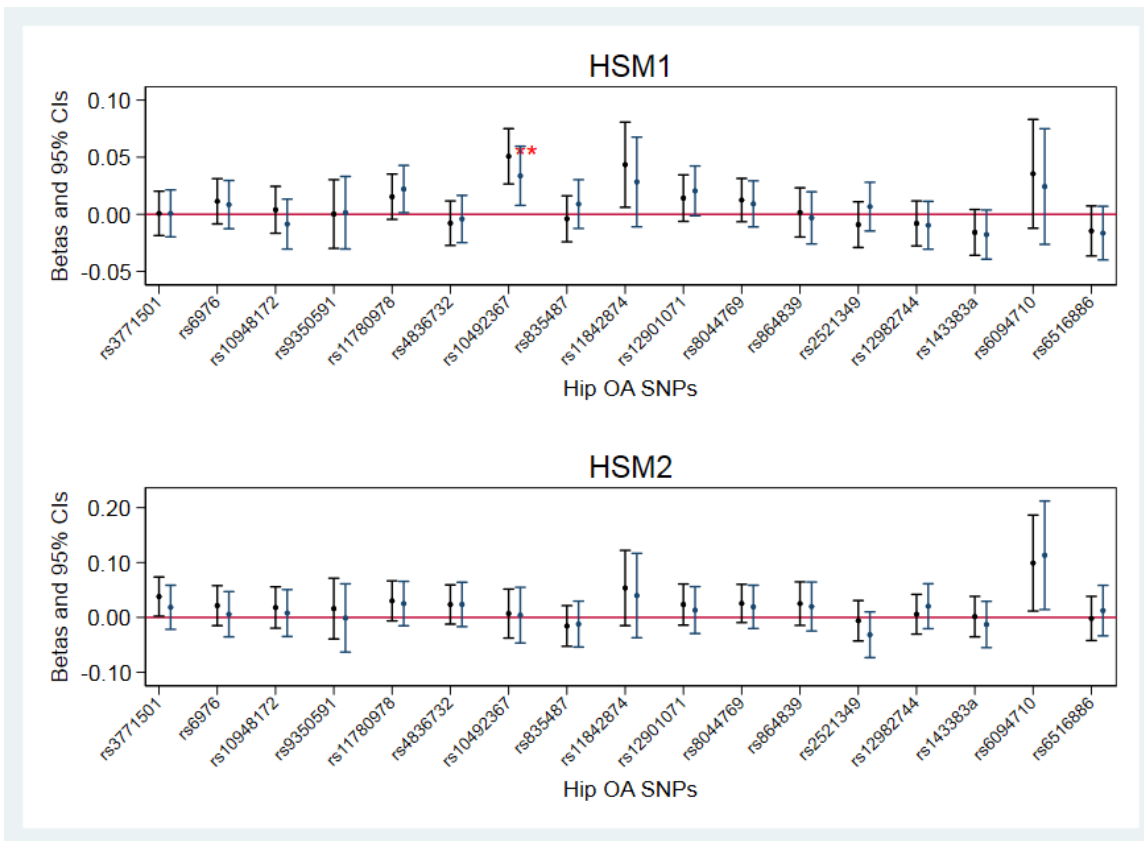


Figure 7.6 A look-up of published hip OA variants in ALSPAC HSM1 and HSM2 GWASes at age 14 (in black) and age 18 (in blue). Figure shows beta coefficients (black and navy dots) with 95% CIs (black and navy lines) for the association between hip OA SNPs and hip shape. Beta coefficients represent SD change in HSM per risk allele (betas were flipped to correspond to OA risk allele, for details see Table 7.1). SNPs with $p < 0.01$ are marked with **.

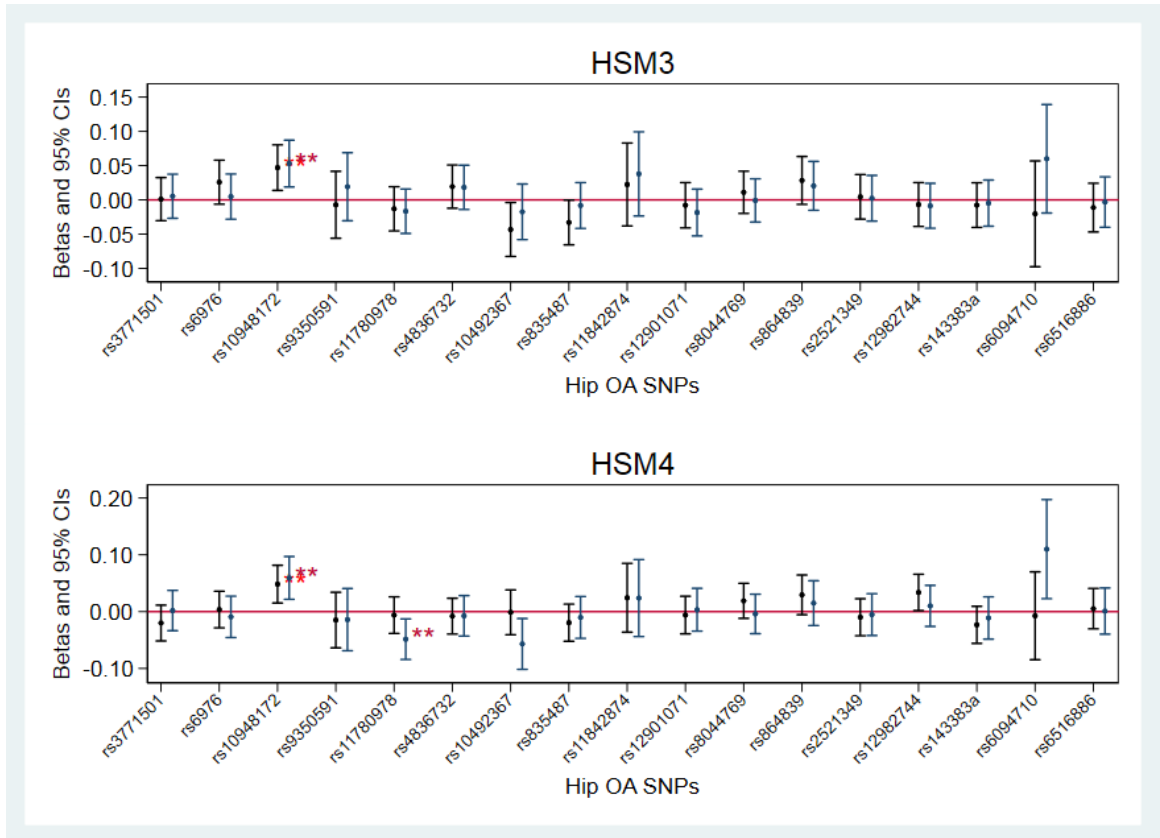


Figure 7.7 A look-up of published hip OA variants in ALSPAC HSM3 and HSM4 GWASes at age 14 (in black) and age 18 (in blue). Figure shows beta coefficients (black and navy dots) with 95% CIs (black and navy lines) for the association between hip OA SNPs and hip shape. Beta coefficients represent SD change in HSM per risk allele (betas were flipped to correspond to OA risk allele, for details see Table 7.1). SNPs with $p < 0.01$ are marked with **.

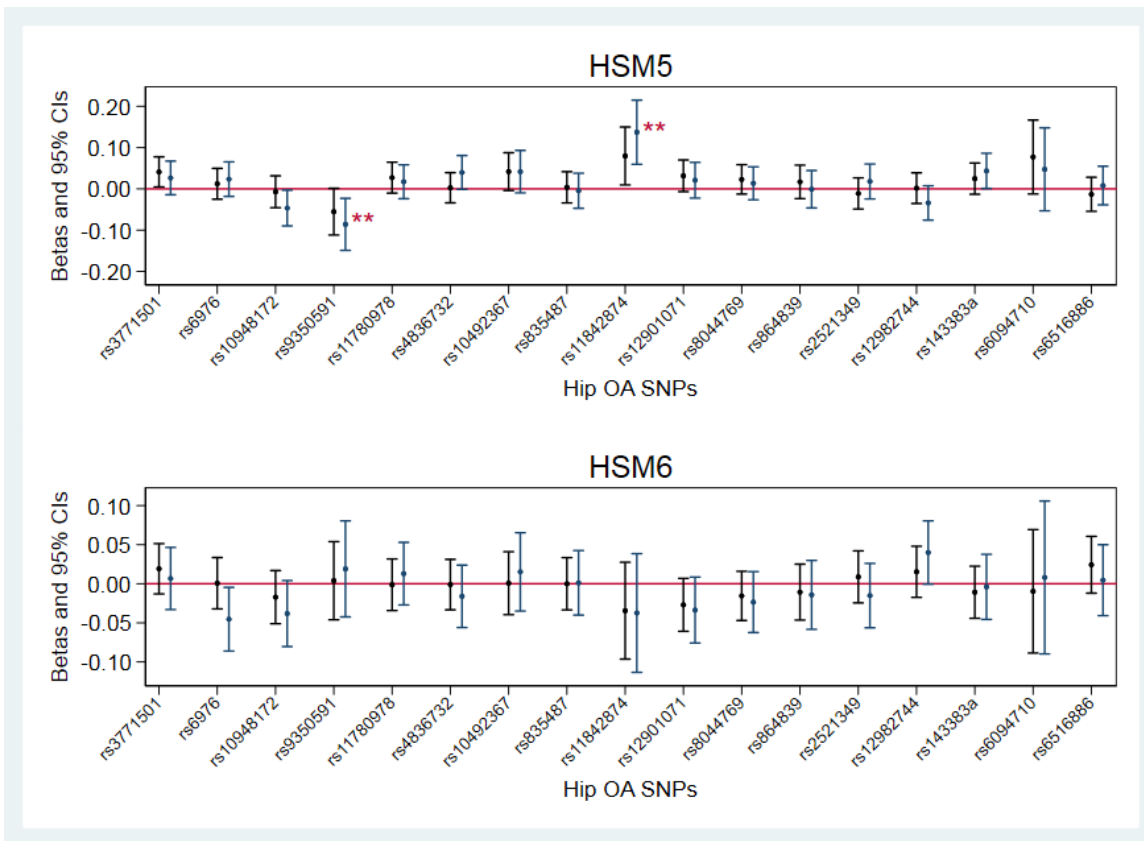


Figure 7.8 A look-up of published hip OA variants in ALSPAC HSM5 and HSM6 GWASes at age 14 (in black) and age 18 (in blue). Figure shows beta coefficients (black and navy dots) with 95% CIs (black and navy lines) for the association between hip OA SNPs and hip shape. Beta coefficients represent SD change in HSM per risk allele (betas were flipped to correspond to OA risk allele, for details see Table 7.1). SNPs with $p < 0.01$ are marked with **.

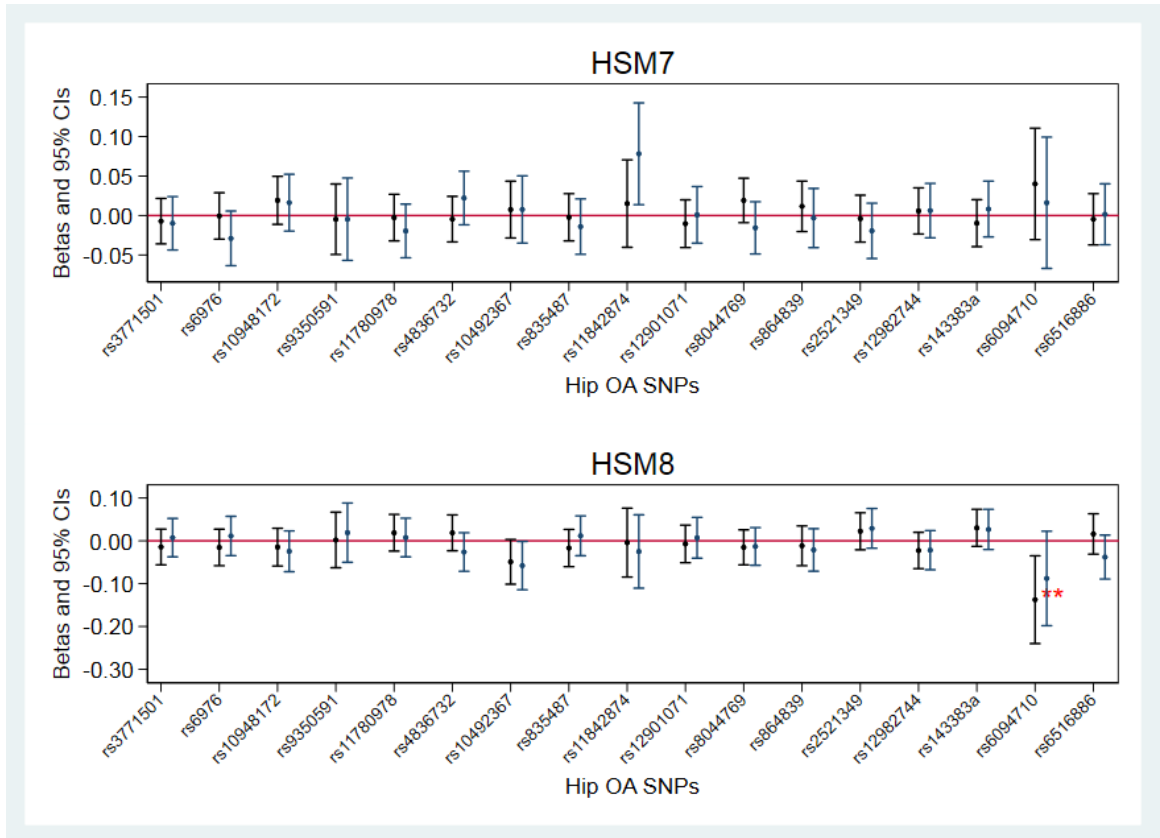


Figure 7.9 A look-up of published hip OA variants in ALSPAC HSM7 and HSM8 GWASes at age 14 (in black) and age 18 (in blue). Figure shows beta coefficients (black and navy dots) with 95% CIs (black and navy lines) for the association between hip OA SNPs and hip shape. Beta coefficients represent SD change in HSM per risk allele (betas were flipped to correspond to OA risk allele, for details see Table 7.1). SNPs with $p < 0.01$ are marked with **.

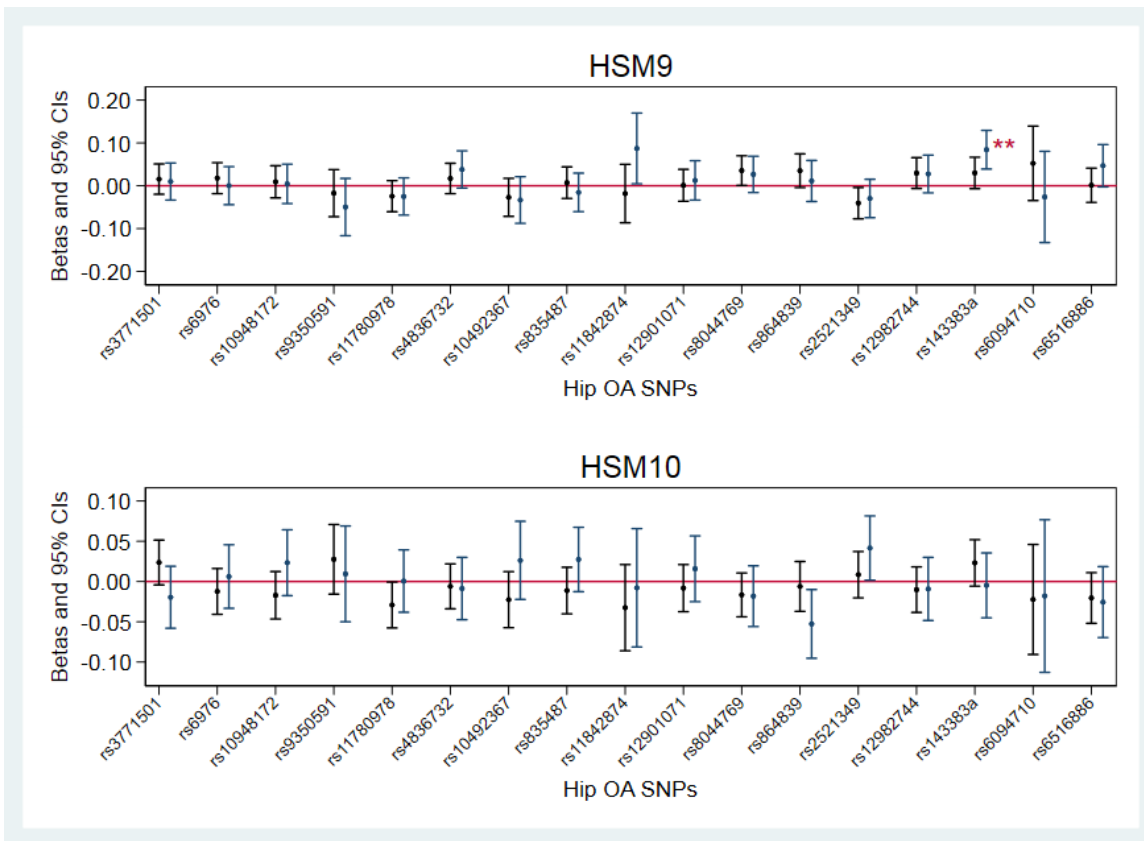


Figure 7.10 A look-up of published hip OA variants in ALSPAC HSM9 and HSM10 GWASes at age 14 (in black) and age 18 (in blue). Figure shows beta coefficients (black and navy dots) with 95% CIs (black and navy lines) for the association between hip OA SNPs and hip shape. Beta coefficients represent SD change in HSM per risk allele (betas were flipped to correspond to OA risk allele, for details see Table 7.1). SNPs with $p < 0.01$ are marked with **.

7.3.5. Genetic correlation between hip shape and other phenotypes

Based on Z-score values, genetic correlations between selected modes and a wide range of traits available in LD hub were performed. Only modes with Z-score values ≥ 2 were selected for analysis, these were HSM1, HSM2, HSM5 and HSM8 at both time points, HSM9 at age 14 and HSM3 and HSM7 at age 18 (a total of 5 modes at age 14 and 6 modes at age 18).

Genetic correlations between HSMs at age 14 and other phenotypes are shown in Figure 7.11-Figure 7.15. In general, there was some evidence for genetic correlations with a wide range of variables including respiratory, educational and anthropometric traits. Both HSM1 (Figure 7.11) and HSM5 (Figure 7.13) showed genetic correlations with respiratory traits and metabolites (primarily lipids), and FN BMD (HSM5 only), however the evidence was weak ($p < 0.05$). HSM2 showed weak evidence of genetic correlation with years of schooling, lipid metabolites and height (Figure 7.12). Similarly, there was weak evidence of genetic correlations between HSM8 and sleep duration, age at menarche and alanine (Figure 7.14). Finally, HSM9 was most strongly genetically correlated with height ($r_g = 0.23$, $p = 0.004$) and there was weaker evidence of genetic correlation with other traits including sleep duration, educational traits or extreme height amongst other traits ($p \sim 0.01$ or less) (Figure 7.15).

Genetic correlations between HSMs at age 18 and other phenotypes are shown in Figure 7.16-Figure 7.21. As for age 14, at age 18 there was weak evidence of genetic correlation between HSM1 and mean diameter for LDL particles, and in contrast with age 14 results there was weak evidence of genetic correlation with autism spectrum disorder ($p < 0.05$) (Figure 7.16). HSM2 showed genetic correlations with a number of traits, the majority of which comprised lipid metabolites, educational traits and obesity (and these traits were also genetically correlated with HSM2 at age 14) with blood lipids, years of schooling and childhood obesity showing the strongest evidence of genetic correlation ($p \leq 0.009$) (Figure 7.17). There was weak evidence of genetic correlation between HSM3 and glucose, autism spectrum disorder and LS BMD ($p < 0.05$) (Figure 7.18). Similarly, to age 14 result, at age 18 HSM5 was genetically correlated with respiratory and lipid traits and unlike age 14 result there was some evidence for genetic

correlation with height ($p=0.01$) (Figure 7.19). HSM7 was genetically correlated with a number of different traits, majority of which represented body size, with BMI showing the strongest evidence of genetic correlation ($p=0.005$) (Figure 7.20). At both time points, HSM8 was genetically correlated with personality trait, whereas at age 18 there was also evidence of genetic correlations with intelligence ($p=0.006$), heart rate ($p=0.009$) and extreme height ($p=0.04$) (Figure 7.21).

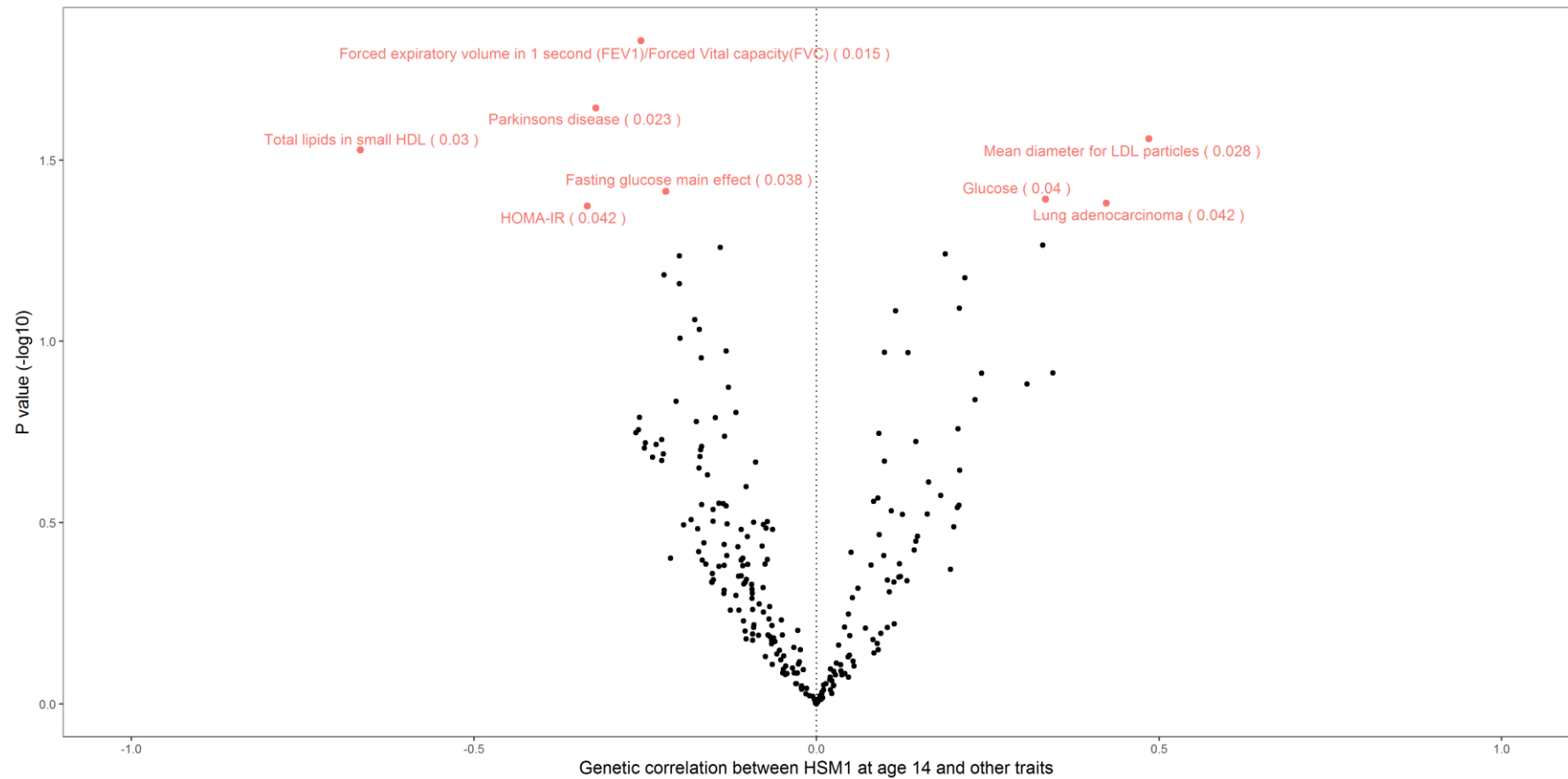


Figure 7.11 Volcano plot for genetic correlation results between HSM1 at age 14 and a range of traits. Each dot represents different trait; pink dots indicate traits with evidence of genetic correlation ($P < 0.05$) and black dots indicate traits with no evidence of genetic correlation. Traits showing evidence of an association are labelled and p value is given in brackets.

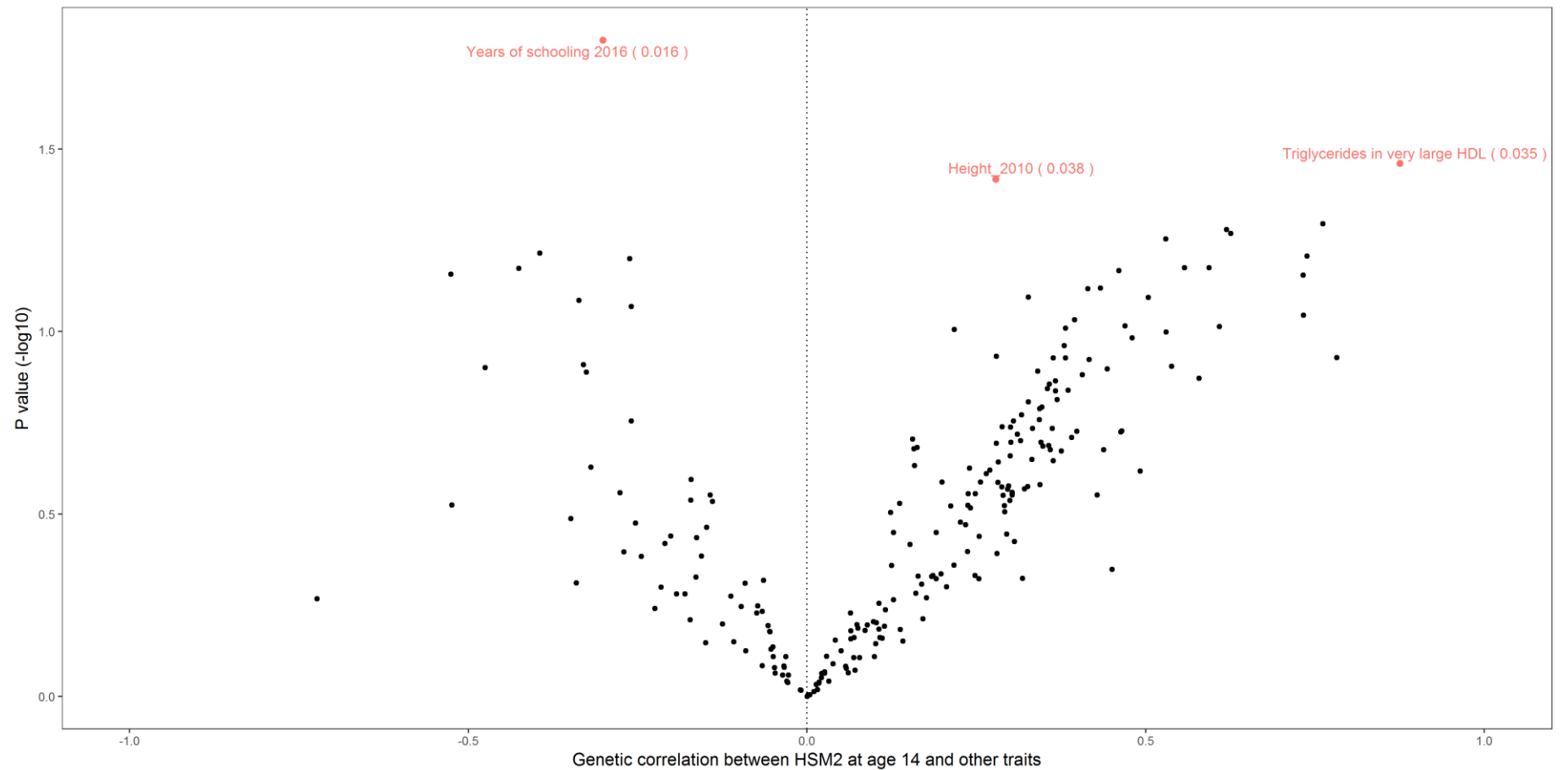


Figure 7.12 Volcano plot for genetic correlation results between HSM2 at age 14 and a range of traits. Each dot represents different trait; pink dots indicate traits with evidence of genetic correlation ($P < 0.05$) and black dots indicate traits with no evidence of genetic correlation. Traits showing evidence of an association are labelled and p value is given in brackets.

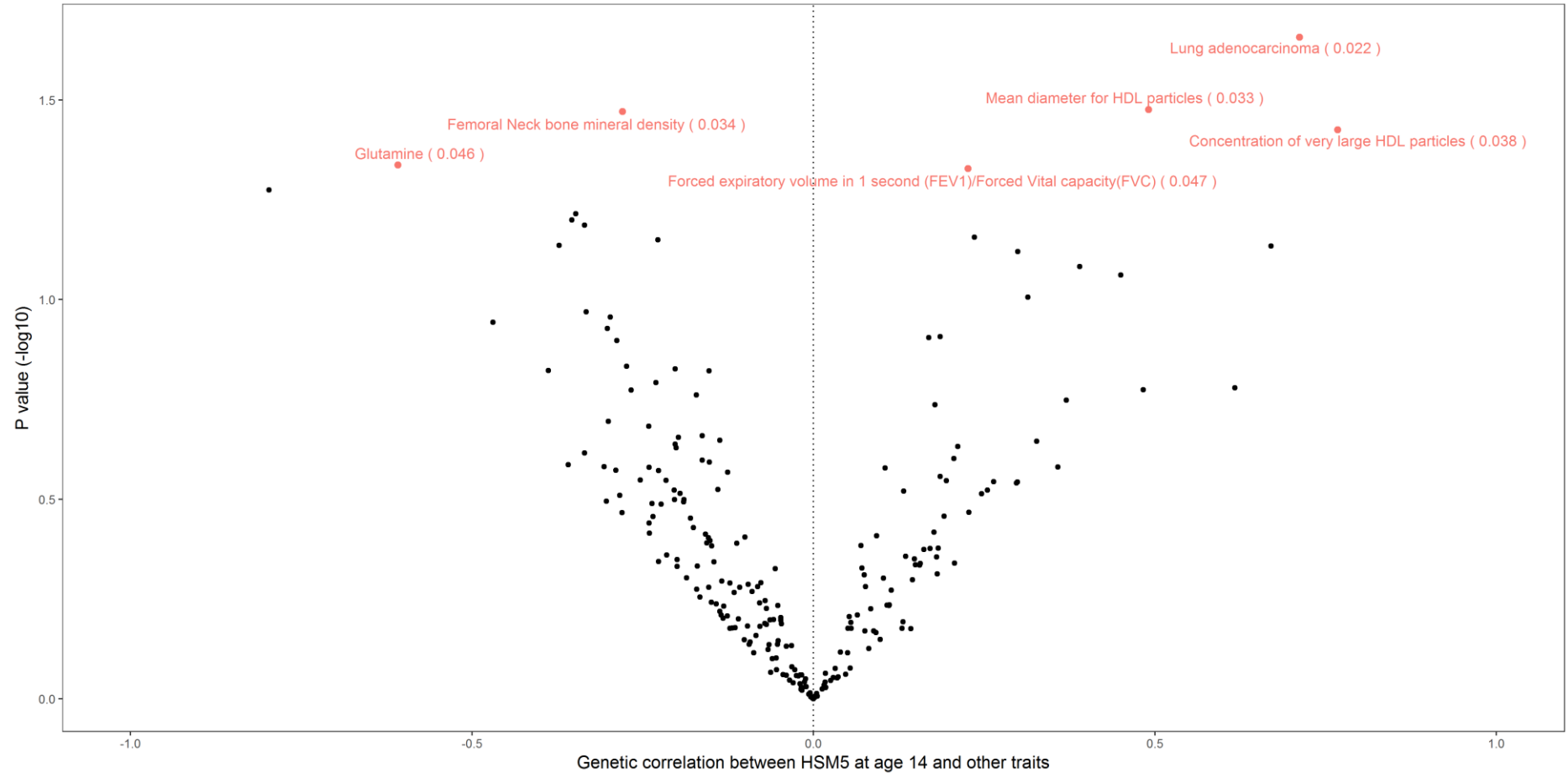


Figure 7.13 Volcano plot for genetic correlation results between HSM5 at age 14 and a range of traits. Each dot represents different trait; pink dots indicate traits with evidence of genetic correlation ($P < 0.05$) and black dots indicate traits with no evidence of genetic correlation. Traits showing evidence of an association are labelled and p value is given in brackets.

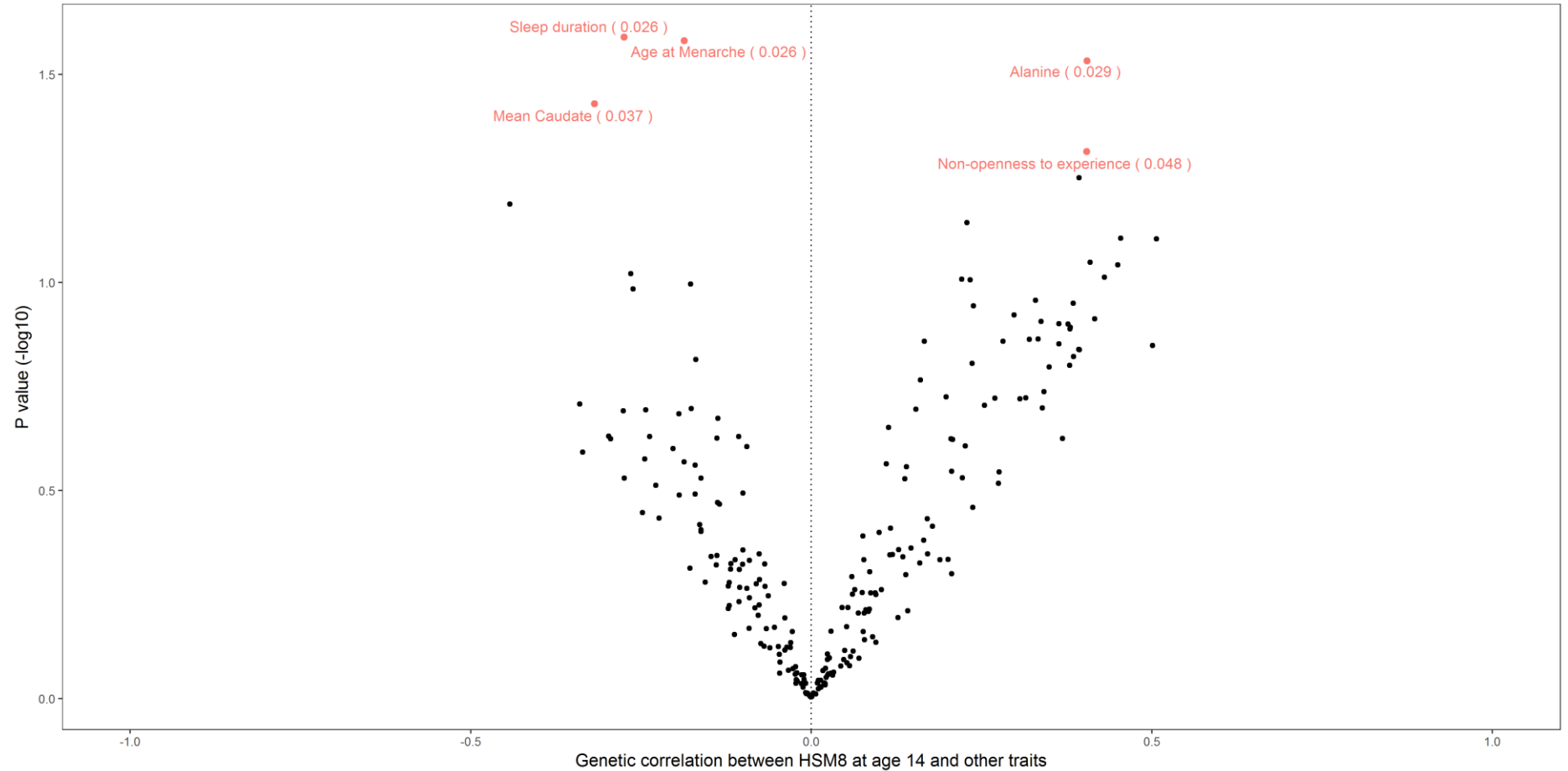


Figure 7.14 Volcano plot for genetic correlation results between HSM8 at age 14 and a range of traits. Each dot represents different trait; pink dots indicate traits with evidence of genetic correlation ($P < 0.05$) and black dots indicate traits with no evidence of genetic correlation. Traits showing evidence of an association are labelled and p value is given in brackets.

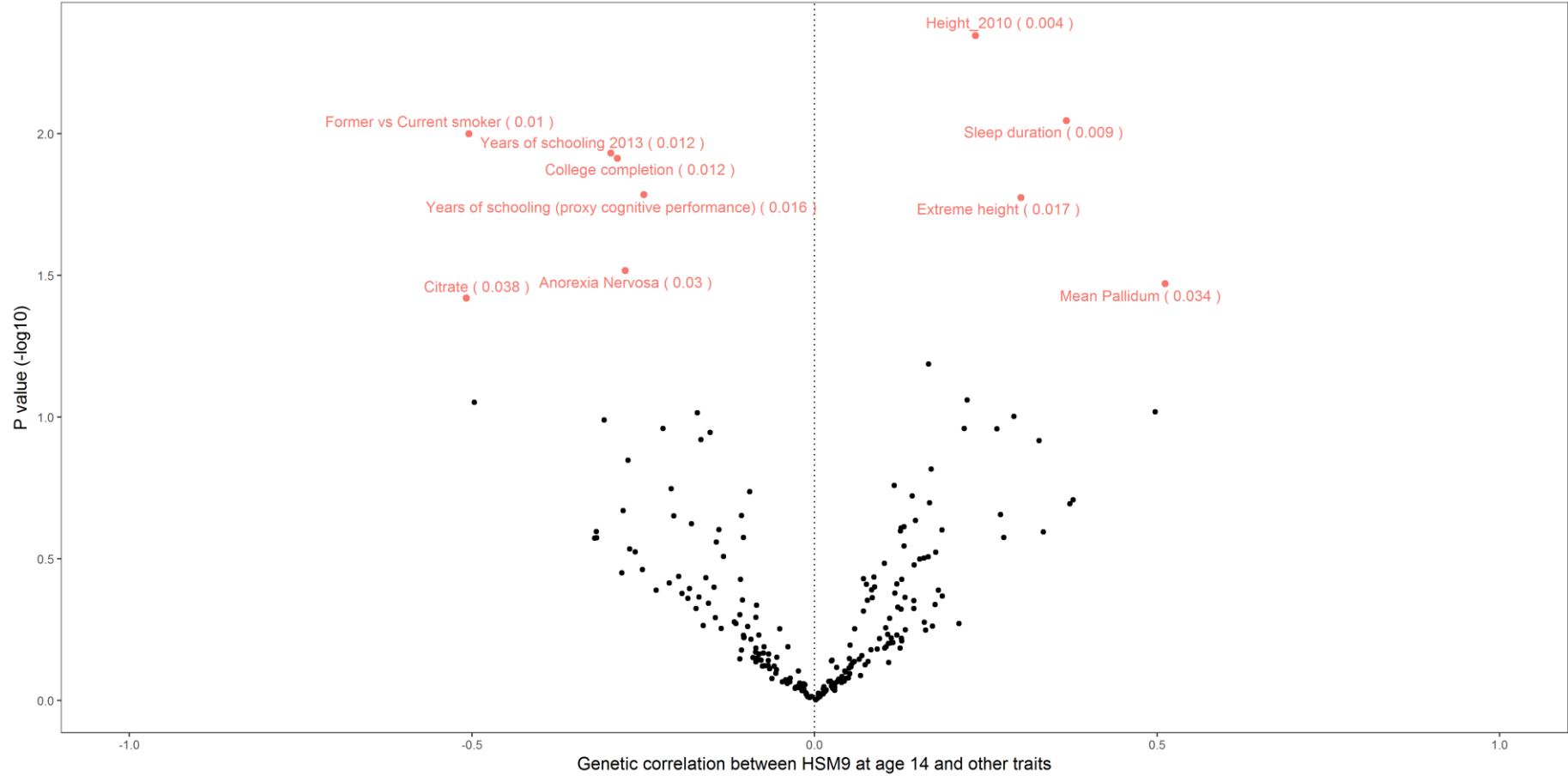


Figure 7.15 Volcano plot for genetic correlation results between HSM9 at age 14 and a range of traits. Each dot represents different trait; pink dots indicate traits with evidence of genetic correlation ($P < 0.05$) and black dots indicate traits with no evidence of genetic correlation. Traits showing evidence of an association are labelled and p value is given in brackets.

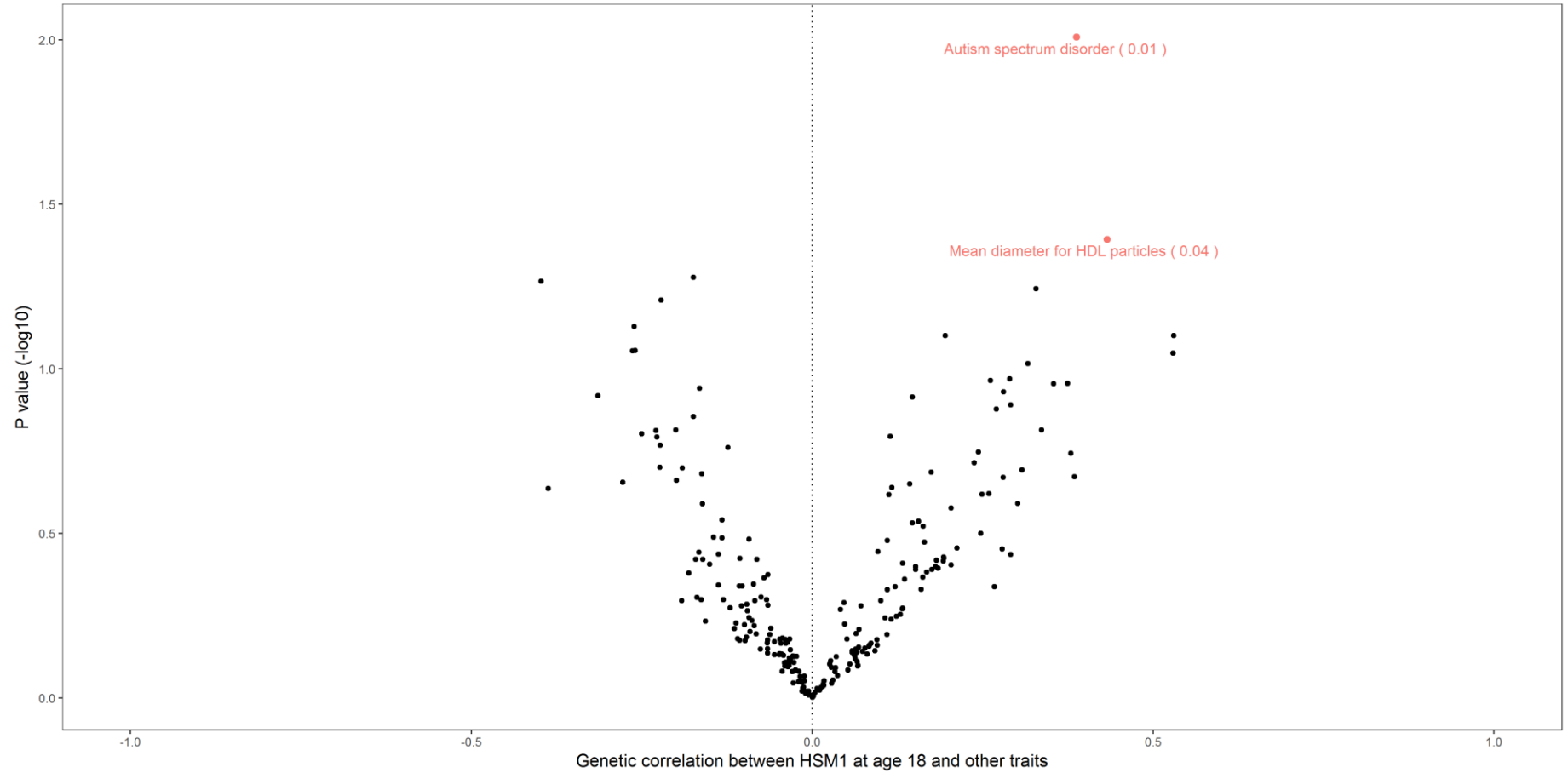


Figure 7.16 Volcano plot for genetic correlation results between HSM1 at age 18 and a range of traits. Each dot represents different trait; pink dots indicate traits with evidence of genetic correlation ($P < 0.05$) and black dots indicate traits with no evidence of genetic correlation. Traits showing evidence of an association are labelled and p value is given in brackets.

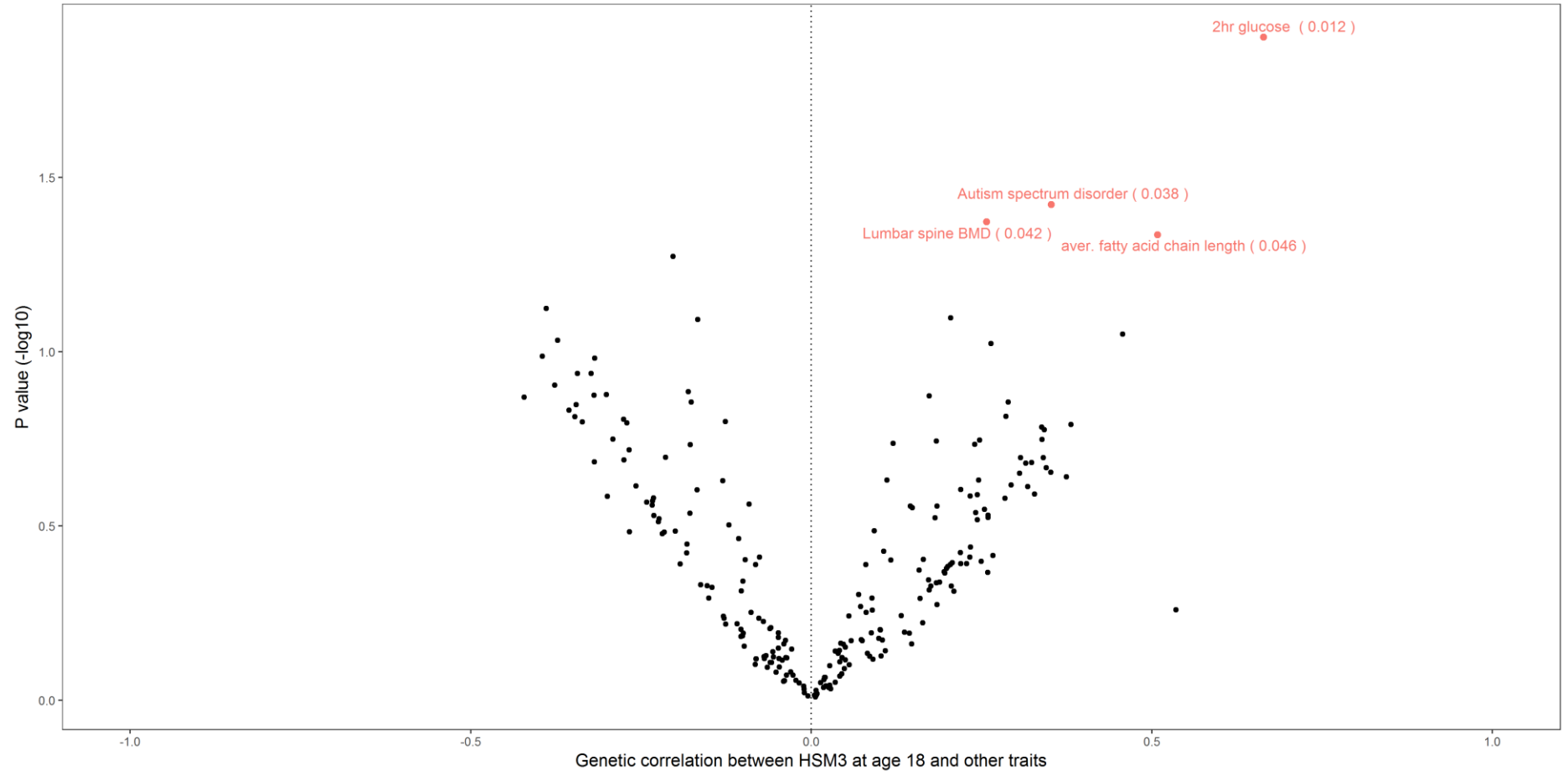


Figure 7.18 Volcano plot for genetic correlation results between HSM3 at age 18 and a range of traits. Each dot represents different trait; pink dots indicate traits with evidence of genetic correlation ($P < 0.05$) and black dots indicate traits with no evidence of genetic correlation. Traits showing evidence of an association are labelled and p value is given in brackets.

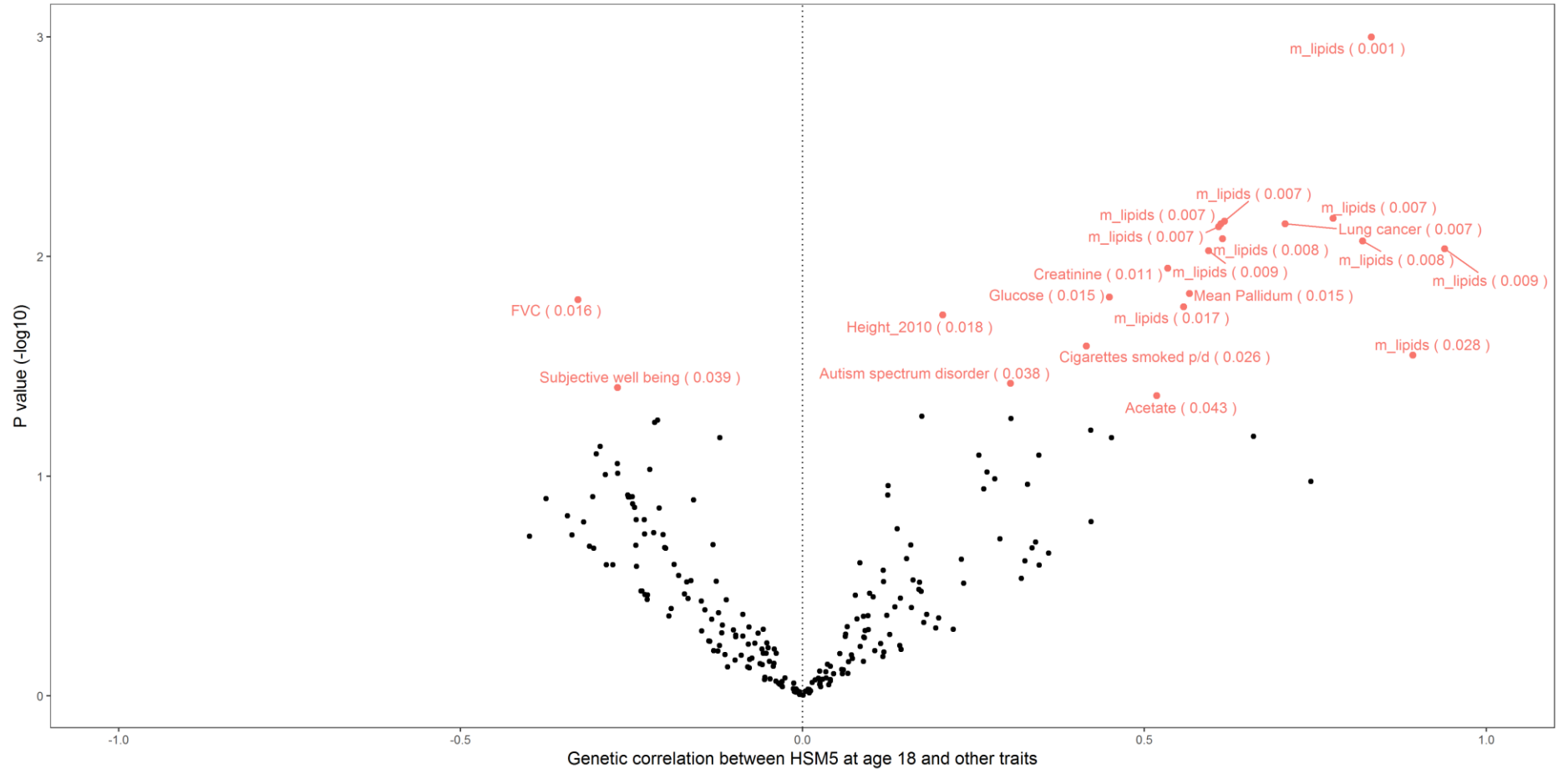


Figure 7.19 Volcano plot for genetic correlation results between HSM5 at age 18 and a range of traits. Each dot represents different trait; pink dots indicate traits with evidence of genetic correlation ($P < 0.05$) and black dots indicate traits with no evidence of genetic correlation. Traits showing evidence of an association are labelled and p value is given in brackets.

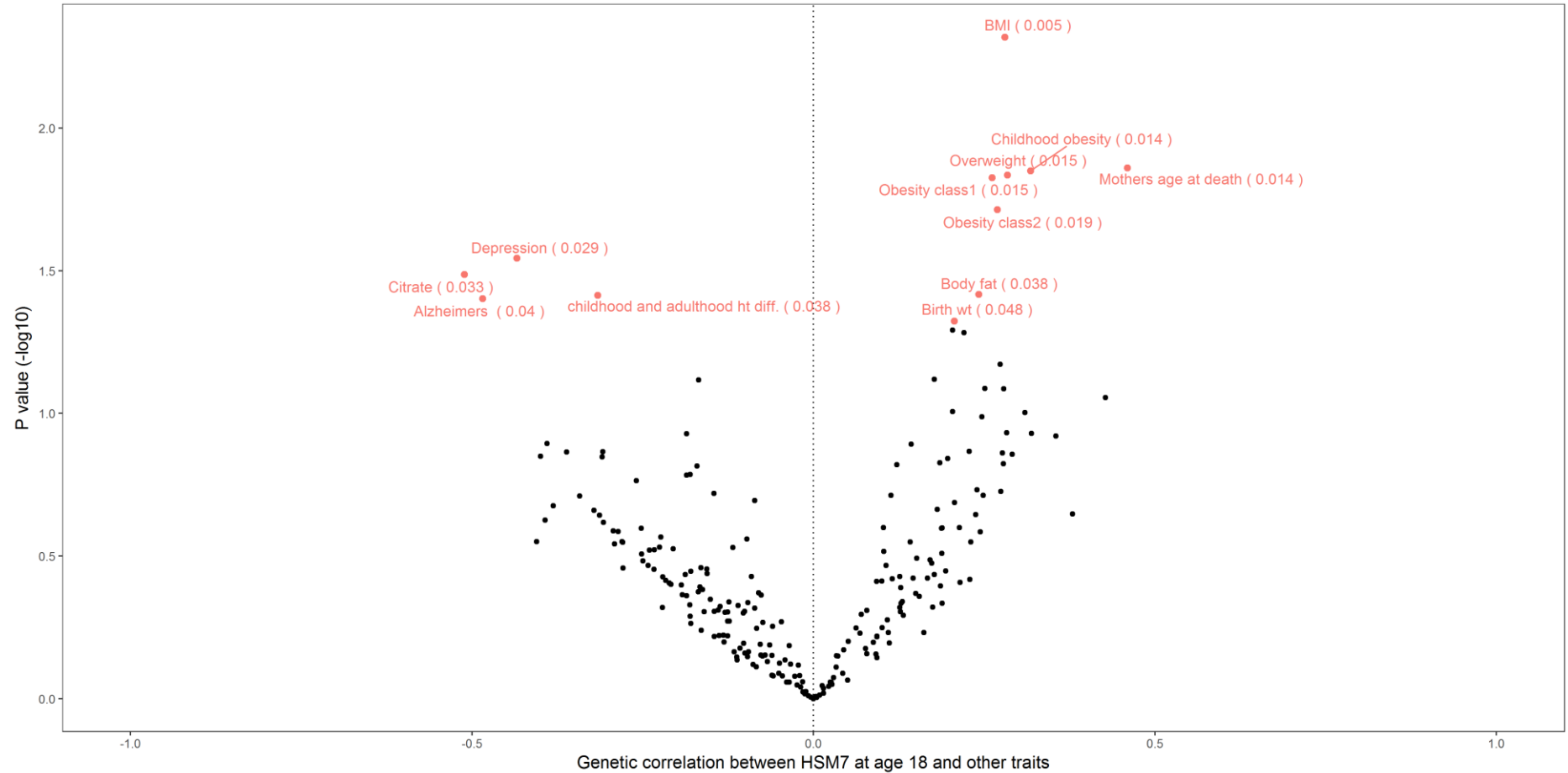


Figure 7.20 Volcano plot for genetic correlation results between HSM7 at age 18 and a range of traits. Each dot represents different trait; pink dots indicate traits with evidence of genetic correlation ($P < 0.05$) and black dots indicate traits with no evidence of genetic correlation. Traits showing evidence of an association are labelled and p value is given in brackets.

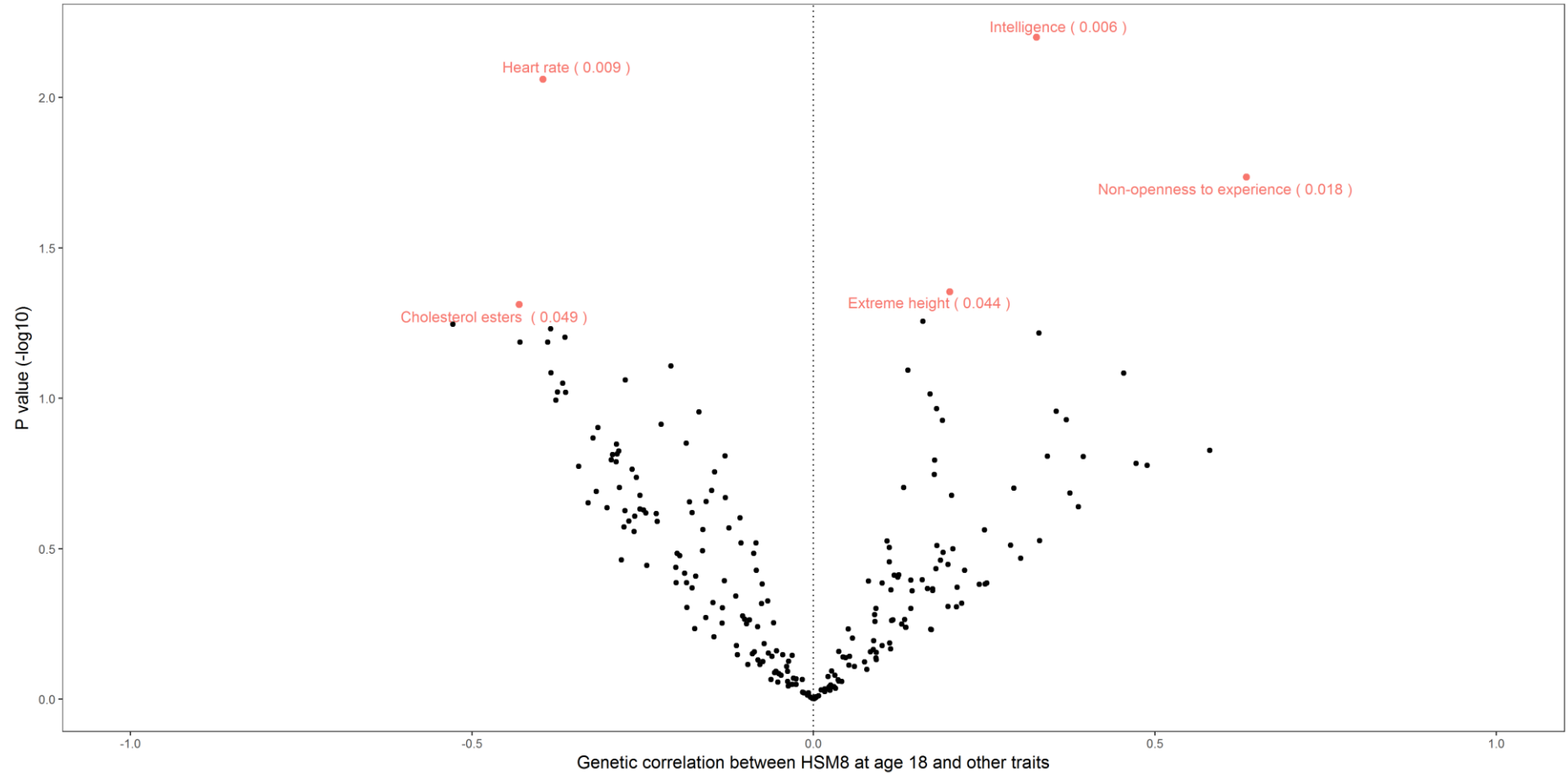


Figure 7.21 Volcano plot for genetic correlation results between HSM8 at age 18 and a range of traits. Each dot represents different trait; pink dots indicate traits with evidence of genetic correlation ($P < 0.05$) and black dots indicate traits with no evidence of genetic correlation. Traits showing evidence of an association are labelled and p value is given in brackets.

7.4. Discussion

In this chapter, I explored the genetic influences on hip shape in adolescents by performing the first GWAS of adolescent hip shape, as quantified by SSM.

There was strong evidence of consistent associations between rs8079830, a variant located near *SOX9*, and HSM1 at both adolescent time points and in adults. HSM1 reflects variation in femoral head and FNW, which both have previously been found to be associated with hip OA and/or fracture risk (Alonso et al., 2000; Baker-LePain & Lane, 2010; Karlsson et al., 1996). Interestingly, rs2158915 (also near *SOX9*) was also found to be associated with both HSM1 and HSM5 in an adult hip shape GWAS meta-analysis. Although in modest linkage with the SNP identified in adolescent GWAS ($r^2 = 0.3315$, $D'=1.0$), further investigation, such as co-localisation analysis (Giambartolomei et al., 2014), is justified to determine whether these associations share the same signal within the genomic region. Consistent with shared genetic influences on hip shape and BMD described in chapters 5 and 6, the *SOX9* locus associated with HSM1 and HSM5 in adult GWAS, was previously found to be related to FN BMD (D. A. Baird et al., 2017). Given the role of *SOX9* (Huang et al., 2001) as a key transcription factor in chondrocyte cell fate specification and in endochondral bone formation, these findings may reflect an influence of longitudinal growth on hip shape which may in turn play a role in OA development. Consistent with this suggestion, a look-up of rs8079830 in MR Base PheWAS showed a strong association with height in the UK Biobank and a recent paper by Zengini et al. (Zengini et al., 2018) confirmed a causal effect of height on OA using a MR approach. Another interesting finding resulting from a look-up in MR Base PheWAS included an association between rs8079830 and knee pain (likely due to OA) in the UK Biobank, consistent with a previous case report in a patient presenting with severe knee pain who was subsequently diagnosed with hip OA (S. Lam & Amies, 2015).

At age 18, there was evidence to suggest an association between rs8111495 and HSM5, which reflects variation in femoral head, FNW and greater and lesser trochanters. While this variant also showed association with hip shape at age 14, there was little evidence of an association in adults. Interestingly, a previous GWAS reported an association

between rs11672517 (in linkage with rs8111495; $R^2 = 0.75$) and Dupuytren's contracture (Ng et al., 2017), a highly heritable disorder of the connective tissue. Additionally, a look up in MR Base PheWAS, revealed strong evidence for an association with fibroblastic disorders in the UK Biobank resource (with Dupuytren's contracture being one of them). Dupuytren's contracture is characterized by development of hardened nodules in the palm of the hand which usually precede the development of bands. As the disease progresses, formed bands lead to contraction and permanent flexion in the affected digits. The nodules are thought to be the result of abnormal deposition of type III collagen, which is usually absent in normal adult palmar fascia (W. L. Lam et al., 2010; Ng et al., 2017; Townley et al., 2006). Previous reports suggest that the presence of type III collagen in regions of adult articular cartilage arise in response to mechanical injury (Aigner et al., 1993). A study by Hosseininia et al. reported that deposition of type III collagen in articular cartilage was more pronounced in femoral heads from OA patients compared with femoral heads from hip fracture patients (Hosseininia et al., 2016). This abnormal deposition of cartilage might be the result of abnormal mechanical loading resulting from altered hip shape and the same biological pathways underlying Dupuytren's contracture may also be implicated in alterations of hip shape. Furthermore, variants implicated in Wnt signalling pathways have been found to be associated with both Dupuytren's contracture (Ng et al., 2017) and knee and hip OA (Lane et al., 2017) .

Finally, rs1111767 was strongly associated with HSM6 at age 18 and there was little evidence to suggest an association at age 14. A look-up of this variant in MR Base PheWAS, revealed strong associations with educational phenotypes. Surprisingly, the largest OA meta-analysis to date reported genetic correlation between OA and educational attainment amongst other traits (Zengini et al., 2018). While these represent seemingly unrelated phenotypes, previous epidemiological studies reported clear relationship between low educational attainment and symptomatic hip OA (Cleveland et al., 2013) as well as radiographic and symptomatic knee OA (Callahan et al., 2011). It has been argued that individuals with higher educational attainment are more likely to make healthier choices (Brennan et al., 2012) (which might in turn reduce their risk of obesity, a well-recognized risk factor for OA (Baker-LePain & Lane, 2010))

which will in turn reduce their risk of OA. It is possible that altered hip shape established early in life coupled with exposure to other risk factors, such as obesity, may predispose individuals to OA in later life, which could potentially explain the observed association with educational attainment. However, the relationship between hip shape and education (as reported in this chapter) may be confounded due to underlying population structure. Haworth et al. demonstrated that individual SNPs were associated with birth location within the UK Biobank (thought to represent a homogenous population) and this structure could not be fully accounted for when adjusting for traditional covariates such as Principal Components or study centre which has the potential to induce bias in genetic studies (Haworth et al., 2018). Although, it is currently unclear to what extent this may confound such relationships.

The effect of adult hip shape variants on adolescent hip shape

There was strong evidence to suggest that variants associated with adult hip shape were also related to adolescent hip shape. In particular, genes implicated by the strongest associations with hip shape in adolescents, namely *SOX9* (associated with HSM1 and HSM5), *PTH1L* (associated with HSM1) and *HHIP* (associated with HSM2) are known to be involved in endochondral bone formation. Both, negative HSM1 and HSM2 scores reflect a larger femoral head (in the inferolateral aspect) and wider FNW, whereas negative HSM5 scores reflect a narrower FNW and larger lesser trochanter. Both FNW and variation in femoral head size have previously been found to be related to the risk of OA in later life. For example, wide FN (Castaño-Betancourt et al., 2013b) and femoral head deformities (Doherty et al., 2008; Heijboer et al., 2012; Ledingham et al., 1992) were found to be associated with increased risk of OA in previous studies. This reinforces the suggestion that subtle morphological changes in hip shape predispose to the onset of OA.

Look-up of known OA variants

When considering the associations between previously established hip OA loci and hip shape in adolescence, the strongest evidence was seen for an effect of rs10492367 (located between *KLHDC5* (Kelch domain containing 5) and *PTH1L* (parathyroid hormone-like hormone)) on HSM1. This SNP is in moderate linkage with rs10743612 ($r^2=0.74$), a variant identified from the adult hip shape GWAS and subsequently found to be

associated with HSM1 in adolescents, as described above. The role of PTHrP in bone remodelling as well as its importance in endochondral bone formation are well recognized (Martin, 2016). However, further studies are justified to confirm the functional role of this variant and how it may modify the relationship between hip shape and OA. While there was suggestive evidence for an effect of other hip OA implicated variants on a number of HSMs, likewise their functional relevance is unknown.

Genetic correlations with other traits

In terms of genetic correlations between hip shape and other traits, I identified a number of correlations with a number of different phenotypes, however considering the number of tests carried out and lack of adjustment for multiple testing the evidence was relatively weak, and these results require replication in an independent sample. FN BMD was negatively correlated with HSM5 at age 14 and LS BMD was positively correlated with HSM3 at age 18, consistent with MR findings presented in chapter 5, which showed associations between BMD and HSM5 at age 14 and HSM3 at age 18. A number of modes showed correlations with height and obesity (i.e. at age 14, HSM2 and HSM9 were positively correlated with height, at age 18 HSM5 and HSM8 were also positively correlated with height, whereas HSM2 and HSM7 were both positively correlated with obesity). This is consistent with previous findings that most variants associated with hip shape in adults were also associated with height (D. A. Baird et al., 2017). It is worth noting that given the relatively small sample size of adolescent hip shape GWAS and heritability Z-scores outside the accepted threshold (less than 2) for some of the modes, these results require further replication with larger sample size (>5000) and this should also be followed up using genome-wide complex trait analysis (GCTA (J. Yang et al., 2011)) which relies on a restricted maximum likelihood approach. However, while these results need to be interpreted with caution, given the well-established role of hip shape in OA and the role obesity plays in increasing the risk of OA, the correlation between BMI and HSM7 ($r_g=0.28$, $p=0.005$) found in this chapter is plausible, i.e. excessive weight might result in excessive wear of the cartilage and thus altered bone proportions (Widhalm et al., 2016) which will in turn predispose individuals to an increased risk of hip OA. Consistent with this suggestion, recent GWAS in the UK Biobank reported genetic correlation between BMI and hip OA ($r_g=0.28$, $p=4 \times 10^{-4}$) and the authors were

able to confirm the causal role of BMI on OA risk using MR approach (Zengini et al., 2018). With regards to genetic correlations between hip shape and other traits observed in this chapter, a MR approach might be usefully employed to further examine these relationships.

Strengths and limitations

This study represents the first GWAS of hip shape in adolescence. Since I used the same SSM template as that in a recent meta-analysis of adult hip shape GWAS (D. A. Baird et al., 2017), I was able to directly compare adolescent results with those of adults. While some of the variants associated with hip shape in adolescence were also replicated in adult cohorts, future studies should aim to replicate these findings in an independent adolescent cohort. Given the fact that some of the adolescent hip shape variants were not replicated in adults, this might suggest that distinct genetic variants are implicated in hip shape development in adolescence as opposed to changes in hip shape occurring in adult life.

One of the primary goals of GWAS is to better understand the architecture of complex traits which might in turn be utilised clinically as better understanding of disease mechanisms might point towards new therapeutic targets. While GWAS is a powerful tool in identifying genetic variants associated with complex traits, the results are not directly informative in terms of the causal gene or underlying biological mechanisms linking the genetic variants with a trait of interest. Further analytical and molecular approaches are necessary to bridge the knowledge gap and better understand mechanisms underlying these associations. In this chapter, GWAS findings were followed up with different analytical approaches and these results, from look-ups and LD score regression, are likely representative of genetic pleiotropy, consistent with the suggestion of pleiotropic abundance in many complex traits (Sivakumaran et al., 2011). Furthermore, while some of the variants identified in this study point towards biologically relevant loci and might thus shed a light on biological pathways relevant to hip shape development and subsequent OA and fracture risk, further functional studies are necessary to determine the likely causal variants and genes. Although eQTL analysis

showed no associations with any of the tissue types available in GTEx, further investigation in relevant tissue types would need to be undertaken (one possibility would be to look-up these hits in an osteoblast eQTL genome-wide dataset (Grundberg et al., 2009)).

Another important limitation of this study includes the modest sample size. Most genetic variants associated with complex traits confer small to modest effects, therefore, large sample sizes are required to detect common variants associated with these traits. Nevertheless, ALSPAC currently represents the only study with repeated measures of hip shape at two critical time points during adolescence (pre- and post-puberty). Despite the sample size, I was able to detect SNPs reaching genome-wide significance and replicate some of these findings in adult cohorts. However, these findings should be replicated in independent adolescent cohorts. For example, the minimum sample size required to detect SNP-trait association of smaller magnitude (i.e. beta of 0.1 SD) with 80% power at GWAS significance level ($p < 5 \times 10^{-8}$) and with MAF of 0.1, the sample size would need to increase to 1 million individuals and even more in the case of rare variants (Visscher et al., 2017).

Conclusions

This study represents the first GWAS of hip shape in adolescents at age 14 and 18. Despite the relatively small sample size, I was able to detect associations with SNPs with potential relevance to bone biology, as exemplified by a variant near *SOX9*, which was also associated with height, and another variant near *PTHLH*, both associated with HSM1. While these results reflect shared influences of longitudinal growth on hip shape, further studies are required to establish role of these variants in mediating OA and hip fracture risk.

CHAPTER 8. DISCUSSION

8.1. Aims of this PhD

OA is the most common form of arthritis associated with a significant economic and health burden, affecting 240 million people worldwide. There is currently no treatment available which would cure it. Despite identifying several risk factors for OA, the pathophysiology still remains to be elucidated. Hip shape is thought to be one of the most important risk factors for hip OA, and it has also been found to be associated with the risk of osteoporotic hip fracture. Therefore, better understanding of factors influencing the development of hip shape, will help to elucidate mechanisms underlying the development of OA and point towards new opportunities for prevention.

The overarching aim of this thesis was to describe the development of hip shape in ALSPAC adolescents and explore factors influencing this process. In order to describe the variation in hip shape and make direct comparison between hip shape measured at age 14 and 18, as well as comparison with adult hip shape, SSM based on adult reference SSM (comprising over 19,000 hip DXA images) was developed and applied to adolescent images. Using this adult reference SSM, I aimed to first describe sex differences in hip shape and associations with pubertal timing. To investigate mechanisms and potential pathways contributing to hip shape development, I investigated the relationships between BMD and hip shape (in adolescents and adult women) before exploring genetic influences on hip shape using GWAS.

8.2. Key findings of this research

8.2.1. Variation in hip shape in relation to sex and pubertal timing

In Chapter 3, I explored sex differences in hip shape in peri-pubertal and post-pubertal children from the ALSPAC cohort and observed sex differences in various aspects of hip shape at both time points investigated. At age 14, males had a larger femoral head and lesser trochanter compared with females and these differences were independent of height, lean and fat mass. At age 18, males had a larger FNW and lesser trochanter whereas females appeared to have larger femoral head medially. However, these differences were largely attenuated following adjustment for height, lean and fat mass with only subtle differences in FNW and lesser trochanter still remaining.

When exploring the relationship between tempo (a marker of pubertal timing) and hip shape (Chapter 4), at age 14 the associations were stronger in males compared with females, however by age 18 these were comparable across sexes showing weak associations with tempo. It needs to be noted that when comparing associations with hip shape between early vs. late maturing males at age 14 clear differences in various aspects of hip shape were observed. Compared with late maturers, early maturing boys had a wider FNW, bigger lesser trochanter and smaller superolateral femoral head, whereas differences in early vs. late maturing females were harder to discern. When these differences were modelled for hip shape measured at age 18, no considerable differences between early vs. late maturers were noted in either sex suggesting no lasting effect of pubertal timing on hip shape. The results observed at age 14 were consistent with published literature. One study in Spanish boys, aged between 9 and 16 years, reported that the size of FN and lesser trochanter increased with age (Pujol et al., 2016). Furthermore, other studies suggest that puberty is a critical period for the development of cam deformity (a well-known risk factor for hip OA related to shape of the superolateral femoral head also found to be related to tempo at age 14) especially as a result of high impact activities. For example, Heijboer et al. followed-up soccer players for a mean period of 2.4 years and noted an increase in cam-type deformities between the ages of 12 and 14 years, which continued to increase from the age of 14

years until closure of the growth plate (Heijboer et al., 2014).

Weak associations between tempo and hip shape at age 18 observed in this thesis are consistent with previous study in females, aged between 20–30 years, which found no relationship between age at menarche and FNW (Pasco et al., 1999) suggesting that pubertal timing does not exert lasting effects on hip shape and its components.

Taken together, findings of this research extend those reported in the literature, suggesting that puberty represents an important period for the development of hip shape, particularly for aspects that are likely to be related to future hip pathology (such as cam-type deformity which is related to hip OA (Heijboer et al., 2012) and variation in FNW, previously investigated in relation to hip fracture (Ahlborg et al., 2005; Alonso et al., 2000; Karlsson et al., 1996; Ego Seeman et al., 2001)).

8.2.2. Relationship between BMD and hip shape

The inverse relationship between OA and OP, as well as the role of hip shape in the development of hip OA and hip fracture risk prediction are well-established (Baker-LePain & Lane, 2010; Geusens & van den Bergh, 2016; Gregory et al., 2004). However, to what extent does the relationship between higher BMD and hip shape contribute to the association between reduced hip fracture risk and hip OA remains to be elucidated. In addition, BMD and hip shape could be influenced by common molecular pathways, consistent with findings from the recent hip shape GWAS which identified a number of loci previously found to be related to BMD (D. A. Baird et al., 2017). Therefore, in Chapters 5 and 6 I explored the previously unknown relationships between BMD and hip shape in ALSPAC children and mothers. Observationally, BMD was associated with a number of HSMs and these associations were consistent across both adolescent time points and in ALSPAC mothers. Higher BMD was associated with a narrower FNW and larger femoral head medially in both adolescents and mothers. The associations between BMD and hip shape, reported in this thesis, could conceivably contribute to the relationship between OP and OA. For example, a previous study in elderly women reported associations between larger femoral heads and increased risk of RHOA (Lynch et al., 2009). On the other hand, I found higher BMD to be associated with narrower

FNW. While wider FNW has been found to be associated with hip OA (Castaño-Betancourt et al., 2013b) these findings would not explain why higher BMD is associated with hip OA. In terms of BMD-hip shape associations and their contribution to hip fracture, a finding of higher BMD associated with narrower FNW was unexpected and is difficult to explain given the known associations between both higher BMD and wider FNW with reduced risk of fracture (Ahlborg et al., 2005; Ego Seeman et al., 2001), although the evidence for the latter is conflicting (Gregory & Aspden, 2008).

Having found strong observational evidence for an association between BMD and hip shape, I followed up these results with a MR approach to determine the extent to which common genetic pathways underlie both BMD and hip shape. In adolescents, I found consistent evidence of associations between BMD with HSM2 and HSM5 across both time points, and evidence of an association with HSM1 and HSM3 at age 14 and 18, respectively. While MR findings suggest that biological pathways underlying BMD variation could contribute to aspects of hip shape (such as variation in FNW described by HSM2, HSM3 and HSM5, and variation in femoral head size described by HSM1) which have previously been found to be associated with increased risk of OA (Castaño-Betancourt et al., 2013b; Lynch et al., 2009) and/or fracture (Ego Seeman et al., 2001), not all observational results were confirmed with MR, either reflecting low power due to limited sample size or simply chance finding. In ALSPAC mothers', MR results showed no robust evidence of an association between BMD and hip shape.

8.2.3. Genetic influences on adolescent hip shape

In Chapter 7, I undertook the first GWAS of hip shape in adolescents and despite the modest sample size, five loci reached genome-wide significance ($P < 5 \times 10^{-8}$). This analysis identified robust associations between a variant near *SOX9* (rs8079830) and HSM1 at age 14 and 18. In addition, this variant was also strongly related to hip shape in adults based on a look-up of adult hip shape GWAS. Another important finding was that a variant residing in an intron of *DUXA* (rs8111495) was found to be associated with HSM5 in adolescents at both time points, but there was no evidence of a corresponding association in adults. Interestingly, a variant in high linkage with rs8111495 (rs11672517

$R^2 = 0.75$) was previously found to be associated with Dupuytren's contracture, which is a disorder of connective tissue (Ng et al., 2017). Finally, rs1111767 was strongly associated with HSM6 at age 18, but there was little evidence to suggest association at age 14 and no compelling evidence of an association in adults. In a look-up of a previous GWAS in the UK Biobank study, this SNP was associated with educational phenotypes. While previous observational evidence showed a strong relationship between educational attainment and symptomatic hip and knee OA (Callahan et al., 2011; Cleveland et al., 2013), recent genetic studies suggest that finer population structure could confound these relationships (Haworth et al., 2018) and may suggest this is an erroneous association. For example, in the UK Biobank geographic location was found to be associated with individual SNPs and these associations persisted when adjusting for traditional measures of population structure such as principal components (Haworth et al., 2018), however to what extent these associations could confound the relationships observed in this thesis is currently unknown.

Based on results from the largest to date meta-analysis of adult hip shape (D. A. Baird et al., 2017) which relied on the same SSM template used throughout this thesis, a look-up in adolescent GWAS showed that a number of variants associated with adult hip shape were also associated with adolescent hip shape. These included consistent associations, across adolescent time points, with variants implicated in endochondral bone formation such as *SOX9* (associated with HSM1 and HSM5), *PTHLH* (associated with HSM1) and *HHIP* (associated with HSM2). Interestingly, in a look-up of previously established OA SNPs, rs10492367 (located between *KLHDC5* and *PTHLH*) was associated with HSM1 and showed the strongest evidence of an association. In addition, this variant was in moderate linkage with rs10743612 ($r^2 = 0.74$), a SNP which showed evidence of associated with HSM1 in both, adults and adolescents.

8.3. Contribution of this research

The findings of this research make several contributions to the current literature. Firstly, this thesis describes the first study to quantify and describe the variation in the shape of proximal femur as measured by SSM in ALSPAC adolescents at two different time points. While previous studies investigated sex differences in hip morphology in adolescents (Forwood et al., 2004; Sayers et al., 2010; M. C. Wang et al., 1997), these mainly focused on individual geometrical indices rather than the entire contour of the proximal femur including the femoral head, trochanters, femoral shaft and acetabular sourcil. Although sexual dimorphism in skeletal size, mass, strength and geometry is well recognized (Callewaert et al., 2010; Sayers et al., 2010; Ego Seeman, 2001), the approach to study sex differences in femoral morphology in this thesis is novel. Nevertheless, the findings were consistent with previous literature showing that males have wider FNW than females (Sayers et al., 2010) and the size of lesser trochanter increased with age as shown in previous study in Spanish males (Pujol et al., 2016). In contrast to the study in Spanish individuals, I was able to describe variation in the entire contour of femoral head as well as variation in the acetabular sourcil.

Furthermore, in line with previous literature, this study confirmed that puberty is a critical period for hip shape development and applying SSM allowed detailed quantification of proximal femur morphology as opposed to single geometrical measurements which are highly correlated with measures of body size. Although no lasting effects of pubertal timing on hip shape were observed in this thesis, previous studies reported an association between delayed puberty and increased risk of fracture in both males and females (Bonjour & Chevalley, 2014; Finkelstein et al., 1996; Finkelstein et al., 1992) likely reflecting relationships with suboptimal bone quality rather than hip morphology.

BMD and hip shape

The relationships between hip shape with hip OA and fracture are well-established. While associations with BMD could partly explain these relationships, the role of hip shape could also contribute. However, to date little is known about the relationship

between BMD and hip shape. The observational results of a positive relationship between BMD and hip shape could reflect a possible shared contribution of femoral head size to associations between BMD and hip OA, whereas the relationship between higher BMD and narrower FNW could have implications for understanding of pathogenesis of hip fracture. In order to explore if BMD and hip shape share common genetic influences, I used a MR approach. I found some evidence for shared genetic mechanisms underlying BMD and hip shape, however further studies are necessary to determine the specific pathways contributing to the BMD-hip shape relationship and their role in OA and OP risk. Although there was no robust evidence of associations in adults, the results were in a consistent direction with the observational results. Both, adolescent and adult MR analyses appear to be underpowered and require further replication in larger samples.

Genetics of hip shape

OA is highly heterogenous and an increasing number of studies focus on OA-related endophenotypes in order to increase power and identify genetic variants with likely functional potential. In this thesis, a number of genetic variants associated with adult hip shape were successfully replicated in adolescents, suggesting that the mechanisms which contributed to later clinically relevant bone phenotypes may start having an impact early in life and therefore highlighting the need for early preventative measures. Of the adults' variants most strongly related to hip shape in adolescents, most loci were implicated in endochondral bone formation, suggesting shared genetic influences on hip shape and longitudinal growth. Furthermore, GWAS in adolescents identified additional SNPs which did not replicate in adults, either reflecting distinct genetic influences on hip shape across the investigated time points or false positive results.

Finally, in the light of the findings of this research, the advice given to young individuals at risk of OP and OA, if they could be identified, should follow the standard guidelines. In terms of reducing future risk of OA, modifiable risk factors such as obesity, joint injury and modification of high impact sporting activities, particularly during growth, should be targeted (Bijlsma & Knahr, 2007; Pun et al., 2015). In terms of future risk of OP,

preventative strategies in adolescence should be aimed at maximising the attainment of peak bone mass (one of the key predictors of BMD in later life (Lane, 2006)), with factors such as exercise, adequate calcium intake and vitamin D levels known to play a role (Coli, 2013; Gordon et al., 2017).

8.4. Strengths and limitations

SSM

One of the strengths of this research includes the use of SSM, which offers a novel approach to study subtle changes in hip morphology and this is the first time SSM has been applied to describe variation in hip shape in a cohort of adolescents. SSM offers a powerful approach which has been successfully applied to study variation in hip shape associated with the incidence (An et al., 2016; Castaño-Betancourt et al., 2013a) and progression of OA (Ahedi et al., 2017), as well as associations with hip fracture (Baker-LePain et al., 2011) in adult cohorts. However, a major drawback is that as each model is data driven, the HSMs generated are unique to the sample used, thus the results cannot be directly cross-compared with other studies. One of the key strengths of this study is the application of an adult reference SSM to adolescent hip DXA data at two different time points, which firstly enabled me to directly compare associations with HSMs between the time points in adolescents and compare these findings with results in adults. However, by using this approach I was unable to estimate the variance explained by each HSM after the adult reference SSM has been applied to the adolescent DXA images. As described previously, this makes the comparison between the magnitude of effect between adolescent and adult results difficult. Conventionally, the first HSM explains the most variance in the dataset with less variance explained by the subsequent modes. However, whether each mode explains the same percentage of variance in adolescent modes after the adult template has been applied remains to be established, but it is reasonable to assume that the top HSMs still capture the largest proportion of variance in the dataset and any future studies should attempt to estimate the variance explained in the model when applying reference template to another dataset.

Furthermore, whilst SSM quantifies the entire contour of the proximal femur, it is not specifically designed to evaluate cam deformities and therefore may not be sensitive enough or there may not be enough cases to detect cam deformities in this population. It has been suggested that exposure to high impact sports in adolescence, before the closure of growth plates, is the most significant risk factor for the development of cam deformity (Zadpoor, 2015) and other factors such as genetics, trauma and male sex are also thought to contribute (Chaudhry & Ayeni, 2014; Kuhns et al., 2015). Previous studies have also suggested that paediatric hip disorders, such as SCFE, predispose to the development of cam FAI (Giles et al., 2013; Pun et al., 2015) suggesting multifactorial influences on cam development. In order to study the development of cam deformity, specific measures for defining the degree of the deformity (alpha angle and femoral head-neck offset are amongst the most commonly used (Ehrmann et al., 2015; Morris et al., 2018)) along with hip images at an earlier age and data on risk factors are needed.

Another potential limitation of this study concerns the magnitude of effects observed and their clinical relevance. For example, unadjusted sex differences described in Chapter 3 ranged from -0.73 to 0.22 SDs, and from -0.6 to 0.49 SDs at the age of 14 and 18, respectively. These were of similar magnitude to differences previously reported between males and females from the MRC NSHD cohort (Pavlova et al., 2017). However, these studies relied on different SSM templates and the results cannot be directly compared.

It needs to be noted that while it is difficult to determine which aspects of hip shape are relevant for specific disease outcomes (such as fracture or hip OA), applying the same template used in this thesis to other disease cohorts will enable the identification of specific hip shapes associated with outcomes of interest (this has already been done in the MrOS cohort; unpublished results). In addition, future studies employing sub-regional models (as demonstrated in previous study by Baird et al. (Baird et al., 2018)) will help to further determine relevant aspects of shape related to disease outcomes. Potential methodological limitations of this research lie in the fact that the SSM was semi-automated, hence required some manual point placement and/or realignment. While this might result in inconsistency in point placement, repeatability and

reproducibility of this method were assessed and intra- and inter-repeatability scores were in good agreement (section 2.4.2, Chapter 2) and within the limit of previously reported values (Faber et al., 2017). Finally, this research was potentially limited by the use of 2D images to study complex, multidimensional shape which could potentially bias the results due to hip rotation. However, the DXA scans in ALSPAC were acquired according to standardized operating procedures whereby the feet are internally rotated, and the positioning is fixed, thus any rotation will represent normal variation. However, it needs to be noted that rotation in the adult population (from whom reference data was acquired and applied to the adolescent data), if present, could arise due to both, anatomical variation or reflect associations with a disease (i.e. the degree of hip rotation required for DXA positioning may be limited in patients with hip pain). In addition, the effect of subtle positioning errors should be accounted for during Procrustes analysis and positioning errors observed in ALSPAC had little influence on the overall model performance as previously described (Chapter 2, section 2.4.1). Finally, it needs to be noted that repeatability studies were only performed at one point in time (following the completion of marking up of TF 4 images). Although both intra- and inter-repeatability scores were in good agreement, if consistency of point placement changed over time this could result in lower precision of the estimated exposure-outcome associations (Kirkwood & Sterne, 2003).

Study design

ALSPAC represents a unique, rich resource of phenotypic, environmental and genetic data spanning across generations. It enabled me to study the development of hip shape in adolescents at two important time points, i.e. in peri-puberty and post-puberty and compare associations with sex and pubertal timing between these time points. In addition, I was able to compare BMD-hip shape associations in adolescents with that of ALSPAC mothers and the availability of genetic data enabled me to further examine whether underlying genetic pathways contribute to these associations. Although I was able to explore BMD-hip shape associations at multiple time points only data from adult females was available thus no comparisons were made with adult males. In addition, the observed sex differences in hip shape were not adjusted for pubertal stage. Consistent

with previous studies (Marshall & Tanner, 1969, 1970), females were considerably more advanced in puberty compared with males (as exemplified by earlier aPHV; 11.8 vs. 13.5 years in females and males, respectively; discussed previously in Chapter 4) and full adjustment for pubertal stage could not be done due to lack of pre-pubertal girls attending the TF 2 assessment clinic. It is therefore possible that the observed sex differences in hip shape at age 14 could partly reflect those in skeletal maturation.

The generalisability of the findings in this thesis are subject to certain limitations. The generalisability of the findings in this thesis are subject to certain limitations. Due to delay in image acquisition and given the time constraints, not all available hip DXA images collected as part of TF 2 clinic were aligned in Shape. During the course of image alignment it was decided that, of the remaining images, only those who had both, genetic data and DXA image acquired at TF 4 clinic will be aligned. It is possible that individuals with scans who were not aligned due to time constraints (1,255 (20.9%) images out of 5,991 singleton images) and those excluded due to issues with image quality were different to those who were included in the analysis. However, I was unable to explicitly compare those with DXA images who were included versus excluded from my analysis as the ALSPAC data team were unable to successfully link all IDs for excluded images, but my comparison of those included in my analysis versus the rest of ALSPAC showed that children attending TF 2 and TF 4 clinics were more likely to be white and of female sex compared with those who did not attend (as described previously (Chapter 2, section 2.6.2)). It needs to be noted that if excluded individuals differ from those included the estimates reported in this thesis (based on complete cases) may be biased. Furthermore, missing data reduces sample size and therefore precision. However, the risk of bias depends on the type of missing data (Sterne et al., 2009). For example, if the outcome (in this case hip shape) is missing at random and the probability of hip shape data being missing is unrelated to unobserved values of hip shape, given the exposure and factors of interest included in the model, the complete-case analysis is unlikely to be biased. Similarly, if the outcome or exposure are missing completely at random the complete case-analysis will be unbiased. However, if the outcome is missing not at random, i.e. the outcome is related to missingness given the other variables included in the model the estimates will be biased (Daniel et al., 2012).

In terms of TF 2 DXA data that were excluded due to time constraints, these were not excluded for any systematic reason and were therefore assumed to be missing completely at random and are thus unlikely to have substantially biased the estimates reported in this thesis. While loss to follow up is inevitable in longitudinal studies and the number of individuals diminishes with time, the numbers available for analysis were still fairly large considering other observational studies which used SSM to study in hip shape (Ahedi et al., 2017; Pavlova et al., 2017). It needs to be noted that while fairly large for observational epidemiology, the sample size for genetic analyses was relatively small. Nevertheless, I was able to perform the first GWAS of hip shape in adolescents and, despite the relatively small sample size in this context, I was able to detect associations with SNPs with potential relevance to bone biology. However, these results need to be confirmed as no replication in independent adolescent cohort of hip shape was performed. Another potential limitation of this study is the fact that approximately 98% of cohort participants were of white European descent. This may have implications for generalisability of these results and given the previously reported ethnic differences in hip morphology (Martel-Pelletier et al., 2016) these results are likely to be generalisable to European populations only.

Although the statistical evidence for a number of observational associations reported in this thesis was strong, these findings are limited by the use of a cross-sectional design, which makes it difficult to establish the direction of effect and causality. However, I used a MR approach (where possible) to overcome shortcomings of conventional epidemiology (predominantly confounding).

Causal analysis

One of the advantages of the ALSPAC dataset is the availability of genetic data which enables the exploration of causal inferences based on observational associations. In this thesis, I was able to follow up observational associations between BMD and hip shape in both ALSPAC adolescents and mothers using a MR approach. However, a number of limitations need to be highlighted. Firstly, the instrument for BMD relied on SNPs discovered in adult cohorts. While this might not be an appropriate instrument of choice

for the adolescent analyses, the GRS was strongly related to BMD at both adolescent time points and a previous study showed that BMD SNPs identified in adults were partly responsible for the rate of bone acquisition in adolescents (Warrington et al., 2015). On one hand, the inclusion of multiple variants in the GRS may improve the precision of an estimate, while on the other hand it may increase the potential for pleiotropy. It needs to be noted that the power of MR analyses in my thesis was low (as shown in Appendix 5, section 10.5.2) and although statistical methods to detect and account for pleiotropy can be used, such as MR-Egger regression and weighted median estimator (Yarmolinsky et al., 2018), these methods often suffer from low power and require large sample sizes (Bowden et al., 2016) and were therefore not performed given the already limited sample sizes in my analyses. In addition, inclusion of a subset of SNPs, with known function and relevance would be more appropriate when using MR in the same context as used in this thesis (as a means for identifying specific biological pathways underlying two related traits). Finally, MR is most commonly used to test for causal relationships between given exposure and an outcome, however, it is possible that assumption 3 (genetic variant used as an instrument must not directly influence the outcome, except through the exposure of interest; as previously outlined in Chapter 2, section 2.6.5) could be violated. Therefore, in my thesis, I used MR in a context of shared genetic influences.

8.5. Future research

A natural progression of this work is to analyse the associations between hip shape and OA-case status applying the same SSM template which was used throughout this thesis. This in turn will enable future research in adolescent studies to focus on those aspects of hip morphology more strongly related to pathology in later life. This has already been done in the MrOS cohort (Blank et al., 2005; Orwoll et al., 2005) which comprised over 4,000 participants with data on hip shape quantified on hip DXA scans at baseline and prevalent RHOA (defined as Croft score ≥ 2) obtained 4.6 years later. Both unadjusted and fully adjusted models (adjusted for site, age, height, weight and ethnicity) showed associations between modes 2, 3, 4 and 9 with RHOA (Faber et al., unpublished results),

with modes 3 and 4 showing the strongest associations. Interestingly, in a look up of known hip OA-associated variants in adolescent hip shape GWAS, rs10948172 (*SUPT3H - CDC5L*) was consistently associated with HSM3 and HSM4 at both time points (as described in Chapter 7, section 7.3.4).

Furthermore, the sample size in adolescent hip shape GWAS was small and therefore requires replication in independent adolescent cohorts in order to confirm the findings reported in this thesis. As previously suggested, the number of loci discovered in GWAS is directly proportional to sample size (Visscher et al., 2017), therefore increasing sample size by using paediatric and/or adolescent cohorts with suitable data (such as the Gothenburg Osteoporosis and Obesity Determinants (GOOD) Study which collected hip DXA scans in men aged 19 years (Lorentzon et al., 2005), The Western Australian Pregnancy Cohort (Raine) which collected hip DXA scans at age 20 years (Straker et al., 2017), the 1990 birth to twenty study in South Africa with repeated hip DXA scans between age 9 -15 years (Richter et al., 2007), or Tasmanian birth cohort with repeated hip DXA scans between ages 8 – 25 years (Y. Yang et al., 2018)) will increase power and may help to identify new variants associated with hip shape. These results can then be followed up using molecular approaches including in vitro studies (relying on cell culture techniques) or in vivo studies (knocking out genes in animal models) in order to identify causal variants underlying these associations.

Using a MR approach, I found evidence that shared genetic factors influence both BMD and hip shape and future studies should be repeated in a larger sample in order to see if these findings are replicated in an adequately powered study. While in Chapter 5 the BMD instrument was based on SNPs previously found to be associated with adult BMD, GRS based on these variants was strongly related to BMD in adolescents. Furthermore, the majority of BMD variants associated with BMD in children and adolescents are also associated with BMD in adults (Kemp et al., 2016). However, it is possible that bone related variants are strongly related to developmental processes occurring earlier in life as opposed to those that occur in adult life (Medina-Gomez et al., 2012). For example, recent GWAS meta-analysis identified age-specific genetic effects on BMD (i.e. rs754388 located within *RIN3* was associated with BMD in children less than 15 years old, but not in adults)(Medina-Gomez et al., 2018). Therefore, future analyses should consider using

GRSs based on pathway specific variants (i.e. those related to Wnt signalling or RANK-RANKL-OPG pathways) or variants specific to paediatric and adolescent BMD. As GWAS sample sizes increase, the discovery of genetic variants will also increase, providing better instruments for MR analysis. The other improvement that could be made to the genetic instrument would be inclusion of SNPs with known functional roles. Having good functional knowledge of SNPs included in GRS, larger sample size and better methods to address pleiotropy will provide valuable insights to our understanding of hip shape development and future pathology associated with hip shape.

My thesis explored the relationship between pubertal growth and hip shape. As described in Chapter 4, puberty is critical for hip shape development and further investigation of factors which may have an unfavourable impact on hip shape during this period is justified. This will enable stratification of individuals into those mostly at risk and provide opportunities for preventative measures early in life which might reduce the risk of fracture and/or OA development in later life. In addition, while the results presented in Chapter 4 most likely represent changes in hip shape associated with pubertal growth rather than the relationship with pubertal timing, further studies using a MR approach could be applied to determine the nature of pubertal timing on hip shape.

A number of studies suggest that cam deformities develop in response to vigorous PA (Palmer et al., 2018; Siebenrock et al., 2011) and changes in hip morphology around puberty are driven by mechanical stimuli, e.g. increase in body mass places greater strain on developing bone (van der Meulen et al., 1996). Data on PA including objective measures, as assessed by accelerometry, as well as questionnaire-based data has been collected in ALSPAC at several time points. It would be of particular interest to explore if associations between PA and modes found to be related to RHOA (i.e. HSM3 and HSM4 identified in MrOS) exist in order to better understand OA pathogenesis.

As described previously, SSM provides the means to quantify the entire outline of proximal femur as opposed to individual geometric measurements. However, for associations with modes describing variation in several components of hip shape (e.g. HSM1 which describes variation in femoral head and neck along with greater and lesser trochanters) it can be difficult to determine whether individual or combinations of these components are driving given associations. Therefore, further sub-regional models

based on a subset of points (focusing on the femoral head, superior joint space and region around anterolateral head-neck junction) can be constructed to distinguish influences acting on global femur morphology from those impacting specific components of shape (this approach has been used previously to explore the associations between known OA loci and hip shape as described by Baird et al. (Baird et al., 2018)). Using the same SSM template employed throughout this thesis, this approach could be first applied to clarify relationships between hip shape and OA in adults and secondly this could be followed up in adolescents to provide better understanding, and perhaps filtering of hip shape components which might be directly associated with OA and other exposures.

8.6. Conclusions

In conclusion, this is the first study to characterise hip shape development across adolescence as assessed by SSM in ALSPAC offspring at age 14 and 18. The findings in this thesis suggest that sexual dimorphism in hip shape can be discerned in early adolescence and consistent with previous studies, I found that puberty is a critical period for the development of hip shape, including aspects of shape previously found to be related to hip pathology in later life. I found strong observational evidence for the association between BMD and hip shape, which in part, could be explained by shared genetic factors underlying these traits. Further studies in a larger sample of adolescents are necessary to confirm these findings and identify specific pathways common to BMD variation and hip shape which will in turn help elucidate shared mechanisms related to OA and OP risk. Finally, genetic variants implicated in endochondral bone formation which were previously found to be associated with adult hip shape appear to influence hip shape in adolescents consistent with a contribution of longitudinal growth on hip shape. In addition, genetic variants associated with adolescent hip shape which did not replicate in adults may suggest distinct genetic influences on hip shape in adolescents vs. adults and warrants further investigation.

CHAPTER 9. REFERENCES

- Abbassi, V. (1998). Growth and normal puberty. *Pediatrics*, 102(Supplement 3), 507-511.
- Agricola, R., Heijboer, M. P., Ginai, A. Z., et al. (2014). A cam deformity is gradually acquired during skeletal maturation in adolescent and young male soccer players: a prospective study with minimum 2-year follow-up. *Am J Sports Med*, 42(4), 798-806.
- Agricola, R., Leyland, K. M., Bierma-Zeinstra, S. M., et al. (2015). Validation of statistical shape modelling to predict hip osteoarthritis in females: data from two prospective cohort studies (Cohort Hip and Cohort Knee and Chingford). *Rheumatology*, 54(11), 2033-2041.
- Ahedi, H. G., Aspden, R. M., Blizzard, L. C., et al. (2017). Hip shape as a predictor of osteoarthritis progression in a prospective population cohort. *Arthritis care & research*, 69(10), 1566-1573.
- Ahlborg, H. G., Nguyen, N. D., Nguyen, T. V., et al. (2005). Contribution of hip strength indices to hip fracture risk in elderly men and women. *J Bone Miner Res*, 20(10), 1820-1827.
- Aigner, T., Bertling, W., Stöss, H., et al. (1993). Independent expression of fibril-forming collagens I, II, and III in chondrocytes of human osteoarthritic cartilage. *J Clin Invest*, 91(3), 829-837.
- Alentorn-Geli, E., Samuelsson, K., Musahl, V., et al. (2017). The Association of Recreational and Competitive running with hip and knee osteoarthritis: a systematic review and meta-analysis. *J Orthop Sports Phys Ther*, 47(6), 373-390.
- Allen, K. D., & Golightly, Y. M. (2015). State of the evidence. *Curr Opin Rheumatol*, 27(3), 276-283.
- Alonso, C. G., Curiel, M. D., Carranza, F. H., et al. (2000). Femoral bone mineral density, neck-shaft angle and mean femoral neck width as predictors of hip fracture in men and women. *Osteoporos Int*, 11(8), 714-720.
- Altman, R., Alarcon, G., Appelrouth, D., et al. (1991). The American College of Rheumatology criteria for the classification and reporting of osteoarthritis of the hip. *Arthritis & Rheumatology*, 34(5), 505-514.
- Altman, R., Alarcon, G., Appelrouth, D., et al. (1990). The American College of Rheumatology criteria for the classification and reporting of osteoarthritis of the hand. *Arthritis & Rheumatology*, 33(11), 1601-1610.
- Altman, R., Asch, E., Bloch, D., et al. (1986). Development of criteria for the classification and reporting of osteoarthritis: classification of osteoarthritis of the knee. *Arthritis & Rheumatology*, 29(8), 1039-1049.
- An, H., Marron, J., Schwartz, T. A., et al. (2016). Novel statistical methodology reveals that hip shape is associated with incident radiographic hip osteoarthritis among African American women. *Osteoarthritis and Cartilage*, 24(4), 640-646.
- Antoniades, L., MacGregor, A. J., Matson, M., et al. (2000). A cotwin control study of the relationship between hip osteoarthritis and bone mineral density. *Arthritis & Rheumatology*, 43(7), 1450-1455.
- Archer, C. W., & Francis-West, P. (2003). The chondrocyte. *Int J Biochem Cell Biol*, 35(4), 401-404.

- Arden, N. K., Griffiths, G. O., Hart, D. J., et al. (1996). The association between osteoarthritis and osteoporotic fracture: the Chingford Study. *Br J Rheumatol*, 35(12), 1299-1304.
- Arden, N. K., & Nevitt, M. C. (2006). Osteoarthritis: epidemiology. *Best Pract Res Clin Rheumatol*, 20(1), 3-25.
- Arden, N. K., Nevitt, M. C., Lane, N. E., et al. (1999). Osteoarthritis and risk of falls, rates of bone loss, and osteoporotic fractures. *Arthritis & Rheumatology*, 42(7), 1378-1385.
- Aresti, N., Kassam, J., Nicholas, N., et al. (2016). Hip osteoarthritis. *BMJ*, 354.
- Arsuaga, J. L., & Carretero, J. M. (1994). Multivariate analysis of the sexual dimorphism of the hip bone in a modern human population and in early hominids. *Am J Phys Anthropol*, 93(2), 241-257.
- Baird, D. A., Gregory, J. S., Barr, R., et al. (2017). Adult hip shape is influenced by variation in genes involved in endochondral bone formation: findings from a genome-wide association study followed by meta-analysis. *J Bone Miner Res*, 32 (Suppl 1).
- Baird, D. A., Paternoster, L., Gregory, J. S., et al. (2018). Investigation of the relationship between susceptibility loci for hip osteoarthritis and DXA-derived hip shape in a population based cohort of peri-menopausal women. *Arthritis & Rheumatology*, 70(12), 1984-1993.
- Baird, J., Walker, I., Smith, C., et al. (2017). Review of methods for determining pubertal status and age of onset of puberty in cohort and longitudinal studies.
- Baker-LePain, J. C., & Lane, N. E. (2010). Relationship between joint shape and the development of osteoarthritis. [Review]. *Current opinion in rheumatology*, 22(5), 538-543.
- Baker-LePain, J. C., Luker, K. R., Lynch, J. A., et al. (2011). Active shape modeling of the hip in the prediction of incident hip fracture. *J Bone Miner Res*, 26(3), 468-474.
- Bass, S., Delmas, P. D., Pearce, G., et al. (1999). The differing tempo of growth in bone size, mass, and density in girls is region-specific. *J Clin Invest*, 104(6), 795-804.
- Beck, T. J. (2007). Extending DXA beyond bone mineral density: understanding hip structure analysis. *Curr Osteoporos Rep*, 5(2), 49-55.
- Bennell, K. L., Hunter, D. J., & Hinman, R. S. (2012). Management of osteoarthritis of the knee. *BMJ*, 345(2), e4934-4934.
- Berendsen, A. D., & Olsen, B. R. (2015). Bone development. *Bone*, 80, 14-18.
- Bergmann, A., Bolm-Audorff, U., Krone, D., et al. (2017). Occupational Strain as a Risk for Hip Osteoarthritis: A Systematic Review of Risk Assessment. *Deutsches Ärzteblatt International*, 114(35-36), 581.
- Betts, J. G., Young, K. A., Wise, J. A., et al. (2013). *Anatomy and Physiology*: OpenStax College
- Bijlsma, J. W. J., & Knahr, K. (2007). Strategies for the prevention and management of osteoarthritis of the hip and knee. *Best Pract Res Clin Rheumatol*, 21(1), 59-76.
- Birrell, F., Howells, N., & Porcheret, M. (2011). Osteoarthritis: pathogenesis and prospects for treatment. *Reports on the Rheumatic Diseases, Series 6 (Autumn 2011) Topical Reviews No 10*, 1-12.
- Blank, J. B., Cawthon, P. M., Carrion-Petersen, M. L., et al. (2005). Overview of recruitment for the osteoporotic fractures in men study (MrOS). *Contemp Clin Trials*, 26(5), 557-568.

- Boer, C. G., Broer, L., Schiphof, D., et al. (2018). Genetic exploration of osteoarthritis endophenotypes identifies new biological pathways in osteoarthritis. *Osteoarthritis and Cartilage*, 26, S30.
- Boese, C. K., Dargel, J., Oppermann, J., et al. (2016). The femoral neck-shaft angle on plain radiographs: a systematic review. *Skeletal Radiol.*, 45(1), 19-28.
- Bonewald, L. F. (2011). The amazing osteocyte. *J Bone Miner Res*, 26(2), 229-238.
- Bonjour, J.-P., & Chevalley, T. (2014). Pubertal timing, bone acquisition, and risk of fracture throughout life. *Endocr Rev*, 35(5), 820-847.
- Boskey, A. L., & Coleman, R. (2010). Aging and bone. *J Dent Res*, 89(12), 1333-1348.
- Bowden, J., Davey Smith, G., Haycock, P. C., et al. (2016). Consistent estimation in Mendelian randomization with some invalid instruments using a weighted median estimator. *Genet Epidemiol*, 40(4), 304-314.
- Boyd, A., Golding, J., Macleod, J., et al. (2012). Cohort profile: the 'children of the 90s'—the index offspring of the Avon Longitudinal Study of Parents and Children. *Int J Epidemiol*, 42(1), 111–127.
- Brandt, K. D., Dieppe, P., & Radin, E. L. (2009). Commentary: is it useful to subset “primary” osteoarthritis? A critique based on evidence regarding the etiopathogenesis of osteoarthritis. *Semin Arthritis Rheum*, 39(2), 81-95.
- Brennan, S. L., Stanford, T., Wluka, A. E., et al. (2012). Cross-sectional analysis of association between socioeconomic status and utilization of primary total hip joint replacements 2006–7: Australian Orthopaedic Association National Joint Replacement Registry. *BMC Musculoskelet Disord*, 13(1), 63.
- Buckwalter, J. A., Glimcher, M. J., Cooper, R. R., et al. (1996). Bone biology. I: Structure, blood supply, cells, matrix, and mineralization. *Instr Course Lect*, 45, 371-386.
- Bulik-Sullivan, B., Finucane, H. K., Anttila, V., et al. (2015). An atlas of genetic correlations across human diseases and traits. *Nat Genet*, 47(11), 1236-1241.
- Bulik-Sullivan, B. K., Loh, P.-R., Finucane, H. K., et al. (2015). LD Score regression distinguishes confounding from polygenicity in genome-wide association studies. *Nat Genet*, 47(3), 291.
- Bundak, R., Darendeliler, F., Gunoz, H., et al. (2007). Analysis of puberty and pubertal growth in healthy boys. *Eur J Pediatr*, 166(6), 595-600.
- Burgess, S., Butterworth, A. S., & Thompson, J. R. (2016a). Beyond Mendelian randomization: how to interpret evidence of shared genetic predictors. *J Clin Epidemiol*, 69, 208-216.
- Burgess, S., Davies, N. M., & Thompson, S. G. (2016b). Bias due to participant overlap in two-sample Mendelian randomization. *Genet Epidemiol*, 40(7), 597-608.
- Burgess, S., Scott, R. A., Timpson, N. J., et al. (2015). Using published data in Mendelian randomization: a blueprint for efficient identification of causal risk factors. *Eur J Epidemiol*, 30(7), 543-552.
- Burgess, S., & Thompson, S. G. (2015). *Mendelian randomization : methods for using genetic variants in causal estimation*: Boca Raton : CRC Press.
- Burr, D. B. (2004). Anatomy and physiology of the mineralized tissues: role in the pathogenesis of osteoarthritis. *Osteoarthritis and Cartilage*, 12, 20-30.
- Burr, D. B., & Gallant, M. A. (2012). Bone remodelling in osteoarthritis. *Nat Rev Rheumatol*, 8(11), 665.
- Callahan, L. F., Cleveland, R. J., Shreffler, J., et al. (2011). Associations of educational attainment, occupation and community poverty with knee osteoarthritis in the

- Johnston County (North Carolina) osteoarthritis project. *Arthritis Res Ther*, 13(5), R169.
- Callewaert, F., Sinnesael, M., Gielen, E., et al. (2010). Skeletal sexual dimorphism: relative contribution of sex steroids, GH-IGF1, and mechanical loading. *J Endocrinol*, 207(2), 127-134.
- Cameron, N. (2015). Can maturity indicators be used to estimate chronological age in children? *Ann Hum Biol*, 42(4), 302-307.
- Capulli, M., Paone, R., & Rucci, N. (2014). Osteoblast and osteocyte: games without frontiers. *Arch Biochem Biophys*, 561, 3-12.
- Castañeda, S., Roman-Blas, J. A., Largo, R., et al. (2012). Subchondral bone as a key target for osteoarthritis treatment. *Biochem Pharmacol*, 83(3), 315-323.
- Castaño-Betancourt, M. C., Cailotto, F., Kerkhof, H. J., et al. (2012). Genome-wide association and functional studies identify the DOT1L gene to be involved in cartilage thickness and hip osteoarthritis. *Proceedings of the National Academy of Sciences*, 109(21), 8218-8223.
- Castaño-Betancourt, M. C., Evans, D. S., Ramos, Y. F. M., et al. (2016). Novel genetic variants for cartilage thickness and hip osteoarthritis. *PLoS Genet*, 12(10), e1006260.
- Castaño-Betancourt, M. C., Rivadeneira, F., Bierma-Zeinstra, S., et al. (2013a). Bone parameters across different types of hip osteoarthritis and their relationship to osteoporotic fracture risk. *Arthritis & Rheumatology*, 65(3), 693-700.
- Castaño-Betancourt, M. C., van Meurs, J. B. J., Bierma-Zeinstra, S., et al. (2013b). The contribution of hip geometry to the prediction of hip osteoarthritis. *Osteoarthritis and Cartilage*, 21(10), 1530-1536.
- Chaganti, R. K., & Lane, N. E. (2011). Risk factors for incident osteoarthritis of the hip and knee. *Curr Rev Musculoskelet Med*, 4(3), 99-104.
- Chapman, K., Takahashi, A., Meulenbelt, I., et al. (2008). A meta-analysis of European and Asian cohorts reveals a global role of a functional SNP in the 5' UTR of GDF5 with osteoarthritis susceptibility. *Hum Mol Genet*, 17(10), 1497-1504.
- Charles, J. F., & Aliprantis, A. O. (2014). Osteoclasts: more than 'bone eaters'. *Trends Mol Med*, 20(8), 449-459.
- Chaudhry, H., & Ayeni, O. R. (2014). The etiology of femoroacetabular impingement: what we know and what we don't. *Sports Health*, 6(2), 157-161.
- Christensen, R., Bartels, E. M., Astrup, A., et al. (2007). Effect of weight reduction in obese patients diagnosed with knee osteoarthritis: a systematic review and meta-analysis. *Ann Rheum Dis*, 66(4), 433-439.
- Chung, C. Y., Park, M. S., Lee, K. M., et al. (2010). Hip osteoarthritis and risk factors in elderly Korean population. *Osteoarthritis and Cartilage*, 18(3), 312-316.
- Cibrián Uhalte, E., Wilkinson, J. M., Southam, L., et al. (2017). Pathways to understanding the genomic aetiology of osteoarthritis. *Hum Mol Genet*, 26(R2), R193-R201.
- Cleveland, R. J., Schwartz, T. A., Prizer, L. P., et al. (2013). Associations of educational attainment, occupation, and community poverty with hip osteoarthritis. *Arthritis care & research*, 65(6), 954-961.
- Cole, T. J., Donaldson, M. D., & Ben-Shlomo, Y. (2010). SITAR—a useful instrument for growth curve analysis. *Int J Epidemiol*, 39(6), 1558-1566.

- Coli, G. (2013). To prevent the osteoporosis playing in advance. *Clin Cases Miner Bone Metab*, 10(2), 83-85.
- Consensus Development Conference. (1993). Consensus Development Conference: diagnosis, prophylaxis, and treatment of osteoporosis. *Am J Med*, 94(6), 646-650.
- Cooper, C., Cook, P. L., Osmond, C., et al. (1991). Osteoarthritis of the hip and osteoporosis of the proximal femur. *Ann Rheum Dis*, 50(8), 540-542.
- Cooper, C., Inskip, H., Croft, P., et al. (1998). Individual risk factors for hip osteoarthritis: obesity, hip injury and physical activity. *Am J Epidemiol*, 147(6), 516-522.
- Cootes, T. F., Taylor, C. J., Cooper, D. H., et al. (1995). Active shape models-their training and application. *Computer vision and image understanding*, 61(1), 38-59.
- Cornelis, F. M. F., Luyten, F. P., & Lories, R. J. (2011). Functional effects of susceptibility genes in osteoarthritis. *Discov Med*, 12(63), 129-139.
- Cross, M., Smith, E., Hoy, D., et al. (2014). The global burden of hip and knee osteoarthritis: estimates from the global burden of disease 2010 study. *Ann Rheum Dis*, 73(7), 1323-1330.
- Cummings, S. R., Black, D. M., Nevitt, M. C., et al. (1990). Appendicular bone density and age predict hip fracture in women. *JAMA* 263(5), 665-668.
- Curtis, E. M., Moon, R. J., Dennison, E. M., et al. (2015). Recent advances in the pathogenesis and treatment of osteoporosis. *Clin Med*, 16(4), 360-364.
- Curtis, E. M., van der Velde, R., Moon, R. J., et al. (2016). Epidemiology of fractures in the United Kingdom 1988–2012: variation with age, sex, geography, ethnicity and socioeconomic status. *Bone*, 87, 19-26.
- Dai, Z., Niu, J., Zhang, Y., et al. (2017). Dietary intake of fibre and risk of knee osteoarthritis in two US prospective cohorts. *Ann Rheum Dis*, 76(8), 1411-1419.
- Daniel, R. M., Kenward, M. G., Cousens, S. N., et al. (2012). Using causal diagrams to guide analysis in missing data problems. *Stat Methods Med Res*, 21(3), 243-256.
- Davey Smith, G., & Ebrahim, S. (2003). 'Mendelian randomization': can genetic epidemiology contribute to understanding environmental determinants of disease? *Int J Epidemiol*, 32(1), 1-22.
- Davey Smith, G., & Hemani, G. (2014). Mendelian randomization: genetic anchors for causal inference in epidemiological studies. *Hum Mol Genet*, 23(R1), R89-R98.
- Day, F. R., Elks, C. E., Murray, A., et al. (2015). Puberty timing associated with diabetes, cardiovascular disease and also diverse health outcomes in men and women: the UK Biobank study. *Scientific reports*, 5, 11208.
- Demirjian, A., Buschang, P. H., Tanguay, R., et al. (1985). Interrelationships among measures of somatic, skeletal, dental, and sexual maturity. *Am J Orthod*, 88(5), 433-438.
- Dequeker, J., Aerssens, J., & Luyten, F. P. (2003). Osteoarthritis and osteoporosis: clinical and research evidence of inverse relationship. *Aging Clin Exp Res*, 15(5), 426-439.
- Dequeker, J., & Johnell, O. (1993). Osteoarthritis protects against femoral neck fracture: the MEDOS study experience. *Bone*, 14, 51-56.
- Dhiman, S., Maheshwari, S., & Verma, S. K. (2015). Assessment of maturity in orthodontics: A review. *Journal of Advanced Clinical & Research Insights*, 2(2), 100-103.
- Di Giovanni, I., Marcovecchio, M. L., Chiavaroli, V., et al. (2017). Being born large for gestational age is associated with earlier pubertal take-off and longer growth duration: a longitudinal study. *Acta Paediatrica*, 106(1), 61-66.

- Dieppe, P., & Kirwan, J. (1994). The localization of osteoarthritis. *Br J Rheumatol*, *33*(3), 201-203.
- Doherty, M., Courtney, P., Doherty, S., et al. (2008). Nonspherical Femoral Head Shape (Pistol Grip Deformity), Neck Shaft Angle, and Risk of Hip Osteoarthritis. *Arthritis and Rheumatism*, *58*(10), 3172-3182.
- Drake, R. L., Vogl, W., Mitchell, A. W. M., et al. (2015). *Gray's Anatomy for students*. In Gray's Anatomy.
- Dreier, R. (2010). Hypertrophic differentiation of chondrocytes in osteoarthritis: the developmental aspect of degenerative joint disorders. *Arthritis Res Ther*, *12*(5), 216.
- Driban, J. B., Hootman, J. M., Sitler, M. R., et al. (2017). Is participation in certain sports associated with knee osteoarthritis? A systematic review. *J Athl Train*, *52*(6), 497-506.
- Dryden, I. L., & Mardia, K. V. (1998). *Statistical shape analysis*. Chichester: Chichester : John Wiley.
- Duboeuf, F., Hans, D., Schott, A. M., et al. (1997). Different morphometric and densitometric parameters predict cervical and trochanteric hip fracture: the EPIDOS Study. *J Bone Miner Res*, *12*(11), 1895-1902.
- Ecker, T. M., Tannast, M., Puls, M., et al. (2007). Pathomorphologic alterations predict presence or absence of hip osteoarthrosis. *Clin Orthop Relat Res*, *465*, 46-52.
- Ehrmann, C., Roskopf, A. B., Pfirrmann, C. W., et al. (2015). Beyond the alpha angle: Alternative measurements for quantifying cam-type deformities in femoroacetabular impingement. *J Magn Reson Imaging*, *42*(4), 1024-1031.
- Engstrom, G., De Verdier, M. G., & Nilsson, P. M. (2009). Incidence of severe knee and hip osteoarthritis in relation to dietary intake of antioxidants beta-carotene, vitamin C, vitamin E and selenium: a population-based prospective cohort study. *Arthritis & Rheumatology*, *60*, s235-s236.
- Estrada, K., Stykarsdottir, U., Evangelou, E., et al. (2012). Genome-wide meta-analysis identifies 56 bone mineral density loci and reveals 14 loci associated with risk of fracture. *Nat Genet*, *44*(5), 491-501.
- Evans, C. H., Ghivizzani, S. C., & Robbins, P. D. (2018a). Arthritis gene therapy is becoming a reality. *Nat Rev Rheumatol*, *14*(7), 381-382.
- Evans, C. H., Ghivizzani, S. C., & Robbins, P. D. (2018b). Gene delivery to joints by intra-articular injection. *Hum Gene Ther*, *29*(1), 2-14.
- Evans, D. M., & Davey Smith, G. (2015). Mendelian randomization: new applications in the coming age of hypothesis-free causality. *Annu Rev Genomics Hum Genet*, *16*, 327-350.
- Faber, B. G., Baird, D., Gregson, C. L., et al. (2017). DXA-derived hip shape is related to osteoarthritis: findings from in the MrOS cohort. *Osteoarthritis and Cartilage*, *25*(12), 2031-2038.
- Fajar, J. K., Taufan, T., & Azharuddin, A. (2018). Hip geometry and femoral neck fractures: A meta-analysis. *J Orthop Translat*, *13*, 1-6.
- Felson, D. T., Zhang, Y., Anthony, J. M., et al. (1992). Weight loss reduces the risk for symptomatic knee osteoarthritis in women: the Framingham Study. *Ann Intern Med*, *116*(7), 535-539.

- Finkelstein, J. S., Klibanski, A., & Neer, R. M. (1996). A longitudinal evaluation of bone mineral density in adult men with histories of delayed puberty. *J Clin Endocrinol Metab*, 81(3), 1152-1155.
- Finkelstein, J. S., Neer, R. M., Biller, B. M., et al. (1992). Osteopenia in men with a history of delayed puberty. *New England Journal of Medicine*, 326(9), 600-604.
- Firestein, G. S., Budd, R., Gabriel, S. E., et al. (2016). *Kelley and Firestein's Textbook of Rheumatology E-Book*: Elsevier Health Sciences.
- Flores-Silva, R., Sasso, G. R. d. S., Sasso-Cerri, E., et al. (2015). Biology of bone tissue: structure, function, and factors that influence bone cells. *Biomed Res Int*, 2015, 17 pages.
- Flynn, T. W., & Soutas-Little, R. W. (1995). Patellofemoral joint compressive forces in forward and backward running. *J Orthop Sports Phys Ther*, 21(5), 277-282.
- Ford, C. A., Nowlan, N. C., Thomopoulos, S., et al. (2017). Effects of imbalanced muscle loading on hip joint development and maturation. *J Orthop Res*, 35(5), 1128-1136.
- Forwood, M. R., Bailey, D. A., Beck, T. J., et al. (2004). Sexual dimorphism of the femoral neck during the adolescent growth spurt: a structural analysis. *Bone*, 35(4), 973-981.
- Foss, M., & Byers, P. (1972). Bone density, osteoarthritis of the hip, and fracture of the upper end of the femur. *Ann Rheum Dis*, 31(4), 259-264.
- Fox, A. J. S., Bedi, A., & Rodeo, S. A. (2009). The basic science of articular cartilage: structure, composition, and function. *Sports Health*, 1(6), 461-468.
- Fraser, A., Macdonald-Wallis, C., Tilling, K., et al. (2013). Cohort profile: the Avon Longitudinal Study of Parents and Children: ALSPAC mothers cohort. *Int J Epidemiol*, 42(1), 97-110.
- Froberg, L., Christensen, F., Pedersen, N. W., et al. (2011). The need for total hip arthroplasty in Perthes disease: a long-term study. *Clin Orthop Relat Res*, 469(4), 1134-1140.
- Frost, H. M. (1987). Bone "mass" and the "mechanostat": a proposal. *Anat Rec*, 219(1), 1-9.
- Frysz, M., Howe, L. D., Tobias, J. H., et al. (2018). Using SITAR (SuperImposition by Translation and Rotation) to estimate age at peak height velocity in Avon Longitudinal Study of Parents and Children [version 1; peer review: 2 approved]. *Wellcome Open Res*, 3.
- Geusens, P. P., & van den Bergh, J. P. (2016). Osteoporosis and osteoarthritis: shared mechanisms and epidemiology. *Curr Opin Rheumatol*, 28(2), 97-103.
- Giambartolomei, C., Vukcevic, D., Schadt, E. E., et al. (2014). Bayesian test for colocalisation between pairs of genetic association studies using summary statistics. *PLoS Genet*, 10(5), e1004383.
- Gilbert, S. F. (2000). Osteogenesis: the development of bones. *Developmental biology*, 6.
- Giles, A. E., Corneman, N. A., Bhachu, S., et al. (2013). Shared morphology of slipped capital femoral epiphysis and femoroacetabular impingement in early-onset arthritis. *Orthopedics*, 36(11), e1365-e1370.
- Giorgi, M., Carriero, A., Shefelbine, S. J., et al. (2015). Effects of normal and abnormal loading conditions on morphogenesis of the prenatal hip joint: application to hip dysplasia. *J Biomech*, 48(12), 3390-3397.

- Glyn-Jones, S., Palmer, A. J. R., Agricola, R., et al. (2015). Osteoarthritis. *Lancet*, 386(9991), 376-387.
- Gnudi, S., Ripamonti, C., Gualtieri, G., et al. (1999). Geometry of proximal femur in the prediction of hip fracture in osteoporotic women. *Br J Radiol*, 72(860), 729-733.
- Goldring, M. B., & Otero, M. (2011). Inflammation in osteoarthritis. *Curr Opin Rheumatol*, 23(5), 471-478.
- Golightly, Y. M., Allen, K. D., Renner, J., et al. (2007). Relationship of limb length inequality with radiographic knee and hip osteoarthritis. *Osteoarthritis and Cartilage*, 15(7), 824-829.
- Gordon, C. M., Zemel, B. S., Wren, T. A. L., et al. (2017). The Determinants of Peak Bone Mass. *J Pediatr*, 180, 261-269.
- Gosvig, K. K., Jacobsen, S., Sonne-Holm, S., et al. (2010). Prevalence of malformations of the hip joint and their relationship to sex, groin pain, and risk of osteoarthritis: a population-based survey. *J Bone Joint Surg Am*, 92(5), 1162-1169.
- Granados, A., Gebremariam, A., & Lee, J. M. (2015). Relationship between timing of peak height velocity and pubertal staging in boys and girls. *J Clin Res Pediatr Endocrinol*, 7(3), 235-237.
- Gregory, J. S., & Aspden, R. M. (2008). Femoral geometry as a risk factor for osteoporotic hip fracture in men and women. *Med Eng Phys*, 30(10), 1275-1286.
- Gregory, J. S., Testi, D., Stewart, A., et al. (2004). A method for assessment of the shape of the proximal femur and its relationship to osteoporotic hip fracture. *Osteoporos Int*, 15(1), 5-11.
- Gregory, J. S., Waarsing, J. H., Day, J., et al. (2007). Early identification of radiographic osteoarthritis of the hip using an active shape model to quantify changes in bone morphometric features: can hip shape tell us anything about the progression of osteoarthritis? *Arthritis & Rheumatism*, 56(11), 3634-3643.
- Grundberg, E., Kwan, T., Ge, B., et al. (2009). Population genomics in a disease targeted primary cell model. *Genome Res*, 19(11), 1942-1952.
- Günther, K. P., Stürmer, T., Sauerland, S., et al. (1998). Prevalence of generalised osteoarthritis in patients with advanced hip and knee osteoarthritis: the Ulm Osteoarthritis Study. *Ann Rheum Dis*, 57(12), 717-723.
- Hackinger, S., Trajanoska, K., Styrkarsdottir, U., et al. (2017). Evaluation of shared genetic aetiology between osteoarthritis and bone mineral density identifies SMAD3 as a novel osteoarthritis risk locus. *Hum Mol Genet*, 26(19), 3850-3858.
- Hannan, M. T., Felson, D. T., Dawson-Hughes, B., et al. (2000). Risk factors for longitudinal bone loss in elderly men and women: the Framingham Osteoporosis Study. *J Bone Miner Res*, 15(4), 710-720.
- Hardcastle, S. A., Dieppe, P., Gregson, C. L., et al. (2015a). Individuals with high bone mass have an increased prevalence of radiographic knee osteoarthritis. *Bone*, 71, 171-179.
- Hardcastle, S. A., Dieppe, P., Gregson, C. L., et al. (2015b). Osteoarthritis and bone mineral density: are strong bones bad for joints? *Bonekey Rep*, 4, 624.
- Hardcastle, S. A., Dieppe, P., Gregson, C. L., et al. (2014). Prevalence of radiographic hip osteoarthritis is increased in high bone mass. *Osteoarthritis and Cartilage*, 22(8), 1120-1128.

- Hardcastle, S. A., Gregson, C. L., Deere, K. C., et al. (2013). High bone mass is associated with an increased prevalence of joint replacement: a case-control study. *Rheumatology*, *52*(6), 1042-1051.
- Harris-Hayes, M., & Royer, N. K. (2011). Relationship of acetabular dysplasia and femoroacetabular impingement to hip osteoarthritis: a focused review. *PM&R*, *3*(11), 1055-1067. e1051.
- Hartwig, F. P., Davies, N. M., Hemani, G., et al. (2016). Two-sample Mendelian randomization: avoiding the downsides of a powerful, widely applicable but potentially fallible technique. *Int J Epidemiol*, *45*(6), 1717-1726.
- Harvey, W. F., Yang, M., Cooke, T. D., et al. (2010). Association of leg-length inequality with knee osteoarthritis: a cohort study. *Ann Intern Med*, *152*(5), 287-295.
- Hatzikotoulas, K., Roposch, A., Shah, K., et al. (2017). The Genetic Epidemiology of Developmental Dysplasia of the Hip: A Genome-Wide Association Study Harnessing National Clinical Audit Data. *bioRxiv*, 154013.
- Hatzikotoulas, K., Roposch, A., Shah, K. M., et al. (2018). Genome-wide association study of developmental dysplasia of the hip identifies an association with GDF5. *Communications Biology*, *1*(1), 56.
- Haworth, S., Mitchell, R., Corbin, L., et al. (2018). Common genetic variants and health outcomes appear geographically structured in the UK Biobank sample: Old concerns returning and their implications. *bioRxiv*, 294876.
- Heijboer, M. P., Bierma-Zeinstra, S. M., Verhaar, J. A., et al. (2012). Cam impingement causes osteoarthritis of the hip: a nationwide prospective cohort study (CHECK). *Ann Rheum Dis*, *72*(6), 918-923.
- Heijboer, M. P., Ginai, A. Z., Roels, P., et al. (2014). A Cam Deformity Is Gradually Acquired During Skeletal Maturation in Adolescent and Young Male Soccer Players A Prospective Study With Minimum 2-Year Follow-up. *Am J Sports Med*, *42*(4), 798-806.
- Hemani, G., Zheng, J., Wade, K. H., et al. (2016). MR-Base: a platform for systematic causal inference across the phenome using billions of genetic associations. *bioRxiv*, 078972.
- Hind, K., Gannon, L., Whatley, E., et al. (2012). Sexual dimorphism of femoral neck cross-sectional bone geometry in athletes and non-athletes: a hip structural analysis study. *J Bone Miner Metab*, *30*(4), 454-460.
- Hirsch, R., Lethbridge-Cejku, M., Scott Jr, W. W., et al. (1996). Association of hand and knee osteoarthritis: evidence for a polyarticular disease subset. *Ann Rheum Dis*, *55*(1), 25-29.
- Ho-Pham, L. T., Nguyen, U. D., & Nguyen, T. V. (2014). Association between lean mass, fat mass, and bone mineral density: a meta-analysis. *J Clin Endocrinol Metab*, *99*(1), 30-38.
- Holroyd, C., Cooper, C., & Dennison, E. (2008). Epidemiology of osteoporosis. *Best Pract Res Clin Endocrinol Metab*, *22*(5), 671-685.
- Hosseini, S., Weis, M. A., Rai, J., et al. (2016). Evidence for enhanced collagen type III deposition focally in the territorial matrix of osteoarthritic hip articular cartilage. *Osteoarthritis and Cartilage*, *24*(6), 1029-1035.
- Hotelling, H. (1933). Analysis of a complex of statistical variables into principal components. *Journal of Educational Psychology*, *24*(6), 417-441.
doi:10.1037/h0071325

- HQIP. (2018). *National Joint Registry 15th Annual Report 2018* Retrieved from [accessed from <https://www.hqip.org.uk/resource/national-joint-registry-15th-annual-report-2018/#.XEC4IVWgKUK>, on 28/01/2019]
- Hsu, Y.-H., & Kiel, D. P. (2012). Genome-wide association studies of skeletal phenotypes: what we have learned and where we are headed. *J Clin Endocrinol Metab*, *97*(10), E1958-E1977.
- Huang, W., Chung, U.-i., Kronenberg, H. M., et al. (2001). The chondrogenic transcription factor Sox9 is a target of signaling by the parathyroid hormone-related peptide in the growth plate of endochondral bones. *Proceedings of the National Academy of Sciences*, *98*(1), 160-165.
- Hunter, D. J., Beavers, D. P., Eckstein, F., et al. (2015). The Intensive Diet and Exercise for Arthritis (IDEA) trial: 18-month radiographic and MRI outcomes. *Osteoarthritis and Cartilage*, *23*(7), 1090-1098.
- Hunter, D. J., & Felson, D. T. (2006). Clinical review: osteoarthritis. *BMJ*, *332*, 639-642.
- Im, G.-I., & Kim, M.-K. (2014). The relationship between osteoarthritis and osteoporosis. *J Bone Miner Metab*, *32*(2), 101-109.
- Ishidou, Y., Matsuyama, K., Sakuma, D., et al. (2017). Osteoarthritis of the hip joint in elderly patients is most commonly atrophic, with low parameters of acetabular dysplasia and possible involvement of osteoporosis. *Arch Osteoporos*, *12*(1), 30.
- Jiang, L., Tian, W., Wang, Y., et al. (2012). Body mass index and susceptibility to knee osteoarthritis: a systematic review and meta-analysis. *Joint Bone Spine*, *79*(3), 291-297.
- Johnson, V. L., & Hunter, D. J. (2014). The epidemiology of osteoarthritis. *Best Pract Res Clin Rheumatol*, *28*(1), 5-15.
- Jones, G., Nguyen, T., Sambrook, P. N., et al. (1995). Osteoarthritis, bone density, postural stability, and osteoporotic fractures: a population based study. *J Rheumatol*, *22*(5), 921-925.
- Jones, H. J., Stergiakouli, E., Tansey, K. E., et al. (2016). Phenotypic manifestation of genetic risk for schizophrenia during adolescence in the general population. *JAMA psychiatry*, *73*(3), 221-228.
- Jordan, J. M., Helmick, C. G., Renner, J. B., et al. (2007). Prevalence of knee symptoms and radiographic and symptomatic knee osteoarthritis in African Americans and Caucasians: the Johnston County Osteoarthritis Project. *J Rheumatol*, *34*(1), 172-180.
- Kandala, N.-B., Connock, M., Pulikottil-Jacob, R., et al. (2015). Setting benchmark revision rates for total hip replacement: analysis of registry evidence. *BMJ*, *350*, h756.
- Kanis, J. A., Johnell, O., Odén, A., et al. (2008). FRAX and the assessment of fracture probability in men and women from the UK. *Osteoporos Int*, *19*(4), 385-397.
- Kaplowitz, P. B. (2008). Link between body fat and the timing of puberty. *Pediatrics*, *121*(Supplement 3), S208-S217.
- Karlsson, K. M., Sernbo, I., Obrant, K. J., et al. (1996). Femoral neck geometry and radiographic signs of osteoporosis as predictors of hip fracture. *Bone*, *18*(4), 327-330.
- Kass, M., Witkin, A., & Terzopoulos, D. (1988). Snakes: Active contour models. *International journal of computer vision*, *1*(4), 321-331.

- Katz, J. N., Earp, B. E., & Gomoll, A. H. (2010). Surgical management of osteoarthritis. *Arthritis Care Res*, 62(9), 1220-1228.
- Kellgren, J. H., & Lawrence, J. S. (1957). Radiological assessment of osteo-arthrosis. *Ann Rheum Dis*, 16(4), 494-502.
- Kemp, J. P., Medina-Gomez, C., Tobias, J. H., et al. (2016). The case for genome-wide association studies of bone acquisition in paediatric and adolescent populations. *Bonekey Rep*, 5.
- Kemp, J. P., Morris, J. A., Medina-Gomez, C., et al. (2017). Identification of 153 new loci associated with heel bone mineral density and functional involvement of GPC6 in osteoporosis. *Nat Genet*, 49(10), 1468.
- Kerkhof, H. J., Meulenbelt, I., Akune, T., et al. (2011). Recommendations for standardization and phenotype definitions in genetic studies of osteoarthritis: the TREAT-OA consortium. *Osteoarthritis and Cartilage*, 19(3), 254-264.
- Khanna, V., & Beaulé, P. E. (2014). Defining structural abnormalities of the hip joint at risk of degeneration. *J Hip Preserv Surg*, 1(1), 12-20.
- Kim, C., Nevitt, M., Guermazi, A., et al. (2018). Leg Length Inequality and Hip Osteoarthritis in the Multicenter Osteoarthritis Study and the Osteoarthritis Initiative. *Arthritis & Rheumatology*, 70(10), 1572-1576.
- Kindblom, J. M., Lorentzon, M., Norjavaara, E., et al. (2006). Pubertal timing predicts previous fractures and BMD in young adult men: the GOOD study. *J Bone Miner Res*, 21(5), 790-795.
- Kirkwood, B. R., & Sterne, J. A. C. (2003). *Essential Medical Statistics*. 2nd ed. Malden, Mass: Blackwell Science.
- Kontulainen, S., Sievänen, H., Kannus, P., et al. (2003). Effect of long-term impact-loading on mass, size, and estimated strength of humerus and radius of female racquet-sports players: a peripheral quantitative computed tomography study between young and old starters and controls. *J Bone Miner Res*, 18(2), 352-359.
- Kraus, V. B., Blanco, F. J., Englund, M., et al. (2015). Call for standardized definitions of osteoarthritis and risk stratification for clinical trials and clinical use. *Osteoarthritis and Cartilage*, 23(8), 1233-1241.
- Kronenberg, H. M. (2003). Developmental regulation of the growth plate. *Nature*, 423(6937), 332-336.
- Kuh, D., Muthuri, S. G., Moore, A., et al. (2016). Pubertal timing and bone phenotype in early old age: findings from a British birth cohort study. *Int J Epidemiol*, 45(4), 1113-1124.
- Kuhns, B. D., Weber, A. E., Levy, D. M., et al. (2015). The natural history of femoroacetabular impingement. *Front Surg*, 2.
- Lam, S., & Amies, V. (2015). Case Report: Hip arthritis presenting as knee pain. *BMJ Case Rep*, 2015.
- Lam, W. L., Rawlins, J. M., Karoo, R. O. S., et al. (2010). Re-visiting Luck's classification: a histological analysis of Dupuytren's disease. *J Hand Surg Eur Vol*, 35(4), 312-317.
- Lane, N. E. (2006). Epidemiology, etiology, and diagnosis of osteoporosis. *Am J Obstet Gynecol*, 194(2), S3-S11.
- Lane, N. E., Corr, M., Baer, N., et al. (2017). Wnt Signaling in Osteoarthritis: a 2017 Update. *Current Treatment Options in Rheumatology*, 3(2), 101-111.
doi:10.1007/s40674-017-0065-z

- Lane, N. E., & Nevitt, M. (2002). Osteoarthritis, bone mass, and fractures: how are they related? *Arthritis & Rheumatology*, *46*(1), 1-4.
- Langdahl, B., Ferrari, S., & Dempster, D. W. (2016). Bone modeling and remodeling: potential as therapeutic targets for the treatment of osteoporosis. *Ther Adv Musculoskelet Dis*, *8*(6), 225-235.
- Lanyon, P., Muir, K., Doherty, S., et al. (2003). Age and sex differences in hip joint space among asymptomatic subjects without structural change: implications for epidemiologic studies. *Arthritis & Rheumatology*, *48*(4), 1041-1046.
- Lawlor, D. A. (2016). Commentary: Two-sample Mendelian randomization: opportunities and challenges. *Int J Epidemiol*, *45*(3), 908-915.
- Lawlor, D. A., Harbord, R. M., Sterne, J. A. C., et al. (2008). Mendelian randomization: using genes as instruments for making causal inferences in epidemiology. *Stat Med*, *27*(8), 1133-1163.
- Lawrence, J. S. (1969). Generalized osteoarthrosis in a population sample. *Am J Epidemiol*, *90*(5), 381-389.
- Ledingham, J., Dawson, S., Preston, B., et al. (1992). Radiographic patterns and associations of osteoarthritis of the hip. *Ann Rheum Dis*, *51*(10), 1111-1116.
- Lee, M. C., & Ebersson, C. P. (2006). Growth and development of the child's hip. *Orthop Clin North Am*, *37*(2), 119-132.
- Lekamwasam, S., Sumith, R., & Lenora, J. (2003). Effect of leg rotation on hip bone mineral density measurements. *J Clin Densitom*, *6*(4), 331-336.
- Leslie, W. D., Lix, L. M., Morin, S. N., et al. (2015). Hip axis length is a FRAX-and bone density-independent risk factor for hip fracture in women. *J Clin Endocrinol Metab*, *100*(5), 2063-2070.
- Li, G., Yin, J., Gao, J., et al. (2013). Subchondral bone in osteoarthritis: insight into risk factors and microstructural changes. *Arthritis Res Ther*, *15*(6), 223.
- Li, H., Zeng, C., Wei, J., et al. (2016). Associations between dietary antioxidants intake and radiographic knee osteoarthritis. *Clin Rheumatol*, *35*(6), 1585-1592.
- Lindner, C., Thiagarajah, S., Wilkinson, J. M., et al. (2015). Investigation of association between hip osteoarthritis susceptibility loci and radiographic proximal femur shape. *Arthritis & Rheumatology*, *67*(8), 2076-2084.
- Litwic, A., Edwards, M. H., Dennison, E. M., et al. (2013). Epidemiology and burden of osteoarthritis. *Br Med Bull*, *105*, 185-199.
- Lodewyckx, L., & Lories, R. J. (2009). WNT Signaling in osteoarthritis and osteoporosis: what is the biological significance for the clinician? *Curr Rheumatol Rep*, *11*(1), 23-30.
- Loeser, R. F. (2010). Age-related changes in the musculoskeletal system and the development of osteoarthritis. *Clin Geriatr Med*, *26*(3), 371-386.
- Looker, A. C., Beck, T. J., & Orwoll, E. (2001). Does body size account for gender differences in femur bone density and geometry? *J Bone Miner Res*, *16*(7), 1291-1299.
- Lorentzon, M., Mellström, D., & Ohlsson, C. (2005). Age of attainment of peak bone mass is site specific in Swedish men—the GOOD study. *J Bone Miner Res*, *20*(7), 1223-1227.
- Lories, R. J., & Luyten, F. P. (2011). The bone–cartilage unit in osteoarthritis. *Nat Rev Rheumatol*, *7*(1), 43.

- Loughlin, J., Mustafa, Z., Smith, A., et al. (2000). Linkage analysis of chromosome 2q in osteoarthritis. *Rheumatology*, 39(4), 377-381.
- Luo, Y., Ferdous, Z., & Leslie, W. (2011). A preliminary dual-energy X-ray absorptiometry-based finite element model for assessing osteoporotic hip fracture risk. *Proc Inst Mech Eng H*, 225(12), 1188-1195.
- Lynch, J. A., Parimi, N., Chaganti, R. K., et al. (2009). The association of proximal femoral shape and incident radiographic hip OA in elderly women. *Osteoarthritis and Cartilage*, 17(10), 1313-1318.
- Mackie, E. J., Ahmed, Y. A., Tatarczuch, L., et al. (2008). Endochondral ossification: how cartilage is converted into bone in the developing skeleton. *Int J Biochem Cell Biol*, 40(1), 46-62.
- Madry, H., van Dijk, C. N., & Mueller-Gerbl, M. (2010). The basic science of the subchondral bone. *Knee Surg Sports Traumatol Arthrosc*, 18(4), 419-433.
- Man, G. S., & Mologhianu, G. (2014). Osteoarthritis pathogenesis—a complex process that involves the entire joint. *J Med Life*, 7(1), 37-41.
- Marks Jr, S. C., & Popoff, S. N. (1988). Bone cell biology: the regulation of development, structure, and function in the skeleton. *Am J Anat*, 183(1), 1-44.
- Marshall, W. A., & Tanner, J. M. (1969). Variations in pattern of pubertal changes in girls. *Arch Dis Child*, 44(235), 291-303.
- Marshall, W. A., & Tanner, J. M. (1970). Variations in the pattern of pubertal changes in boys. *Arch Dis Child*, 45(239), 13-23.
- Martel-Pelletier, J., Barr, A. J., Cicuttini, F. M., et al. (2016). Osteoarthritis. *Nature Reviews Disease Primers*, 2, 16072. doi:10.1038/nrdp.2016.72
- Martel-Pelletier, J., Boileau, C., Pelletier, J.-P., et al. (2008). Cartilage in normal and osteoarthritis conditions. *Best Pract Res Clin Rheumatol*, 22(2), 351-384.
- Martin, T. J. (2016). Parathyroid hormone-related protein, its regulation of cartilage and bone development, and role in treating bone diseases. *Physiol Rev*, 96(3), 831-871.
- Mayhew, A. J., & Meyre, D. (2017). Assessing the heritability of complex traits in humans: methodological challenges and opportunities. *Curr Genomics*, 18(4), 332-340.
- McAlindon, T., LaValley, M., Schneider, E., et al. (2013). Effect of vitamin D supplementation on progression of knee pain and cartilage volume loss in patients with symptomatic osteoarthritis: a randomized controlled trial. *JAMA*, 309(2), 155-162.
- McCarthy, M. I., Abecasis, G. R., Cardon, L. R., et al. (2008). Genome-wide association studies for complex traits: consensus, uncertainty and challenges. *Nat Rev Genet*, 9(5), 356-369.
- McKiernan, F., & Washington, W. (2005). Effect of subtle positioning flaws on measured bone mineral density of the hip. *J Clin Densitom*, 8(3), 330-334.
- Medina-Gomez, C., Kemp, J. P., Estrada, K., et al. (2012). Meta-analysis of genome-wide scans for total body BMD in children and adults reveals allelic heterogeneity and age-specific effects at the WNT16 locus. *PLoS Genet*, 8(7), e1002718.
- Medina-Gomez, C., Kemp, J. P., Trajanoska, K., et al. (2018). Life-course genome-wide association study meta-analysis of total body BMD and assessment of age-specific effects. *Am J Hum Genet*, 102(1), 88-102.

- Michelotti, J., & Clark, J. (1999). Femoral neck length and hip fracture risk. *J Bone Miner Res*, *14*(10), 1714-1720.
- Moayyeri, A., Hammond, C. J., Hart, D. J., et al. (2013). The UK adult twin registry (TwinsUK Resource). *Twin Res Hum Genet*, *16*(1), 144-149.
- Moro, M., Van der Meulen, M. C. H., Kiratli, B. J., et al. (1996). Body mass is the primary determinant of midfemoral bone acquisition during adolescent growth. *Bone*, *19*(5), 519-526.
- Morris, W. Z., Li, R. T., Liu, R. W., et al. (2018). Origin of cam morphology in femoroacetabular impingement. *Am J Sports Med*, *46*(2), 478-486.
- Murphy, N. J., Eyles, J. P., & Hunter, D. J. (2016). Hip osteoarthritis: etiopathogenesis and implications for management. *Adv Ther*, *33*(11), 1921-1946.
- Murray, K. J., & Azari, M. F. (2015). Leg length discrepancy and osteoarthritis in the knee, hip and lumbar spine. *J Can Chiropr Assoc*, *59*(3), 226-237.
- Mustafa, Z., Chapman, K., Irlen, C., et al. (2000). Linkage analysis of candidate genes as susceptibility loci for osteoarthritis—suggestive linkage of COL9A1 to female hip osteoarthritis. *Rheumatology*, *39*(3), 299-306.
- Nelson, A. E. (2018). Osteoarthritis year in review 2017: clinical. *Osteoarthritis and Cartilage*, *26*(3), 319-325.
- Nelson, A. E., Smith, M. W., Golightly, Y. M., et al. (2014). “Generalized osteoarthritis”: a systematic review. *Semin Arthritis Rheum*, *43*(6), 713-720.
- Neogi, T., & Zhang, Y. (2013). Epidemiology of osteoarthritis. *Rheumatic Disease Clinics*, *39*(1), 1-19.
- Nevitt, M. C., Cummings, S. R., Lane, N. E., et al. (1996). Association of estrogen replacement therapy with the risk of osteoarthritis of the hip in elderly white women. *Arch Intern Med*, *156*(18), 2073-2080.
- Ng, M., Thakkar, D., Southam, L., et al. (2017). A genome-wide association study of Dupuytren disease reveals 17 additional variants implicated in fibrosis. *Am J Hum Genet*, *101*(3), 417-427.
- Nguyen, N. D., Eisman, J. A., Center, J. R., et al. (2007). Risk factors for fracture in nonosteoporotic men and women. *J Clin Endocrinol Metab*, *92*(3), 955-962.
- NICE. (2008). Osteoarthritis: the care and management of osteoarthritis in adults. *London: Royal College of Physicians*.
- Nieuwenhuijse, M., & Nelissen, R. (2015). Hip pain and radiographic signs of osteoarthritis. *BMJ*, *351*.
- Novais, E. N., Shefelbine, S. J., Kienle, K.-P., et al. (2018). Body Mass Index Affects Proximal Femoral but Not Acetabular Morphology in Adolescents Without Hip Pathology. *J Bone Joint Surg Am*, *100*(1), 66-74.
- Nüesch, E., Dieppe, P., Reichenbach, S., et al. (2011). All cause and disease specific mortality in patients with knee or hip osteoarthritis: population based cohort study. *BMJ*, *342*, d1165.
- OARSI. (2016). Osteoarthritis: A Serious Disease. *Osteoarthritis Research Society International*, pp. 1-103.
- Oliveria, S. A., Felson, D. T., Reed, J. I., et al. (1995). Incidence of symptomatic hand, hip, and knee osteoarthritis among patients in a health maintenance organization. *Arthritis & Rheumatology*, *38*(8), 1134-1141.
- Ombregt, L. (2013). *A System of Orthopaedic Medicine-E-Book*: Elsevier Health Sciences.

- Ornitz, D. M., & Marie, P. J. (2002). FGF signaling pathways in endochondral and intramembranous bone development and human genetic disease. *Genes Dev*, 16(12), 1446-1465.
- Orwoll, E., Blank, J. B., Barrett-Connor, E., et al. (2005). Design and baseline characteristics of the osteoporotic fractures in men (MrOS) study—a large observational study of the determinants of fracture in older men. *Contemp Clin Trials*, 26(5), 569-585.
- Ozer, B. H., Krueger, D., & Binkley, N. (2010). Slight abduction/adduction deviations in femur positioning for dual-energy X-ray absorptiometry are inconsequential. *J Clin Densitom*, 13(1), 10-17.
- Paans, N., van den Akker-Scheek, I., Dilling, R. G., et al. (2013). Effect of exercise and weight loss in people who have hip osteoarthritis and are overweight or obese: a prospective cohort study. *Phys Ther*, 93(2), 137-146.
- Packer, J. D., & Safran, M. R. (2015). The etiology of primary femoroacetabular impingement: genetics or acquired deformity? *J Hip Preserv Surg*, 2(3), 249-257.
- Palazzo, C., Nguyen, C., Lefevre-Colau, M.-M., et al. (2016). Risk factors and burden of osteoarthritis. *Ann Phys Rehabil Med*, 59(3), 134-138.
- Palmer, A., Fernquest, S., Gimpel, M., et al. (2018). Physical activity during adolescence and the development of cam morphology: a cross-sectional cohort study of 210 individuals. *Br J Sports Med*, 52(9), 601-610.
- Panoutsopoulou, K., Thiagarajah, S., Zengini, E., et al. (2016). Radiographic endophenotyping in hip osteoarthritis improves the precision of genetic association analysis. *Ann Rheum Dis*, 76(7), 1199-1206.
- Panoutsopoulou, K., & Zeggini, E. (2013). Advances in osteoarthritis genetics. *J Med Genet*, 50(11), 715-724.
- Pasco, J. A., Panahi, S., Henry, M. J., et al. (1999). Femoral neck dimensions are unlikely to be associated with age at menarche. *Osteoporos Int*, 9(6), 557-559.
- Pavlova, A. V., Saunders, F. R., Muthuri, S. G., et al. (2017). Statistical shape modelling of hip and lumbar spine morphology and their relationship in the MRC National Survey of Health and Development. *J Anat*, 231(2), 248-259.
- Pereira, D., Peleteiro, B., Araujo, J., et al. (2011). The effect of osteoarthritis definition on prevalence and incidence estimates: a systematic review. *Osteoarthritis and Cartilage*, 19(11), 1270-1285.
- Pers, T. H., Timshel, P., & Hirschhorn, J. N. (2014). SNPsnap: a Web-based tool for identification and annotation of matched SNPs. *Bioinformatics*, 31(3), 418-420.
- Pollard, T. C. B., Batra, R. N., Judge, A., et al. (2013). The hereditary predisposition to hip osteoarthritis and its association with abnormal joint morphology. *Osteoarthritis and Cartilage*, 21(2), 314-321.
- Poole, A. R. (2010, 08/03/2011). Chapter 3: The Normal Synovial Joint. *OARSI online Primer*. Yves Henrotin, David Hunter, Hiroshi Kawaguchi. Retrieved from <http://primer.oarsi.org/content/chapter-3-normal-synovial-joint>
- Poole, K. E. S., & Compston, J. E. (2006). Osteoporosis and its management. *BMJ*, 333(7581), 1251-1256.
- Poole, K. E. S., Treece, G. M., Mayhew, P. M., et al. (2012). Cortical thickness mapping to identify focal osteoporosis in patients with hip fracture. *PLoS ONE [Electronic Resource]*, 7(6), e38466.

- Prieto-Alhambra, D., Judge, A., Javaid, M. K., et al. (2014). Incidence and risk factors for clinically diagnosed knee, hip and hand osteoarthritis: influences of age, gender and osteoarthritis affecting other joints. *Ann Rheum Dis*, *73*(9), 1659-1664.
- Prieto-Alhambra, D., Nogues, X., Javaid, M. K., et al. (2013). An increased rate of falling leads to a rise in fracture risk in postmenopausal women with self-reported osteoarthritis: a prospective multinational cohort study (GLOW). *Ann Rheum Dis*, *72*(6), 911-917.
- Pujol, A., Rissech, C., Ventura, J., et al. (2014). Ontogeny of the female femur: geometric morphometric analysis applied on current living individuals of a Spanish population. *J Anat*, *225*(3), 346-357.
- Pujol, A., Rissech, C., Ventura, J., et al. (2016). Ontogeny of the male femur: Geometric morphometric analysis applied to a contemporary Spanish population. *Am J Phys Anthropol*, *159*(1), 146-163.
- Pun, S. (2016). Hip dysplasia in the young adult caused by residual childhood and adolescent-onset dysplasia. *Curr Rev Musculoskelet Med*, *9*(4), 427-434.
- Pun, S., Kumar, D., & Lane, N. E. (2015). Femoroacetabular impingement. *Arthritis Rheumatol*, *67*(1), 17-27.
- Purcell, S., Neale, B., Todd-Brown, K., et al. (2007). PLINK: a tool set for whole-genome association and population-based linkage analyses. *Am J Hum Genet*, *81*(3), 559-575.
- Quasnichka, H. L., Anderson-MacKenzie, J. M., & Bailey, A. J. (2006). Subchondral bone and ligament changes precede cartilage degradation in guinea pig osteoarthritis. *Biorheology*, *43*(3, 4), 389-397.
- Racunica, T. L., Teichtahl, A. J., Wang, Y., et al. (2007). Effect of physical activity on articular knee joint structures in community-based adults. *Arthritis care & research*, *57*(7), 1261-1268.
- Ralphs, J. R., & Benjamin, M. (1994). The joint capsule: structure, composition, ageing and disease. *J Anat*, *184*(Pt 3), 503-509.
- Rauch, F. (2005). Bone growth in length and width: the Yin and Yang of bone stability. *J Musculoskelet Neuronal Interact*, *5*(3), 194-201.
- Resnick, D. (1976). The 'tilt deformity' of the femoral head in osteoarthritis of the hip: a poor indicator of previous epiphysiolysis. *Clin Radiol*, *27*(3), 355-363.
- Reyes, C., Leyland, K. M., Peat, G., et al. (2016). Association Between Overweight and Obesity and Risk of Clinically Diagnosed Knee, Hip, and Hand Osteoarthritis: A Population-Based Cohort Study. *Arthritis & Rheumatology*, *68*(8), 1869-1875.
- Richter, L., Norris, S., Pettifor, J., et al. (2007). Cohort profile: Mandela's children: the 1990 Birth to Twenty study in South Africa. *Int J Epidemiol*, *36*(3), 504-511.
- Rickham, P. P. (1964). Human experimentation. Code of Ethics of the World Medical Association. Declaration of Helsinki. *BMJ*, *2*(5402), 177.
- Rizzoli, R., & Bonjour, J.-P. (1999). Determinants of peak bone mass and mechanisms of bone loss. *Osteoporos Int*, *9*(8), S17-S23.
- Roberts, S. J., van Gastel, N., Carmeliet, G., et al. (2015). Uncovering the periosteum for skeletal regeneration: the stem cell that lies beneath. *Bone*, *70*, 10-18.
- Rogol, A. D., Roemmich, J. N., & Clark, P. A. (2002). Growth at puberty. *J Adolesc Health*, *31*(6), 192-200.
- Rosen, V. (2013). Mechanisms of endochondral ossification in the pathogenesis of OA. *Osteoarthritis and Cartilage*, *21*, S1.

- Salter, D. M., Su, S.-L., & Lee, H.-S. (2014). Epidemiology and genetics of osteoarthritis. *Journal of Medical Sciences*, 34(6), 252.
- Sayers, A., Marcus, M., Rubin, C., et al. (2010). Investigation of sex differences in hip structure in peripubertal children. *J Clin Endocrinol Metab*, 95(8), 3876-3883.
- Schuiling, K. D., Robinia, K., & Nye, R. (2011). Osteoporosis update. *J Midwifery Womens Health*, 56(6), 615-627.
- Schwarz, G. (1978). Estimating the dimension of a model. *The annals of statistics*, 6(2), 461-464.
- Seeman, E. (1999). The structural basis of bone fragility in men. *Bone*, 25(1), 143-147.
- Seeman, E. (2001). Sexual dimorphism in skeletal size, density, and strength. *J Clin Endocrinol Metab*, 86(10), 4576-4584.
- Seeman, E., Duan, Y., Fong, C., et al. (2001). Fracture site-specific deficits in bone size and volumetric density in men with spine or hip fractures. *J Bone Miner Res*, 16(1), 120-127.
- Šešelj, M., Nahhas, R. W., Sherwood, R. J., et al. (2012). The influence of age at menarche on cross-sectional geometry of bone in young adulthood. *Bone*, 51(1), 38-45.
- Sherar, L. B., Cumming, S. P., Eisenmann, J. C., et al. (2010). Adolescent biological maturity and physical activity: biology meets behavior. *Pediatr Exerc Sci*, 22(3), 332-349.
- Shim, K. S. (2015). Pubertal growth and epiphyseal fusion. *Ann Pediatr Endocrinol Metab*, 20(1), 8-12.
- Siebenrock, K. A., Ferner, F., Noble, P. C., et al. (2011). The cam-type deformity of the proximal femur arises in childhood in response to vigorous sporting activity. *Clin Orthop Relat Res*, 469(11), 3229-3240.
- Sivakumaran, S., Agakov, F., Theodoratou, E., et al. (2011). Abundant pleiotropy in human complex diseases and traits. *Am J Hum Genet*, 89(5), 607-618.
- Solomon, L. (1976). Patterns of osteoarthritis of the hip. *J Bone Joint Surg Br*, 58(2), 176-183.
- Spector, T. D., & MacGregor, A. J. (2004). Risk factors for osteoarthritis: genetics. *Osteoarthritis and Cartilage*, 12, 39-44.
- Spector, T. D., & Williams, F. M. (2006). The UK adult twin registry (TwinsUK). *Twin Res Hum Genet*, 9(6), 899-906.
- Staiger, D., & Stock, J. (1997). Instrumental Variables Regression with Weak Instruments. *Econometrica*, 65(3), 557-586.
- Stecher, R. M. (1941). Heberden's nodes: heredity in hypertrophic arthritis of the finger joints. *Am J Med Sci*, 201, 801-809.
- Stegmann, M. B., & Gomez, D. D. (2002). A brief introduction to statistical shape analysis. *Informatics and mathematical modelling, Technical University of Denmark, DTU*, 15(11).
- Sterne, J. A. C., White, I. R., Carlin, J. B., et al. (2009). Multiple imputation for missing data in epidemiological and clinical research: potential and pitfalls. *BMJ*, 338, b2393.
- Straker, L., Mountain, J., Jacques, A., et al. (2017). Cohort Profile: The Western Australian Pregnancy Cohort (Raine) Study—Generation 2. *Int J Epidemiol*, 46(5), 1384-1385j.

- Sun, M. M.-G., Beier, F., & Pest, M. A. (2017). Recent developments in emerging therapeutic targets of osteoarthritis. *Curr Opin Rheumatol*, 29(1), 96-102.
- Sun, X., Yu, W., & Hu, C. (2014). Genetics of type 2 diabetes: insights into the pathogenesis and its clinical application. *Biomed Res Int*, 2014, 15 pages.
- Suttorp, M. M., Siegerink, B., Jager, K. J., et al. (2014). Graphical presentation of confounding in directed acyclic graphs. *Nephrol Dial Transplant*, 30(9), 1418-1423.
- Swerdlow, D. I., Kuchenbaecker, K. B., Shah, S., et al. (2016). Selecting instruments for Mendelian randomization in the wake of genome-wide association studies. *Int J Epidemiol*, 45(5), 1600-1616.
- Symmons, D., Mathers, C., & Pflieger, B. (2003). Global burden of osteoarthritis in the year 2000. *World Health Organization*.
- Tamer, T. M. (2013). Hyaluronan and synovial joint: function, distribution and healing. *Interdiscip Toxicol*, 6(3), 111-125.
- Taylor, A. E., Jones, H. J., Sallis, H., et al. (2018). Exploring the association of genetic factors with participation in the Avon Longitudinal Study of Parents and Children. *Int J Epidemiol*, 47(4), 1207-1216.
- Timpson, N. J., Sayers, A., Davey-Smith, G., et al. (2009). How does body fat influence bone mass in childhood? A Mendelian randomization approach. *J Bone Miner Res*, 24(3), 522-533.
- Townley, W. A., Baker, R., Sheppard, N., et al. (2006). Dupuytren's contracture unfolded. *BMJ*, 332(7538), 397-400.
- Tran, B. H., Center, J. R., & Nguyen, T. V. (2013). Translational genetics of osteoporosis: from population association to individualized prognosis. *Primer on the Metabolic Bone Diseases and Disorders of Mineral Metabolism*, 376-388.
- Valdes, A. M., & Spector, T. D. (2010). The genetic epidemiology of osteoarthritis. *Curr Opin Rheumatol*, 22(2), 139-143.
- Van Der Kraan, P. M., Berenbaum, F., Blanco, F. J., et al. (2016). Translation of clinical problems in osteoarthritis into pathophysiological research goals. *RMD open*, 2(1), e000224.
- van der Meulen, M. C. H., Ashford Jr, M. W., Kiratli, B. J., et al. (1996). Determinants of femoral geometry and structure during adolescent growth. *J Orthop Res*, 14(1), 22-29.
- Vestergaard, P., Rejnmark, L., & Mosekilde, L. (2009). Osteoarthritis and risk of fractures. *Calcif Tissue Int*, 84(4), 249-256.
- Vigdorichik, J. M., Nepple, J. J., Eftekhary, N., et al. (2017). What is the association of elite sporting activities with the development of hip osteoarthritis? *Am J Sports Med*, 45(4), 961-964.
- Vina, E. R., & Kwok, C. K. (2018). Epidemiology of osteoarthritis: literature update. *Curr Opin Rheumatol*, 30(2), 160-167.
- Visscher, P. M., Wray, N. R., Zhang, Q., et al. (2017). 10 years of GWAS discovery: biology, function, and translation. *Am J Hum Genet*, 101(1), 5-22.
- Waarsing, J. H., Rozendaal, R. M., Verhaar, J. A., et al. (2010). A statistical model of shape and density of the proximal femur in relation to radiological and clinical OA of the hip. *Osteoarthritis and Cartilage*, 18(6), 787-794.
- Walker, J. M. (1991). Musculoskeletal development: a review. *Phys Ther*, 71(12), 878-889.

- Wang, M. C., Aguirre, M., Bhudhikanok, G. S., et al. (1997). Bone mass and hip axis length in healthy Asian, black, Hispanic, and white American youths. *J Bone Miner Res*, *12*(11), 1922-1935.
- Wang, Q., Chen, D., Cheng, S. M., et al. (2015). Growth and aging of proximal femoral bone: a study with women spanning three generations. *J Bone Miner Res*, *30*(3), 528-534.
- Wang, Y., Simpson, J. A., Wluka, A. E., et al. (2010). Is physical activity a risk factor for primary knee or hip replacement due to osteoarthritis? A prospective cohort study. *J Rheumatol*, *38*(2), 350-357.
- Warner, S. C., & Valdes, A. M. (2016). The genetics of osteoarthritis: A review. *Journal of Functional Morphology and Kinesiology*, *1*(1), 140-153.
- Warrington, N. M., Kemp, J. P., Tilling, K., et al. (2015). Genetic variants in adult bone mineral density and fracture risk genes are associated with the rate of bone mineral density acquisition in adolescence. *Hum Mol Genet*, *24*(14), 4158-4166.
- Wegener, V., Jorysz, G., Arnoldi, A., et al. (2017). Normal radiological unossified hip joint space and femoral head size development during growth in 675 children and adolescents. *Clinical Anatomy*, *30*(2), 267-275.
- Wehby, G. L., Ohsfeldt, R. L., & Murray, J. C. (2008). 'Mendelian randomization' equals instrumental variable analysis with genetic instruments. *Stat Med*, *27*(15), 2745-2749.
- Weinstein, S. L., & Dolan, L. A. (2018). Proximal femoral growth disturbance in developmental dysplasia of the hip: what do we know? *J Child Orthop*, *12*(4), 331-341.
- Wells, J. C. K., & Cole, T. J. (2002). Adjustment of fat-free mass and fat mass for height in children aged 8 y. *Int J Obes Relat Metab Disord*, *26*(7), 947-952.
- White, T. D. (2005). *The human bone manual* Tim D. White, Pieter A. Folkens. Burlington, Mass. London: Burlington, Mass. London : Elsevier.
- WHO, S. G. (2003). *Prevention and management of osteoporosis: report of a WHO scientific group*: World Health Organization.
- Widhalm, H. K., Seemann, R., Hamboeck, M., et al. (2016). Osteoarthritis in morbidly obese children and adolescents, an age-matched controlled study. *Knee Surg Sports Traumatol Arthrosc*, *24*(3), 644-652.
- Williams, F. M. K., & Spector, T. D. (2006). Recent advances in the genetics of osteoporosis. *J Musculoskelet Neuronal Interact*, *6*(1), 27-35.
- Wluka, A. E., Cicuttini, F. M., & Spector, T. D. (2000). Menopause, oestrogens and arthritis. *Maturitas*, *35*(3), 183-199.
- Wolf, A. D., & Pflieger, B. (2003). Burden of major musculoskeletal conditions. *Bulletin of the World Health Organization*, *81*(9), 646-656.
- Wu, C. W., Morrell, M. R., Heinze, E., et al. (2005). Validation of American College of Rheumatology classification criteria for knee osteoarthritis using arthroscopically defined cartilage damage scores. *Semin Arthritis Rheum*, *35*(3), 197-201.
- Yang, J., Lee, S. H., Goddard, M. E., et al. (2011). GCTA: a tool for genome-wide complex trait analysis. *Am J Hum Genet*, *88*(1), 76-82.
- Yang, Y., Wu, F., Winzenberg, T., et al. (2018). Tracking of Areal Bone Mineral Density From Age Eight to Young Adulthood and Factors Associated With Deviation From Tracking: A 17-Year Prospective Cohort Study. *J Bone Miner Res*, *33*(5), 832-839.

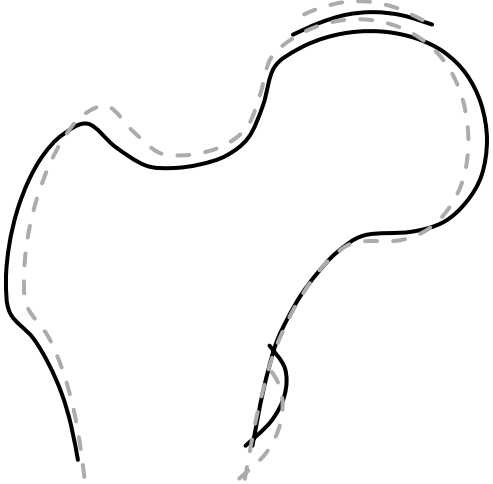
- Yarmolinsky, J., Wade, K. H., Richmond, R. C., et al. (2018). Causal inference in cancer epidemiology: what is the role of Mendelian randomization? *Cancer Epidemiol Biomarkers Prev*, 27(9), 995-1010.
- Yerges-Armstrong, L. M., Nevitt, M. C., Yau, M. S., et al. (2014). Genetic association analysis of radiographic hip osteoarthritis with established loci for bone mineral density: data from the osteoarthritis initiative. *Osteoarthritis and Cartilage*, 22, S234.
- Yerges-Armstrong, L. M., Yau, M. S., Liu, Y., et al. (2014). Association Analysis of BMD-associated SNPs with Knee Osteoarthritis. *J Bone Miner Res*, 29(6), 1373-1379.
- Yoshida, K., Barr, R. J., Galea-Soler, S., et al. (2015). Reproducibility and diagnostic accuracy of Kellgren-Lawrence grading for osteoarthritis using radiographs and dual-energy X-ray absorptiometry images. *J Clin Densitom*, 18(2), 239-244.
- Zadpoor, A. A. (2015). Etiology of femoroacetabular impingement in athletes: a review of recent findings. *Sports Med*, 45(8), 1097-1106.
- Zeggini, E., Panoutsopoulou, K., Southam, L., et al. (2012). Identification of new susceptibility loci for osteoarthritis (arcOGEN): a genome-wide association study. *Lancet*, 380(9844), 815-823.
- Zengini, E., Finan, C., & Wilkinson, J. M. (2016). The genetic epidemiological landscape of hip and knee osteoarthritis: where are we now and where are we going? *J Rheumatol*, 43(2), 260-266.
- Zengini, E., Hatzikotoulas, K., Tachmazidou, I., et al. (2018). Genome-wide analyses using UK Biobank data provide insights into the genetic architecture of osteoarthritis. *Nat Genet*, 50(4), 549.
- Zhang, F., Tan, L.-J., Lei, S.-F., et al. (2010). The differences of femoral neck geometric parameters: effects of age, gender and race. *Osteoporos Int*, 21(7), 1205-1214.
- Zhang, W., Moskowitz, R. W., Nuki, G., et al. (2008). OARSI recommendations for the management of hip and knee osteoarthritis, Part II: OARSI evidence-based, expert consensus guidelines. *Osteoarthritis and Cartilage*, 16(2), 137-162.
- Zheng, J., Erzurumluoglu, A. M., Elsworth, B. L., et al. (2017). LD Hub: a centralized database and web interface to perform LD score regression that maximizes the potential of summary level GWAS data for SNP heritability and genetic correlation analysis. *Bioinformatics*, 33(2), 272-279.
- Zmuda, J. M., Sheu, Y. T., & Moffett, S. P. (2006). The search for human osteoporosis genes. *J Musculoskelet Neuronal Interact*, 6(1), 3-15.

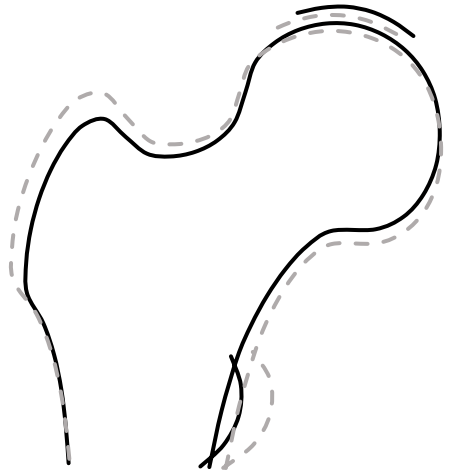
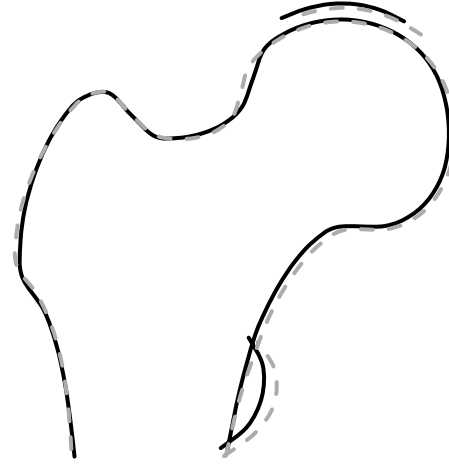
CHAPTER 10. APPENDICES

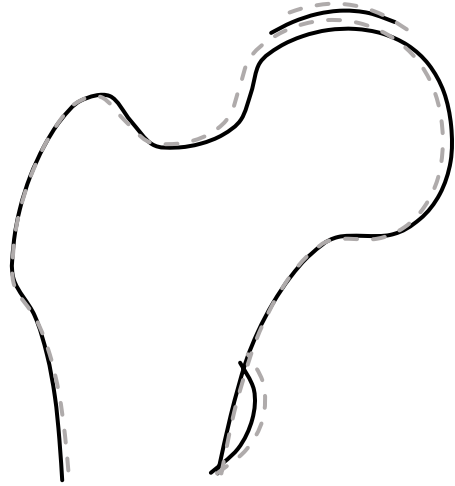
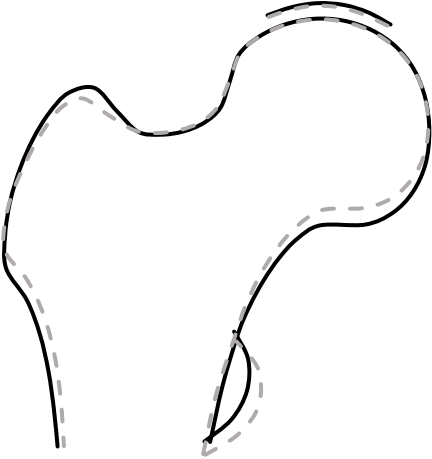
10.1. Appendix 1

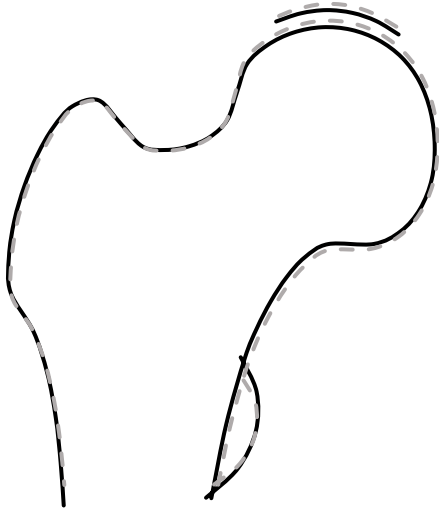
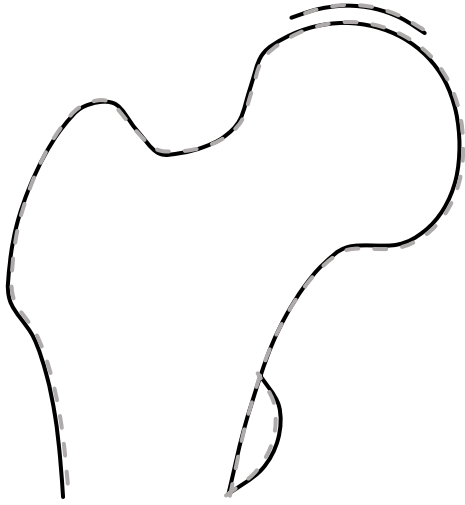
Appendix for chapter 2

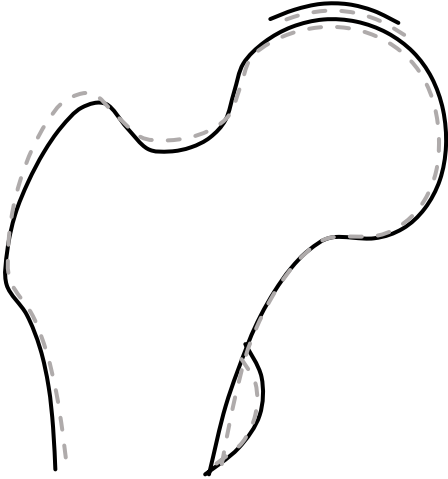
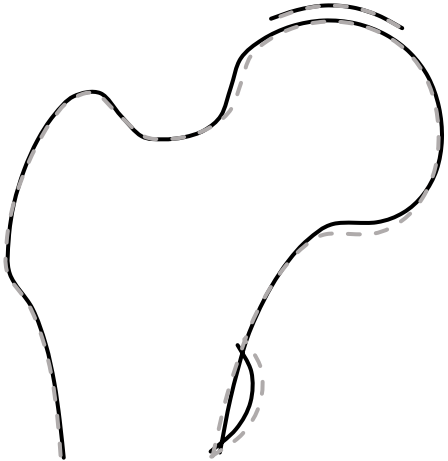
Supplementary Table 10.1.1; Variation described by the top ten modes based on adult reference SSM

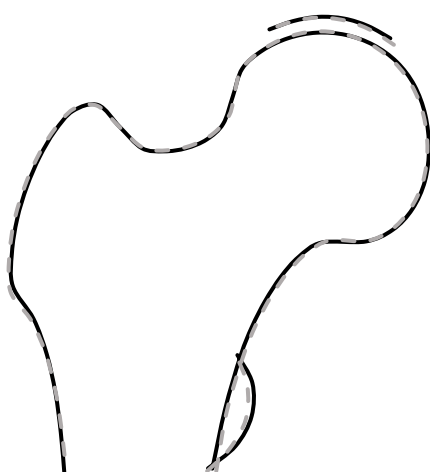
HSM (% of variatio n)	Key features: +2 SDs (solid line) -2 SDs (dashed line)	Graphical representation
1 (42%)	<p>Positive scores (solid line)</p> <ul style="list-style-type: none"> - Loss of femoral head curvature - Narrower FN <p>Negative scores (dashed line)</p> <ul style="list-style-type: none"> - Wider FN - Smaller NSA 	<p style="text-align: center;">HSM1</p> 

<p>2 (13%)</p>	<p>Positive scores (solid line)</p> <ul style="list-style-type: none"> - Narrower FN and shaft - Smaller greater trochanter - Smaller femoral head (inferior aspect proximal to lesser trochanter) <p>Negative scores (dashed line)</p> <ul style="list-style-type: none"> - Wider FN - Larger greater and lesser trochanter <p>-</p>	<p>HSM2</p>  <p>The diagram shows a lateral view of the femoral head and neck. A solid line represents the positive features: a narrower femoral neck (FN) and shaft, a smaller greater trochanter, and a smaller femoral head. A dashed line represents the negative features: a wider FN and shaft, and larger greater and lesser trochanters. The femoral head is shown with a slight indentation at the inferior aspect proximal to the lesser trochanter.</p>
<p>3 (8.5%)</p>	<p>Positive scores (solid line)</p> <ul style="list-style-type: none"> - Smaller lesser trochanter - Narrower FN <p>Negative scores (dashed line)</p> <ul style="list-style-type: none"> - Wider FN - Larger lesser trochanter 	<p>HSM3</p>  <p>The diagram shows a lateral view of the femoral head and neck. A solid line represents the positive features: a smaller lesser trochanter and a narrower femoral neck (FN). A dashed line represents the negative features: a wider FN and a larger lesser trochanter. The femoral head is shown with a slight indentation at the inferior aspect proximal to the lesser trochanter.</p>

<p>4 (6.1%)</p>	<p>Positive scores (solid line)</p> <ul style="list-style-type: none"> - Narrower femoral neck - Smaller neck shaft angle <p>Negative scores (dashed line)</p> <ul style="list-style-type: none"> - Cam-type deformity - Wider FN 	<p>HSM4</p> 
<p>5 (4.1%)</p>	<p>Positive scores (solid line)</p> <ul style="list-style-type: none"> - Larger femoral head (inferior aspect proximal to lesser trochanter) - Larger greater trochanter - Wider FN <p>Negative scores (dashed line)</p> <ul style="list-style-type: none"> - Smaller femoral head (inferior aspect proximal to lesser trochanter) - Narrower FN 	<p>HSM5</p> 

<p>6 (3.4%)</p>	<p>Positive scores (solid line)</p> <ul style="list-style-type: none"> - Narrower FN - Smaller femoral head <p>Negative scores (dashed line)</p> <ul style="list-style-type: none"> - Larger femoral head - Wider FN 	<p>HSM6</p> 
<p>7 (2.6%)</p>	<p>Positive scores (solid line)</p> <ul style="list-style-type: none"> - Larger femoral head (medial aspect and inferior aspect proximal to lesser trochanter) - Wider femoral shaft <p>Negative scores (dashed line)</p> <ul style="list-style-type: none"> - Smaller femoral head (medial aspect and inferior aspect proximal to lesser trochanter) 	<p>HSM7</p> 

<p>8 (2.5%)</p>	<p>Positive scores (solid line)</p> <ul style="list-style-type: none"> - Larger femoral head - Narrower FN <p>Negative scores (dashed line)</p> <ul style="list-style-type: none"> - Smaller femoral head - Larger greater trochanter - Loss of femoral neck to head curvature 	<p>HSM8</p> 
<p>9 (1.8%)</p>	<p>Positive scores (solid line)</p> <ul style="list-style-type: none"> - Cam-type deformity - Smaller lesser trochanter <p>Negative scores (dashed line)</p> <ul style="list-style-type: none"> - Larger femoral head (inferior aspect proximal to lesser trochanter) - Larger lesser trochanter 	<p>HSM9</p> 

<p>10 (1.5%)</p>	<p>Positive scores (solid line) - Larger lesser trochanter</p> <p>Negative scores (dashed line) - Smaller lesser trochanter</p>	<p>HSM10</p> 
----------------------	---	---

10.2. Appendix 2

Appendix for chapter 3

Supplementary Table 10.2.1; Associations between age at clinic attendance and the top ten HSMs at both time points

HSM	Age 14 (N=4,428)		Age 18 (N=4,369)	
	β (95% CI)	p	β (95% CI)	p
1	0.08 (0.02,0.14)	0.008	0.00 (-0.03,0.03)	0.781
2	-0.05 (-0.16,0.06)	0.348	-0.01 (-0.07,0.05)	0.772
3	-0.11 (-0.20,-0.01)	0.034	-0.01 (-0.06,0.04)	0.773
4	0.08 (-0.02,0.17)	0.131	0.01 (-0.04,0.07)	0.639
5	-0.08 (-0.20,0.03)	0.154	-0.05 (-0.11,0.01)	0.094
6	0.13 (0.03,0.23)	0.011	0.12 (0.05,0.18)	<0.001
7	0.11 (0.02,0.20)	0.017	-0.01 (-0.06,0.04)	0.709
8	-0.40 (-0.54,-0.26)	<0.001	0.06 (-0.01,0.12)	0.105
9	-0.07 (-0.18,0.04)	0.231	-0.05 (-0.12,0.01)	0.112
10	-0.08 (-0.17,0.01)	0.069	-0.03 (-0.09,0.03)	0.301

Abbreviations: HSM (hip shape mode), CI (confidence interval). Table shows results of linear regression analysis between age at clinic attendance and the top ten HSMs in ALSPAC adolescents at age 14 and age 18. Regression coefficients represent SD change in HSM per one-year increase in age at clinic attendance, 95% CIs and p value.

Supplementary Table 10.2.2; Associations between height and the top ten HSMs at both time points

HSM	Age 14 (N=4,428)		Age 18 (N=4,369)	
	β (95% CI)	p	β (95% CI)	p
1	0.004 (0.002,0.01)	<0.001	0.00 (0.00,0.00)	0.796
2	-0.02 (-0.02,-0.02)	<0.001	-0.02 (-0.03,-0.02)	<0.001
3	-0.01 (-0.01,-0.01)	<0.001	0.00 (0.00,0.00)	0.632
4	-0.01 (-0.01,-0.01)	<0.001	-0.01 (-0.01,0.00)	<0.001
5	-0.02 (-0.02,-0.01)	<0.001	-0.02 (-0.02,-0.02)	<0.001
6	0.00 (0.00,0.00)	0.999	0.02 (0.02,0.02)	<0.001
7	0.01 (0.01,0.01)	<0.001	0.00 (0.00,0.00)	0.058
8	-0.02 (-0.03,-0.02)	<0.001	0.00 (0.00,0.01)	0.121
9	-0.02 (-0.02,-0.01)	<0.001	-0.02 (-0.02,-0.02)	<0.001
10	-0.01 (-0.01,0.00)	<0.001	0.00 (0.00,0.00)	0.389

Abbreviations: HSM (hip shape mode), CI (confidence interval). Table shows results of linear regression analysis between height and the top ten HSMs in ALSPAC adolescents at age 14 and age 18. Regression coefficients represent SD change in HSM per unit increase in height, 95% CIs and p value.

Supplementary Table 10.2.3; Associations between lean mass and the top ten HSMs at both time points

HSM	Age 14 (N=4,428)		Age 18 (N=4,369)	
	β (95% CI)	p	β (95% CI)	p
1	0.003 (0.002,0.01)	<0.001	0.0002 (0.00,0.00)	0.629
2	-0.03 (-0.03,-0.03)	<0.001	-0.03 (-0.03,-0.02)	<0.001
3	-0.02 (-0.02,-0.02)	<0.001	-0.01 (-0.01,-0.01)	<0.001
4	-0.01 (-0.02,-0.01)	<0.001	-0.01 (-0.01,0.00)	<0.001
5	-0.01 (-0.02,-0.01)	<0.001	-0.02 (-0.02,-0.02)	<0.001
6	0.01 (0.00,0.01)	<0.001	0.03 (0.02,0.03)	<0.001
7	0.001 (-0.001,0.004)	0.435	0.00 (-0.01,0.00)	<0.001
8	-0.01 (-0.01,-0.01)	<0.001	0.01 (0.00,0.01)	<0.001
9	-0.03 (-0.03,-0.02)	<0.001	-0.02 (-0.02,-0.02)	<0.001
10	-0.01 (-0.01,-0.01)	<0.001	0.00 (0.00,0.00)	0.039

Abbreviations: HSM (hip shape mode), CI (confidence interval). Table shows results of linear regression analysis between lean mass and the top ten HSMs in ALSPAC adolescents at age 14 and age 18. Regression coefficients represent SD change in HSM per unit increase in lean mass, 95% CIs and p value.

Supplementary Table 10.2.4; Associations between fat mass and the top ten HSMs at both time points

HSM	Age 14 (N=4,428)		Age 18 (N=4,369)	
	β (95% CI)	p	β (95% CI)	p
1	0.00 (0.00,0.01)	<0.001	0.001 (0.0003,0.003)	0.006
2	-0.02 (-0.02,-0.02)	<0.001	-0.01 (-0.01,-0.01)	<0.001
3	-0.02 (-0.02,-0.02)	<0.001	-0.01 (-0.01,0.00)	<0.001
4	0.00 (0.00,0.01)	0.004	0.00 (0.00,0.00)	0.797
5	0.00 (-0.01,0.00)	0.076	0.01 (0.00,0.01)	<0.001
6	-0.01 (-0.01,-0.01)	<0.001	-0.01 (-0.02,-0.01)	<0.001
7	0.00 (0.00,0.00)	0.445	-0.01 (-0.01,-0.01)	<0.001
8	-0.03 (-0.03,-0.03)	<0.001	-0.02 (-0.02,-0.01)	<0.001
9	0.00 (0.00,0.00)	0.534	0.01 (0.01,0.01)	<0.001
10	-0.01 (-0.01,-0.01)	<0.001	-0.02 (-0.02,-0.01)	<0.001

Abbreviations: HSM (hip shape mode), CI (confidence interval). Table shows results of linear regression analysis between fat mass and the top ten HSMs in ALSPAC adolescents at age 14 and age 18. Regression coefficients represent SD change in HSM per unit increase in fat mass, 95% CIs and p value.

10.3. Appendix 3

Appendix for chapter 4



DATA NOTE

Using SITAR (SuperImposition by Translation and Rotation) to estimate age at peak height velocity in Avon Longitudinal Study of Parents and Children [version 1; referees: 1 approved]

Monika Frysz ^{1,2}, Laura D. Howe ^{1,2}, Jonathan H. Tobias ³,
Lavinia Paternoster ^{1,2}

¹MRC Integrative Epidemiology Unit at the University of Bristol, University of Bristol, Bristol, UK

²Population Health Sciences, Bristol Medical School, University of Bristol, Bristol, UK

³Musculoskeletal Research Unit, University of Bristol, Bristol, UK

v1 First published: 25 Jul 2018, 3:90 (doi: [10.12688/wellcomeopenres.14708.1](https://doi.org/10.12688/wellcomeopenres.14708.1))
Latest published: 25 Jul 2018, 3:90 (doi: [10.12688/wellcomeopenres.14708.1](https://doi.org/10.12688/wellcomeopenres.14708.1))

Abstract

Puberty is a time of substantial biological and psychological changes. One of the hallmarks of puberty is a rapid growth spurt, however its timing varies between individuals. The impact of pubertal timing on later health outcomes has been of interest in life course epidemiology, however its measurement can be challenging. Age at peak height velocity (aPHV) offers an objective measure of pubertal timing without having to rely on physical examination or self-report. We describe the derivation of aPHV estimates in Avon Longitudinal Study of Parents and Children (ALSPAC) offspring, using Superimposition by Translation And Rotation (SITAR) mixed effects growth curve analysis. ALSPAC is a rich source of phenotypic and genotypic data and given the importance of pubertal timing for later health outcomes, these data offer an opportunity to explore the determinants and consequences of aPHV.

Keywords

ALSPAC, pubertal timing, growth, age at peak height velocity



This article is included in the Avon Longitudinal Study of Parents and Children (ALSPAC) gateway.

Open Peer Review

Referee Status:

Invited Referees
1

version 1
published 25 Jul 2018 [report](#)

1 **Shane A Norris**, University of the Witwatersrand, South Africa
John M. Pettifor , University of the Witwatersrand, South Africa

Discuss this article

Comments (0)

Corresponding author: Monika Frysz (monika.frysz@bristol.ac.uk)

Author roles: **Frysz M:** Data Curation, Formal Analysis, Writing – Original Draft Preparation, Writing – Review & Editing; **Howe LD:** Conceptualization, Data Curation, Writing – Review & Editing; **Tobias JH:** Conceptualization, Writing – Review & Editing; **Paternoster L:** Conceptualization, Writing – Review & Editing

Competing interests: No competing interests were disclosed.

Grant information: This work was supported by the Wellcome Trust through a PhD Studentship to MF [105504] and the ALSPAC core programme grant [102215]. The UK Medical Research Council and Wellcome [102215] and the University of Bristol provide core support for ALSPAC. LDH is supported by a Career Development Award fellowship from the UK Medical Research Council [MR/M020894/1]. MF, LDH and LP work in a unit that receives support from the UK Medical Research Council and the University of Bristol [MC_UU_12013/4 & MC_UU_12013/5]. *The funders had no role in study design, data collection and analysis, decision to publish, or preparation of the manuscript.*

Copyright: © 2018 Frysz M *et al.* This is an open access article distributed under the terms of the [Creative Commons Attribution Licence](#), which permits unrestricted use, distribution, and reproduction in any medium, provided the original work is properly cited.

How to cite this article: Frysz M, Howe LD, Tobias JH and Paternoster L. Using SITAR (SuperImposition by Translation and Rotation) to estimate age at peak height velocity in Avon Longitudinal Study of Parents and Children [version 1; referees: 1 approved] Wellcome Open Research 2018, 3:90 (doi: [10.12688/wellcomeopenres.14708.1](https://doi.org/10.12688/wellcomeopenres.14708.1))

First published: 25 Jul 2018, 3:90 (doi: [10.12688/wellcomeopenres.14708.1](https://doi.org/10.12688/wellcomeopenres.14708.1))

Introduction

Puberty is a period of significant biological and psychological changes in human development. One of its hallmarks includes a rapid growth spurt, the timing and speed of which varies between individuals, with marked sexual dimorphism.

The relationship of pubertal timing with adverse health outcomes in later life has been investigated previously¹. For example, previous studies reported an association between late menarche and increased risk of osteoporosis², whereas early pubertal timing has been found to be related to higher risk of obesity and cardiovascular disease in both men and women³. Thus, investigating the influences of pubertal timing and understanding its relationship with later health outcomes is of great public health importance. While clinical assessment remains the gold standard for the assessment of pubertal status, this is difficult to achieve in large-scale studies. Self-reported puberty measures lack reliability^{4,5}, and may be unpopular with study participants, potentially leading to large amounts of missing data. Another measure, age at peak height velocity (aPHV) provides an objective and non-invasive assessment of pubertal status.

The Avon Longitudinal Study of Parents and Children (ALSPAC) is a longitudinal birth cohort, which was established in the 1990s in the South West of England⁶. ALSPAC is a rich source of data, including phenotypic and genetic data collected for the mothers, fathers and children.

This paper describes the application of Superimposition by Translation And Rotation (SITAR) mixed effects growth curve model (described previously by Cole *et al.*)⁷ for analysis of height in puberty and estimating aPHV in ALSPAC offspring which resulted in a new dataset being generated. Previous studies have shown this to be a suitable method for estimating aPHV⁸, even with fairly sparse data⁹.

Methods

ALSPAC recruited a total of 14,541 pregnant women with expected delivery date between 1st April 1991 and 31st December 1992. Of these pregnancies, 68 have no known birth outcome, 195 were twin, 3 were triplet and 1 was quadruplet. In total, these pregnancies resulted in 14,062 live births of which 13,988 children were alive at 1 year of age.

In order to increase sample size additional recruitment took place when the children were on average 7 years old (Phase II) and again between age 8 – 18 years (Phase III) resulting in a total of 15,247 enrolled pregnancies, of which 14,701 were alive at 1 year of age. For more details regarding eligibility and recruitment please refer to Boyd *et al.*⁶.

These children have been followed up from birth (those recruited during Phases II and III were followed up from the time they joined the study) and data collection included questionnaires and clinical assessments. For the purpose of estimating age at PHV, only height measurements obtained by trained fieldworkers during assessment clinics were used. These clinics encompassed 'children in focus clinics' (CIF) to which a

random 10% subsample of children were invited between the age 2 and 5 years, and six assessment clinics in late childhood (between age 7 and 13 years), three further assessment clinics in adolescence (ages 13, 15 and 17 years). These data were restricted to include height measurements collected when the children were between 5 to 20 years of age which resulted in a total of 61,290 height measurements available for 10,236 participants of whom 5,099 were female and 5,137 were male. To maximise accuracy of estimate aPHV, these data were further restricted to include individuals with at least one height measurement for the following time periods: 5 to <10 years, 10 to < 15 years and 15 to 20 years. A total of 46,246 height measurements for 5,707 individuals (3,019 females, 2,688 males) were available for SITAR analysis.

SITAR is a mixed effects shape-invariant growth curve model, consisting of a mean growth curve along with three transformations (size, tempo and velocity), used to describe how each individual differs from the mean curve. The three SITAR parameters are size, reflecting up/down shift from the mean curve; tempo, reflecting left/right shift (on the age scale) which corresponds to the relative timing of puberty based on aPHV, and velocity reflecting stretching/shrinking of the age scale and hence describing differences in the rate at which individuals pass through puberty. For a detailed description of the method please refer to Cole *et al.*⁷.

Height data were uploaded into R and following outlier removal of people with velocity exceeding 4 SDs (using velout function; for more details see sitar package documentation in R¹⁰), an initial SITAR model was fitted, for males and females separately, in R version 3.4.1. Following initial model fitting, standardized residuals exceeding 4 in absolute value were removed leaving a total of 40,037 height measurements for 5,707 individuals available for analysis with an average of 8 measurements (range 1–10 measurements) available per participant (see Figure 1 for details regarding participant recruitment).

Dataset validation

The final SITAR model was fitted with 5 degrees of freedom, for males and females separately, and it explained 98% and 98.3% of variance in the dataset for males and females, respectively. Mean aPHV (SD) was 13.6 (0.9) for males (Figure 2) and 11.7 (0.8) for females (Figure 3) and these estimates are similar to those reported in the literature^{11,12}.

Table 1 shows mean and SD of additional variables that were estimated, which include: size (cm) (negative values indicating smaller whereas positive taller children and zero represents the mean), tempo (years) (negative values indicating early puberty, positive late puberty and zero represents the mean), velocity (years) (measure of intensity, positive values indicating short growth spurt, zero corresponding to mean velocity) along with peak velocity (cm).

Ethical approval and consent

Ethical approval for the study was obtained from the ALSPAC Ethics and Law Committee and the Local Research Ethics

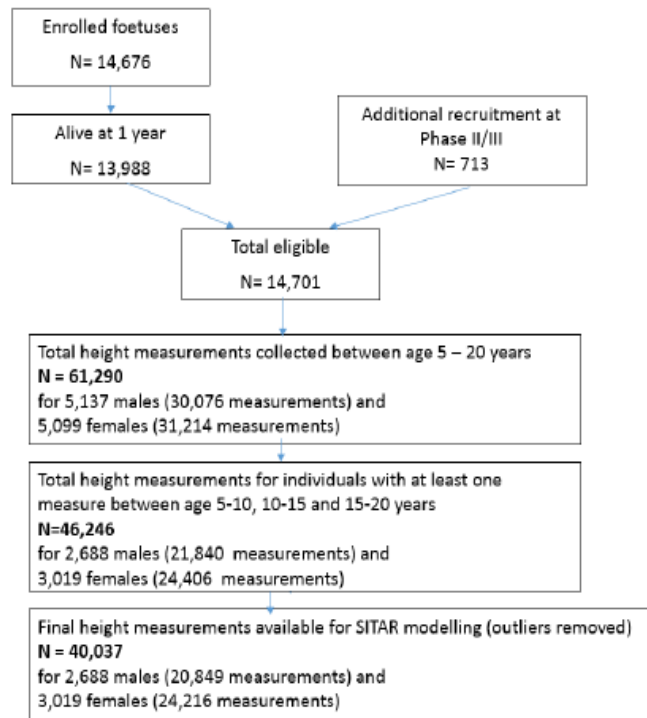


Figure 1. Avon Longitudinal Study of Parents and Children (ALSPAC) participant recruitment and height measurements available for analysis.

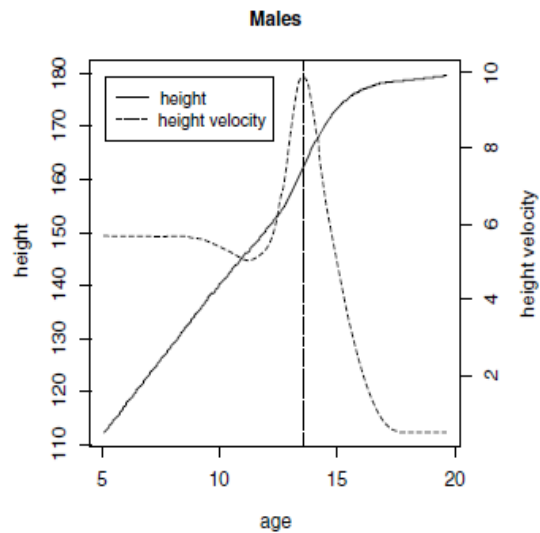


Figure 2. Mean growth curve (solid line) and velocity (dashed line) plots estimated by Superimposition by Translation and Rotation (SITAR) for males. Vertical dotted line represents mean age at peak height velocity.

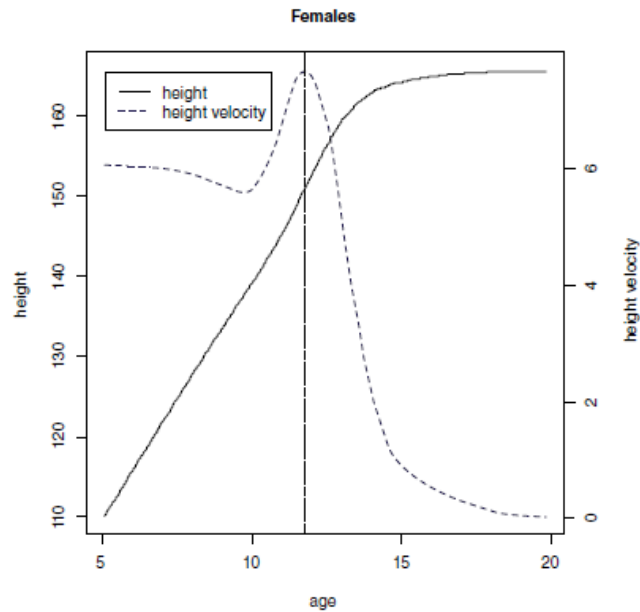


Figure 3. Mean growth curve (solid line) and velocity (dashed line) plots estimated by SuperImposition by Translation and Rotation (SITAR) for females. Vertical dotted line represents mean age at peak height velocity.

Table 1. Means and standard deviations of estimated SITAR growth parameters in Avon Longitudinal Study of Parents and Children (ALSPAC) offspring.

	Combined (N= 5,707)	Males (N=2,688)	Females (N=3019)
Variable name	Mean (SD)	Mean (SD)	Mean (SD)
aPHV (years)	12.6 (1.3)	13.6 (0.9)	11.7 (0.8)
Size (cm)	0.0 (6.3)	0.0 (6.5)	0.0 (6.0)
Tempo (years)	0.0 (0.9)	0.0 (0.9)	0.0 (0.9)
Velocity (years)	0.0 (0.1)	0.0 (0.1)	0.0 (0.1)
Peak velocity (cm)	8.8 (1.5)	10.0 (1.1)	7.7 (0.8)

Abbreviations: aPHV (age at peak height velocity), SD (standard deviation)

Committees, full details of the approvals obtained are available from the study website (<http://www.bristol.ac.uk/alspac/researchers/research-ethics/>).

Written informed consent was obtained from parents, and children were invited to give consent where appropriate. Study members have the right to withdraw their consent for elements of the study or from the study entirely at any time.

Data availability

ALSPAC data access is through a system of managed open access. The steps below highlight how to apply for access to the data included in this data note and all other ALSPAC data. The

dataset generated in this data note has been deposited within the ALSPAC data resource and is linked to ALSPAC project number B2325. Please quote this number to request required variables which have been described in this dataset (size, tempo, velocity, aPHV and peak velocity).

1. Please read the [ALSPAC access policy \(PDF, 627kB\)](#) which describes the process of accessing the data and samples in detail, and outlines the costs associated with doing so.
2. You may also find it useful to browse our fully searchable [research proposals database](#), which lists all research projects that have been approved since April 2011.

3. Please submit your research proposal for consideration by the ALSPAC Executive Committee using the online process. You will receive a response within 10 working days to advise you whether your proposal has been approved.

If you have any questions about accessing data, please email alspac-data@bristol.ac.uk.

The ALSPAC data management plan describes in detail the policy regarding data sharing, which is through a system of managed open access.

Competing interests

No competing interests were disclosed.

Grant information

This work was supported by the Wellcome Trust through a PhD Studentship to MF [105504] and the ALSPAC core programme grant [102215].

The UK Medical Research Council and Wellcome [102215] and the University of Bristol provide core support for ALSPAC. LDH is supported by a Career Development Award fellowship from the UK Medical Research Council [MR/M020894/1]. MF, LDH and LP work in a unit that receives support from the UK Medical Research Council and the University of Bristol [MC_UU_12013/4 & MC_UU_12013/5].

The funders had no role in study design, data collection and analysis, decision to publish, or preparation of the manuscript.


Acknowledgements

We are extremely grateful to all the families who took part in this study, the midwives for their help in recruiting them, and the whole ALSPAC team, which includes interviewers, computer and laboratory technicians, clerical workers, research scientists, volunteers, managers, receptionists, and nurses.

References

- Day FR, Elks CE, Murray A, et al.: Puberty timing associated with diabetes, cardiovascular disease and also diverse health outcomes in men and women: the UK Biobank study. *Sci Rep.* 2015; 5: 11208. [PubMed Abstract](#) | [Publisher Full Text](#) | [Free Full Text](#)
- Parker SE, Troisi R, Wise LA, et al.: Menarche, menopause, years of menstruation, and the incidence of osteoporosis: the influence of prenatal exposure to diethylstilbestrol. *J Clin Endocrinol Metab.* 2014; 99(2): 594–601. [PubMed Abstract](#) | [Publisher Full Text](#) | [Free Full Text](#)
- Prentice P, Viner RM: Pubertal timing and adult obesity and cardiometabolic risk in women and men: a systematic review and meta-analysis. *Int J Obes (Lond).* 2013; 37(8): 1036–43. [PubMed Abstract](#) | [Publisher Full Text](#)
- Haasmussen AR, Wohlschlag-Veje C, Tetre de Henzy-Martin K, et al.: Validity of self-assessment of pubertal maturation. *Pediatrics.* 2015; 135(1): 86–93. [PubMed Abstract](#) | [Publisher Full Text](#)
- Desmangles JC, Lappe JM, Lipaczewski G, et al.: Accuracy of pubertal Tanner staging self-reporting. *J Pediatr Endocrinol Metab.* 2006; 19(3): 213–222. [PubMed Abstract](#) | [Publisher Full Text](#)
- Boyd A, Golding J, Macleod J, et al.: Cohort profile: the 'children of the 90s'—the index offspring of the Avon Longitudinal Study of Parents and Children. *Int J Epidemiol.* 2013; 42(1): 111–27. [PubMed Abstract](#) | [Publisher Full Text](#) | [Free Full Text](#)
- Cole TJ, Donaldson MD, Ben-Shlomo Y: SITAR—a useful instrument for growth curve analysis. *Int J Epidemiol.* 2010; 39(6): 1568–1566. [PubMed Abstract](#) | [Publisher Full Text](#) | [Free Full Text](#)
- Simpkin AJ, Sayers A, Gilthorpe MS, et al.: Modelling height in adolescence: a comparison of methods for estimating the age at peak height velocity. *Ann Hum Biol.* 2017; 44(8): 715–722. [PubMed Abstract](#) | [Publisher Full Text](#) | [Free Full Text](#)
- Cole TJ: Optimal design for longitudinal studies to estimate pubertal height growth in individuals. *Ann Hum Biol.* 2018; 1–7. [PubMed Abstract](#) | [Publisher Full Text](#)
- Cole T: Sitar: Super Imposition by Translation and Rotation Growth Curve Analysis. 2015. [Reference Source](#)
- Khairullah A, May MT, Tilling K, et al.: Height-based Indices of Pubertal Timing in Male Adolescents. *Int J Dev Sci.* 2013; 7(2): 105–116. [PubMed Abstract](#) | [Free Full Text](#)
- Marshall WA, Tanner JM: Variations in the pattern of pubertal changes in boys. *Arch Dis Child.* 1970; 45(239): 13–23. [PubMed Abstract](#) | [Publisher Full Text](#) | [Free Full Text](#)

Open Peer Review

Current Referee Status: 

Version 1

Referee Report 16 August 2018

doi:10.21956/wellcomeopenres.16018.r33565



Shane A Norris¹, **John M. Pettifor** ²

¹ MRC/Wits Developmental Pathways for Health Research Unit, Faculty of Health Sciences, University of the Witwatersrand, Johannesburg, South Africa

² MRC/Wits Developmental Pathways for Health Research Unit, Faculty of Health Sciences, University of the Witwatersrand, Johannesburg, South Africa

Frysz and colleagues from the University of Bristol describe the use of the statistical programme, Superimposition by Translation and Rotation (SITAR), to determine the age of peak height velocity (aPHV) in a cohort of children participating in the Avon Longitudinal Study of Parents and Children (ALSPAC). The results they obtained for both boys and girls (13.6 years and 11.7 years respectively) are similar to those obtained by other researchers in well-resourced countries.

SITAR, a recently developed modelling approach by Tim Cole¹, has been used increasingly in longitudinal studies to describe secular and population trends in childhood growth and pubertal development using skeletal development (Tanner RUS score) and aPHV in both poorly- and well-resourced communities²⁻⁴. Its advantages are that it assesses each individual's curve against the mean curve and is able to determine the size (amplitude of change), tempo (the timing of the onset of change) and velocity (rate of change) of each individual curve in relation to the mean curve. It is also robust with missing data. Cole in a paper published this year assessed the interval required between height measurements in individual adolescent children to optimize the determination of aPHV⁵. Cole concluded that height measurements need not be taken more frequently than biennially to obtain an accurate assessment of the average aPHV.

The reviewers have a few minor comments, which might help to provide further clarity on the participants included in the cohort. The authors describe the recruitment of participants from the ALSPAC cohort and the inclusion criteria for height measurements to be included into the database used for this particular aspect of the study. It is however unclear if black or Asian children were included in the analytical cohort sample. The reason for this comment is that data are available to suggest the age of pubertal development and aPHV in black children may differ from that of white children living in both well- and poorly-resourced countries^{3,6}. Thus their inclusion might have influenced the mean values of aPHV obtained and the subsequent comparisons with other cohorts.

The inclusion of an individual into the SITAR study required that at least one height measurement was available at each of three different time periods, 5-10 years, 10-15 years and 15-20 years. Yet in their analysis of the average number of measurements available per individual, the average is given as 8 with a range from 1-10. It is unclear how children with only one measurement were included based on

the criteria for inclusion given above. It is possible that the authors meant that the participants included had at least one measurement in any of the age bands.

In the second paragraph of the Methods section, line 3, Phase II is referred to as being between age 8 - 18 years. We believe this should be Phase III.

References

1. Cole TJ, Donaldson MD, Ben-Shlomo Y: SITAR—a useful instrument for growth curve analysis. *Int J Epidemiol.* 2010; **39** (6): 1558-66 [PubMed Abstract](#) | [Publisher Full Text](#)
2. Cole TJ, Mori H: Fifty years of child height and weight in Japan and South Korea: Contrasting secular trend patterns analyzed by SITAR. *Am J Hum Biol.* 2018; **30** (1). [PubMed Abstract](#) | [Publisher Full Text](#)
3. Cole TJ, Rousham EK, Hawley NL, Cameron N, Norris SA, Pettifor JM: Ethnic and sex differences in skeletal maturation among the Birth to Twenty cohort in South Africa. *Arch Dis Child.* 2015; **100** (2): 138-43 [PubMed Abstract](#) | [Publisher Full Text](#)
4. Prentice A, Dibba B, Sawo Y, Cole TJ: The effect of prepubertal calcium carbonate supplementation on the age of peak height velocity in Gambian adolescents. *Am J Clin Nutr.* 2012; **96** (5): 1042-50 [PubMed Abstract](#) | [Publisher Full Text](#)
5. Cole TJ: Optimal design for longitudinal studies to estimate pubertal height growth in individuals. *Ann Hum Biol.* 2018. 1-7 [PubMed Abstract](#) | [Publisher Full Text](#)
6. Ramnitz MS, Lodish MB: Racial disparities in pubertal development. *Semin Reprod Med.* 2013; **31** (5): 333-9 [PubMed Abstract](#) | [Publisher Full Text](#)

Is the rationale for creating this work clearly stated? <http://dx.doi.org/10.1055/s-0033-1348891>

Yes

Are the protocols appropriate and is the work technically sound?

Yes

Are sufficient details of methods and materials provided to allow replication by others?

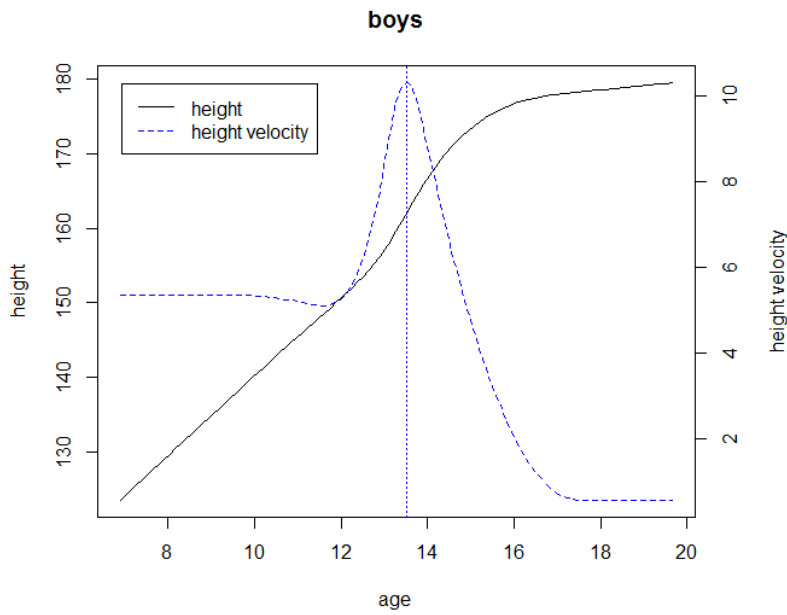
Partly

Are the datasets clearly presented in a useable and accessible format?

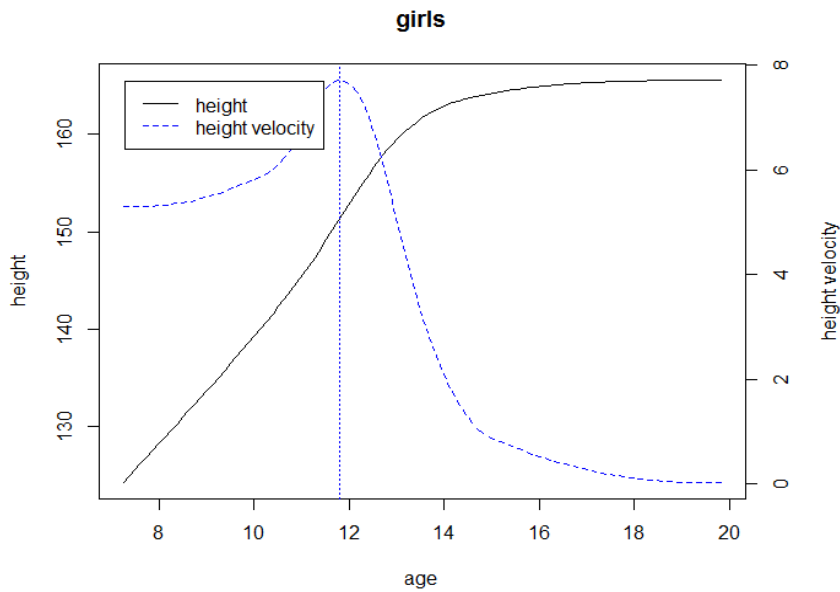
Yes

Competing Interests: No competing interests were disclosed.

We have read this submission. We believe that we have an appropriate level of expertise to confirm that it is of an acceptable scientific standard.



Supplementary Figure 10.3.1 Mean growth curve (black line) and velocity (blue dashed-line) plots estimated by SITAR for males. Vertical dotted line represents age at peak height velocity (equivalent to tempo measure).



Supplementary Figure 10.3.2 Mean growth curve (black line) and velocity (blue dashed-line) plots estimated by SITAR for females. Vertical dotted line represents age at peak height velocity (equivalent to tempo measure).

10.4. Appendix 4

Appendix for chapter 5

Supplementary Table 10.4.1; The association between FN BMD and top ten HSMs in ALSPAC offspring at age 14 (N=4,428)

HSM	Model 1		Model 2	
	β (95% CI)	p	β (95% CI)	p
1	0.08 (0.07,0.10)	<0.001	0.07 (0.06,0.09)	1.3 x10 ⁻²²
2	-0.01 (-0.03,0.01)	0.327	0.16 (0.13,0.18)	7.3 x10 ⁻³⁴
3	-0.02 (-0.04,0.00)	0.05	0.13 (0.11,0.15)	6.3 x10 ⁻³⁰
4	0.07 (0.05,0.09)	7.1 x10 ⁻¹¹	0.13 (0.11,0.15)	1.8 x10 ⁻²⁶
5	0.06 (0.03,0.08)	1.4 x10 ⁻⁰⁶	0.19 (0.16,0.21)	<0.0001
6	0.02 (0.00,0.04)	0.085	0.03 (0.01,0.05)	0.015
7	0.03 (0.01,0.05)	3.8 x10 ⁻⁰³	0.01 (-0.01,0.03)	0.275
8	-0.15 (-0.18,-0.12)	6.7 x10 ⁻²⁹	-0.02 (-0.05,0.02)	0.328
9	-0.04 (-0.07,-0.02)	0.0001	0.06 (0.03,0.08)	2.5 x10 ⁻⁰⁵
10	-0.05 (-0.07,-0.03)	2.4 x10 ⁻⁰⁸	-0.01 (-0.03,0.01)	0.45

Abbreviations: HSM (hip shape mode), CI (confidence interval). Table shows results of linear regression analysis between FN BMD and the top ten HSMs in ALSPAC adolescents. Results are unit change in HSM per standard deviation increase in exposure, 95% CIs and p value. Model 1 age and sex adjusted; model 2 additionally adjusted for height, lean and fat mass.

Supplementary Table 10.4.2; The association between FN BMD and top ten HSMs in ALSPAC offspring at age 14, stratified by gender

		Model 1		Model 2	
	HSM	β (95% CI)	p	β (95% CI)	p
Males N= 2,117	1	0.11 (0.09,0.13)	1.8 x10 ⁻³⁰	0.10 (0.07,0.12)	2.2 x10 ⁻¹⁶
	2	-0.05 (-0.08,-0.02)	2.3 x10 ⁻⁰³	0.15 (0.11,0.19)	1.0 x10 ⁻¹⁴
	3	-0.06 (-0.09,-0.03)	2.8 x10 ⁻⁰⁵	0.12 (0.09,0.16)	1.8 x10 ⁻¹²
	4	0.05 (0.02,0.08)	3.2 x10 ⁻⁰⁴	0.15 (0.11,0.18)	1.8 x10 ⁻¹⁵
	5	0.01 (-0.03,0.04)	0.634	0.20 (0.16,0.24)	2.7 x10 ⁻²²
	6	0.02 (-0.01,0.05)	0.209	0.02 (-0.02,0.05)	0.407
	7	0.05 (0.03,0.08)	7.5 x10 ⁻⁰⁵	0.00 (-0.03,0.03)	0.881
	8	-0.21 (-0.24,-0.17)	2.8 x10 ⁻²⁴	-0.03 (-0.07,0.02)	0.246
	9	-0.11 (-0.14,-0.08)	5.3 x10 ⁻¹²	0.01 (-0.03,0.05)	0.524
	10	-0.06 (-0.08,-0.03)	2.5 x10 ⁻⁰⁵	-0.02 (-0.05,0.01)	0.267
Females N=2,311	1	0.06 (0.05,0.08)	6.9 x10 ⁻¹⁴	0.06 (0.04,0.08)	2.2 x10 ⁻⁰⁹
	2	0.03 (0.00,0.06)	0.097	0.16 (0.13,0.20)	2.3 x10 ⁻¹⁹
	3	0.02 (-0.01,0.05)	0.142	0.14 (0.11,0.17)	7.6 x10 ⁻¹⁸
	4	0.08 (0.05,0.10)	1.9 x10 ⁻⁰⁸	0.12 (0.09,0.15)	5.8 x10 ⁻¹⁴
	5	0.10 (0.07,0.13)	1.9 x10 ⁻¹⁰	0.16 (0.13,0.20)	1.2 x10 ⁻¹⁷
	6	0.02 (-0.01,0.04)	0.238	0.04 (0.01,0.07)	7.8E ⁻⁰³
	7	0.00 (-0.02,0.03)	0.814	0.04 (0.01,0.07)	0.022
	8	-0.10 (-0.13,-0.06)	3.1 x10 ⁻⁰⁸	-0.01 (-0.05,0.03)	0.727
	9	0.02 (-0.01,0.05)	0.271	0.09 (0.05,0.13)	3.0 x10 ⁻⁰⁶
	10	-0.04 (-0.07,-0.02)	2.5 x10 ⁻⁰⁴	0.00 (-0.03,0.03)	0.994

Abbreviations: HSM (hip shape mode), CI (confidence interval). Table shows results of linear regression analysis between FN BMD and the top ten HSMs in male and female adolescents. Results are unit change in HSM per standard deviation increase in exposure, 95% CIs and p value. Model 1 age adjusted; model 2 additionally adjusted for height, lean and fat mass.

Supplementary Table 10.4.3; The association between FN BMD and top ten HSMs in ALSPAC offspring at age 18 (N=4,369)

HSM	Model 1		Model 2	
	β (95% CI)	p	β (95% CI)	p
1	0.04 (0.03,0.06)	9.5×10^{-12}	0.04 (0.03,0.06)	3.6×10^{-08}
2	0.03 (0.01,0.06)	0.017	0.13 (0.11,0.16)	9.6×10^{-21}
3	0.02 (-0.01,0.04)	0.14	0.06 (0.04,0.09)	3.1×10^{-08}
4	0.07 (0.05,0.10)	1.4×10^{-10}	0.11 (0.08,0.13)	2.9×10^{-16}
5	0.12 (0.10,0.15)	1.0×10^{-20}	0.17 (0.14,0.20)	1.5×10^{-30}
6	0.01 (-0.02,0.03)	0.452	0.01 (-0.02,0.04)	0.619
7	-0.04 (-0.06,-0.02)	2.6×10^{-04}	0.01 (-0.01,0.04)	0.316
8	-0.01 (-0.04,0.02)	0.543	0.05 (0.02,0.08)	1.3×10^{-03}
9	0.05 (0.03,0.08)	1.5×10^{-04}	0.09 (0.05,0.12)	7.5×10^{-08}
10	-0.05 (-0.08,-0.03)	8.8×10^{-06}	0.02 (-0.01,0.04)	0.25

Abbreviations: HSM (hip shape mode), CI (confidence interval). Table shows results of linear regression analysis between FN BMD and the top ten HSMs in ALSPAC adolescents. Results are unit change in HSM per standard deviation increase in exposure, 95% CIs and p value. Model 1 age and sex adjusted; model 2 additionally adjusted for height, lean and fat mass.

Supplementary Table 10.4.4; The association between FN BMD and top ten HSMs in ALSPAC offspring at age 18, stratified by gender

	HSM	Model 1		Model 2	
		β (95% CI)	p	β (95% CI)	p
Males N = 1,931	1	0.04 (0.03,0.06)	2.6 x10 ⁻⁰⁶	0.04 (0.02,0.07)	9.6 x10 ⁻⁰⁵
	2	0.00 (-0.03,0.04)	0.864	0.09 (0.05,0.12)	2.6 x10 ⁻⁰⁵
	3	-0.01 (-0.04,0.02)	0.424	0.03 (0.00,0.07)	0.043
	4	0.07 (0.04,0.10)	4.7 x10 ⁻⁰⁶	0.11 (0.07,0.15)	5.4 x10 ⁻⁰⁹
	5	0.08 (0.05,0.12)	5.0 x10 ⁻⁰⁷	0.13 (0.09,0.17)	1.9 x10 ⁻¹⁰
	6	0.05 (0.01,0.08)	0.011	0.05 (0.01,0.10)	0.012
	7	-0.09 (-0.11,-0.06)	4.0 x10 ⁻¹⁰	-0.04 (-0.07,-0.01)	0.022
	8	0.01 (-0.03,0.05)	0.534	0.08 (0.04,0.13)	4.2 x10 ⁻⁰⁴
	9	-0.03 (-0.06,0.01)	0.117	0.00 (-0.04,0.04)	0.836
	10	-0.04 (-0.07,-0.01)	0.014	0.03 (-0.01,0.07)	0.12
Females N=2,438	1	0.04 (0.03,0.06)	9.2 x10 ⁻⁰⁷	0.04 (0.02,0.06)	4.6 x10 ⁻⁰⁵
	2	0.06 (0.03,0.10)	0.001	0.18 (0.14,0.22)	1.5 x10 ⁻¹⁸
	3	0.05 (0.02,0.08)	0.003	0.10 (0.06,0.13)	6.6 x10 ⁻⁰⁹
	4	0.08 (0.04,0.11)	6.9 x10 ⁻⁰⁶	0.11 (0.08,0.15)	1.2 x10 ⁻⁰⁹
	5	0.16 (0.13,0.20)	1.4 x10 ⁻¹⁶	0.21 (0.17,0.25)	5.3 x10 ⁻²²
	6	-0.03 (-0.07,0.00)	0.083	-0.04 (-0.07,0.00)	0.082
	7	0.01 (-0.02,0.05)	0.435	0.06 (0.02,0.10)	1.1 x10 ⁻⁰³
	8	-0.03 (-0.07,0.01)	0.10	0.03 (-0.02,0.07)	0.243
	9	0.14 (0.10,0.18)	6.4 x10 ⁻¹¹	0.17 (0.12,0.22)	1.9 x10 ⁻¹²
	10	-0.07 (-0.11,-0.03)	1.1 x10 ⁻⁰⁴	0.00 (-0.04,0.04)	0.898

Abbreviations: HSM (hip shape mode), CI (confidence interval). Table shows results of linear regression analysis between FN BMD and the top ten HSMs in male and female adolescents. Results are unit change in HSM per standard deviation increase in exposure, 95% CIs and p value. Model 1 age adjusted; model 2 additionally adjusted for height, lean and fat mass.

Supplementary Table 10.4.5; List of SNPs used to generate genetic risk score for FN BMD

	CHR	nearest gene	SNP	EAF	BMD increasing allele	Other allele
1	1	<i>DNM3</i>	rs479336	0.25	G	T
2	1	<i>WLS</i>	rs17482952	0.92	A	G
3	1	<i>WLS</i>	rs12407028	0.6	T	C
4	1	<i>WNT4</i>	rs7521902	0.76	C	A
5	1	<i>ZBTB40</i>	rs6426749	0.18	C	G
6	2	<i>PKDCC</i>	rs7584262	0.22	T	C
7	2	<i>ANAPC1</i>	rs17040773	0.81	A	C
8	2	<i>GALNT3</i>	rs1346004	0.51	G	A
9	3	<i>KIAA2018</i>	rs1026364	0.34	T	G
10	3	<i>CTNNB1</i>	rs430727	0.57	C	T
11	4	<i>IDUA</i>	rs3755955	0.84	G	A
12	4	<i>MEPE</i>	rs6532023	0.33	T	G
13	5	<i>MEF2C</i>	rs1366594	0.54	A	C
14	6	<i>CDKAL1/SOX4</i>	rs9466056	0.62	G	A
15	6	<i>RSPO3</i>	rs13204965	0.77	A	C
16	6	<i>ESR1</i>	rs7751941	0.77	G	A
17	6	<i>C6orf97</i>	rs4869742	0.71	C	T
18	7	<i>WNT16</i>	rs3801387	0.27	G	A
19	7	<i>ABCF2</i>	rs7812088	0.12	A	G
20	7	<i>STARD3NL</i>	rs6959212	0.66	C	T
21	7	<i>SLC25A13</i>	rs4727338	0.66	C	G
22	8	<i>TNFRSF11B/OPG</i>	rs2062377	0.43	T	A
23	9	<i>FUBP3</i>	rs7851693	0.64	C	G
24	10	<i>MBL2/DKK1</i>	rs1373004	0.89	G	T
25	10	<i>CPN1</i>	rs7084921	0.42	T	C
26	11	<i>ARHGAP1</i>	rs7932354	0.3	T	C

27	11	<i>DCDC5</i>	rs163879	0.32	C	T
28	11	<i>SOX6</i>	rs7108738	0.17	G	T
29	11	<i>LRP5</i>	rs3736228	0.84	C	T
30	12	<i>KLHDC5/PTHLH</i>	rs7953528	0.18	A	T
31	12	<i>ERC1/WNT5B</i>	rs2887571	0.25	G	A
32	12	<i>C12orf23</i>	rs1053051	0.48	C	T
33	12	<i>HOXC6</i>	rs736825	0.64	C	G
34	12	<i>SP7</i>	rs2016266	0.32	G	A
35	13	<i>TNFSF11/RANKL</i>	rs9533090	0.51	C	T
36	14	<i>RPS6KA5</i>	rs1286083	0.18	C	T
37	14	<i>MARK3</i>	rs11623869	0.65	G	T
38	16	<i>NTAN1</i>	rs4985155	0.33	G	A
39	16	<i>AXIN1</i>	rs9921222	0.52	C	T
40	16	<i>C16orf38/CLCN7</i>	rs13336428	0.59	G	A
41	16	<i>SALL1/CYLD</i>	rs1566045	0.20	C	T
42	16	<i>FOXL1</i>	rs10048146	0.81	A	G
43	17	<i>SMG6</i>	rs4790881	0.70	A	C
44	17	<i>SOX9</i>	rs7217932	0.47	A	G
45	17	<i>SOST</i>	rs4792909	0.38	T	G
46	17	<i>C17orf53</i>	rs227584	0.29	C	A
47	18	<i>FAM210A</i>	rs4796995	0.64	A	G
48	18	<i>TNFRSF11A/RANK</i>	rs884205	0.76	C	A
49	20	<i>JAG1</i>	rs3790160	0.52	T	C

Supplementary Table 10.4.6; Mendelian randomization (using two-stage least squares) and observational analyses to explore associations between hip BMD and top ten hip shape modes in ALSPAC adolescents at age 14

HSM	OBS - Model 1		OBS -Model 2		TSLS (unweighted GRS)	
	β (95% CIs)	p	β (95% CIs)	p	β (95% CIs)	p
1	0.10 (0.08,0.11)	2.9×10^{-46}	0.09 (0.07,0.11)	1.2×10^{-28}	0.10 (0.03,0.18)	0.008
2	0.03 (0.01,0.06)	0.016	0.21 (0.18,0.24)	2.6×10^{-48}	0.17 (0.02,0.31)	0.023
3	-0.02 (-0.05,0.00)	0.029	0.13 (0.10,0.15)	2.5×10^{-24}	0.10 (-0.03,0.23)	0.144
4	0.05 (0.03,0.08)	2.2×10^{-06}	0.10 (0.08,0.13)	3.1×10^{-14}	-0.04 (-0.17,0.09)	0.561
5	0.07 (0.05,0.10)	2.7×10^{-08}	0.20 (0.17,0.23)	9.2×10^{-41}	0.22 (0.07,0.37)	0.004
6	0.02 (-0.01,0.04)	0.139	0.03 (0.00,0.06)	0.029	-0.04 (-0.17,0.10)	0.523
7	0.04 (0.02,0.06)	7.1×10^{-05}	0.03 (0.01,0.05)	0.015	0.07 (-0.03,0.20)	0.150
8	-0.14 (-0.17,-0.11)	1.9×10^{-20}	-0.01 (-0.05,0.02)	0.477	-0.17 (-0.35,0.02)	0.074
9	-0.06 (-0.08,-0.03)	1.4×10^{-05}	0.05 (0.02,0.08)	0.001	0.11 (-0.04,0.25)	0.151
10	-0.04 (-0.06,-0.02)	1.0×10^{-04}	0.01 (-0.02,0.03)	0.658	-0.02 (-0.14,0.09)	0.662

Table shows results of linear regression analysis (OBS) and two-stage least squares Mendelian randomization analysis (TSLS) between total hip BMD and genetic risk score (GRS) for hip BMD and the top ten hip shape modes (HSMs) in 3,553 ALSPAC adolescents (analysis restricted to individuals with complete phenotypic and genotypic data). Model 1 = age and gender adjusted, Model 2 = model 1 plus height, lean and fat mass. Results are standard deviation (SD) change in HSM per SD increase in exposure, 95% CIs and p value.

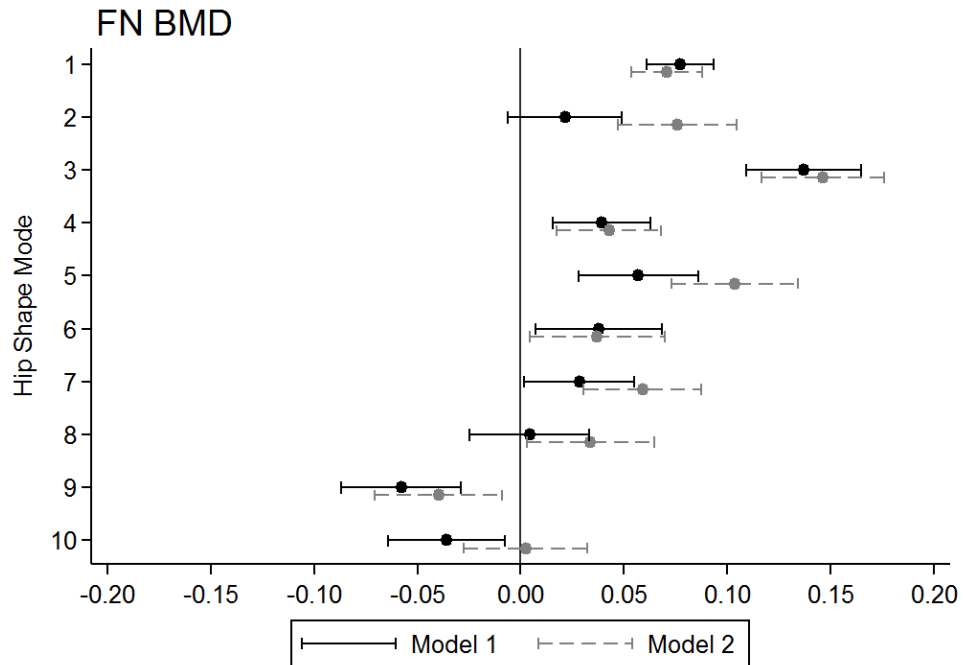
Supplementary Table 10.4.7; Mendelian randomization (using two-stage least squares) and observational analyses to explore associations between hip BMD and top ten hip shape modes in ALSPAC adolescents at age 18

HSM	OBS - Model 1		OBS -Model 2		TSLS (unweighted GRS)	
	β (95% CIs)	p	β (95% CIs)	p	β (95% CIs)	p
1	0.04 (0.04,0.02)	3.2×10^{-06}	0.03 (0.02,0.05)	2.4×10^{-04}	0.07 (-0.03,0.16)	0.159
2	0.10 (0.10,0.07)	3.8×10^{-11}	0.23 (0.20,0.26)	3.0×10^{-40}	0.21 (0.13,0.40)	0.036
3	0.01 (0.01,-0.01)	0.408	0.06 (0.03,0.09)	1.9×10^{-05}	0.16 (0.01,0.31)	0.041
4	0.06 (0.06,0.03)	7.6×10^{-06}	0.09 (0.06,0.13)	3.2×10^{-09}	-0.03 (-0.19,0.13)	0.685
5	0.10 (0.10,0.07)	2.2×10^{-10}	0.16 (0.13,0.20)	4.3×10^{-19}	0.20 (0.01,0.40)	0.039
6	0.04 (0.04,0.01)	0.008	0.04 (0.01,0.08)	0.02	-0.04 (-0.23,0.15)	0.678
7	-0.01 (-0.01,-0.03)	0.642	0.06 (0.03,0.08)	2.4×10^{-04}	-0.04 (-0.19,0.11)	0.628
8	-0.06 (-0.06,-0.09)	6.3×10^{-04}	-0.02 (-0.06,0.02)	0.296	-0.05 (-0.23,0.17)	0.650
9	0.04 (0.04,0.01)	0.021	0.08 (0.04,0.11)	1.1×10^{-04}	0.03 (-0.17,0.23)	0.750
10	-0.03 (-0.03,-0.06)	0.048	0.05 (0.02,0.08)	0.003	0.07 (-0.11,0.24)	0.443

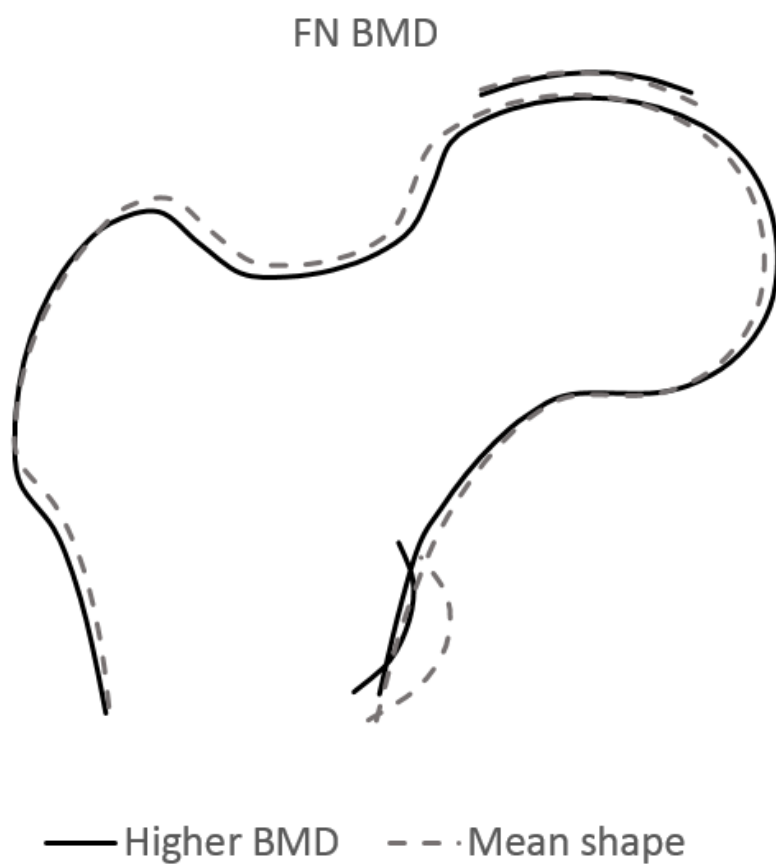
Table shows results of linear regression analysis (OBS) and two-stage least squares Mendelian randomization analysis (TSLS) between total hip BMD and genetic risk score (GRS) for hip BMD and the top ten hip shape modes (HSMs) in 3,175 ALSPAC adolescents (analysis restricted to individuals with complete phenotypic and genotypic data). Model 1 = age and gender adjusted, Model 2 = model 1 plus height, lean and fat mass. Results are standard deviation (SD) change in HSM per SD increase in exposure, 95% CIs and p value.

10.5. Appendix 5

Appendix for chapter 6



Supplementary Figure 10.5.1 Linear regression coefficients (black and dashed grey lines) with 95% CIs for the association between FN BMD and the top ten HSMs. Model 1 adjusted for age, Model 2 additionally adjusted for height, lean and fat mass.



Supplementary Figure 10.5.2 Hip shape changes observed per SD increase in FN BMD based on fully adjusted coefficients (model 2) (to aid visualisation each coefficient was multiplied by a factor of 10). Multiple regression coefficients, showing associations with FN BMD (see Supplementary Table 10.5.2 in Appendix 5), were entered into Shape software and the combined relationship between FN BMD and hip shape plotted. Dotted line represents mean hip shape, solid line represents composite change in hip shape per 10 x SD increase in FN BMD.

Supplementary Table 10.5.1; Association between hip BMD and top ten HSMs in ALSPAC mothers (N= 4,286)

HSM	Model 1		Model 2	
	β (95% CI)	p	β (95% CI)	p
1	0.10 (0.08,0.11)	<0.001	0.10 (0.08,0.11)	<0.001
2	0.03 (0.01,0.06)	0.015	0.13 (0.10,0.15)	<0.001
3	0.14 (0.12,0.17)	<0.001	0.16 (0.13,0.19)	<0.001
4	0.02 (0.00,0.05)	0.075	0.02 (-0.01,0.05)	0.158
5	0.07 (0.04,0.10)	<0.001	0.13 (0.10,0.16)	<0.001
6	0.05 (0.02,0.08)	0.003	0.05 (0.01,0.08)	0.009
7	0.05 (0.02,0.08)	<0.001	0.10 (0.07,0.13)	<0.001
8	-0.02 (-0.05,0.01)	0.144	0.00 (-0.03,0.03)	0.987
9	-0.07 (-0.10,-0.04)	<0.001	-0.06 (-0.09,-0.02)	<0.001
10	-0.01 (-0.04,0.02)	0.526	0.04 (0.01,0.07)	0.011

Abbreviations: HSM (hip shape mode), CI (confidence interval). Table shows results of linear regression analysis between total hip BMD and the top ten HSMs in male and female adolescents. Results are unit change in HSM per standard deviation increase in exposure, 95% CIs and p value. Model 1 age adjusted; model 2 additionally adjusted for height, lean and fat mass.

Supplementary Table 10.5.2; Association between FN BMD and top ten HSMs in ALSPAC mothers

HSM	Model 1		Model 2	
	β (95% CI)	p	β (95% CI)	p
1	0.08 (0.06,0.09)	<0.001	0.07 (0.05,0.09)	<0.001
2	0.02 (-0.01,0.05)	0.154	0.08 (0.05,0.10)	<0.001
3	0.14 (0.11,0.16)	<0.001	0.15 (0.12,0.18)	<0.001
4	0.04 (0.02,0.06)	0.001	0.04 (0.02,0.07)	<0.001
5	0.06 (0.03,0.09)	<0.001	0.10 (0.07,0.13)	<0.001
6	0.04 (0.01,0.07)	0.012	0.04 (0.00,0.07)	0.026
7	0.03 (0.00,0.05)	0.041	0.06 (0.03,0.09)	<0.001
8	0.00 (-0.03,0.03)	0.866	0.03 (0.00,0.07)	0.031
9	-0.06 (-0.09,-0.03)	<0.001	-0.04 (-0.07,-0.01)	0.012
10	-0.04 (-0.06,-0.01)	0.015	0.00 (-0.03,0.03)	0.869

Abbreviations: HSM (hip shape mode), CI (confidence interval). Table shows results of linear regression analysis between FN BMD and the top ten HSMs in male and female adolescents. Results are unit change in HSM per standard deviation increase in exposure, 95% CIs and p value. Model 1 age adjusted; model 2 additionally adjusted for height, lean and fat mass.

Supplementary Table 10.5.3; Estimated effects of genome-wide significant SNPs associated with FN BMD based on meta-analysis of GWA studies in 83,894 individuals (discovery and replication stages combined)

	chr	gene	SNP	beta	EA	EAF	pval
1	1	WLS	rs12407028	0.05	T	0.6	3.44 x10 ⁻²³
2	1	WLS	rs17482952	0.08	A	0.93	1.30 x10 ⁻¹¹
3	1	DNM3	rs479336	0.04	G	0.26	8.50 x10 ⁻¹⁵
4	1	ZBTB40	rs6426749	0.11	C	0.17	7.40 x10 ⁻⁵⁷
5	1	WNT4	rs7521902	0.04	C	0.69	2.80 x10 ⁻⁰⁹
6	2	GALNT3	rs1346004	0.05	G	0.5	1.10 x10 ⁻²⁵
7	2	ANAPC1	rs17040773	0.04	A	0.76	1.51 x10 ⁻⁰⁹
8	2	PKDCC	rs7584262	0.04	T	0.23	1.27 x10 ⁻⁰⁹
9	3	KIAA2018	rs1026364	0.03	T	0.37	4.80 x10 ⁻¹⁰
10	3	CTNNB1	rs430727	0.06	C	0.52	4.40 x10 ⁻²⁵
11	4	IDUA	rs3755955	0.06	G	0.84	1.46 x10 ⁻¹⁴
12	4	MEPE	rs6532023	0.06	T	0.34	4.90 x10 ⁻²⁶
13	5	MEF2C	rs1366594	0.08	A	0.54	4.50 x10 ⁻⁶¹
14	6	RSPO3	rs13204965	0.04	A	0.76	8.10 x10 ⁻¹²
15	6	C6orf97	rs4869742	0.05	C	0.69	4.10 x10 ⁻¹⁸
16	6	ESR1	rs7751941	0.04	G	0.79	1.60 x10 ⁻⁰⁹
17	6	CDKAL1/SOX4	rs9466056	0.04	G	0.62	2.73 x10 ⁻¹³
18	7	WNT16	rs3801387	0.08	G	0.26	5.20 x10 ⁻⁴⁰
19	7	SLC25A13	rs4727338	0.08	C	0.67	8.10 x10 ⁻⁴⁸
20	7	STARD3NL	rs6959212	0.04	C	0.68	1.20 x10 ⁻¹³
21	7	ABCF2	rs7812088	0.05	A	0.13	7.28 x10 ⁻⁰⁹
22	8	TNFRSF11B/OPG	rs2062377	0.06	T	0.43	9.10 x10 ⁻²⁵
23	9	FUBP3	rs7851693	0.05	C	0.64	3.37 x10 ⁻²²
24	10	MBL2/DKK1	rs1373004	0.04	G	0.87	1.45 x10 ⁻⁰⁸
25	10	CPN1	rs7084921	0.03	T	0.39	9.30 x10 ⁻¹⁰
26	11	DCDC5	rs163879	0.03	C	0.32	2.10 x10 ⁻⁰⁸
27	11	LRP5	rs3736228	0.05	C	0.84	4.80 x10 ⁻¹¹

28	11	SOX6	rs7108738	0.08	G	0.17	1.10 x10 ⁻³²
29	11	ARHGAP1	rs7932354	0.05	T	0.31	5.10 x10 ⁻¹⁸
30	12	C12orf23	rs1053051	0.03	C	0.48	9.60 x10 ⁻¹⁰
31	12	SP7	rs2016266	0.03	G	0.32	3.70 x10 ⁻¹⁰
32	12	ERC1/WNT5B	rs2887571	0.03	G	0.23	6.49 x10 ⁻⁰⁹
33	12	HOXC6	rs736825	0.04	C	0.56	1.10 x10 ⁻⁰⁹
34	12	KLHDC5/PTHLH	rs7953528	0.05	A	0.18	1.87 x10 ⁻¹²
35	13	TNFSF11/RANKL	rs9533090	0.054	C	0.51	9.84 x10 ⁻¹¹
36	14	MARK3	rs11623869	0.04	G	0.65	5.20 x10 ⁻¹⁶
37	14	RPS6KA5	rs1286083	0.05	C	0.19	2.20 x10 ⁻¹⁵
38	16	FOXL1	rs10048146	0.05	A	0.8	1.00 x10 ⁻¹⁴
39	16	C16orf38/CLCN7	rs13336428	0.04	G	0.57	1.49 x10 ⁻¹⁶
40	16	SALL1/CYLD	rs1566045	0.06	C	0.2	1.94 x10 ⁻²²
41	16	NTAN1	rs4985155	0.03	G	0.33	1.74 x10 ⁻¹⁰
42	16	AXIN1	rs9921222	0.03	C	0.52	5.18 x10 ⁻¹²
43	17	C17orf53	rs227584	0.06	C	0.3	2.56 x10 ⁻²⁴
44	17	SMG6	rs4790881	0.05	A	0.69	9.75 x10 ⁻¹⁹
45	17	SOST	rs4792909	0.04	T	0.37	1.95 x10 ⁻¹¹
46	17	SOX9	rs7217932	0.03	A	0.46	1.92 x10 ⁻¹¹
47	18	FAM210A	rs4796995	0.03	A	0.63	4.85 x10 ⁻⁰⁸
48	18	TNFRSF11A/RANK	rs884205	0.04	C	0.73	3.18 x10 ⁻¹⁰
49	20	JAG1	rs3790160	0.04	T	0.5	3.61 x10 ⁻¹²

Abbreviations: EA: effect allele, EAF: effect allele frequency

Analysis was based on 45 SNPs (4 SNPs were removed due to harmonization issues: rs17482952, rs4792909, rs2062377, rs736825)

Supplementary Table 10.5.4; Observational associations between femoral neck BMD and the top ten HSMs

HSM	Model 1		Model 2	
	β (95% CI)	p	β (95% CI)	p
1	0.08 (0.06,0.09)	<0.001	0.07 (0.05,0.09)	<0.001
2	0.02 (-0.01,0.05)	0.15	0.08 (0.05,0.10)	<0.001
3	0.14 (0.11,0.16)	<0.001	0.15 (0.12,0.18)	<0.001
4	0.04 (0.02,0.06)	0.001	0.04 (0.02,0.07)	<0.001
5	0.06 (0.03,0.09)	<0.001	0.10 (0.07,0.13)	<0.001
6	0.04 (0.01,0.07)	0.01	0.04 (0.00,0.07)	0.03
7	0.03 (0.00,0.05)	0.04	0.06 (0.03,0.09)	<0.001
8	0.00 (-0.03,0.03)	0.87	0.03 (0.00,0.06)	0.03
9	-0.06 (-0.08,-0.03)	<0.001	-0.04 (-0.07,-0.01)	0.01
10	-0.03 (-0.06,-0.01)	0.02	0.00 (-0.03,0.03)	0.87

Table shows results of the association between FN BMD and the top ten HSMs in 4,286 adult ALSPAC women. Model 1 was adjusted for age, model 2 was additionally adjusted for height, and fat and lean mass.

Supplementary Table 10.5.5; Results for two sample MR to investigate association between BMD and the top ten HSMs in ALSPAC mothers

HSM	Method	est (95% CI)	pval
1	MR Egger	-0.25 (-0.56,0.05)	0.11
1	Weighted median	0.07 (-0.07,0.21)	0.34
1	Inverse variance weighted	0.02 (-0.09,0.12)	0.72
2	MR Egger	-0.01 (-0.61,0.59)	0.98
2	Weighted median	0.08 (-0.15,0.32)	0.49
2	Inverse variance weighted	0.17 (-0.03,0.37)	0.09
3	MR Egger	-0.09 (-0.62,0.43)	0.74
3	Weighted median	0.06 (-0.17,0.29)	0.60
3	Inverse variance weighted	0.10 (-0.07,0.27)	0.26
4	MR Egger	0.08 (-0.38,0.53)	0.74
4	Weighted median	-0.09 (-0.30,0.11)	0.36
4	Inverse variance weighted	-0.06 (-0.21,0.09)	0.40
5	MR Egger	-0.45 (-1.00,0.10)	0.12
5	Weighted median	-0.09 (-0.32,0.14)	0.44
5	Inverse variance weighted	-0.01 (-0.19,0.18)	0.96
6	MR Egger	0.22 (-0.27,0.72)	0.38
6	Weighted median	-0.06 (-0.31,0.20)	0.66
6	Inverse variance weighted	0.00 (-0.16,0.17)	0.97
7	MR Egger	0.15 (-0.28,0.58)	0.50
7	Weighted median	0.05 (-0.17,0.27)	0.66
7	Inverse variance weighted	0.07 (-0.07,0.21)	0.34
8	MR Egger	-0.62 (-1.20,-0.05)	0.04
8	Weighted median	-0.20 (-0.45,0.05)	0.12
8	Inverse variance weighted	-0.13 (-0.33,0.06)	0.19
9	MR Egger	-0.02 (-0.52,0.48)	0.94
9	Weighted median	-0.12 (-0.34,0.11)	0.31
9	Inverse variance weighted	-0.11 (-0.27,0.06)	0.20
10	MR Egger	0.34 (-0.11,0.80)	0.15
10	Weighted median	0.03 (-0.19,0.25)	0.78
10	Inverse variance weighted	0.001 (-0.15,0.15)	0.99

Abbreviations: HSM (hip shape mode), est (estimate), CI (confidence interval)
 Analysis was based on 45 SNPs.

10.5.2. Power in MR analysis

While there is currently no online calculator for two-sample MR, as an approximation an online calculator for power calculations in one-sample setting was used

<https://sb452.shinyapps.io/power/>.

The power to detect an effect of 0.13, given sample size of 3,111, would be 65%.

Assuming the R^2 (variance explained in BMD by the genetic instrument) in this study was similar to that reported in adults. Sample size required in order to achieve 80% power would be 4700.

Supplementary Table 10.5.6; Univariate associations between potential confounders and FN BMD in a sample of 4,286 adult women

Exposure	Outcome	β (95% CI)	p
Age	FN BMD	-0.04 (-0.05,-0.03)	<0.001
Height	FN BMD	0.03 (0.03,0.04)	<0.001
Lean mass	FN BMD	0.06 (0.06,0.07)	<0.001
Fat mass	FN BMD	0.03 (0.02,0.03)	<0.001

Abbreviations: CI (confidence interval). Table shows results of linear regression analysis between each confounder and FN BMD in ALSPAC mothers. Regression coefficients represent unit change in outcome per unit change in exposure, 95% CIs and p value.

Supplementary Table 10.5.7; Univariate associations between potential confounders and total hip BMD in a sample of 4,286 adult women

Exposure	Outcome	β (95% CI)	p
Age	hip BMD	-0.03 (-0.04,-0.03)	<0.001
Height	hip BMD	0.02 (0.01,0.02)	<0.001
Lean mass	hip BMD	0.07 (0.06,0.07)	<0.001
Fat mass	hip BMD	0.03 (0.03, 0.04)	<0.001

Abbreviations: CI (confidence interval). Table shows results of linear regression analysis between each confounder and total hip BMD in ALSPAC mothers. Regression coefficients represent unit change in outcome per unit change in exposure, 95% CIs and p value.

Supplementary Table 10.5.8; Univariate associations between potential confounders and the top ten HSMs in a sample of 4,286 adult women

exposure	HSM	β (95% CI)	p
Age	1	0.000 (-0.003,0.004)	0.802
Age	2	-0.001 (-0.007,0.005)	0.716
Age	3	0.012 (0.006,0.018)	1.5x10 ⁻⁰⁴
Age	4	0.009 (0.004,0.015)	3.7x10 ⁻⁰⁴
Age	5	0.002 (-0.004,0.008)	0.56
Age	6	0.000 (-0.006,0.007)	0.943
Age	7	0.004 (-0.001,0.010)	0.136
Age	8	0.003 (-0.003,0.009)	0.347
Age	9	-0.001 (-0.008,0.005)	0.666
Age	10	-0.007 (-0.014,-0.001)	0.021
Height	1	0.000 (-0.003,0.003)	0.947
Height	2	0.006 (0.002,0.011)	0.004
Height	3	0.000 (-0.005,0.004)	0.855
Height	4	-0.003 (-0.007,0.000)	0.089
Height	5	-0.010 (-0.015,-0.006)	1.5x10 ⁻⁰⁵
Height	6	-0.001 (-0.006,0.004)	0.715
Height	7	-0.001 (-0.005,0.004)	0.817
Height	8	-0.015 (-0.020,-0.010)	1.7x10 ⁻¹⁰
Height	9	-0.003 (-0.008,0.002)	0.212
Height	10	-0.008 (-0.013,-0.004)	2.3x10 ⁻⁰⁴
Fat mass	1	0.004 (0.003,0.005)	9.4x10 ⁻⁰⁸
Fat mass	2	-0.014 (-0.016,-0.011)	4.2x10 ⁻²⁷
Fat mass	3	0.004 (0.001,0.006)	5.9x10 ⁻⁰³
Fat mass	4	0.000 (-0.002,0.002)	0.782
Fat mass	5	-0.005 (-0.007,-0.002)	2.9x10 ⁻⁰⁴
Fat mass	6	0.002 (-0.001,0.005)	0.166

Fat mass	7	-0.004 (-0.006,-0.002)	1.3x10 ⁻⁰³
Fat mass	8	-0.005 (-0.008,-0.003)	1.2x10 ⁻⁰⁴
Fat mass	9	-0.004 (-0.007,-0.001)	2.6x10 ⁻⁰³
Fat mass	10	-0.008 (-0.010,-0.005)	5.3x10 ⁻⁰⁹
Lean mass	1	0.006 (0.003,0.009)	3.2x10 ⁻⁰⁴
Lean mass	2	-0.019 (-0.024,-0.014)	1.2x10 ⁻¹²
Lean mass	3	0.000 (-0.005,0.006)	0.933
Lean mass	4	0.002 (-0.003,0.006)	0.405
Lean mass	5	-0.018 (-0.024,-0.013)	4.1x10 ⁻¹¹
Lean mass	6	0.003 (-0.003,0.008)	0.392
Lean mass	7	-0.015 (-0.020,-0.010)	9.3x10 ⁻⁰⁹
Lean mass	8	-0.009 (-0.015,-0.004)	9.1x10 ⁻⁰⁴
Lean mass	9	-0.011 (-0.017,-0.006)	4.7x10 ⁻⁰⁵
Lean mass	10	-0.016 (-0.021,-0.011)	4.1x10 ⁻⁰⁹
Lean mass	5	-0.018 (-0.024,-0.013)	4.1x10 ⁻¹¹
Lean mass	6	0.003 (-0.003,0.008)	0.392
Lean mass	7	-0.015 (-0.020,-0.010)	9.3x10 ⁻⁰⁹
Lean mass	8	-0.009 (-0.015,-0.004)	9.1x10 ⁻⁰⁴
Lean mass	9	-0.011 (-0.017,-0.006)	4.7x10 ⁻⁰⁵
Lean mass	10	-0.016 (-0.021,-0.011)	4.1x10 ⁻⁰⁹

Abbreviations: HSM (hip shape mode), CI (confidence interval). Table shows results of linear regression analysis between each confounder and the top ten HSMs in ALSPAC mothers. Regression coefficients represent SD change in HSM per unit change in exposure, 95% CIs and p value.

10.6. Appendix 6

Appendix for chapter 7

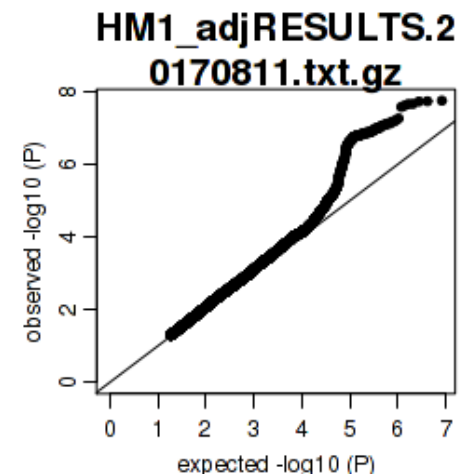
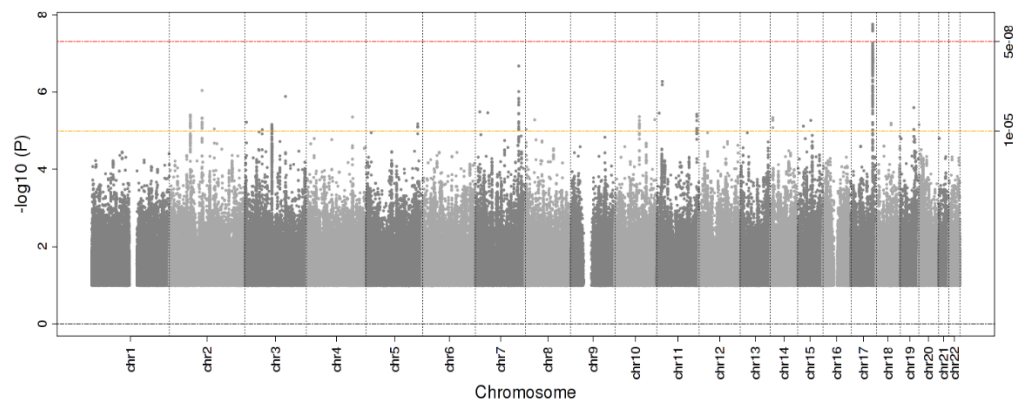
Template code to run GWAS analysis of hip shape in ALSPAC adolescents using SNPTEST.

Code adapted from Lavinia Paternoster's script (available here

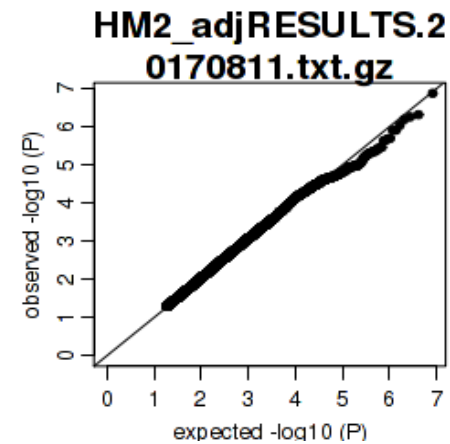
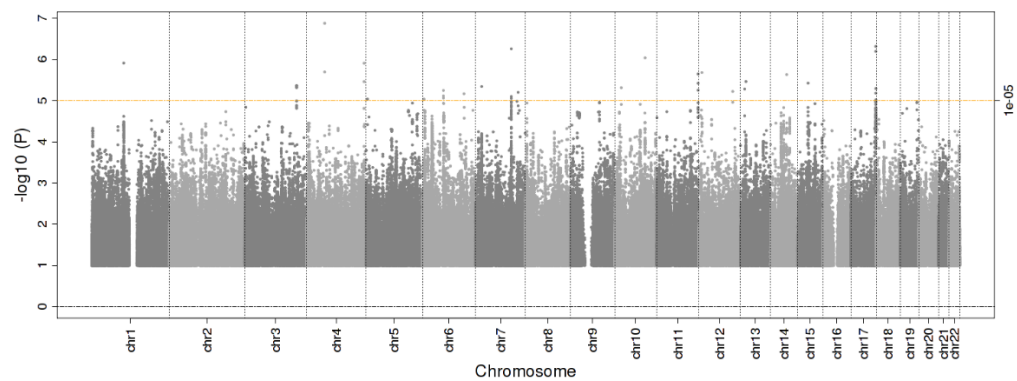
https://github.com/epxlp/GWAS_scripts)

```
#!/bin/bash
#PBS -r n
#
#PBS -l walltime=36:00:00,nodes=1:ppn=1
#PBS -j oe
#PBS -o
/panfs/panasas01/sscm/mf13567/GWAS_hip_shape_MF/kids13/ALS13vsCOMB/age_sex_adj/scripts/GWAS_HSM_template.log
#
# -----
cd
/panfs/panasas01/sscm/mf13567/GWAS_hip_shape_MF/kids13/ALS13vsCOMB/age_sex_adj/scripts
module add apps/snptest.2.5.0

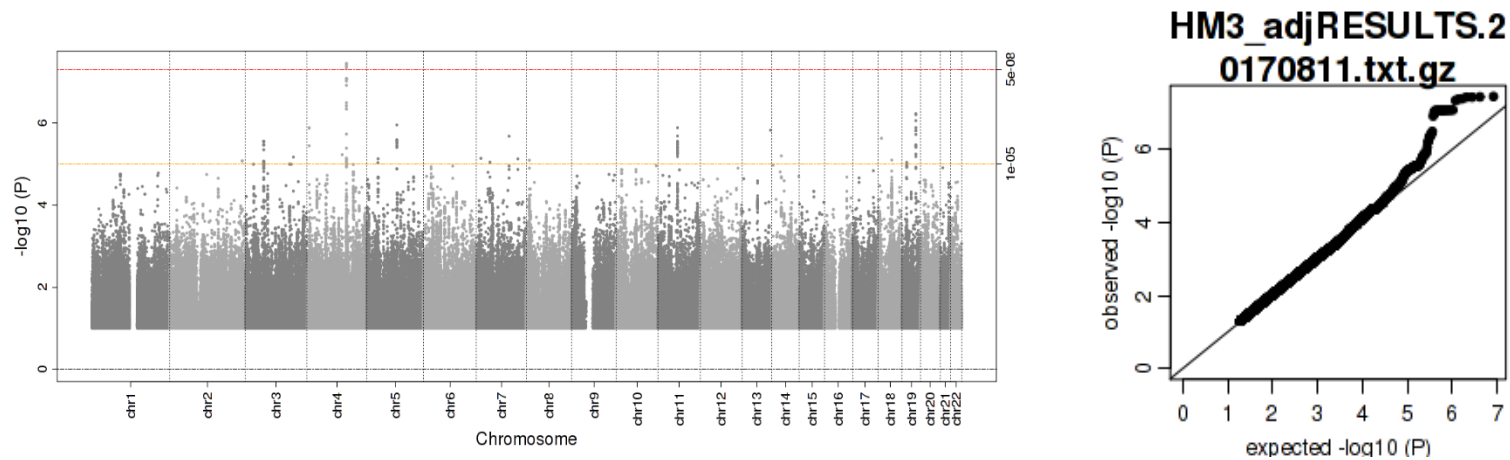
snptest_v2.5 -data
/panfs/panasas01/shared/alspac/studies/latest/alspac/genetic/variants/arrays/gwas/imputed/1000genomes/released/2015-10-30/data/dosage_bgen/data_chr0template.bgen \
/panfs/panasas01/sscm/mf13567/GWAS_hip_shape_MF/kids13/data/ALS13_merged.sample \
-exclude_samples
/panfs/panasas01/sscm/mf13567/GWAS_hip_shape_MF/kids13/data/exclusion_list_children.txt \
-assume_chromosome template \
-frequentist 1 \
-method expected \
-pheno HSMmode_13vsComb \
-use_raw_phenotypes \
-cov_names age_at_clinic_13 sex \
-sex_column sex \
-log
/panfs/panasas01/sscm/mf13567/GWAS_hip_shape_MF/kids13/ALS13vsCOMB/age_sex_adj/outputs/logs/SNPTEST_ALS13vcCOMB_HSMmode_chrtemplate.log \
-o
/panfs/panasas01/sscm/mf13567/GWAS_hip_shape_MF/kids13/ALS13vsCOMB/age_sex_adj/outputs/SNPTEST_ALS13vcCOMB_HSMmode_chrtemplate.out
```



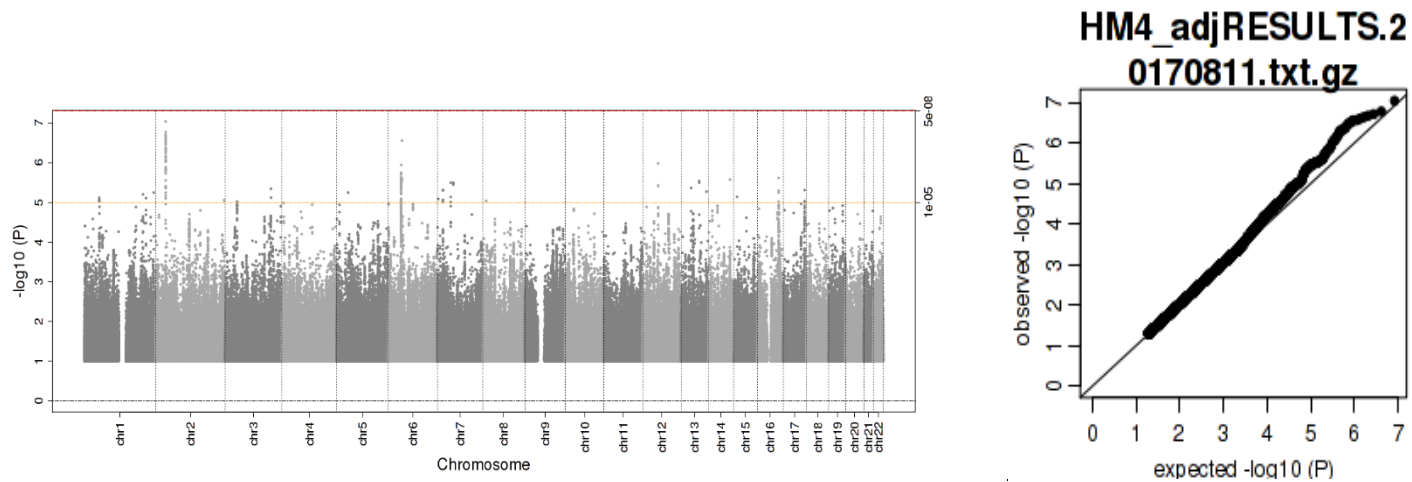
Supplementary Figure 10.6.1 Manhattan (left-hand side) and QQ (right hand-side) plots for HSM1 GWAS at age 14



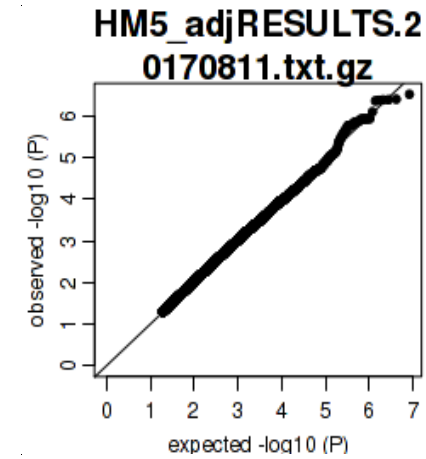
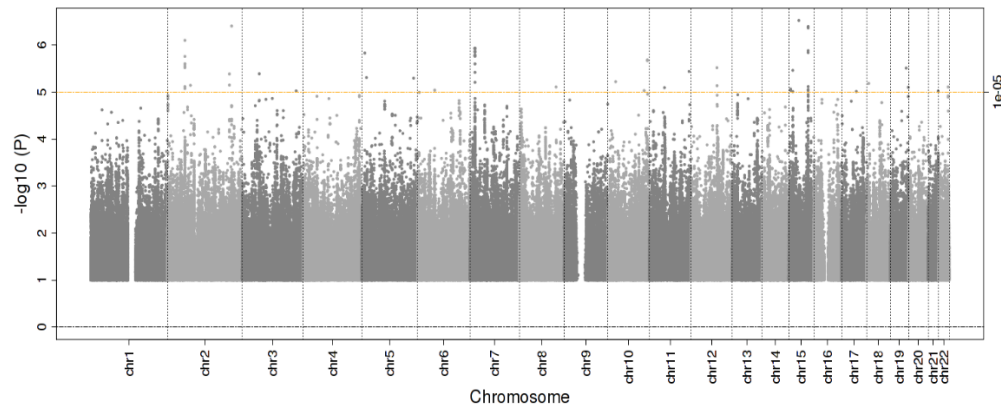
Supplementary Figure 10.6.2 Manhattan (left-hand side) and QQ (right hand-side) plots for HSM2 GWAS at age 14



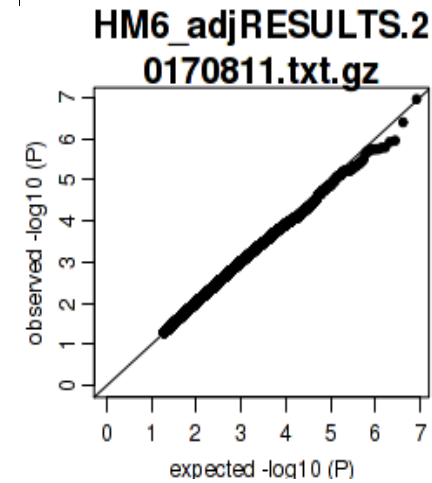
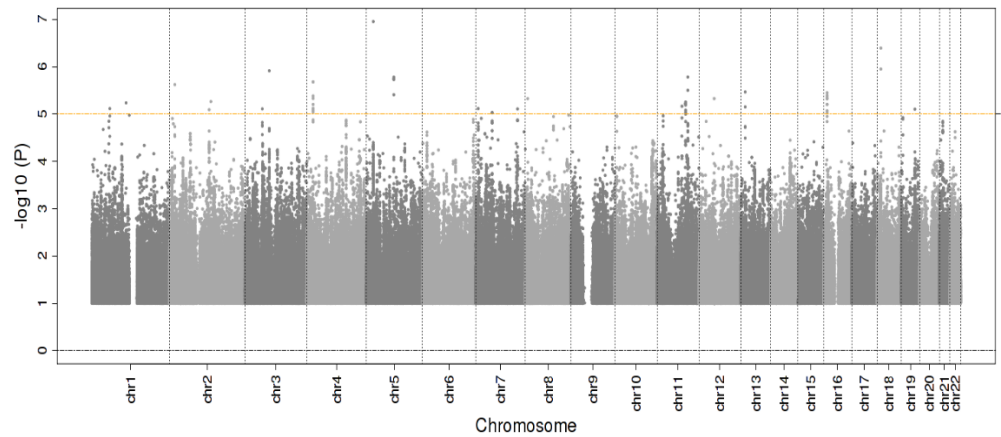
Supplementary Figure 10.6.3 Manhattan (left-hand side) and QQ (right hand-side) plots for HSM3 GWAS at age 14



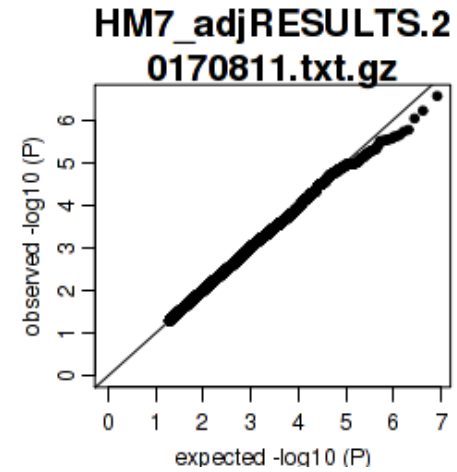
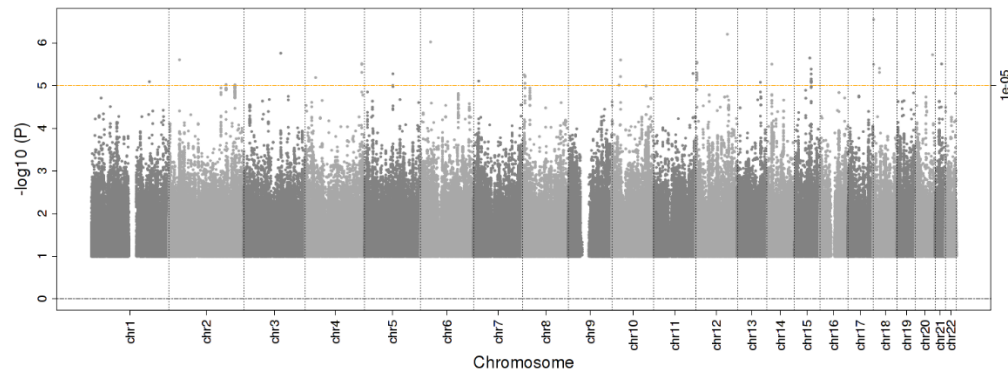
Supplementary Figure 10.6.4 Manhattan (left-hand side) and QQ (right hand-side) plots for HSM4 GWAS at age 14



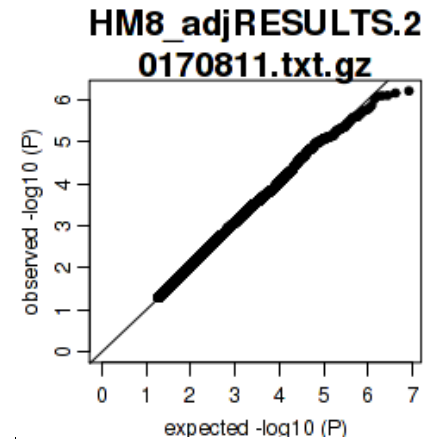
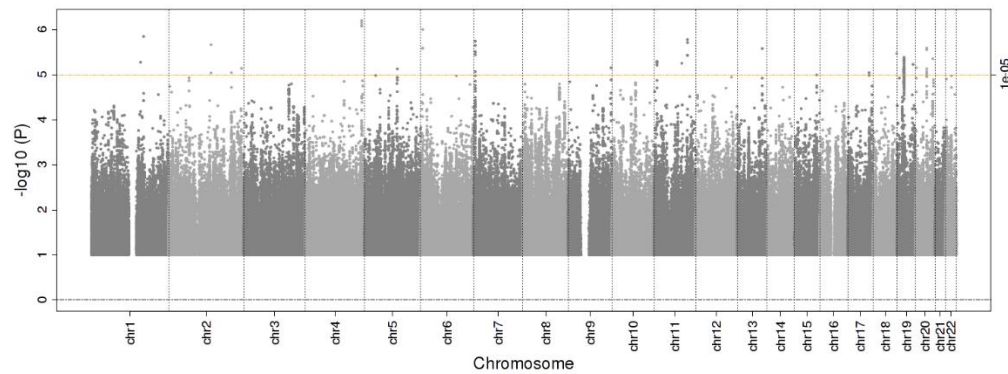
Supplementary Figure 10.6.5 Manhattan (left-hand side) and QQ (right hand-side) plots for HSM5 GWAS at age 14



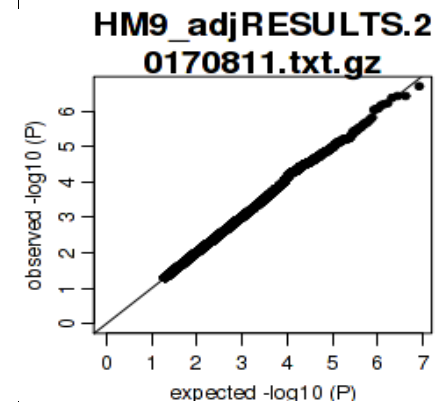
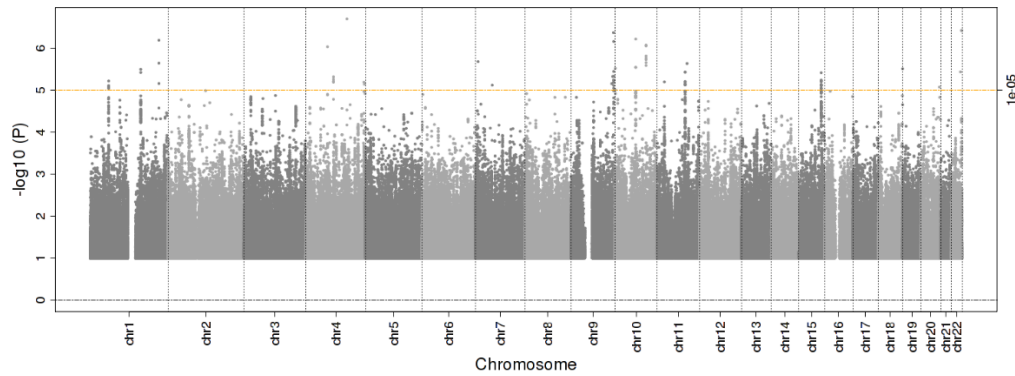
Supplementary Figure 10.6.6 Manhattan (left-hand side) and QQ (right hand-side) plots for HSM6 GWAS at age 14



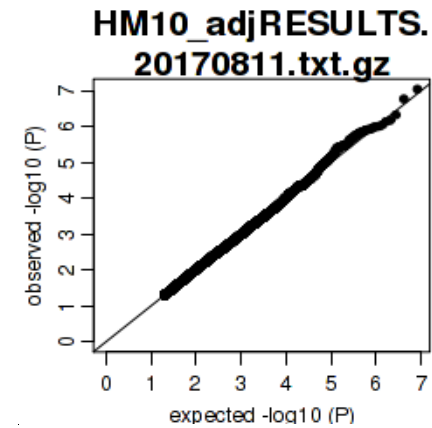
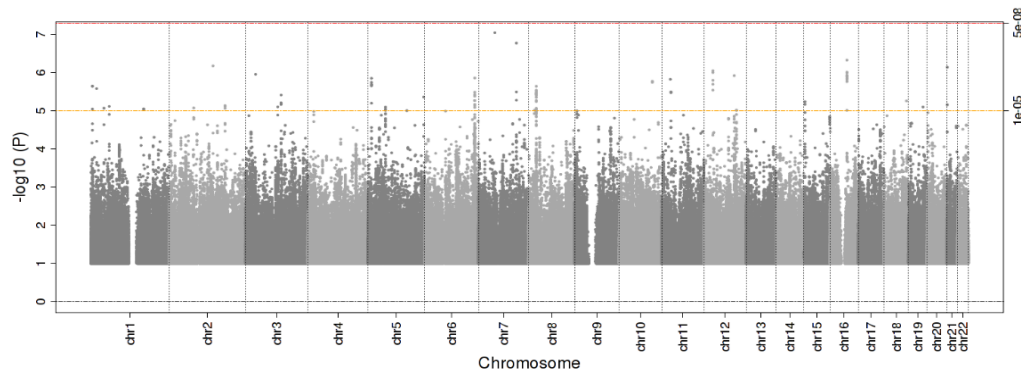
Supplementary Figure 10.6.7 Manhattan (left-hand side) and QQ (right hand-side) plots for HSM7 GWAS at age 14



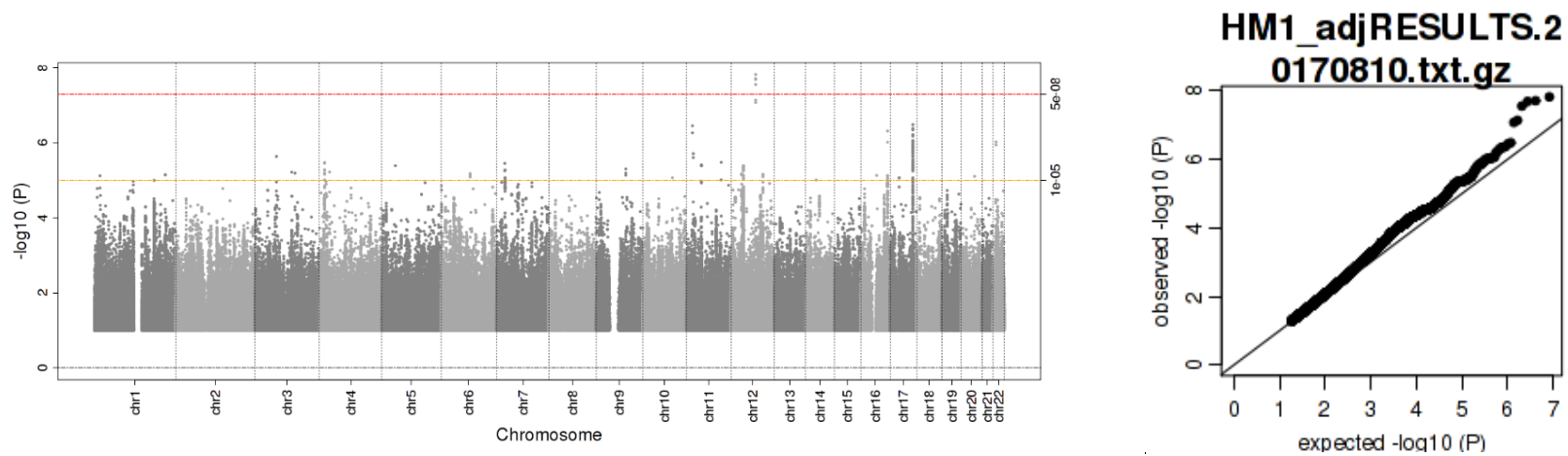
Supplementary Figure 10.6.8 Manhattan (left-hand side) and QQ (right hand-side) plots for HSM8 GWAS at age 14



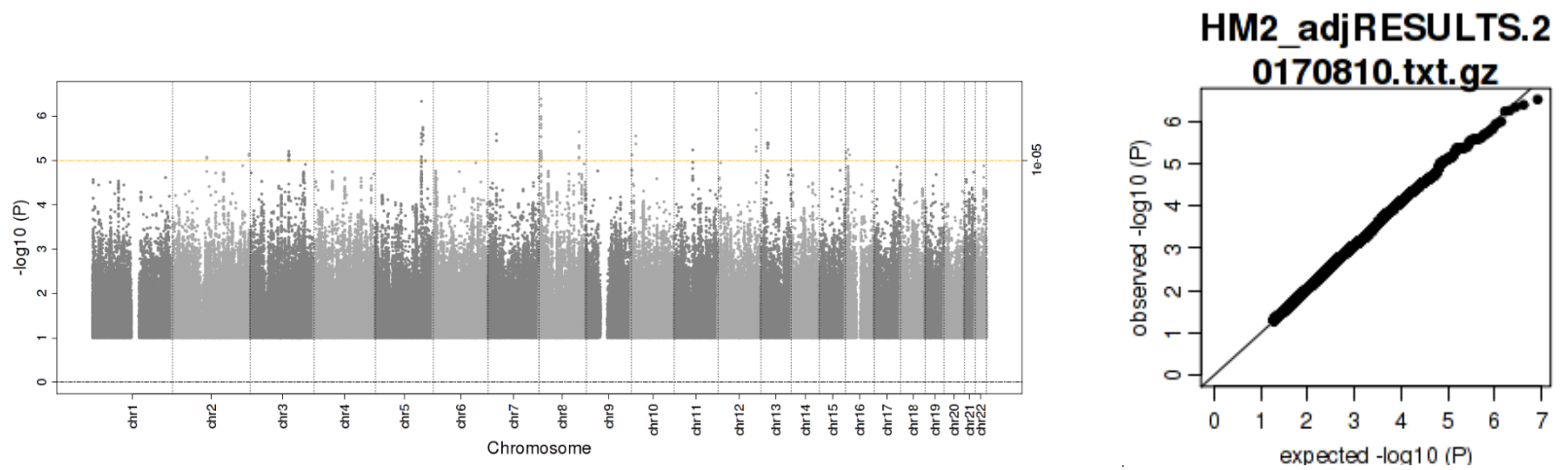
Supplementary Figure 10.6.9 Manhattan (left-hand side) and QQ (right hand-side) plots for HSM9 GWAS at age 14



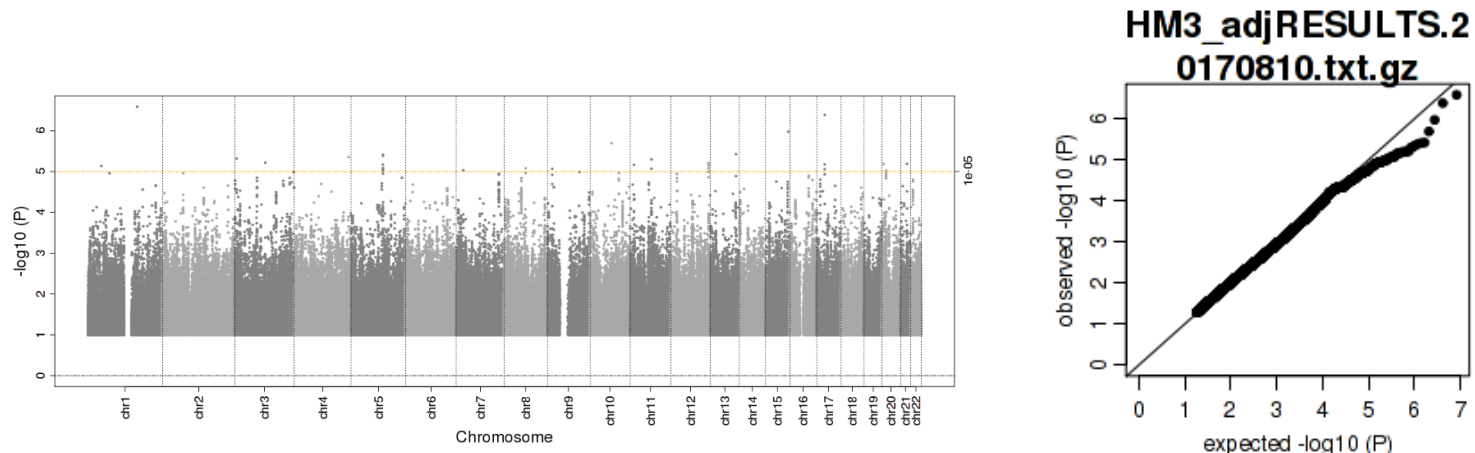
Supplementary Figure 10.6.10 Manhattan (left-hand side) and QQ (right hand-side) plots for HSM10 GWAS at age 14



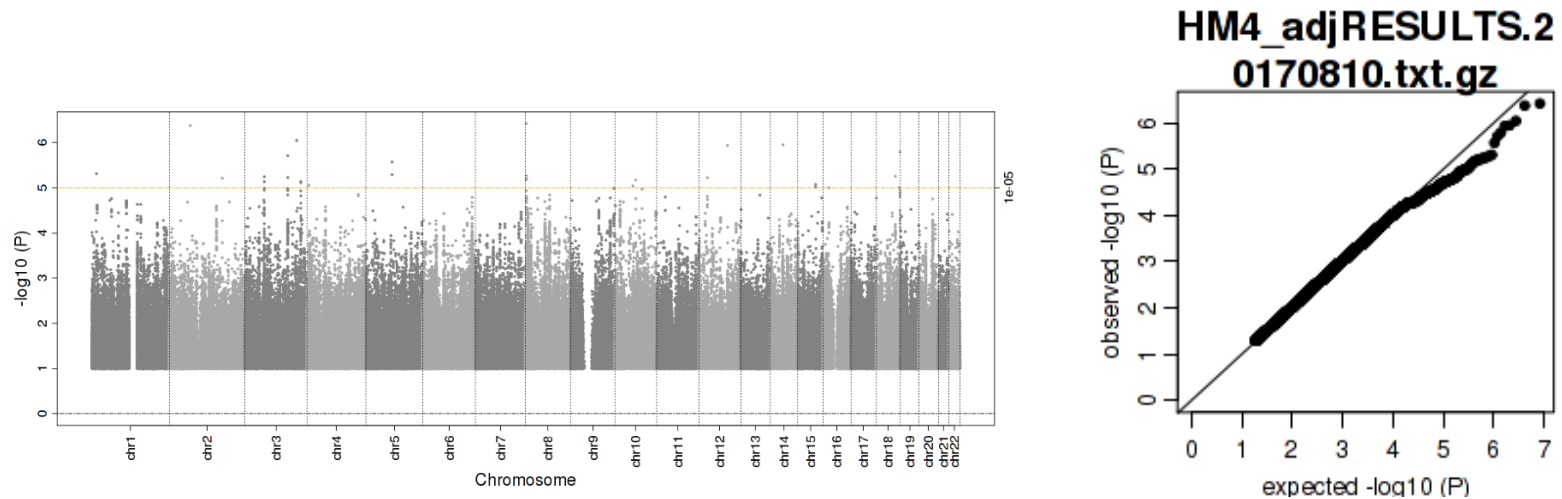
Supplementary Figure 10.6.11 Manhattan (left-hand side) and QQ (right hand-side) plots for HSM1 GWAS at age 18



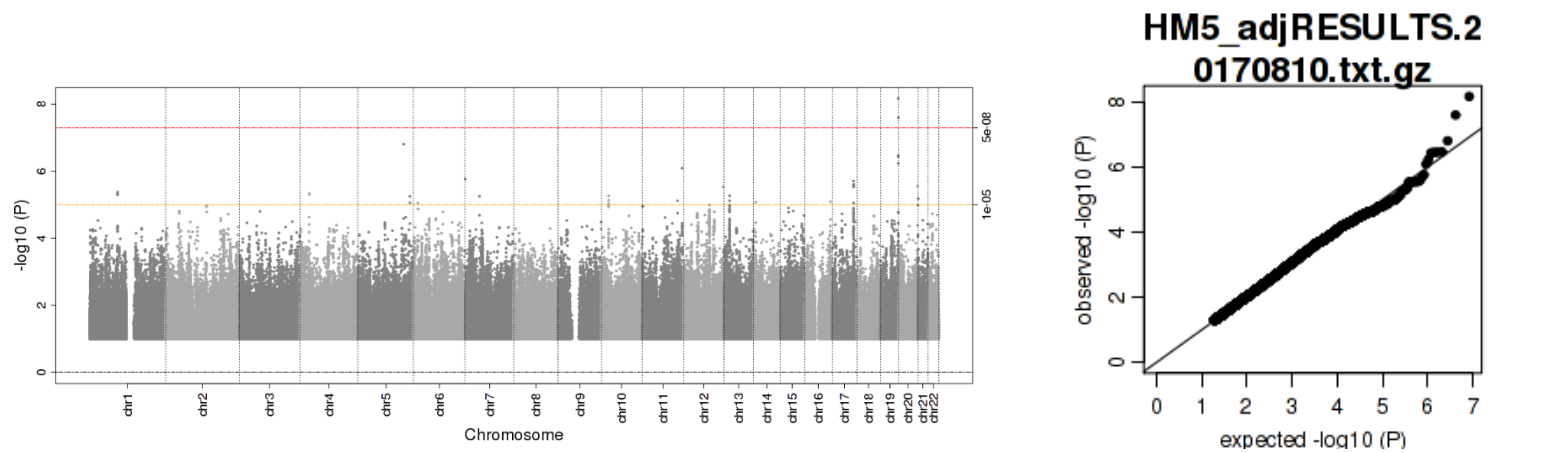
Supplementary Figure 10.6.12 Manhattan (left-hand side) and QQ (right hand-side) plots for HSM2 GWAS at age 18



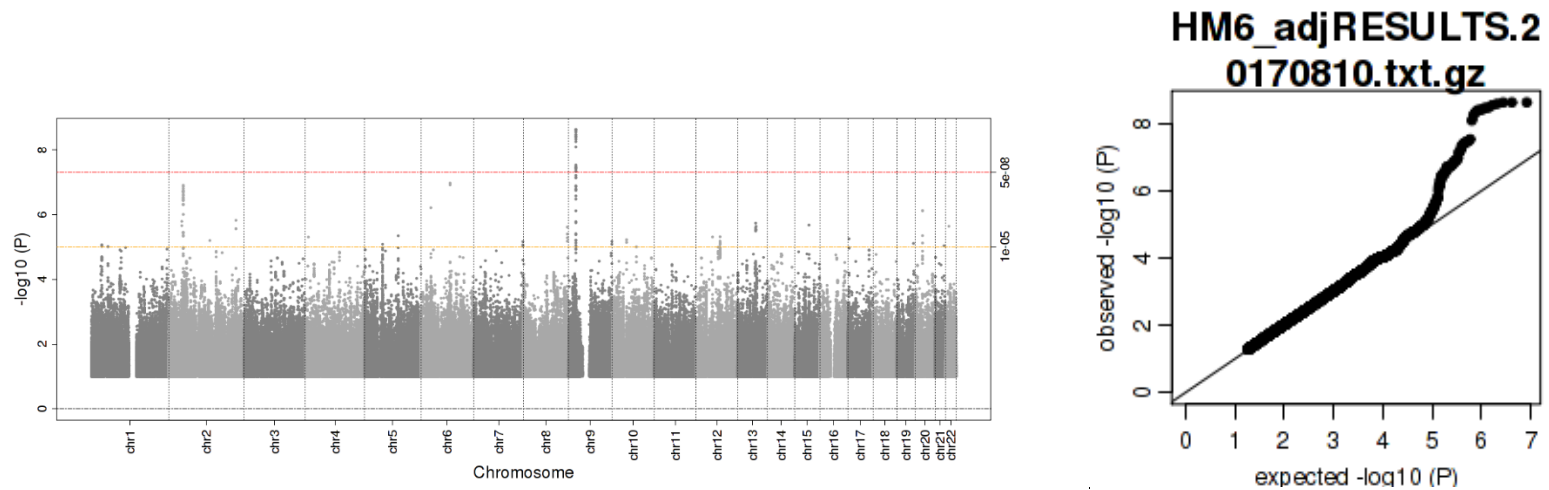
Supplementary Figure 10.6.13 Manhattan (left-hand side) and QQ (right hand-side) plots for HSM3 GWAS at age 18



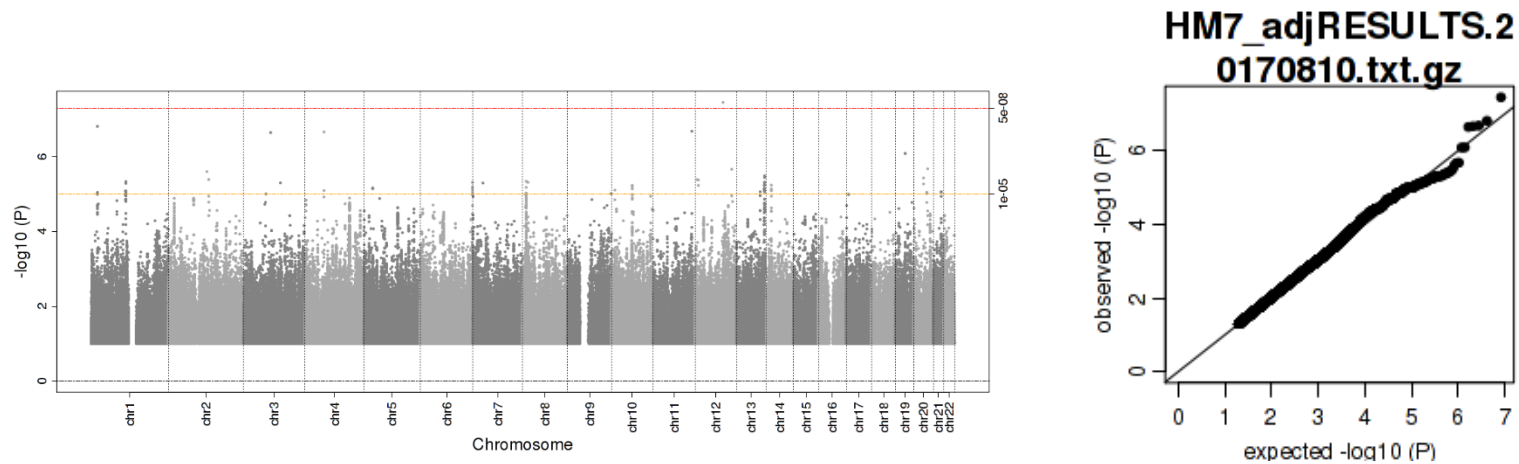
Supplementary Figure 10.6.14 Manhattan (left-hand side) and QQ (right hand-side) plots for HSM4 GWAS at age 18



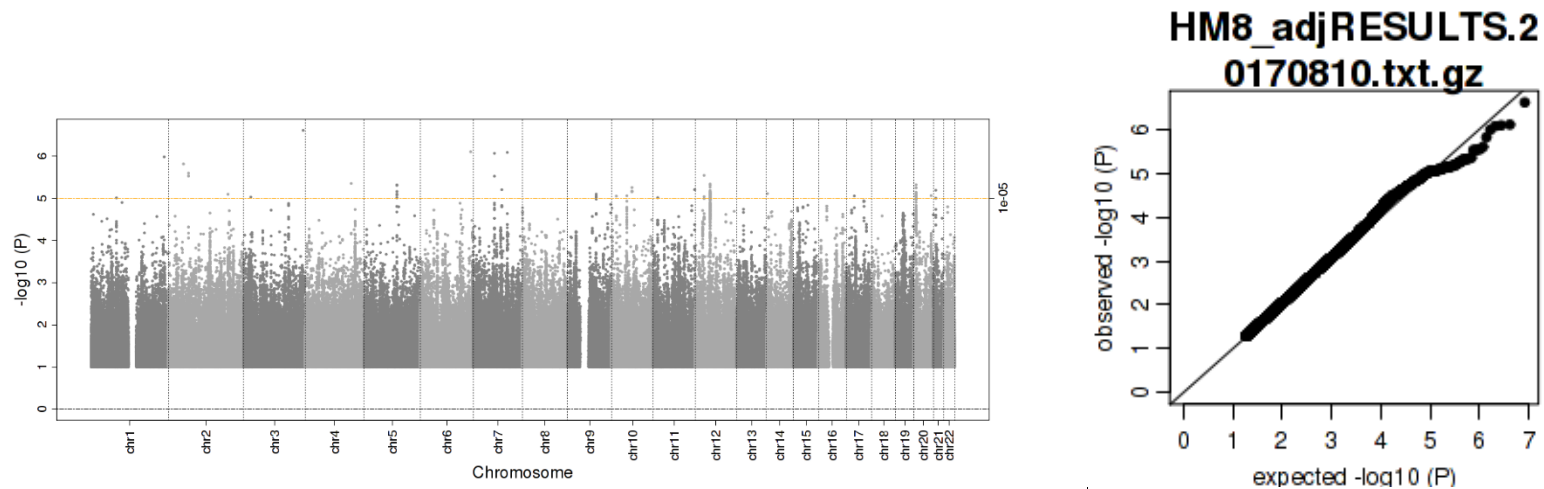
Supplementary Figure 10.6.15 Manhattan (left-hand side) and QQ (right hand-side) plots for HSM5 GWAS at age 18



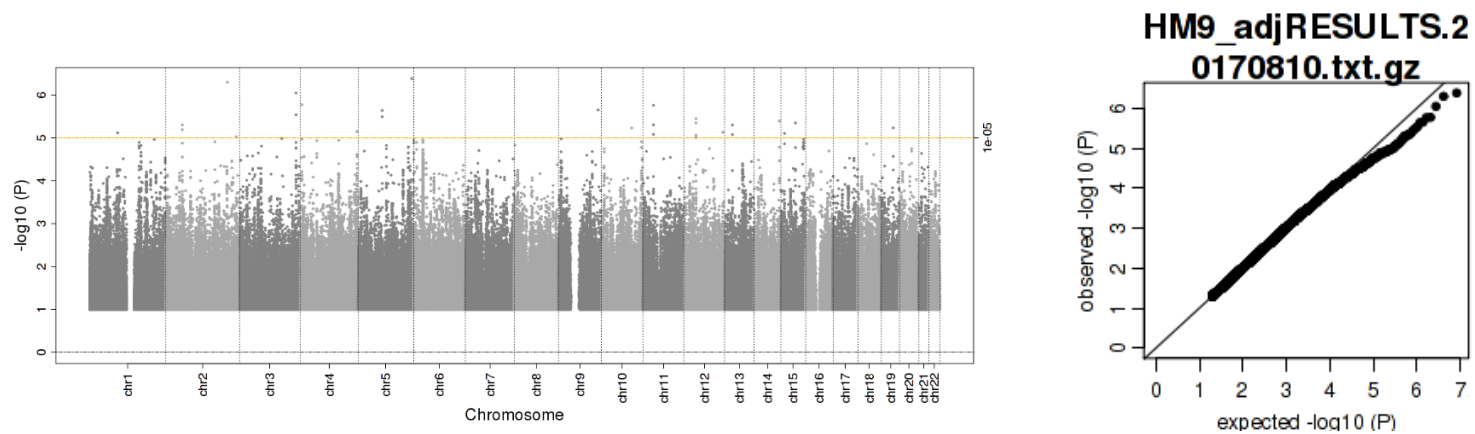
Supplementary Figure 10.6.16 Manhattan (left-hand side) and QQ (right hand-side) plots for HSM6 GWAS at age 18



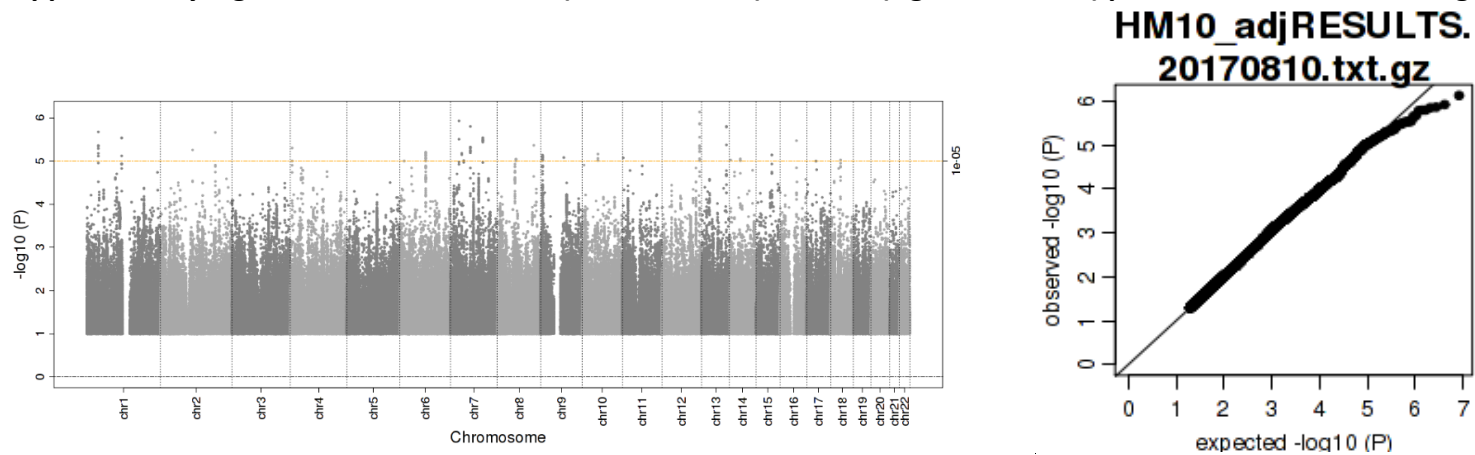
Supplementary Figure 10.6.17 Manhattan (left-hand side) and QQ (right hand-side) plots for HSM7 GWAS at age 18



Supplementary Figure 10.6.18 Manhattan (left-hand side) and QQ (right hand-side) plots for HSM8 GWAS at age 18



Supplementary Figure 10.6.19 Manhattan (left-hand side) and QQ (right hand-side) plots for HSM9 GWAS at age 18



Supplementary Figure 10.6.20 Manhattan (left-hand side) and QQ (right hand-side) plots for HSM10 GWAS at age 18